Multispectral Remote Sensing

Lectures in Brienza
20 Sep 2011

Paul Menzel
UW/CIMSS/AOS

Applications with Multispectral Remote Sensing Data

Satellite Remote Sensing

Energy Balance

VIS, IR, and MW Radiative Transfer

EOS Terra & Aqua MODIS

Multispectral Signatures

(Ocean Color, Snow/Ice, Vegetation, Aerosols, Clouds, Moisture, Fires, Volcanic Ash)

Detecting Climate Trends

Satellite remote sensing of the Earth-atmosphere

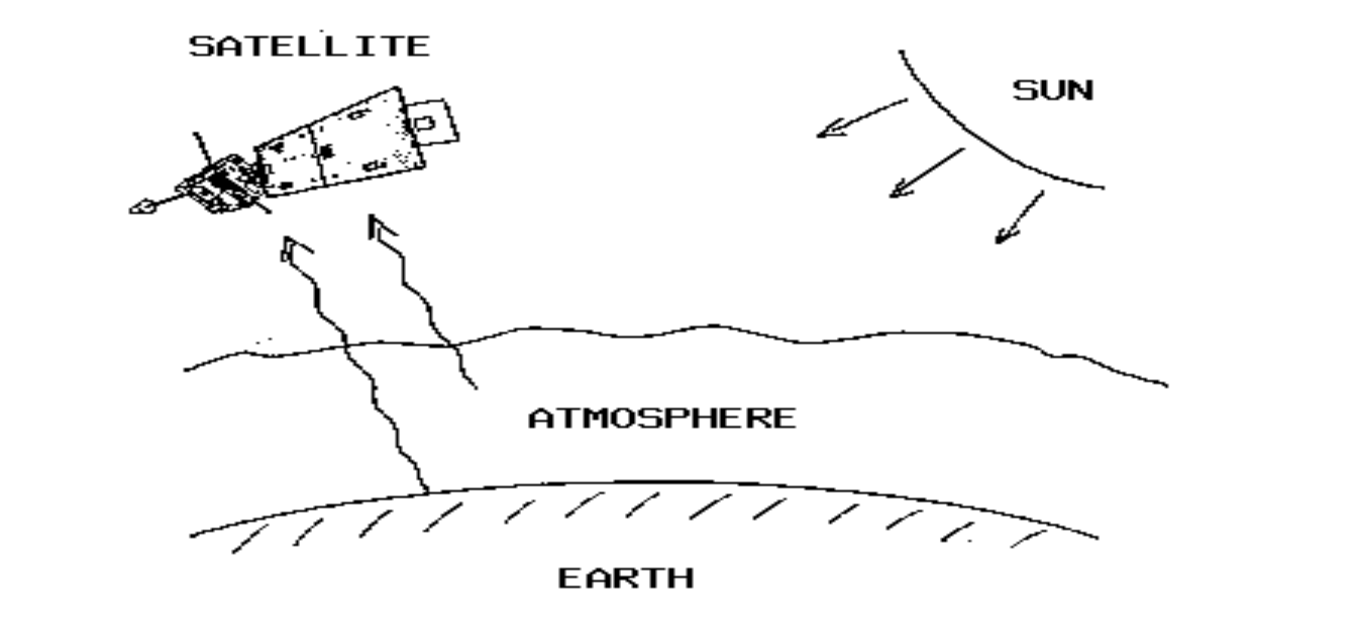

Observations depend on

telescope characteristics (resolving power, diffraction)
detector characteristics (signal to noise)
communications bandwidth (bit depth)
spectral intervals (window, absorption band)
time of day (daylight visible)
atmospheric state (T, Q, clouds)
earth surface (Ts, vegetation cover)

Solar (visible) and Earth emitted (infrared) energy

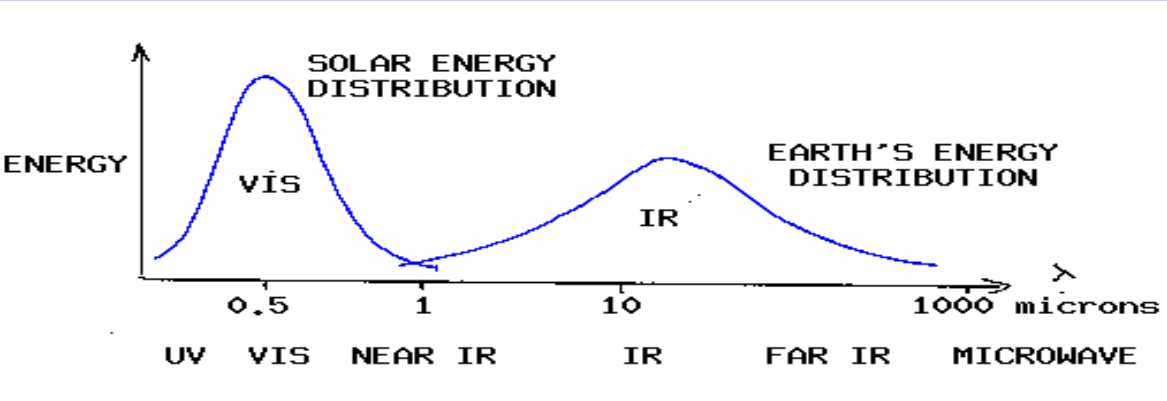

Incoming solar radiation (mostly visible) drives the earth-atmosphere (which emits infrared).

Over the annual cycle, the incoming solar energy that makes it to the earth surface (about 50 %) is balanced by the outgoing thermal infrared energy emitted through the atmosphere.

The atmosphere transmits, absorbs (by H2O, O2, O3, dust) reflects (by clouds), and scatters (by aerosols) incoming visible; the earth surface absorbs and reflects the transmitted visible. Atmospheric H2O, CO2, and O3 selectively transmit or absorb the outgoing infrared radiation. The outgoing microwave is primarily affected by H2O and O2.

Radiative Energy Balance

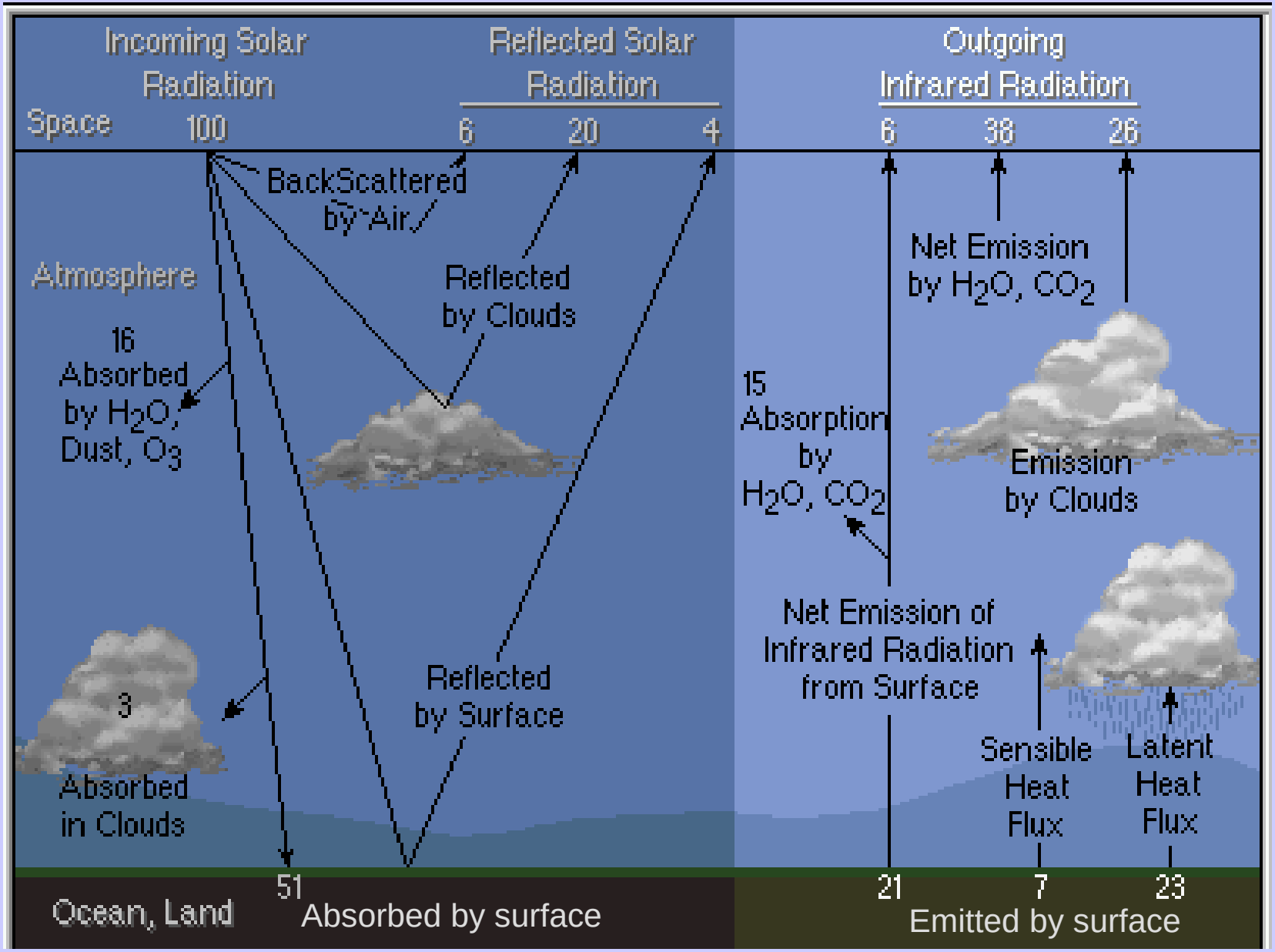

Solar Spectrum

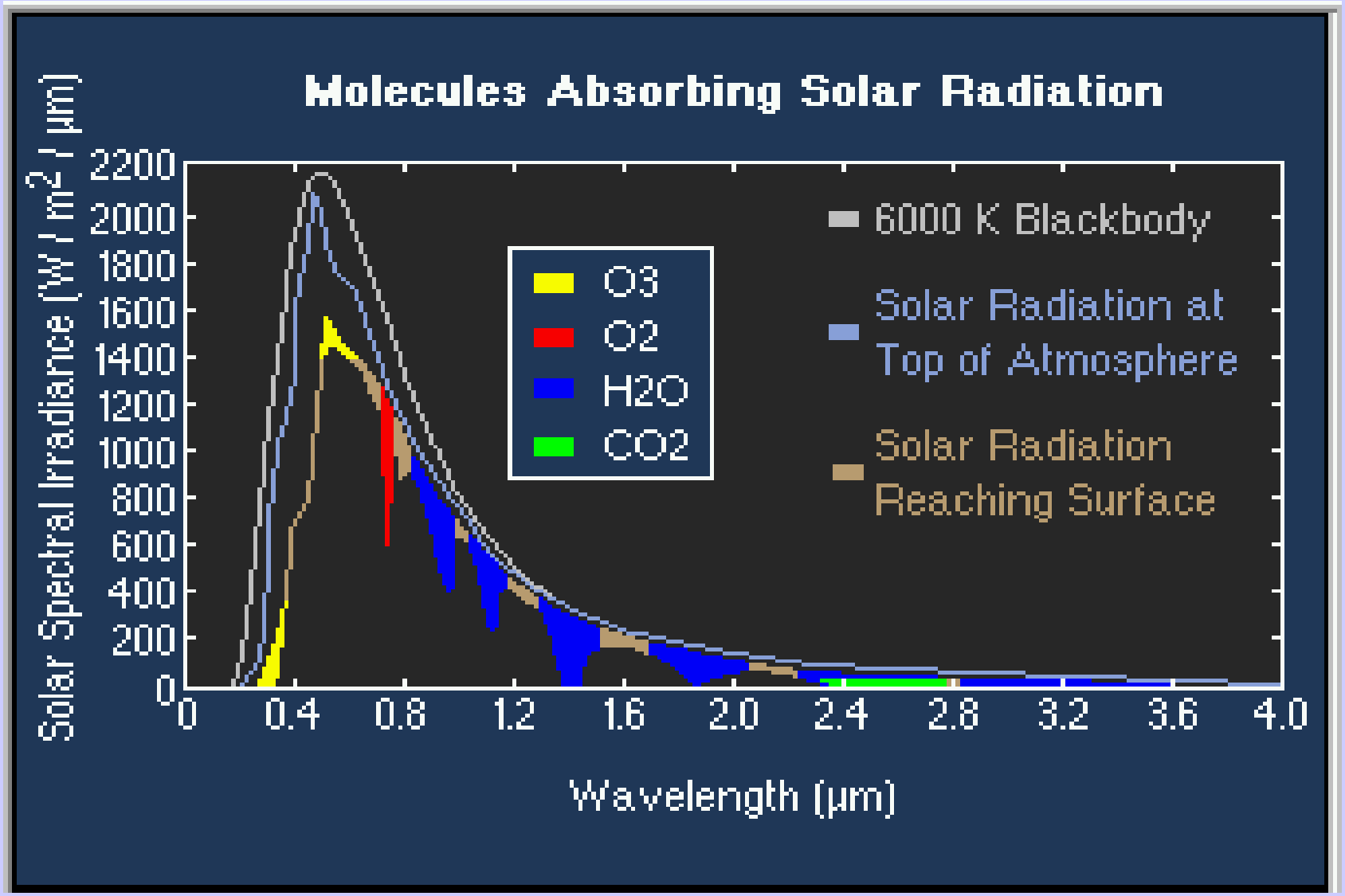

Earth emitted spectra overlaid on Planck function envelopes

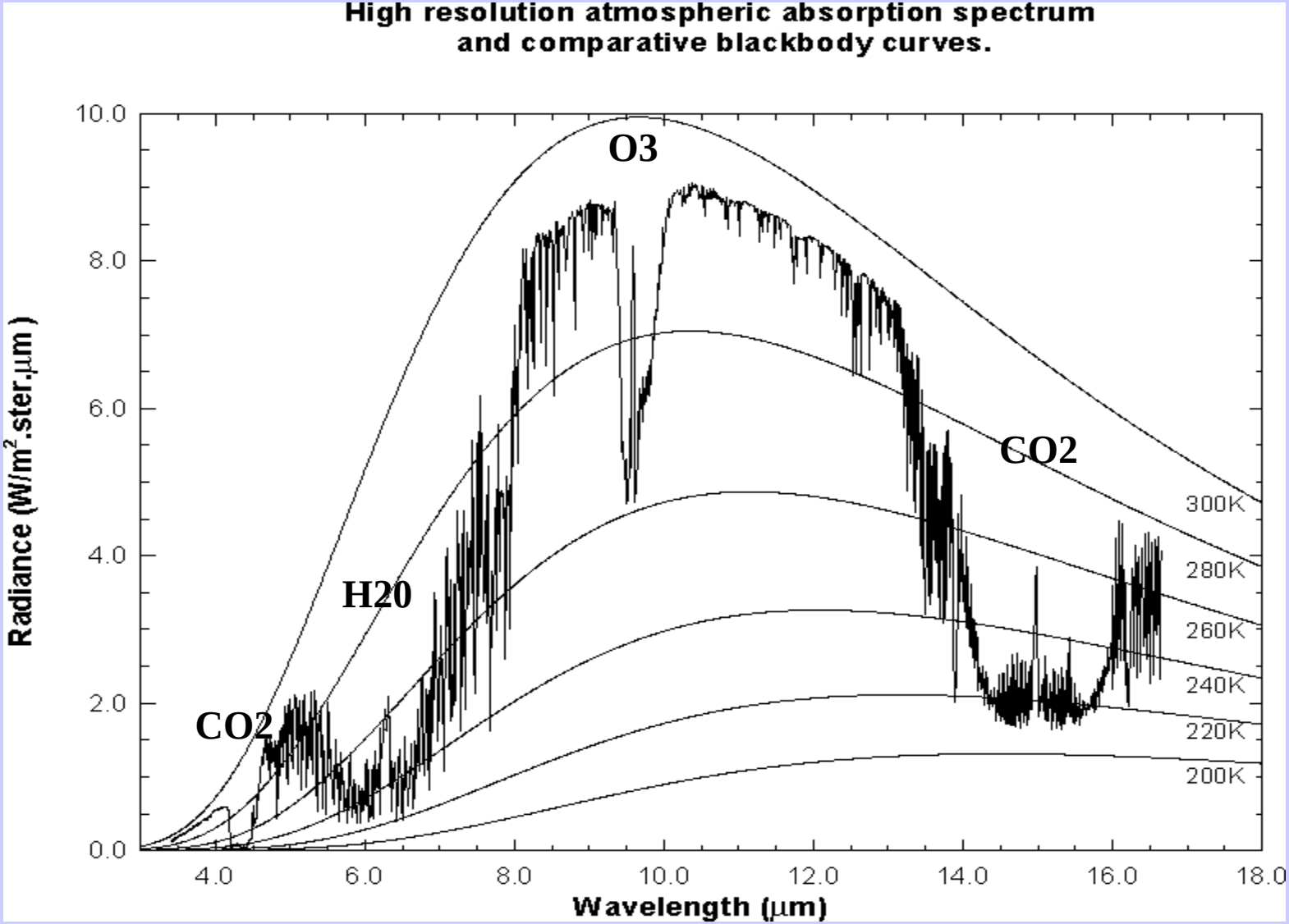

Radiative Transfer through the Atmosphere

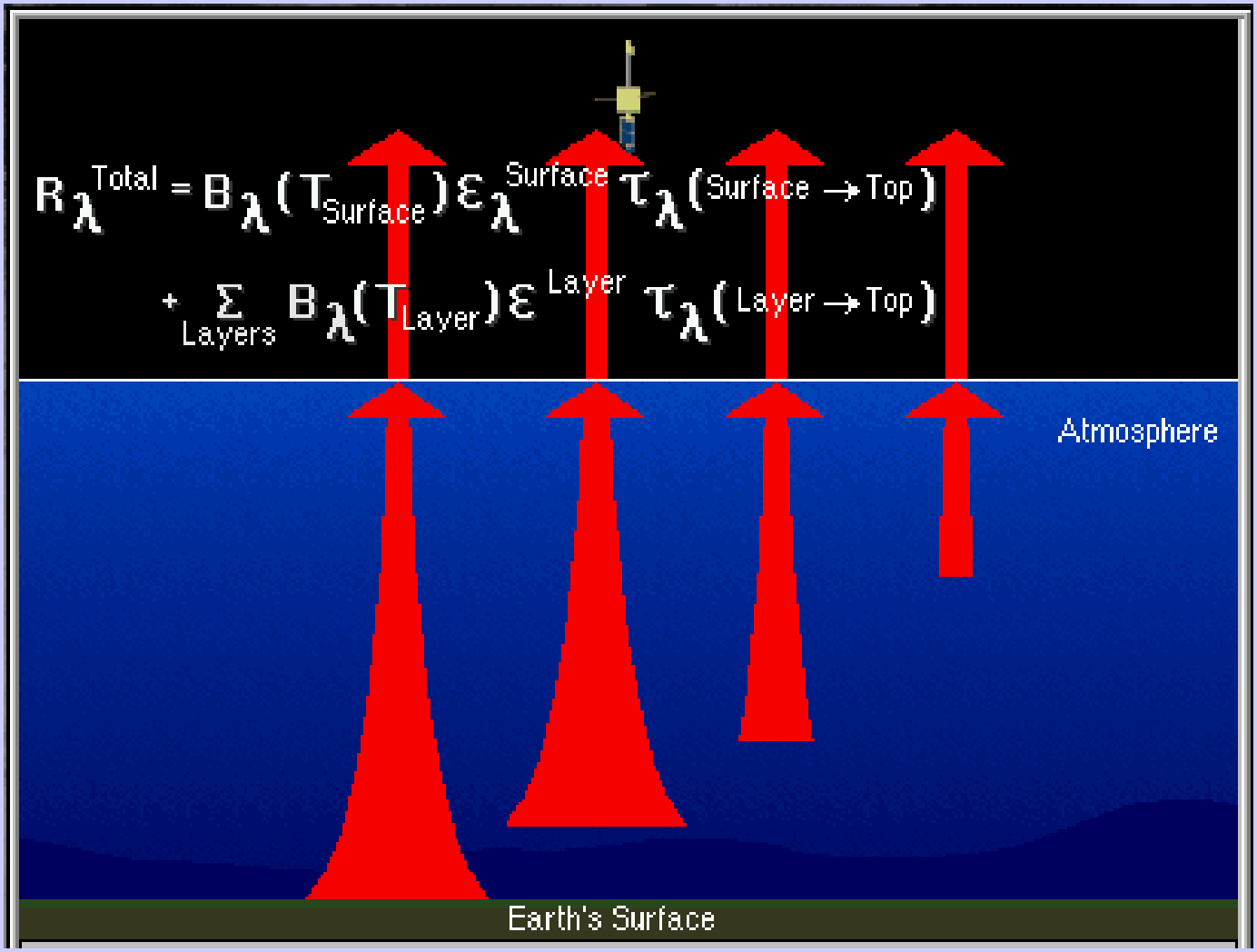

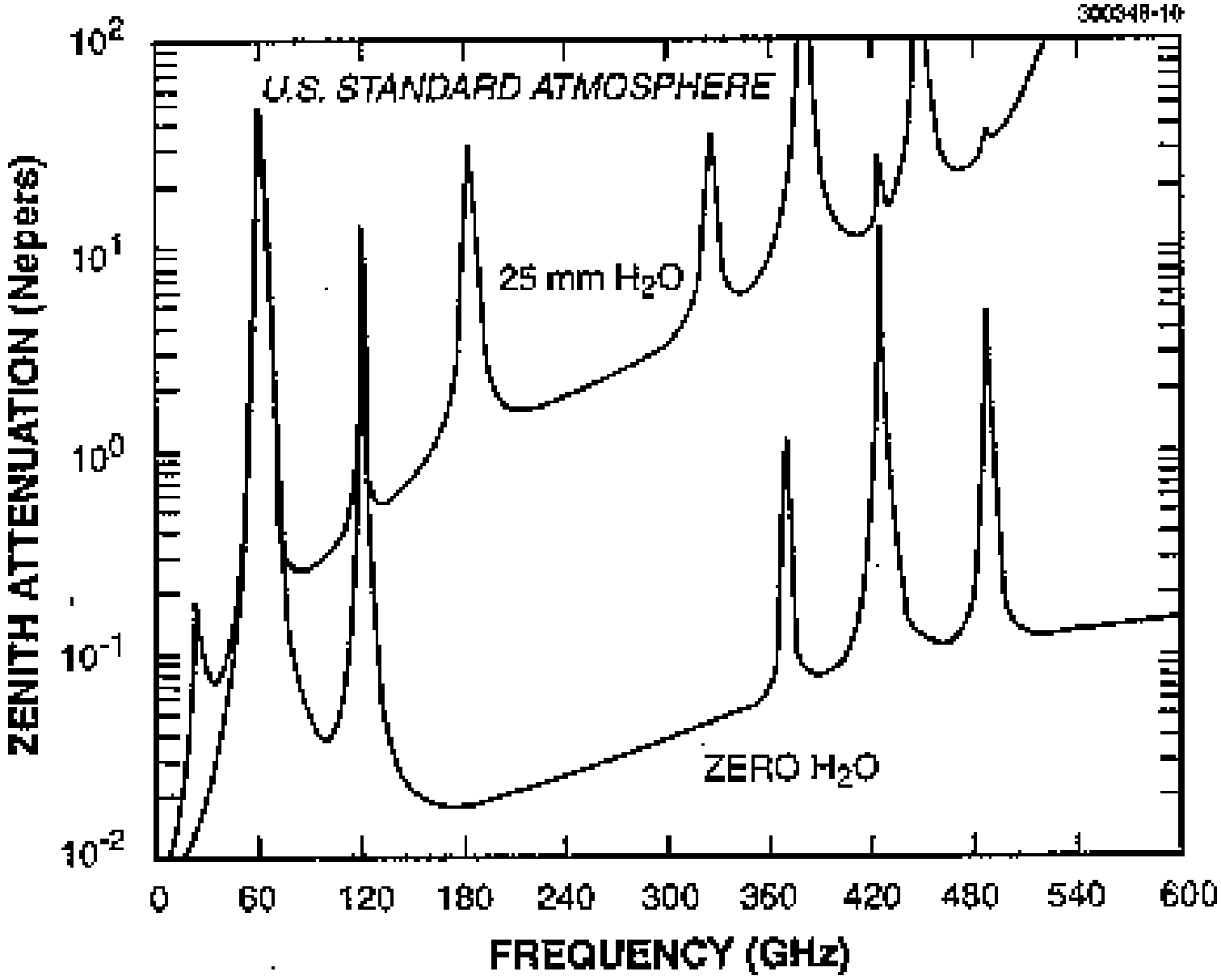
U.S. STANDARD ATMOSPHERE
25 mm H_2O
ZERO H_2O
ZENITH ATTENUATION (Nepers)
10^2
10^1
10^0
10^{-1}
10^{-2}
0
60
120
180
240
300
360
420
480
540
600
FREQUENCY (GHz)

Applications with Multispectral Remote Sensing Data

Satellite Remote Sensing

Energy Balance

VIS, IR, and MW Radiative Transfer

EOS Terra & Aqua MODIS

Multispectral Signatures

(Ocean Color, Snow/Ice, Vegetation, Aerosols, Clouds, Moisture, Fires, Volcanic Ash)

Detecting Climate Trends

Evolution of Leo Obs

Terra was launched in 1999 and the EOS Era began

MODIS, CERES, MOPITT, ASTER, and MISR reach polar orbit

Aqua and ENVISAT followed in 2002

MODIS and MERIS to be followed by VIIRS
AIRS and IASI to be followed by CrIS
AMSU leading to ATMS

MODIS ON THE EOS TERRA AND AQUA MISSIONS

Terra Launch: Dec. 18, 1999
First Image: Feb. 24, 2000

Aqua Launch: May 04, 2002
First Image: June 26, 2002

VIIRS, MODIS, FY-1C, AVHRR

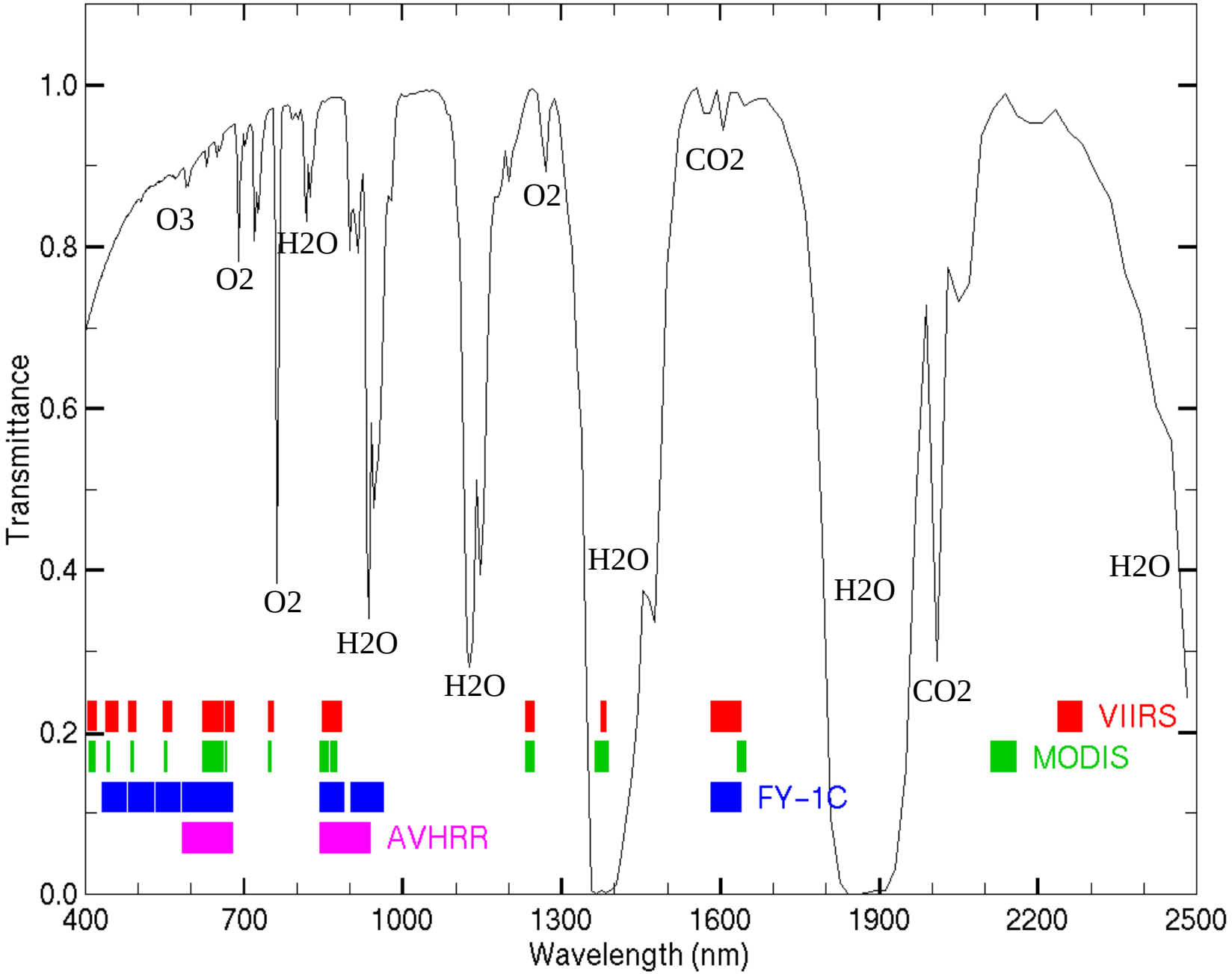

MODIS IR Spectral Bands

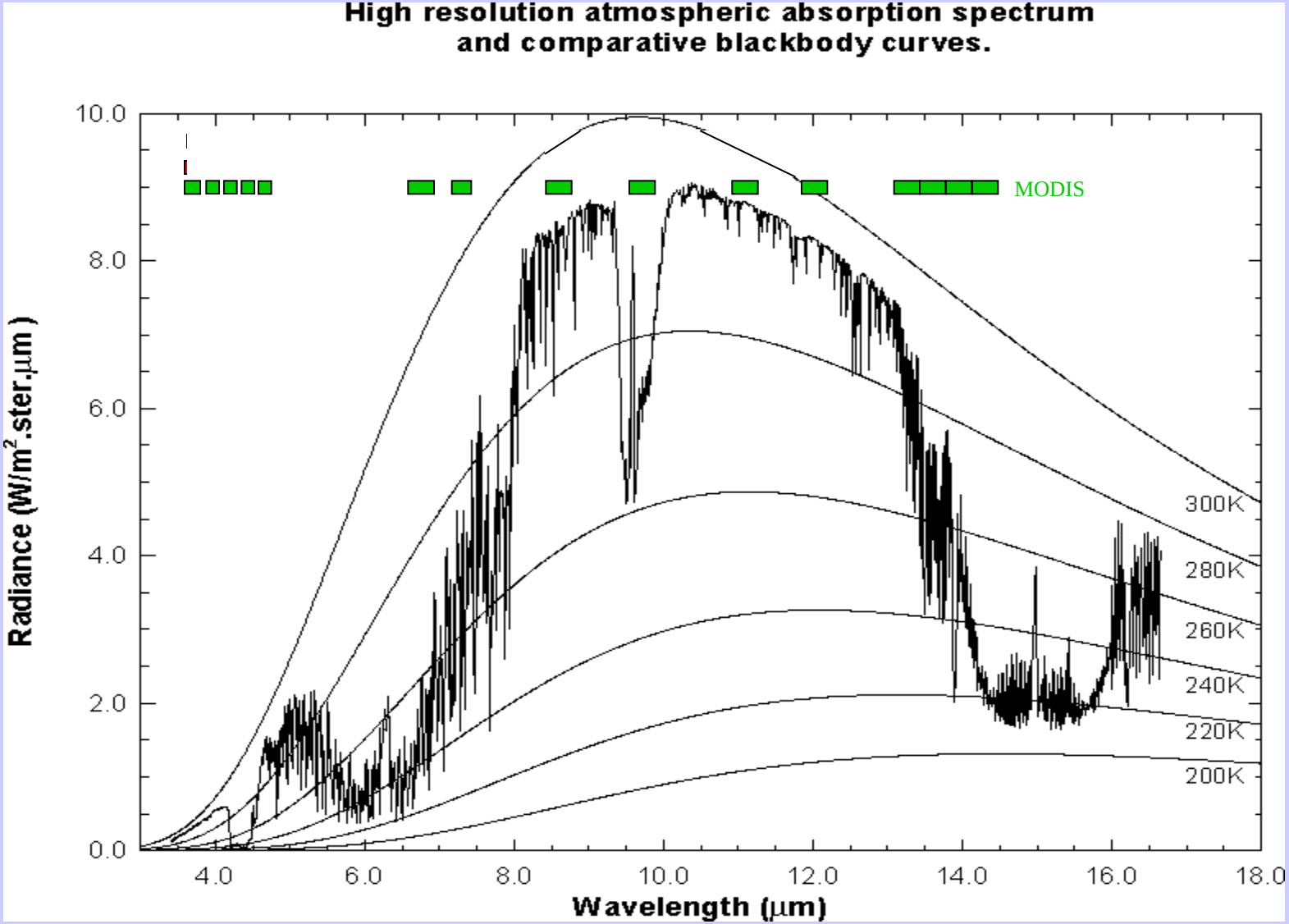

Applications with Multispectral Remote Sensing Data

Satellite Remote Sensing

Energy Balance

VIS, IR, and MW Radiative Transfer

EOS Terra & Aqua MODIS

Multispectral Signatures

*(**Ocean Color, SST**, Snow/Ice, Vegetation, Aerosols, Clouds, Moisture, Fires, Volcanic Ash)*

Detecting Climate Trends

OCEAN-SOLAR RADIATION

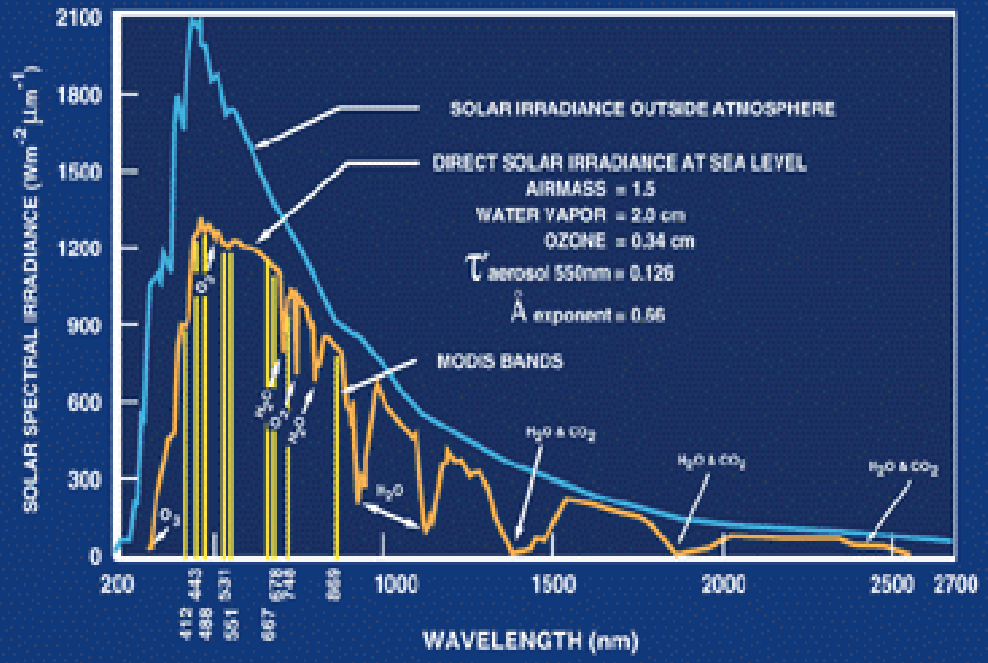

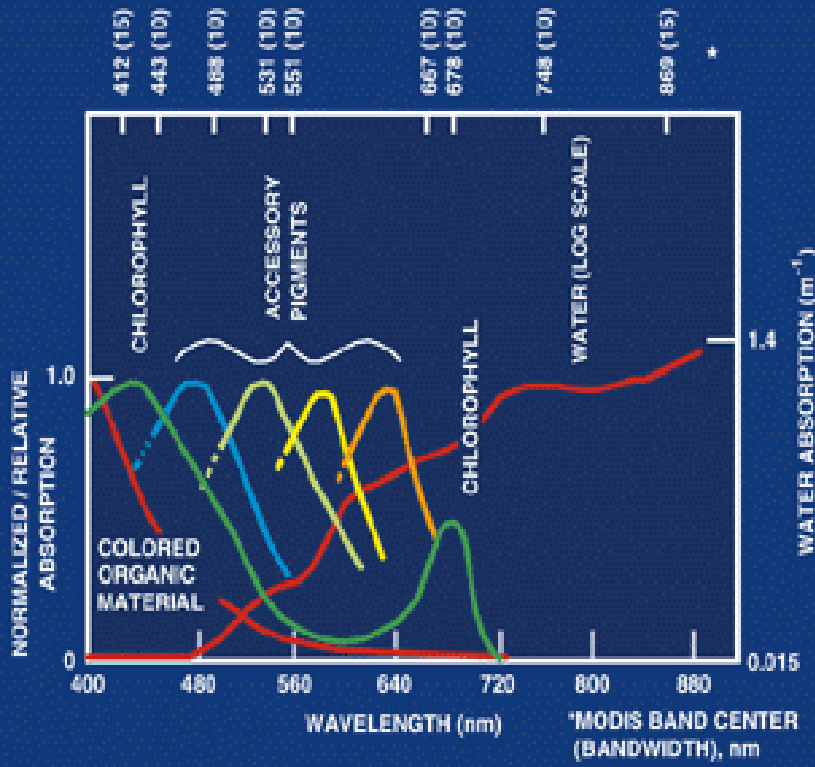

Good Agreement in Derived Chlorphyll

2002 289

SeaWiFS

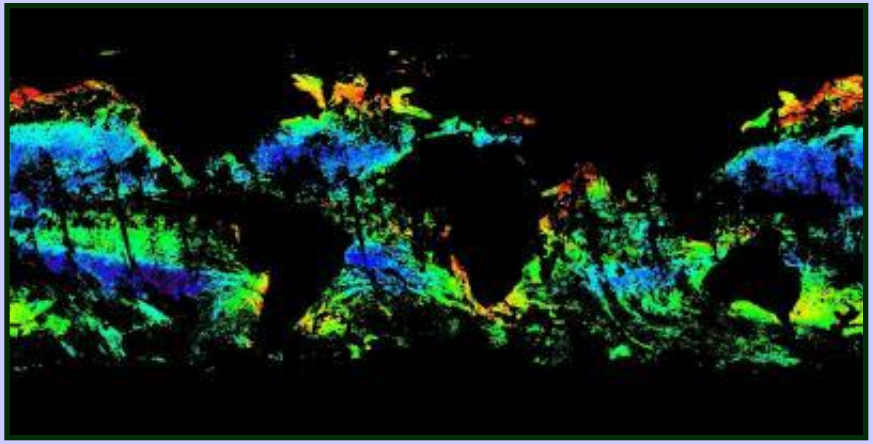

MODISA

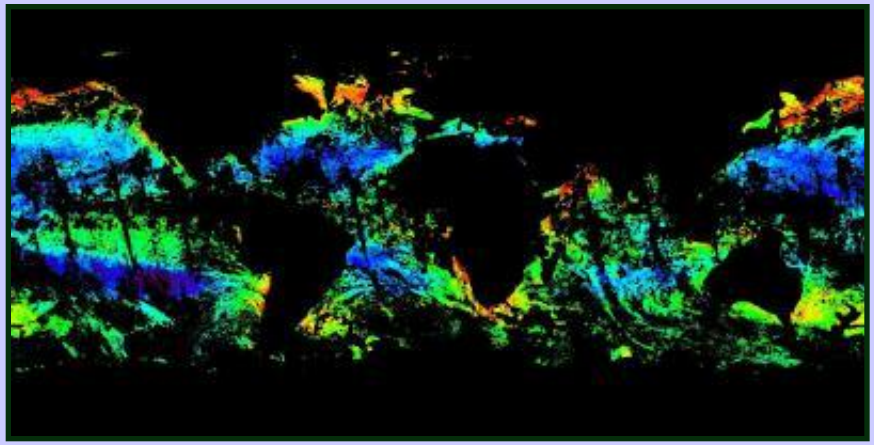

2008 289

SeaWiFS

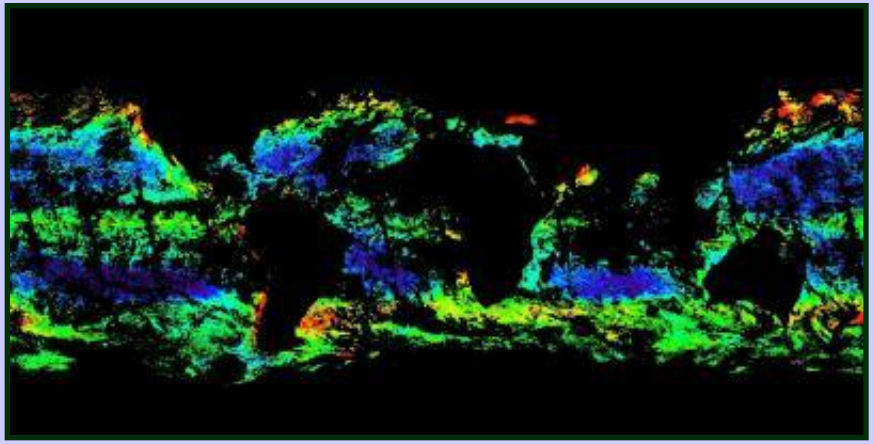

MODISA

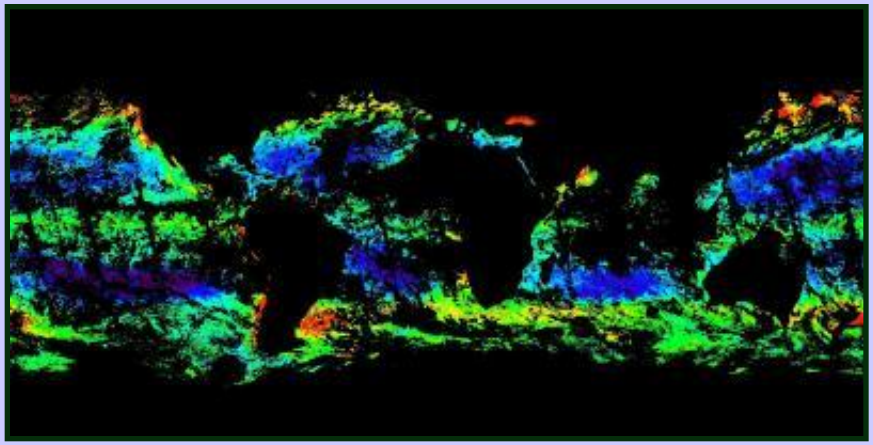

Studying the Chesapeake Bay with SeaDAS

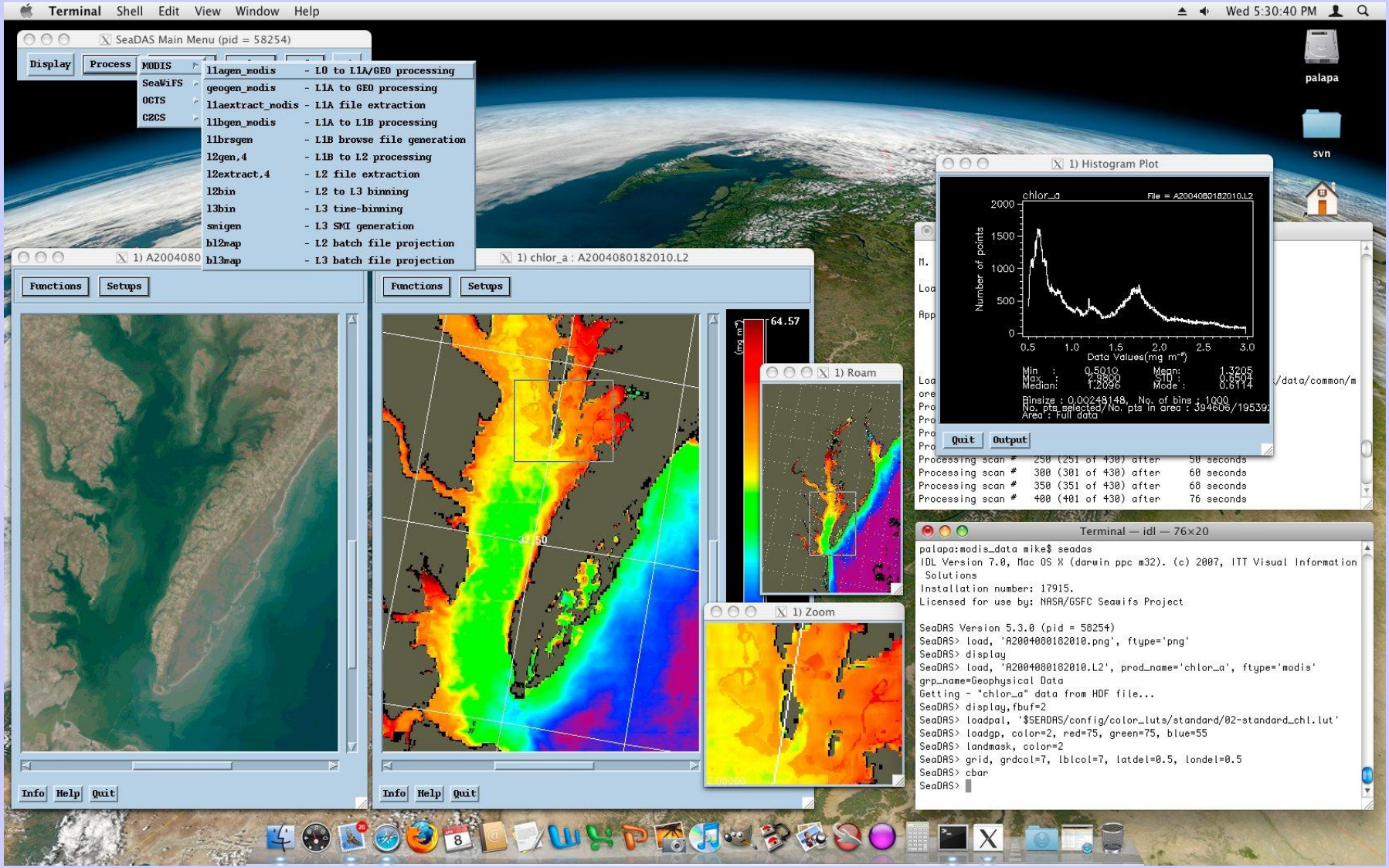

15 years in distribution, free, open-source, linux/os-x/solaris/windows(vm)
~1400 downloads in 2009 alone

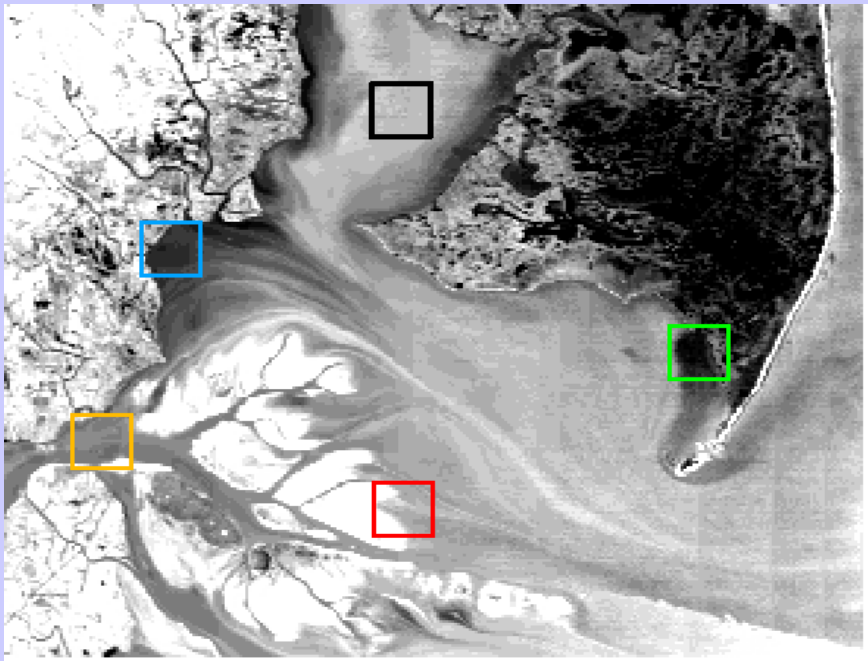

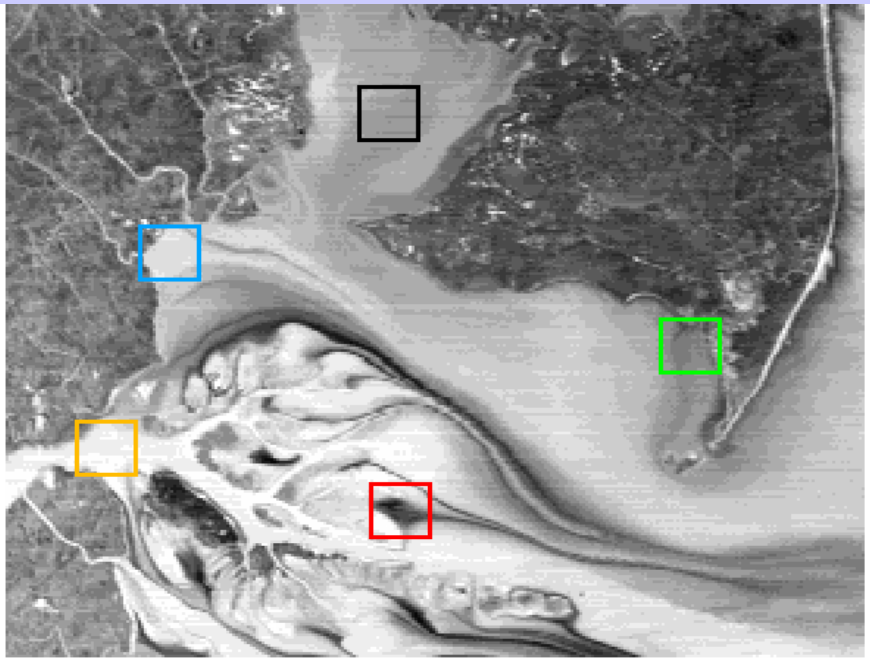

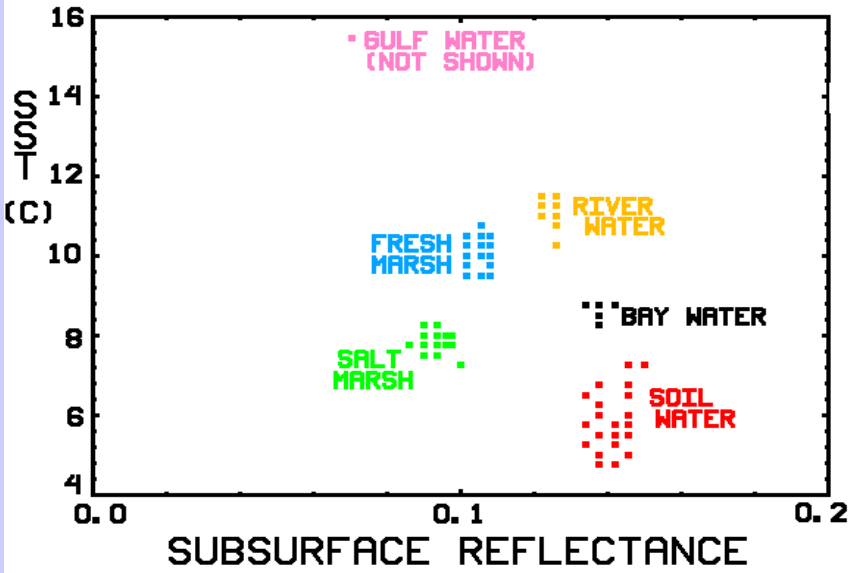

MAMS WATER TYPE ANALYSIS
DEC 4 1990

SHOWN:
* .66um REFLECTANCE (LEFT)
* SPLIT WINDOW SST (RIGHT)

Aircraft Observations of the Mississippi Delta

0005 ACFT 09 4 DEC 91338 164701 53491 00035 01.50

First Order Estimation of SST

Moisture attenuation in atmospheric windows varies linearly with optical depth.

$$\tau_\lambda = e^{-k_\lambda u} = 1 - k_\lambda u$$

For same atmosphere, deviation of brightness temperature from surface temperature is a linear function of absorbing power. Thus moisture corrected SST can inferred by using split window measurements and extrapolating to zero k_λ

$$T_s = T_{bw1} + [\, k_{w1} / (k_{w2} - k_{w1}) \,] [T_{bw1} - T_{bw2}] \ .$$

Moisture content of atmosphere inferred from slope of linear relation.

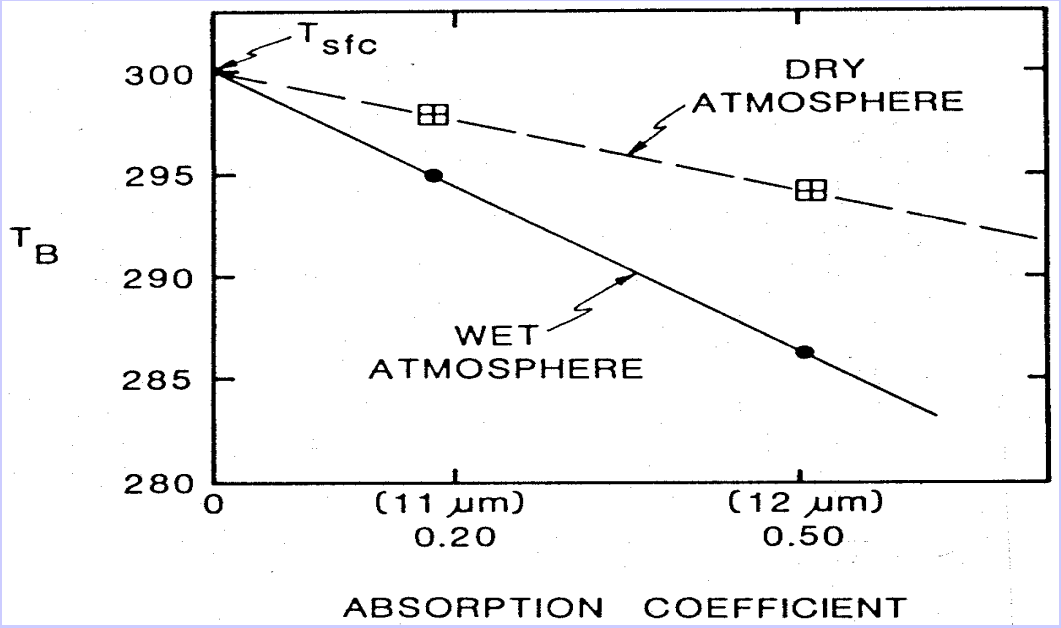

MODIS SEA SURFACE TEMPERATURE

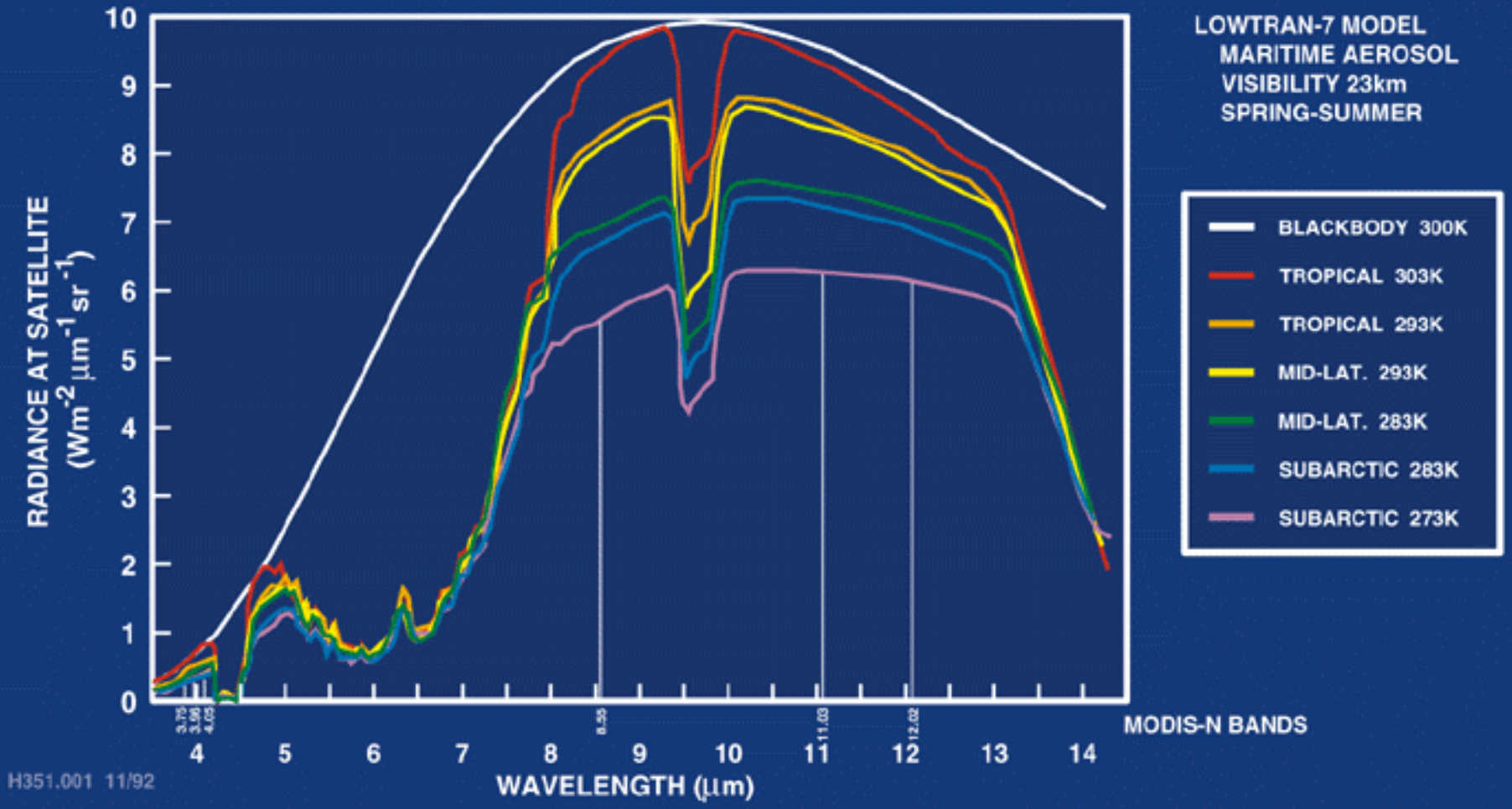

SST - MODIS and AVHRR

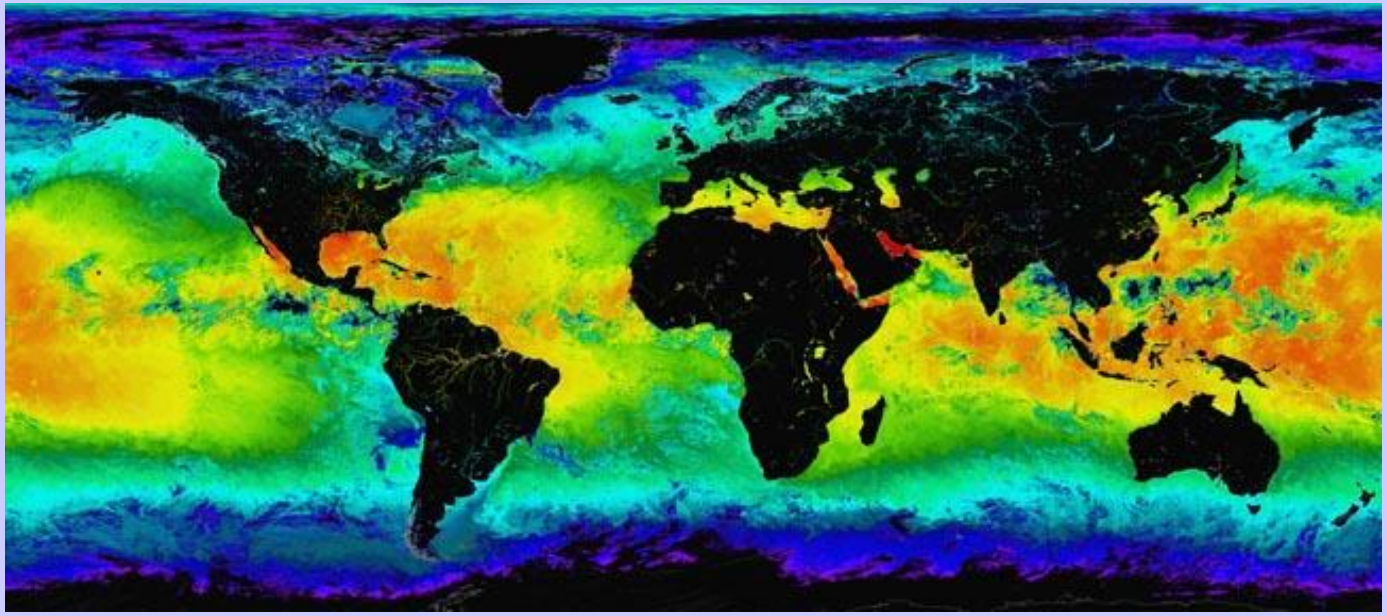

MODIS 4 µm Night SST

←

Improved coverage in tropical regions. Color scales are not identical, cloud mask is not applied.

AVHRR Night SST

→

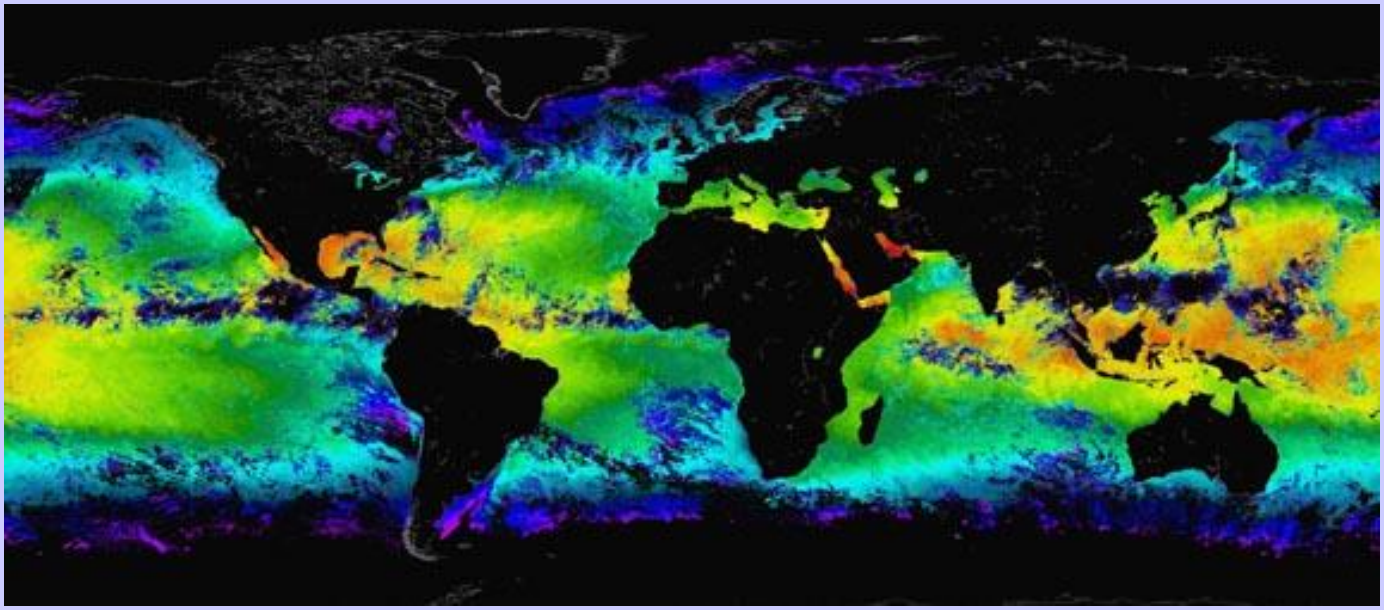

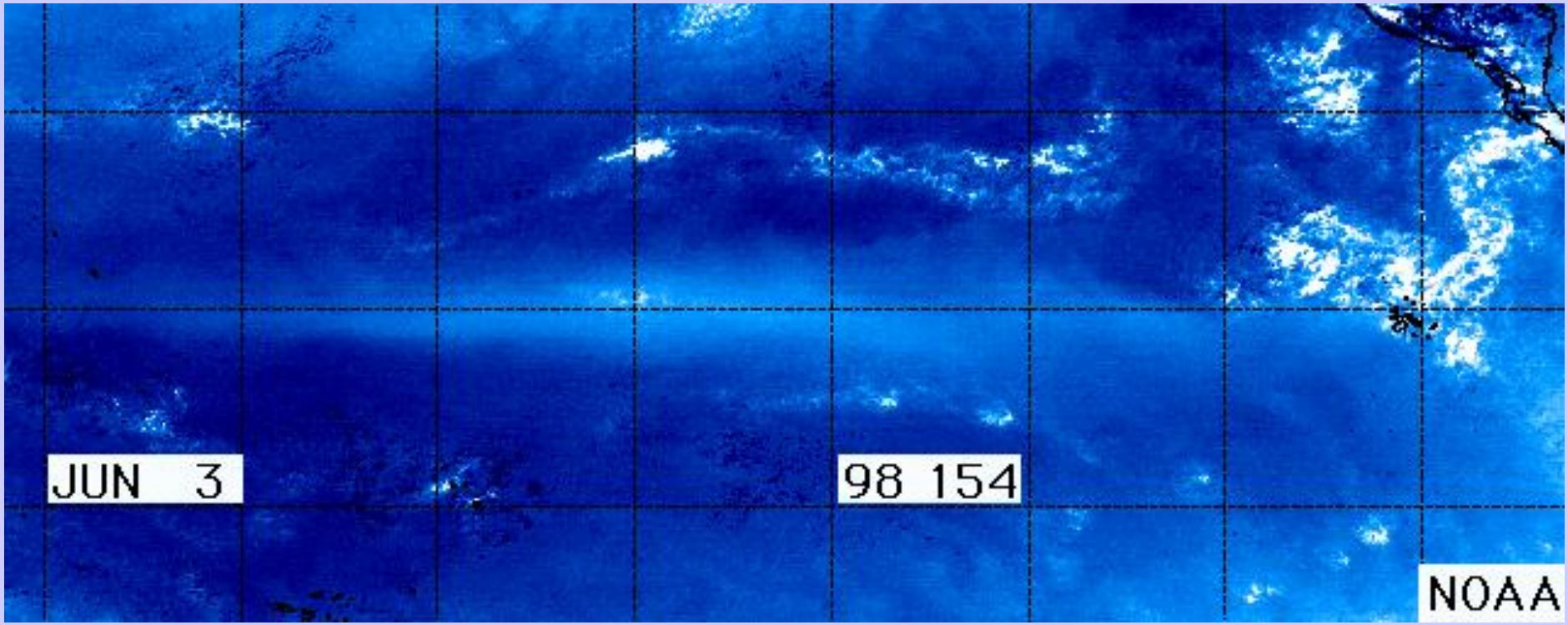

SST Waves from Legeckis

Applications with Multispectral Remote Sensing Data

Satellite Remote Sensing

Energy Balance

VIS, IR, and MW Radiative Transfer

EOS Terra & Aqua MODIS

Multispectral Signatures

*(Ocean Color, SST, **Snow/Ice, Vegetation**, Aerosols, Clouds, Moisture, Fires, Volcanic Ash)*

Detecting Climate Trends

LAND - THERMAL RADIATION

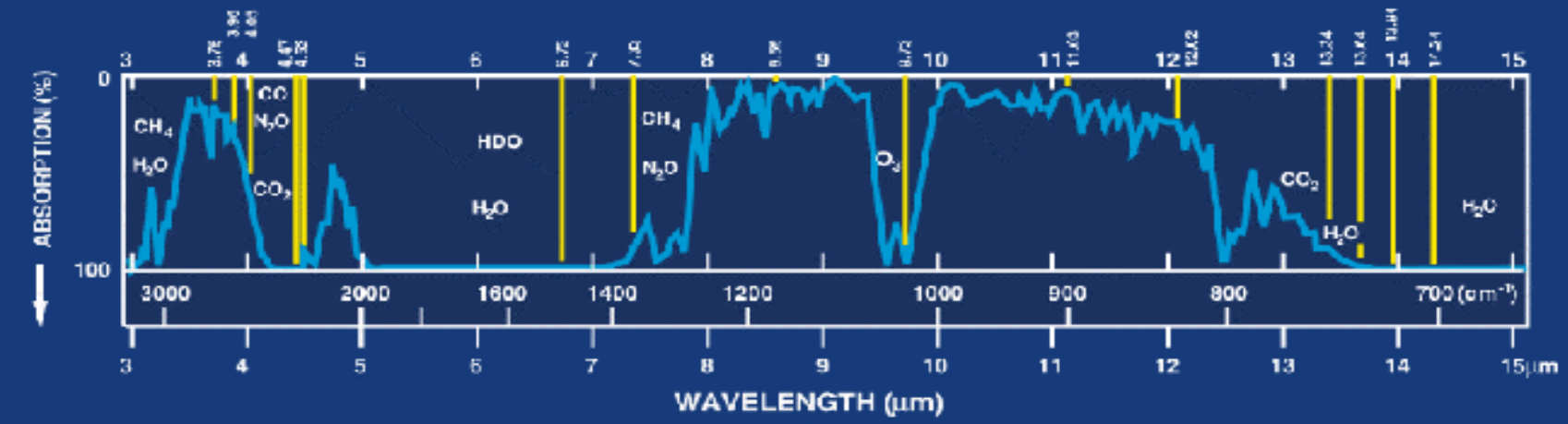

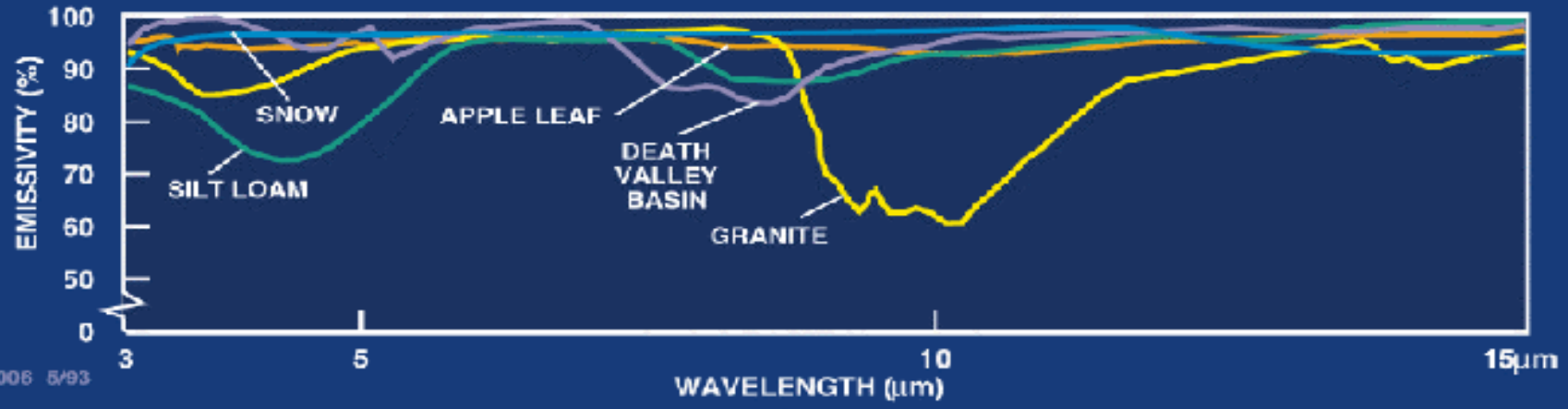

C351.006 5/93

LAND-SOLAR RADIATION

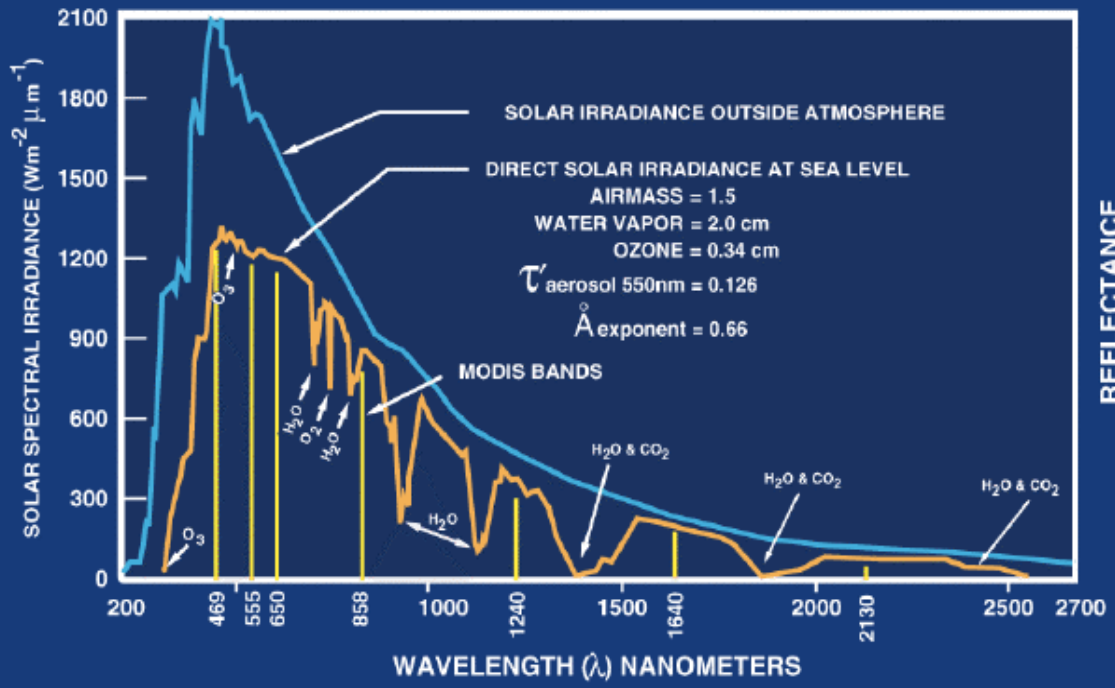

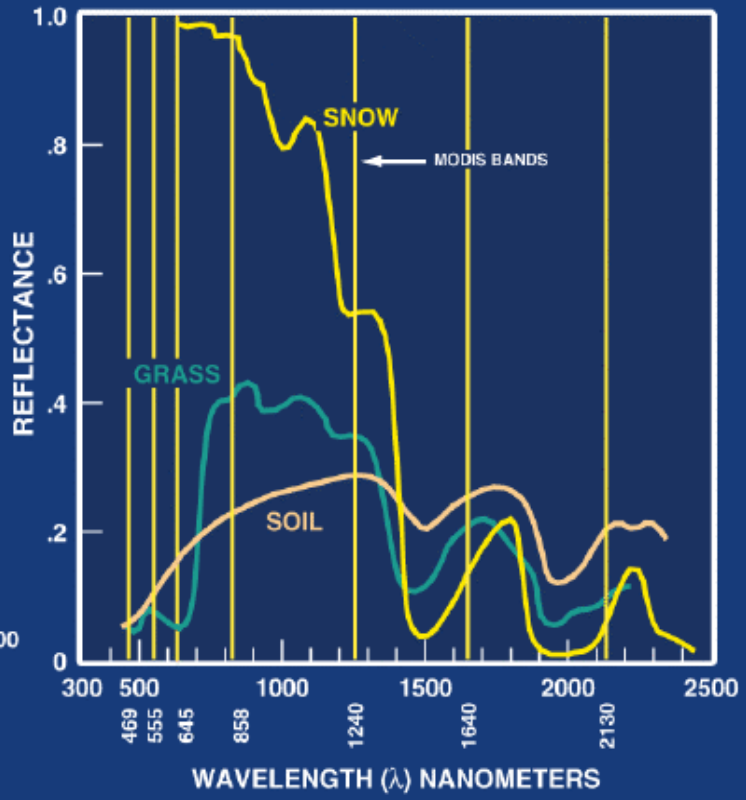

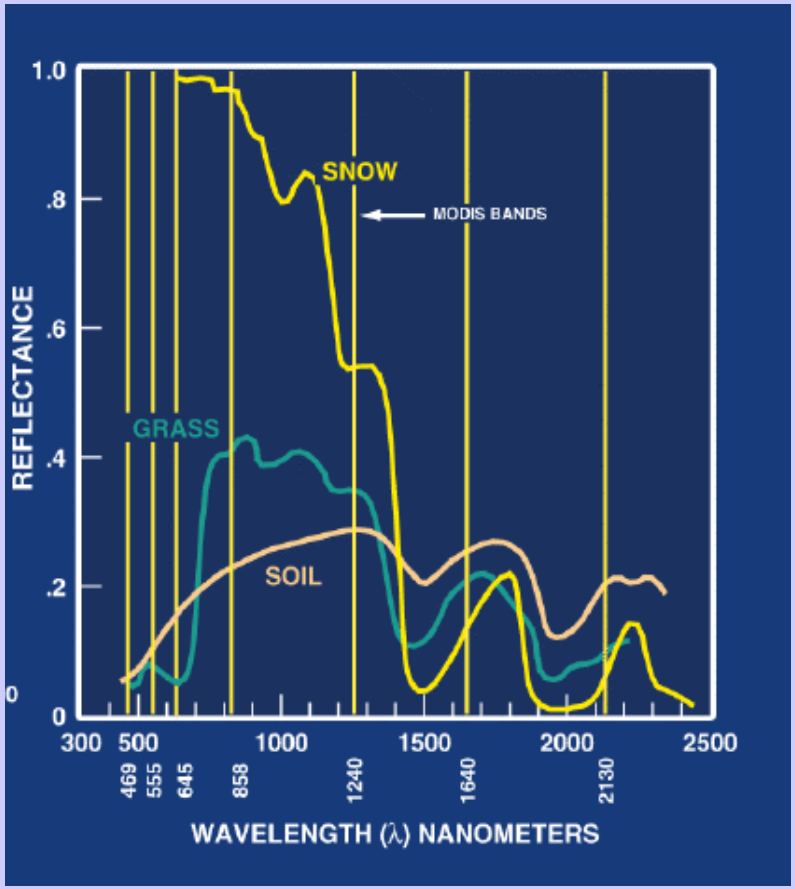

Investigating with Multi-spectral Combinations

Given the spectral response of a surface or atmospheric feature

Select a part of the spectrum where the reflectance or absorption changes with wavelength

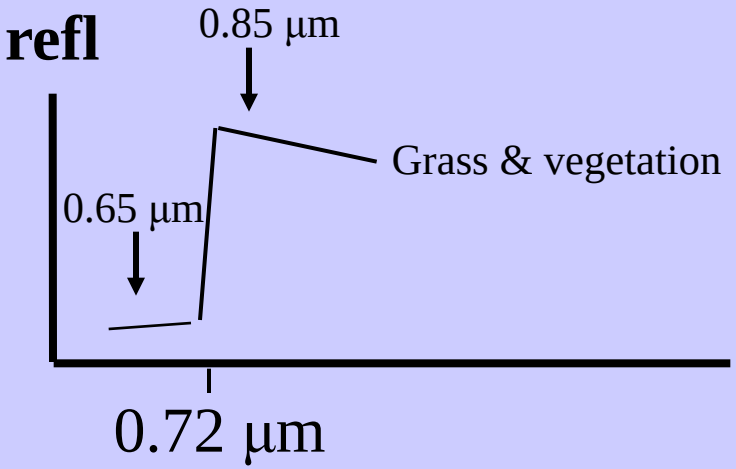

e.g. reflection from grass

If 0.65 μm and 0.85 μm channels see the same reflectance than surface viewed is not grass;
if 0.85 μm sees considerably higher reflectance than 0.65 μm then surface might be grass

The signal reaching any space borne sensor is a complex mixture of surface and atmospheric components.

One of the advantages of MODIS is its broad spectral range. The wider the spectral range the more information content we have when we observe the Earth - Atmosphere system.

Aspen Leaves - very uniform

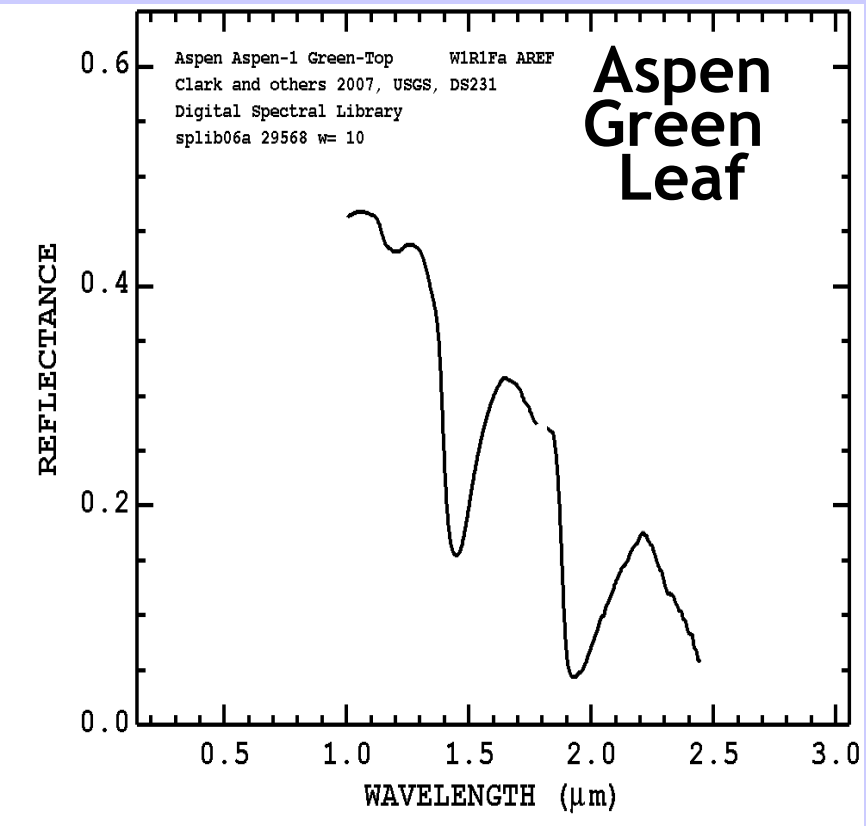

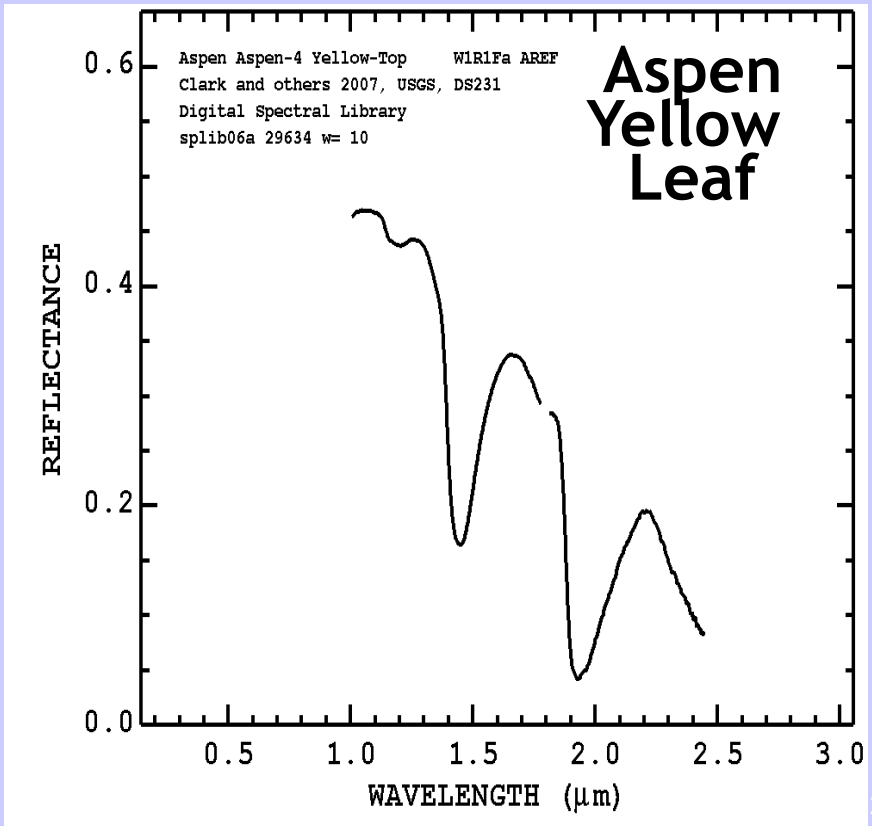

Leaves top - Forest bottom

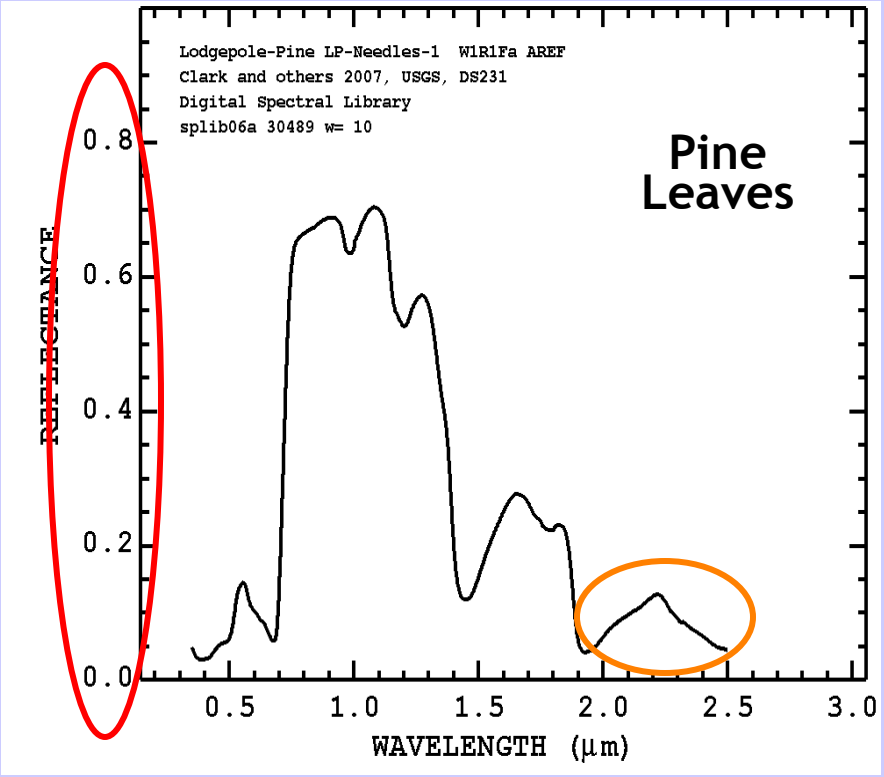

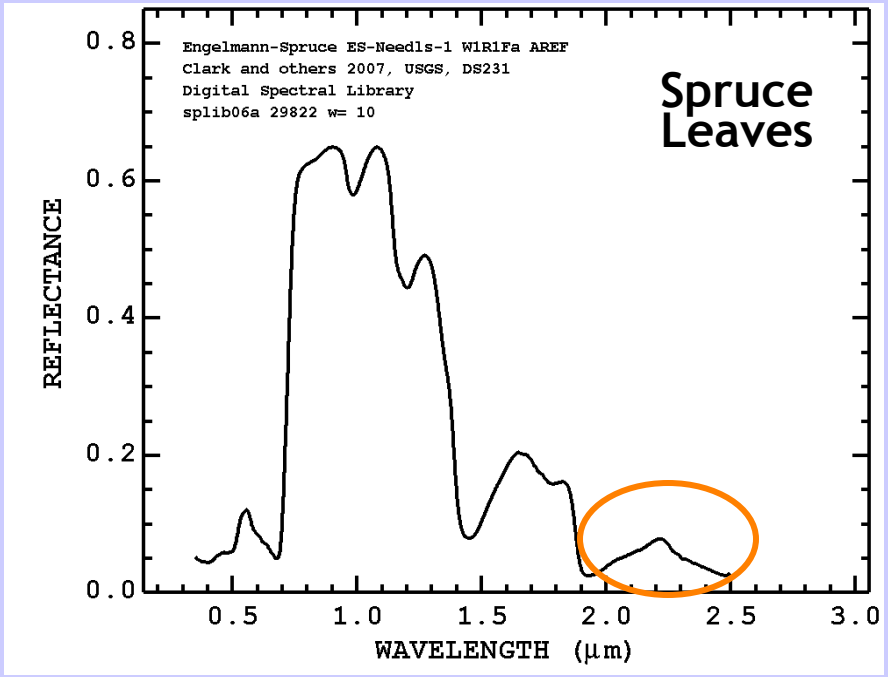

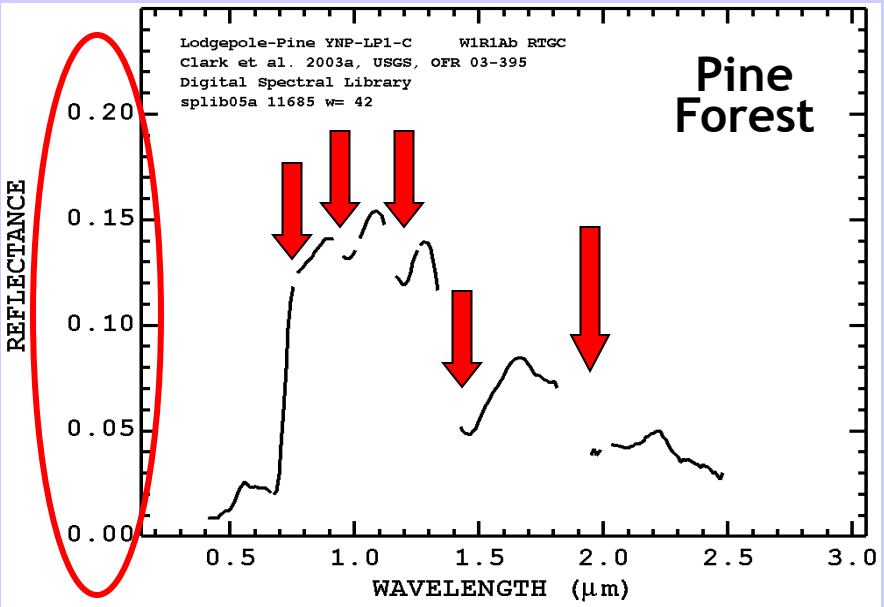

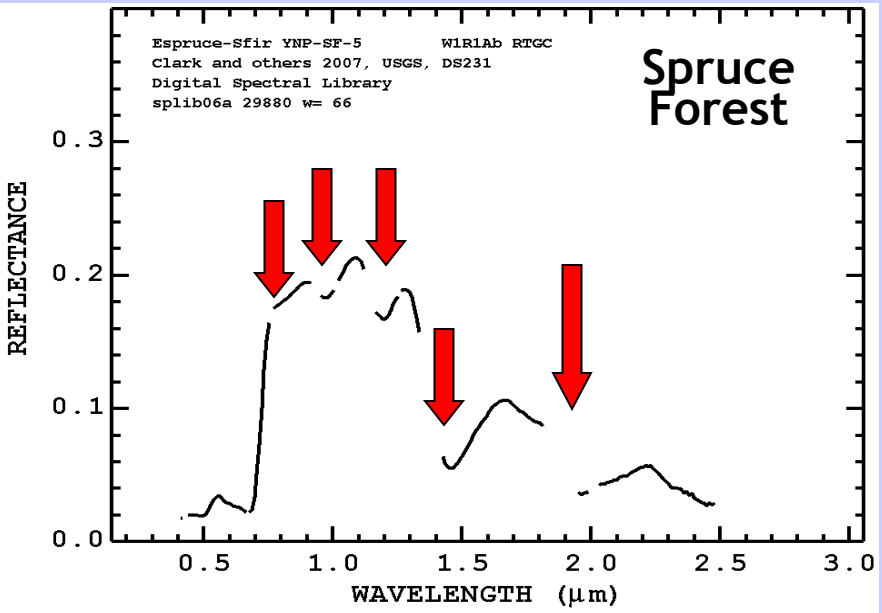

NDVI versus EVI

EVI is a useful proxy for 'greenness' or photosynthetically active vegetation in optically dense canopies, as found throughout the Amazon (LAI= 4 -7), by relying on the more sensitive NIR canopy reflectance which is less prone to saturate

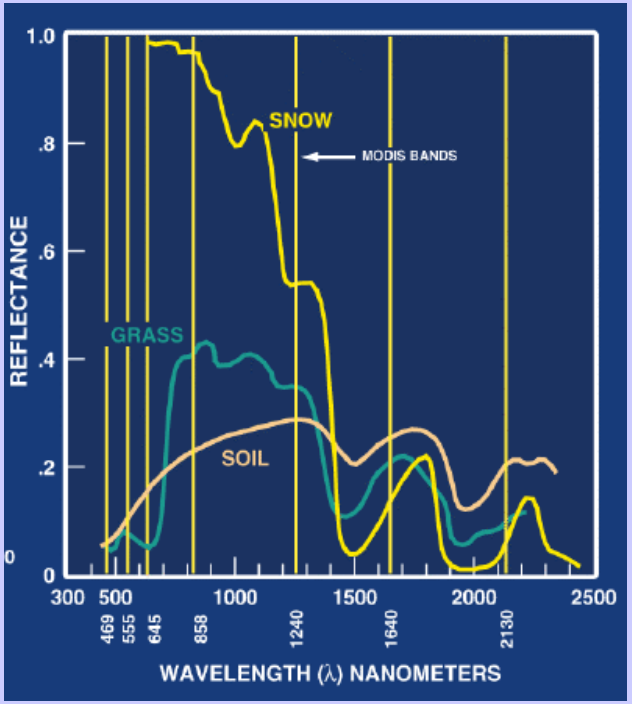

$$NDVI = (\rho 0.8 - \rho 0.6) / (\rho 0.8 + \rho 0.6)$$

$$EVI = 2.5 \times \frac{\rho_{NIR} - \rho_{red}}{1 + \rho_{NIR} + (6 \times \rho_{red} - 7.5 \times \rho_{blue})}$$

Basin-wide greening in dry season

October EVI (dry) minus June EVI (wet season) CMG

from Huete et al

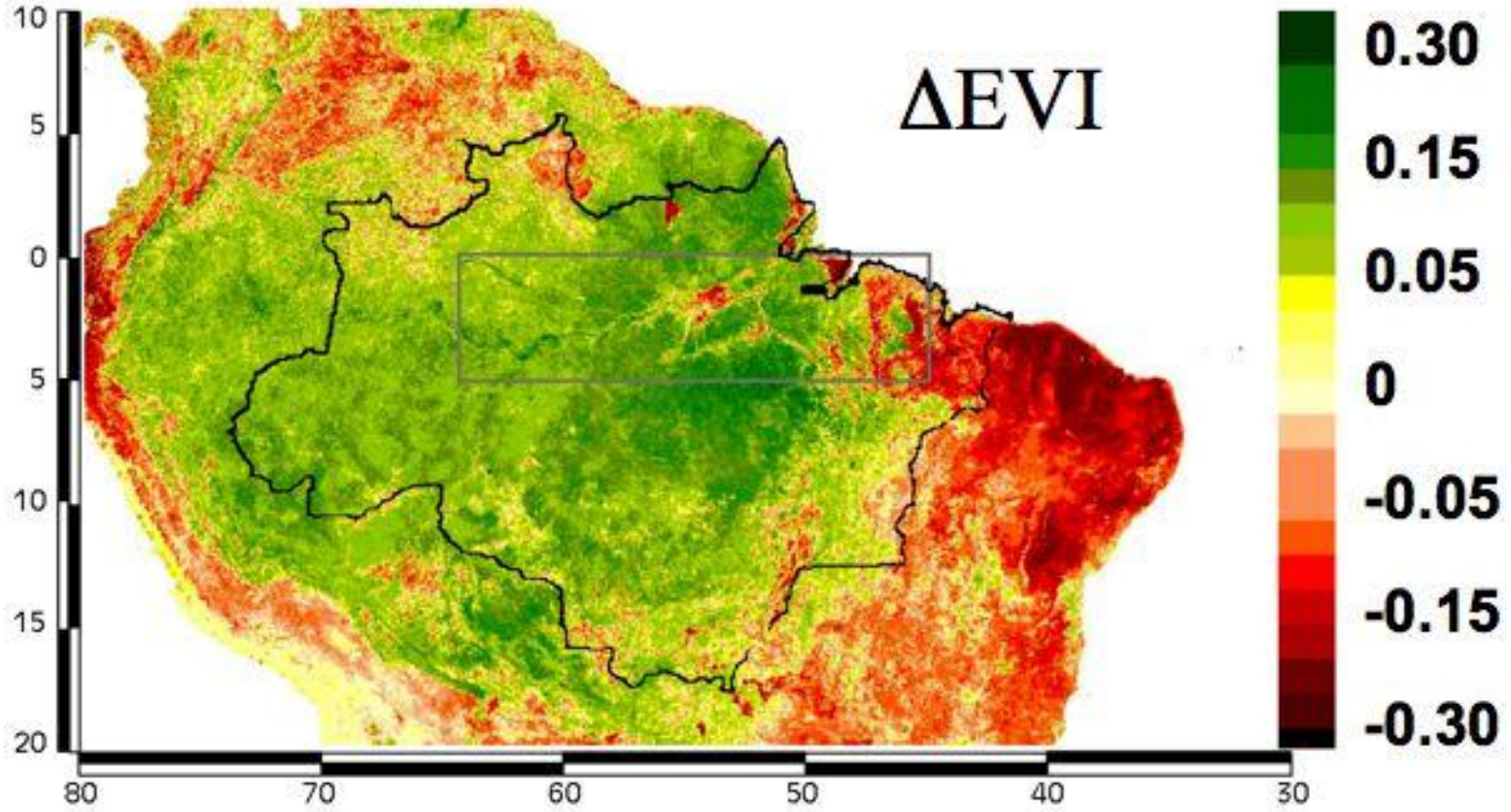

- green colors depict 'greening' and red colors depict 'browning' in the dry season

Vegetation Continuous Fields produced by year from MODIS at 250 m

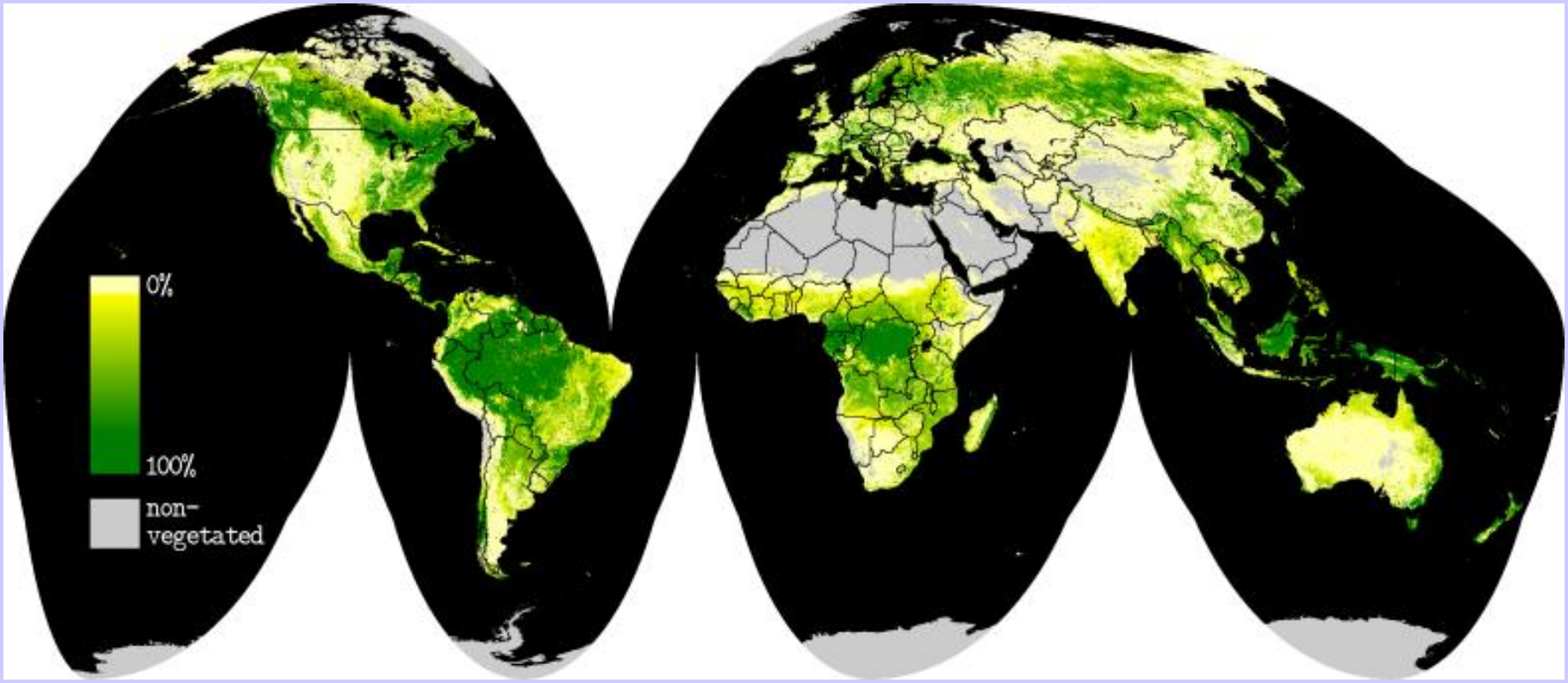

Vegetation Continuous Fields Percent tree cover from MODIS year 2001.

Slide from J. Townshend, UMd

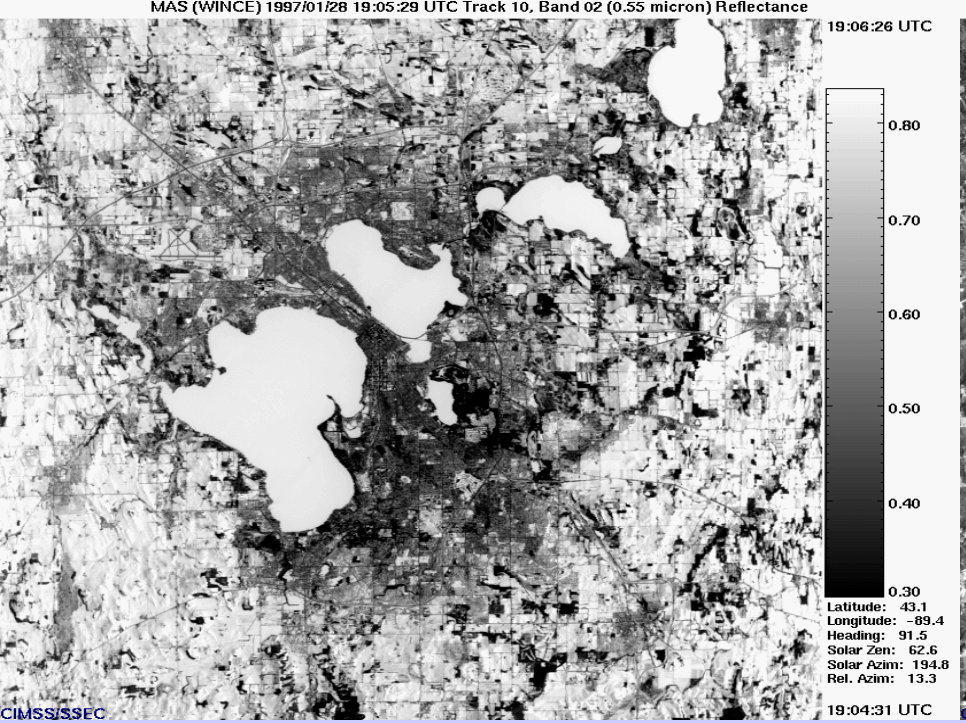

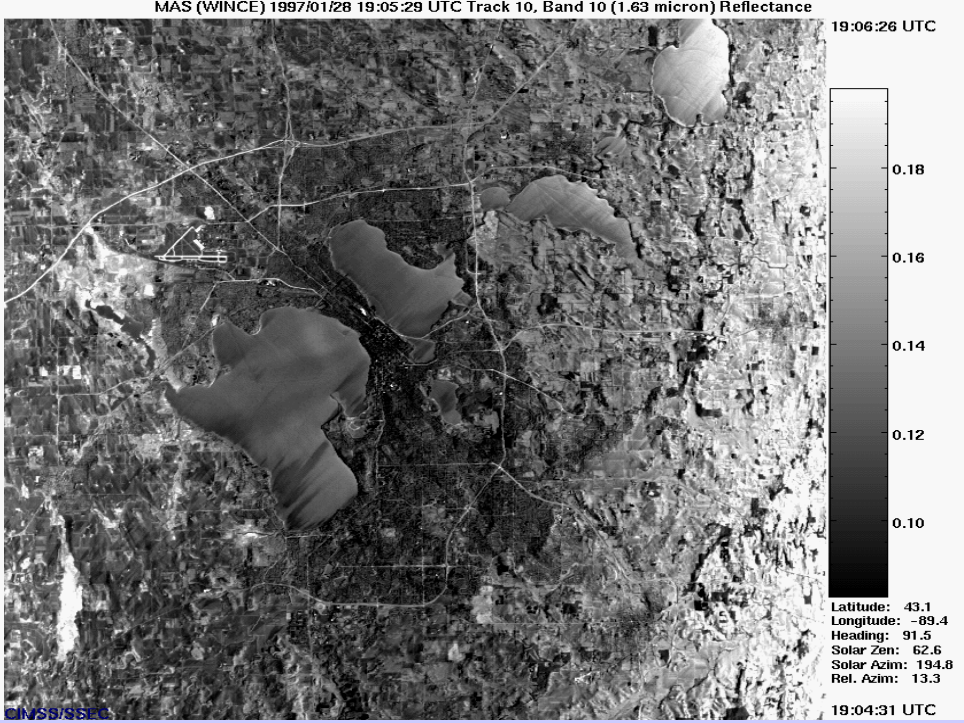

MODIS Airborne Simulator (MAS)
0.6, 1.6, & 11.0 um data over Madison in Jan 97

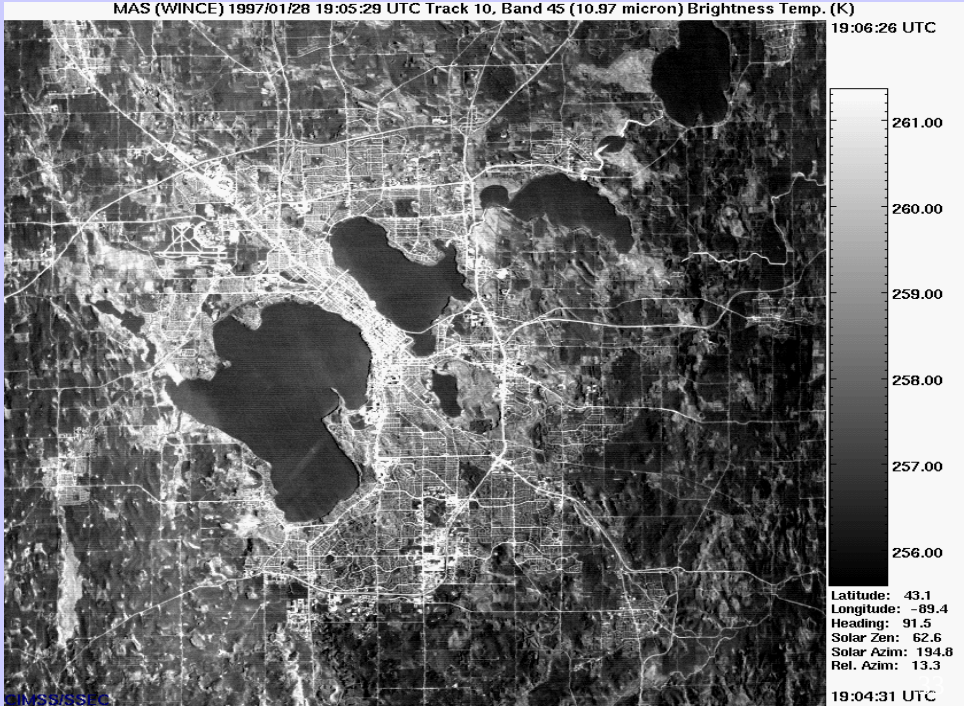

Example with MODIS

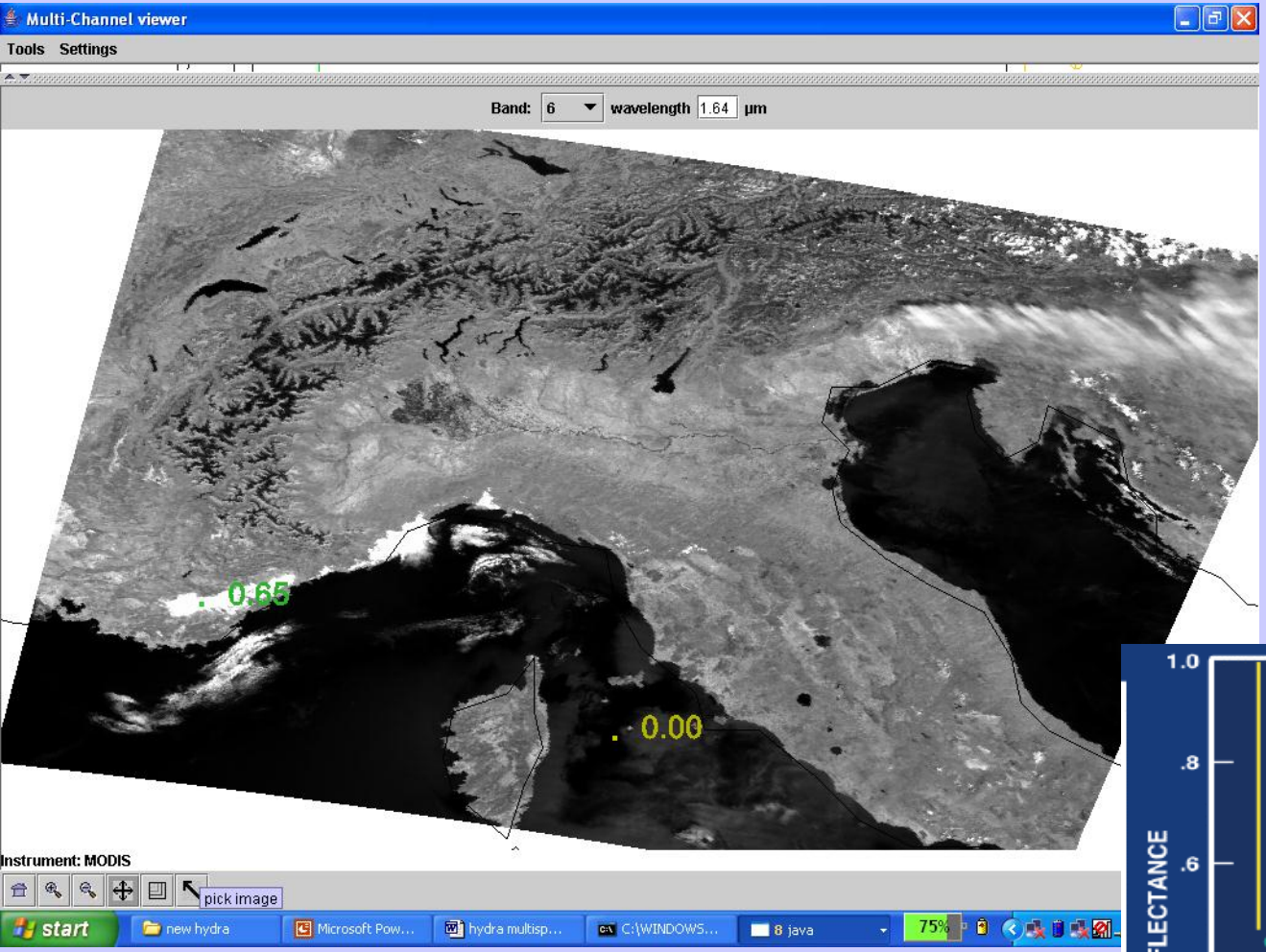

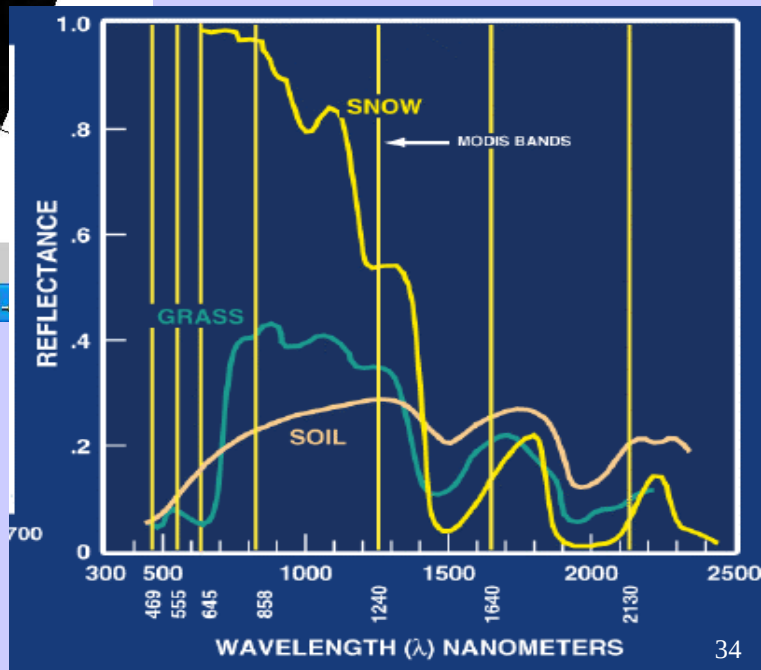

low refl at 1.6 um from snow in mountains

Applications with Multispectral Remote Sensing Data

Satellite Remote Sensing
Energy Balance
VIS, IR, and MW Radiative Transfer
EOS Terra & Aqua MODIS
Multispectral Signatures
(Ocean Color, SST, Snow/Ice, Vegetation, ***Aerosols****,*
Clouds, Moisture, Fires, Volcanic Ash)
Detecting Climate Trends

Aerosol Types and Origin

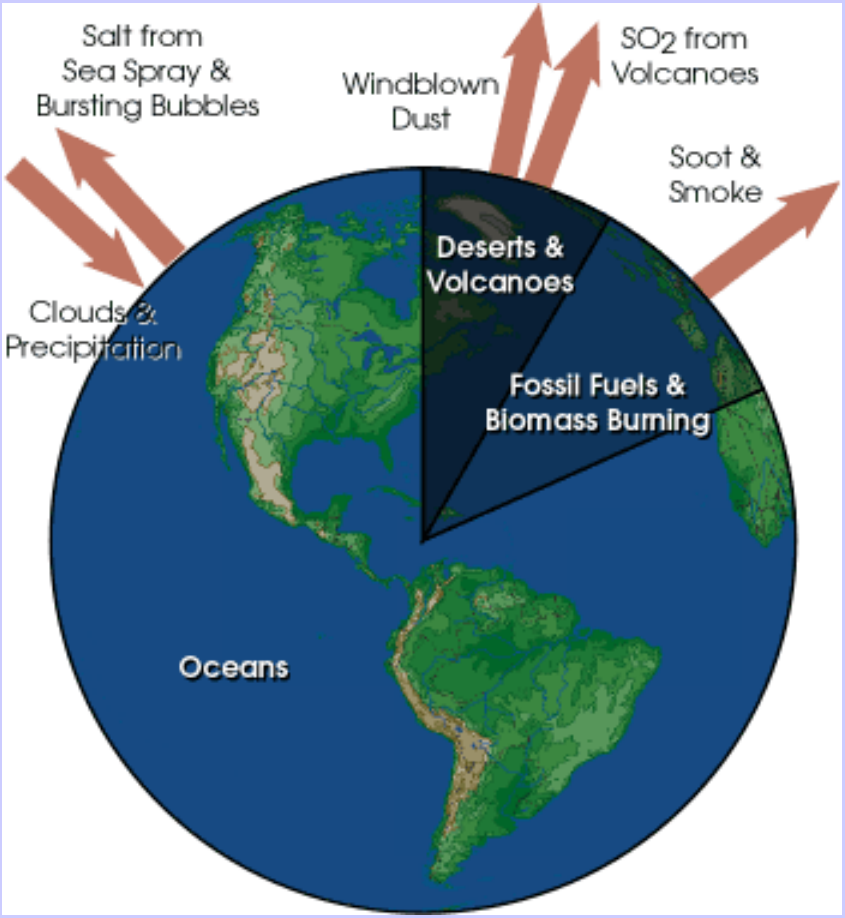

- Aerosol particles larger than about 1 μm in size are produced by windblown dust and sea salt from sea spray and bursting bubbles
- Aerosols smaller than 1 μm are mostly formed by condensation processes such as conversion of sulfur dioxide (SO2) gas (released from volcanic eruptions) to sulfate particles and by formation of soot and smoke during burning processes.
- After formation, aerosols are mixed and transported by atmospheric motions and are primarily removed by clouds and precipitation.

Aerosol Size Distribution

There are 3 modes :

- « **nucleation** »: radius is between 0.002 and 0.05 µm. They result from combustion processes, photo-chemical reactions, etc.

- « **accumulation** »: radius is between 0.05 µm and 0.5 µm. Coagulation processes.

- « **coarse** »: larger than 1 µm. From mechanical processes like aeolian erosion.

« fine » particles (nucleation and accumulation) result from anthropogenic activities, coarse particles come from natural processes.

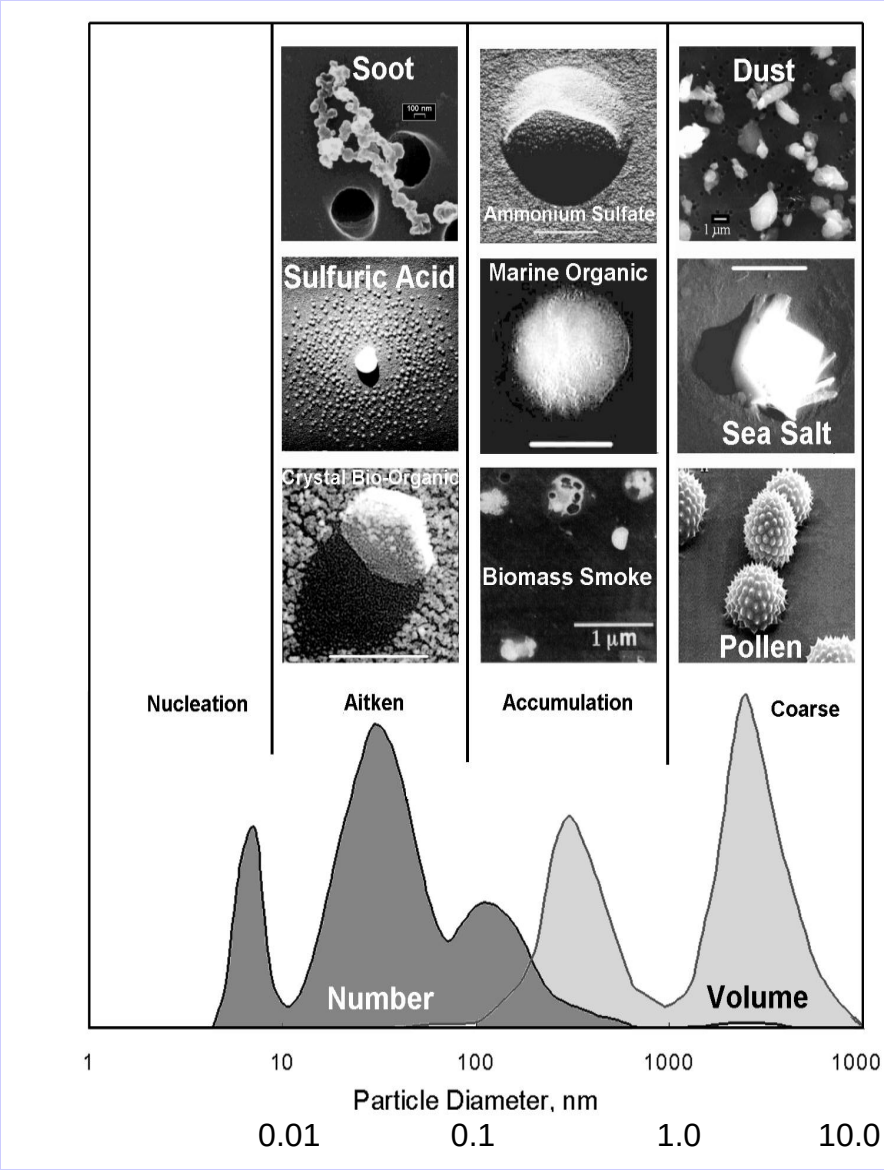

Physical Properties

These Aerosols have the largest impacts on radiative budget, visibility, cloud processes and health issues

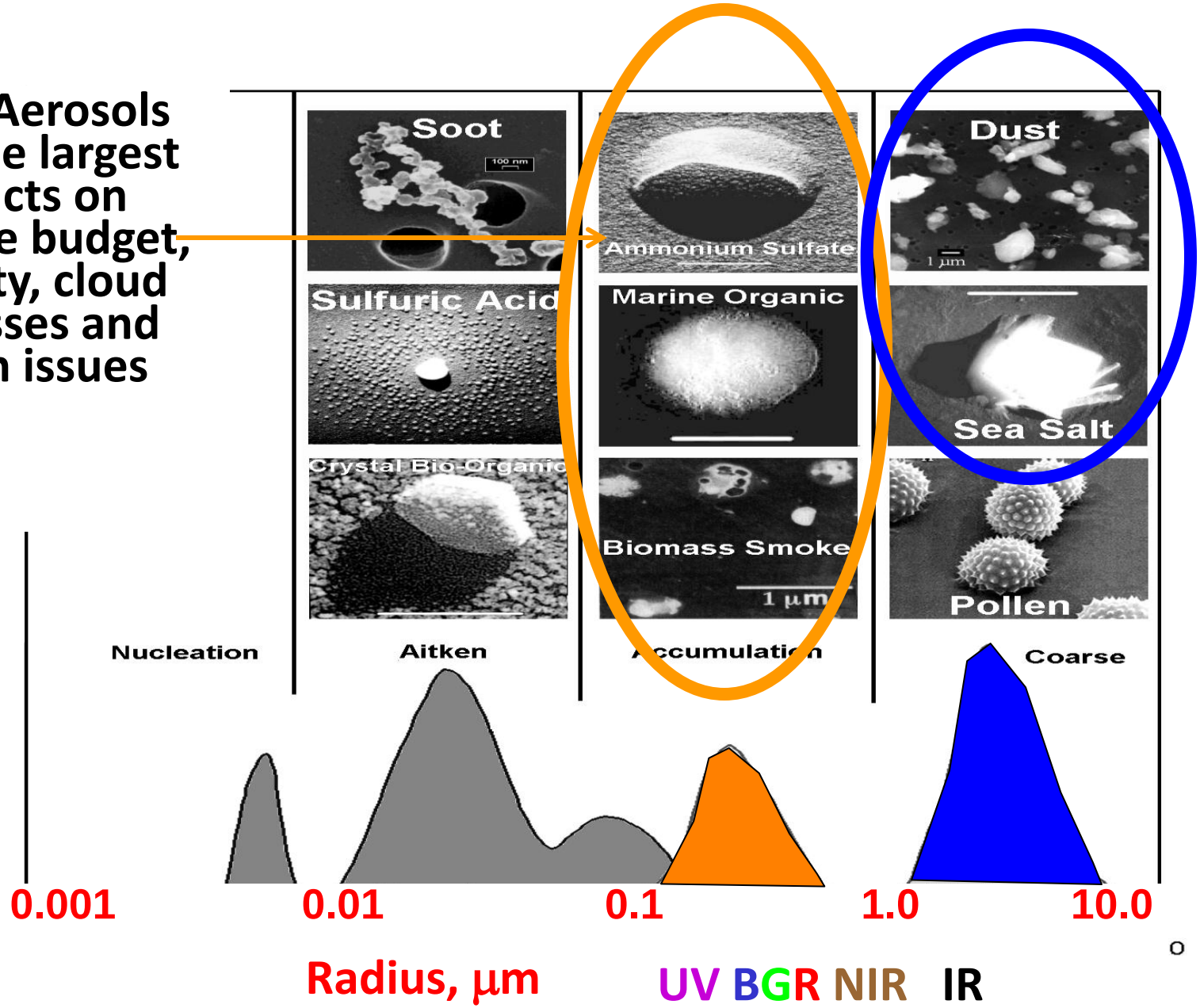

Aerosols over Ocean

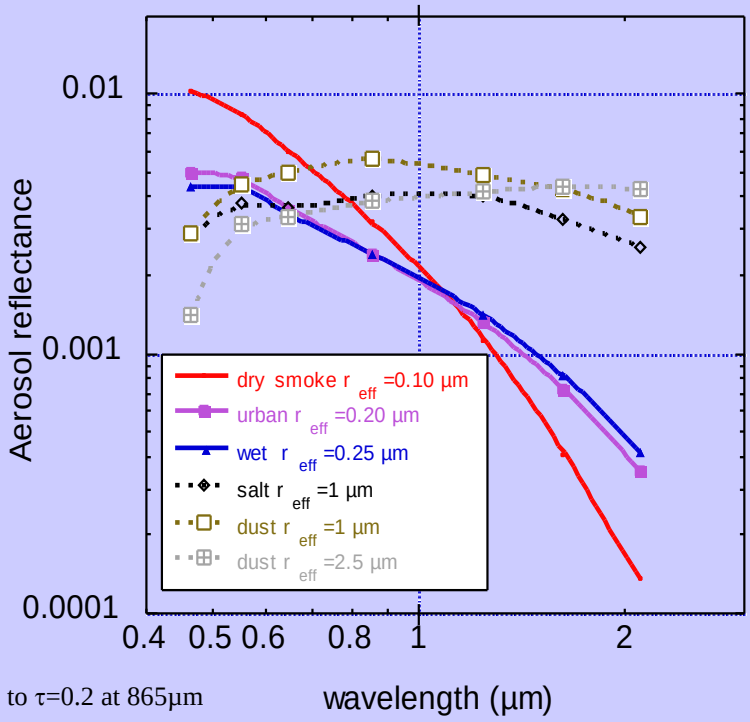

Normalized to τ=0.2 at 865μm

- Radiance data in 6 bands (550-2130nm).
- Spectral radiances (LUT) to derive the aerosol size distribution
- Two modes (accumulation 0.10-0.25μm; coarse1.0-2.5μm); ratio is a free parameter
- Radiance at 865μm to derive τ

Ocean products :

- The total Spectral Optical thickness
- The effective radius
- The optical thickness of small & large modes/ratio between the 2 modes

Spectral optical properties of aerosol

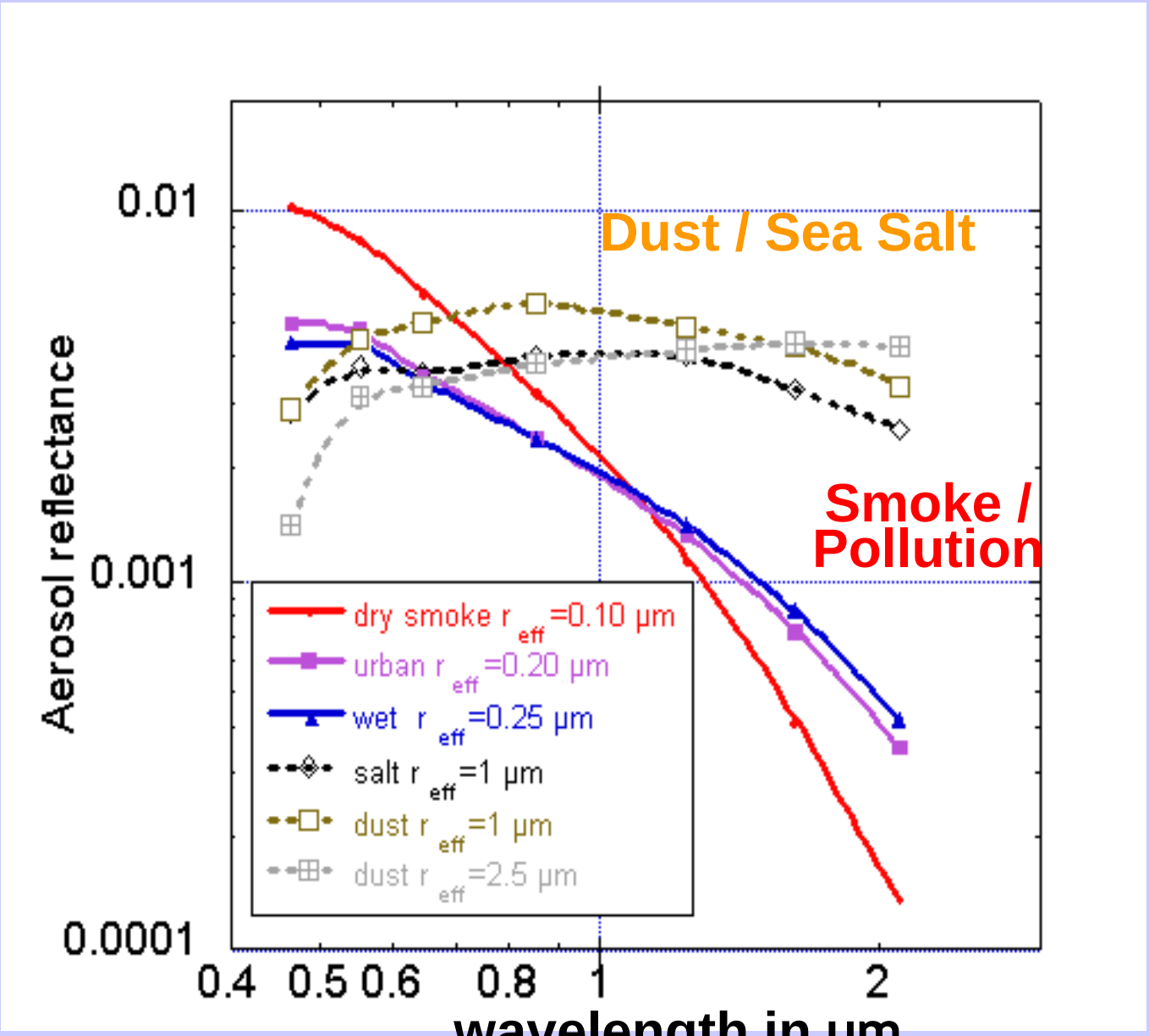

Global aerosol AOT trends

Remer et al 2005

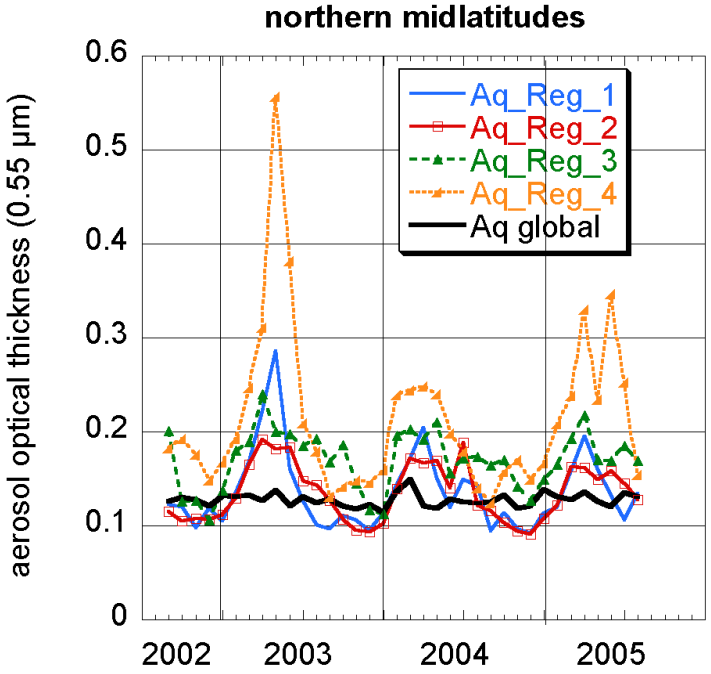

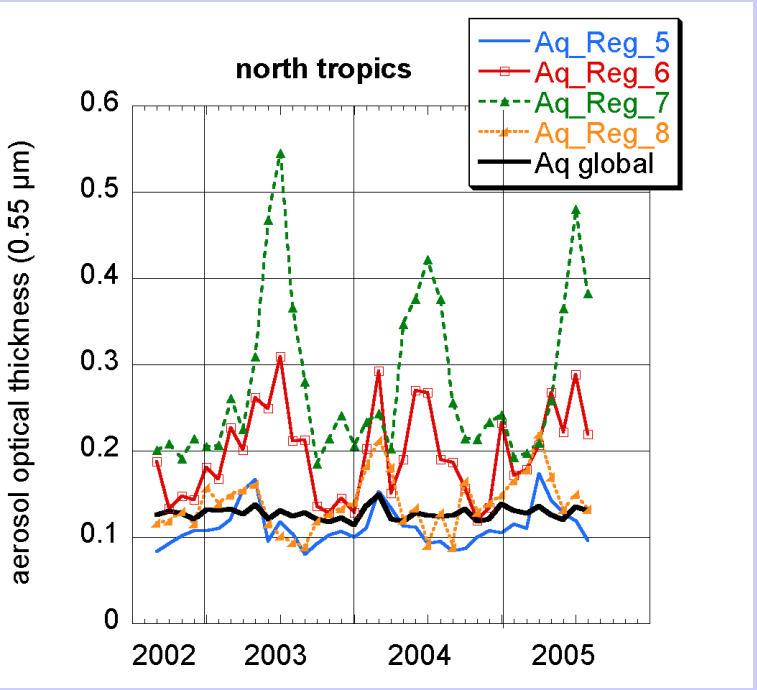

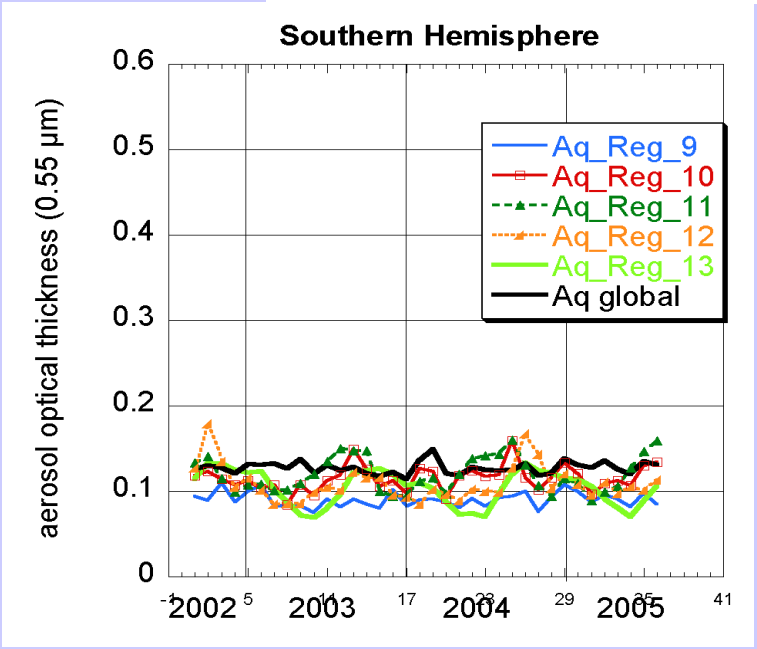

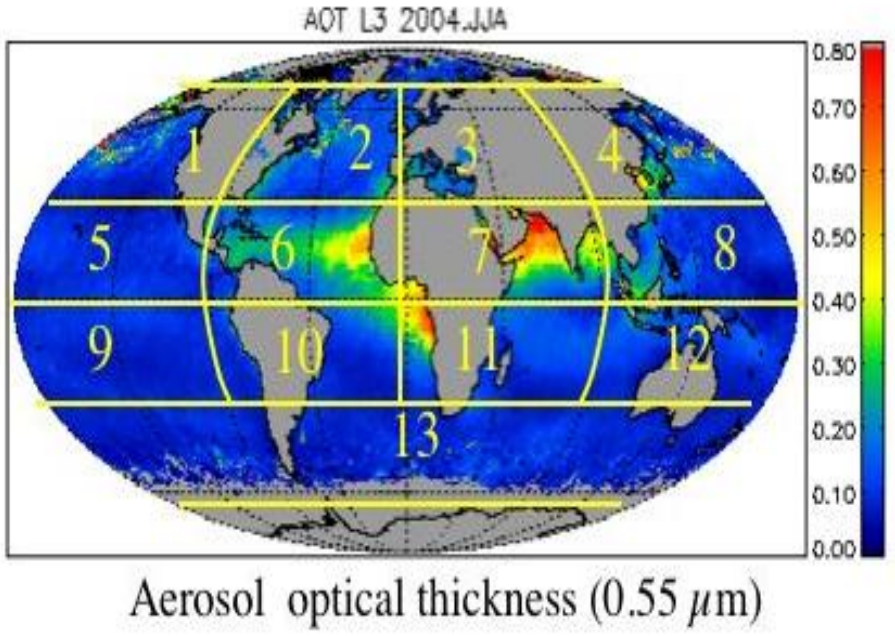

Aerosol effects on cloud cover

over the Atlantic Ocean - several aerosol types interact with clouds June-Aug 2002

Pollution zone

Dust zone

Smoke zone

Marine aerosol

aerosol forcing increased cloud cover 5% (~ 6 W/m2) and height 40 hPa (~ 400 m) over Atlantic Ocean

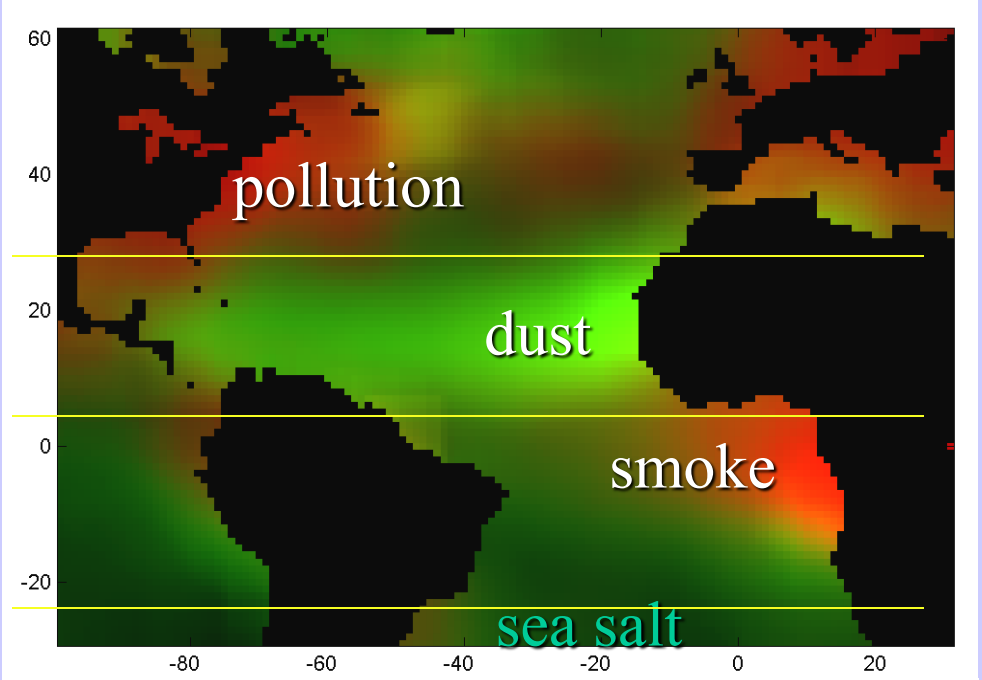

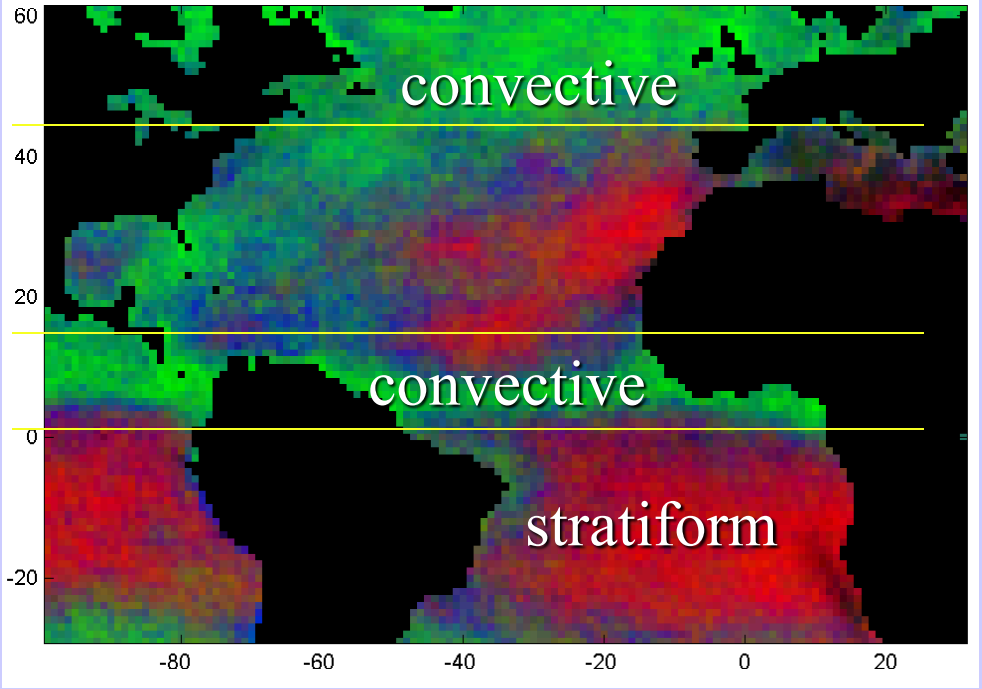

clean

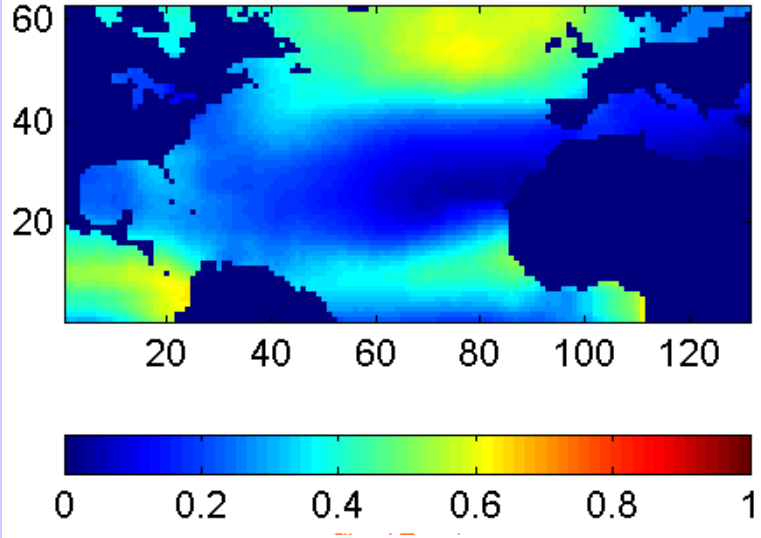

Cloud fraction

hazy

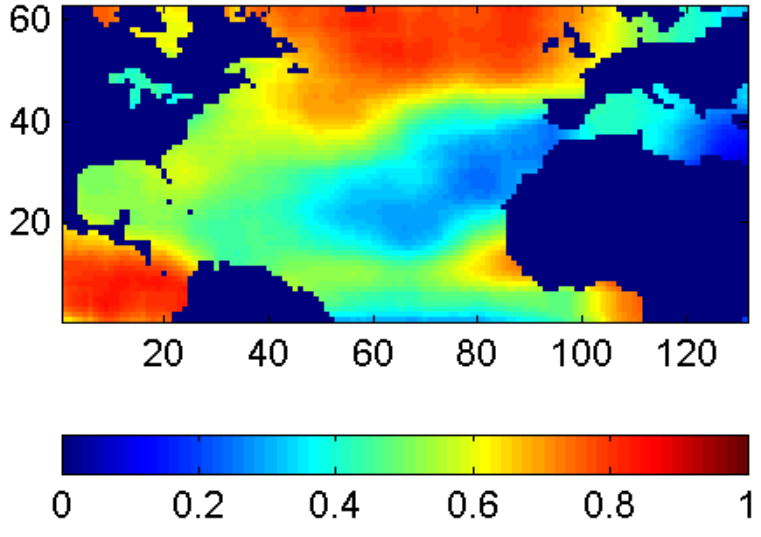

Cloud fraction

clean

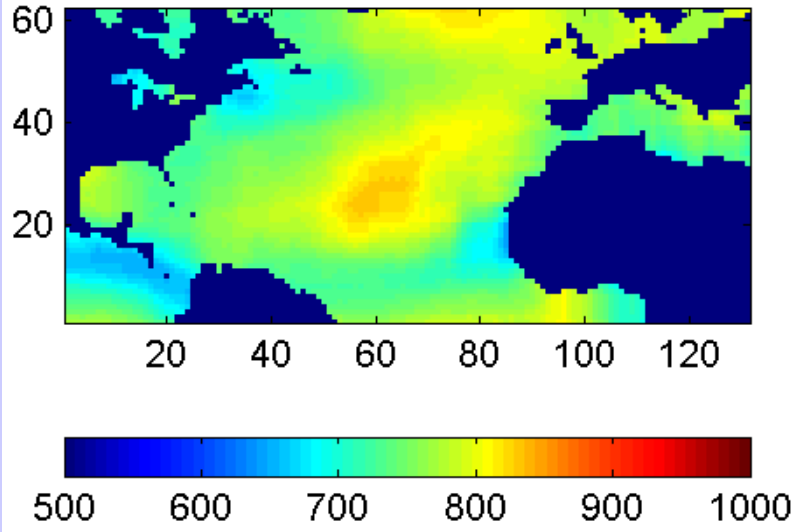

Cloud top pressure

hazy

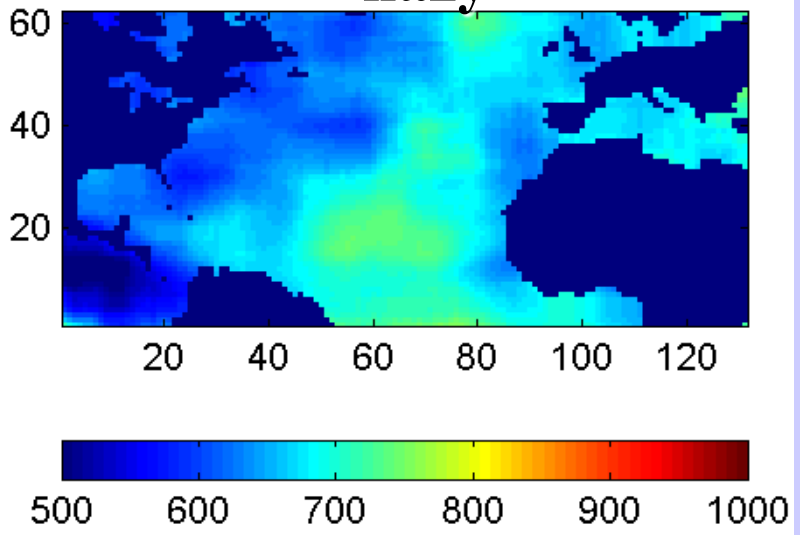

Cloud top pressure

Applications with Multispectral Remote Sensing Data

Satellite Remote Sensing

Energy Balance

VIS, IR, and MW Radiative Transfer

EOS Terra & Aqua MODIS

Multispectral Signatures

(Ocean Color, SST, Snow/Ice, Vegetation, Aerosols,

***Clouds**, Moisture, Fires, Volcanic Ash)*

Detecting Climate Trends

ATMOSPHERE-SOLAR RADIATION

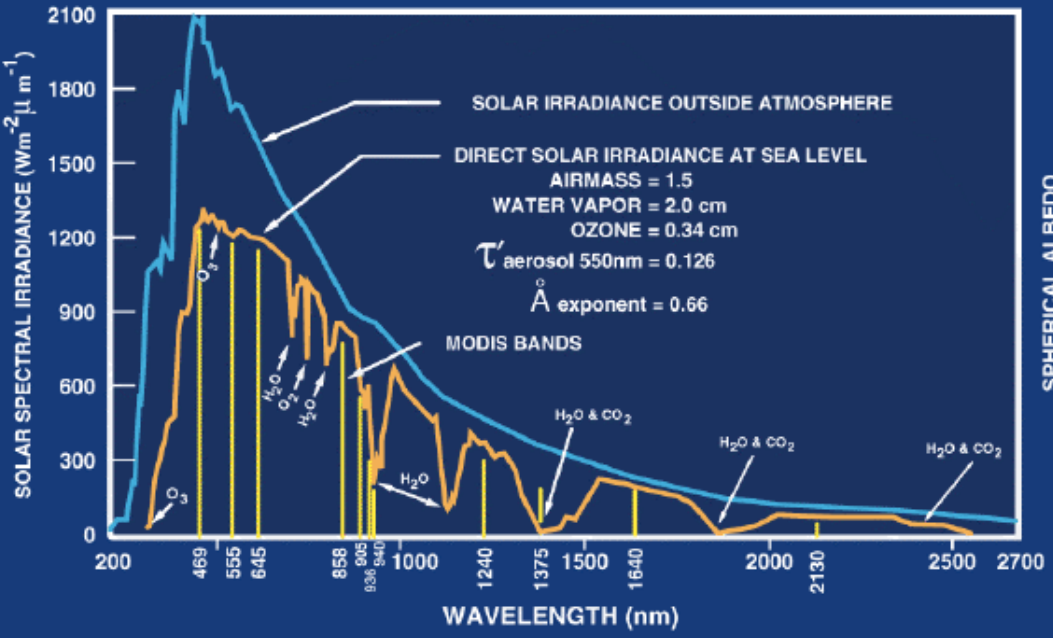

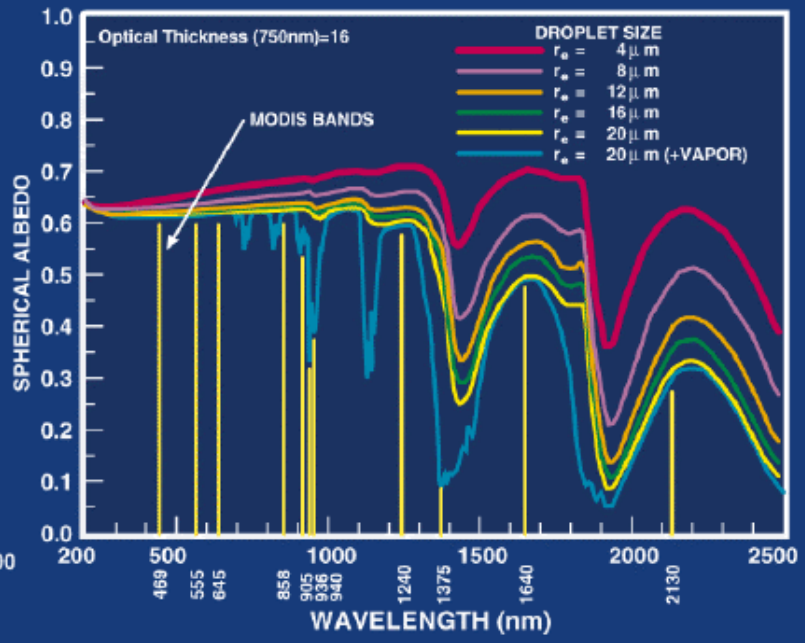

C351.008 5/93

ATMOSPHERE - THERMAL RADIATION

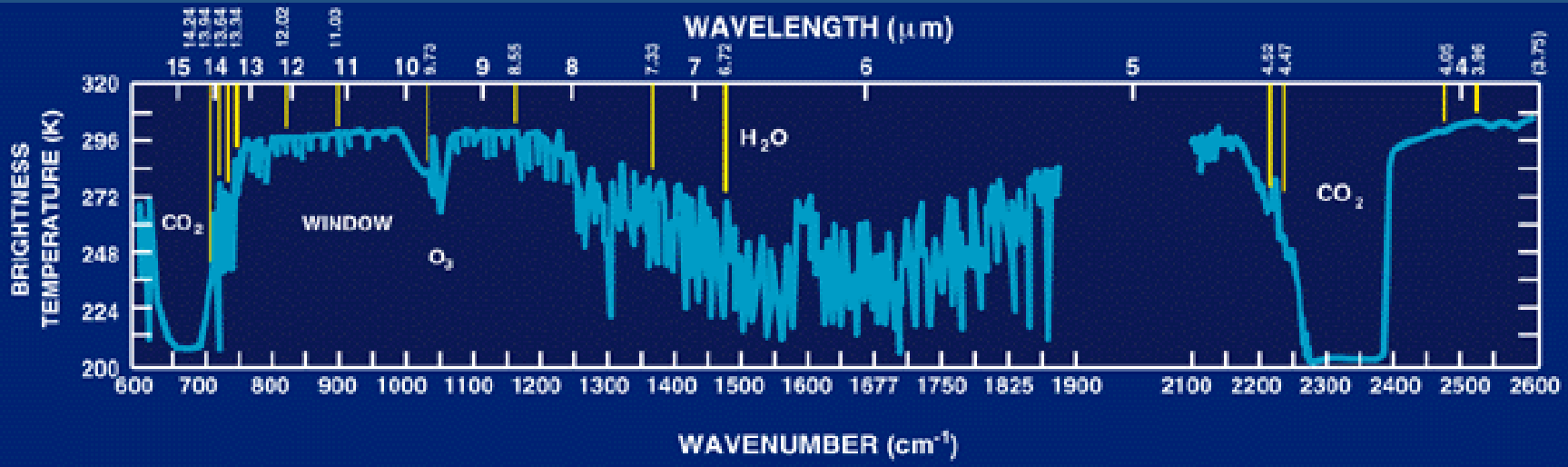

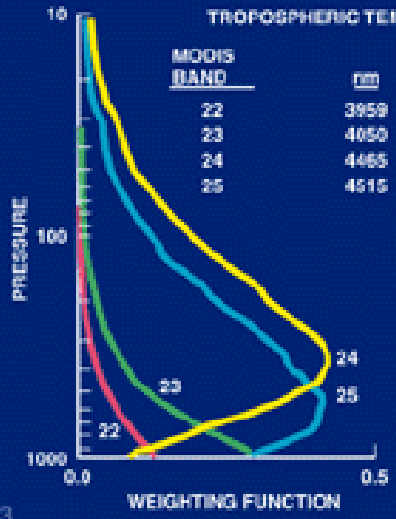

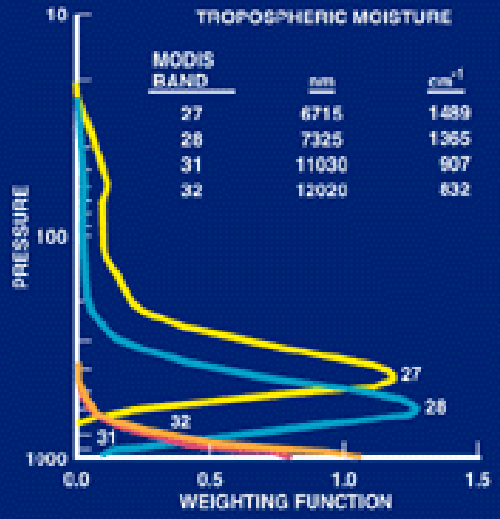

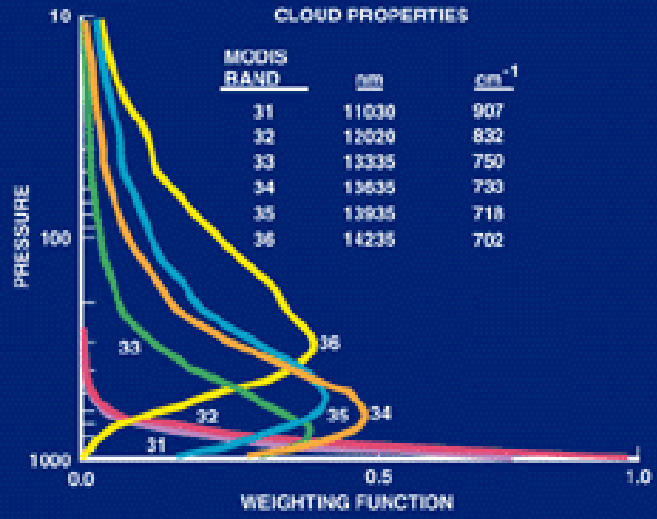

E351.002 5/93

ATMOSPHERE - CLEAR SKY THERMAL EMISSION

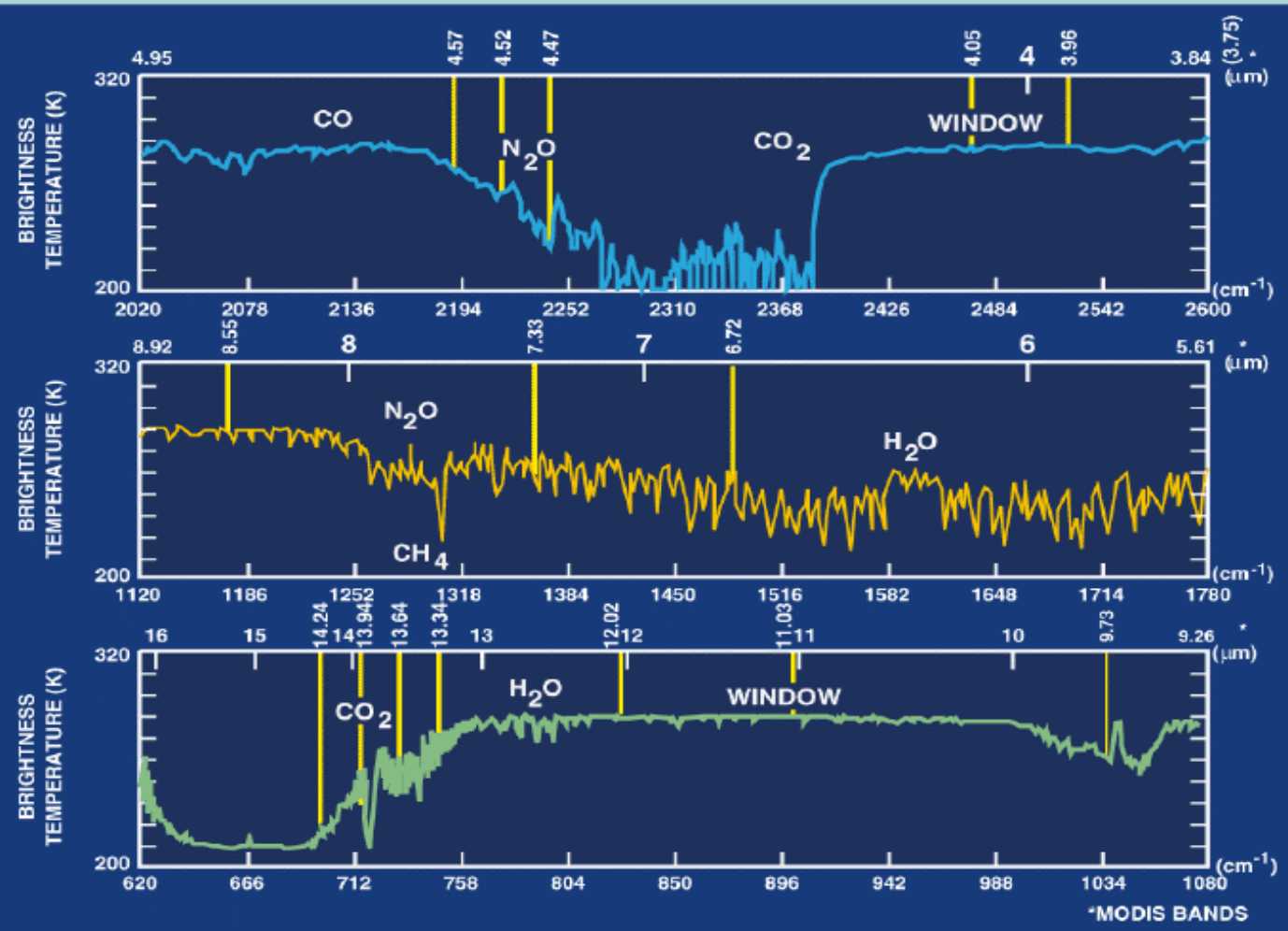

002 11/92

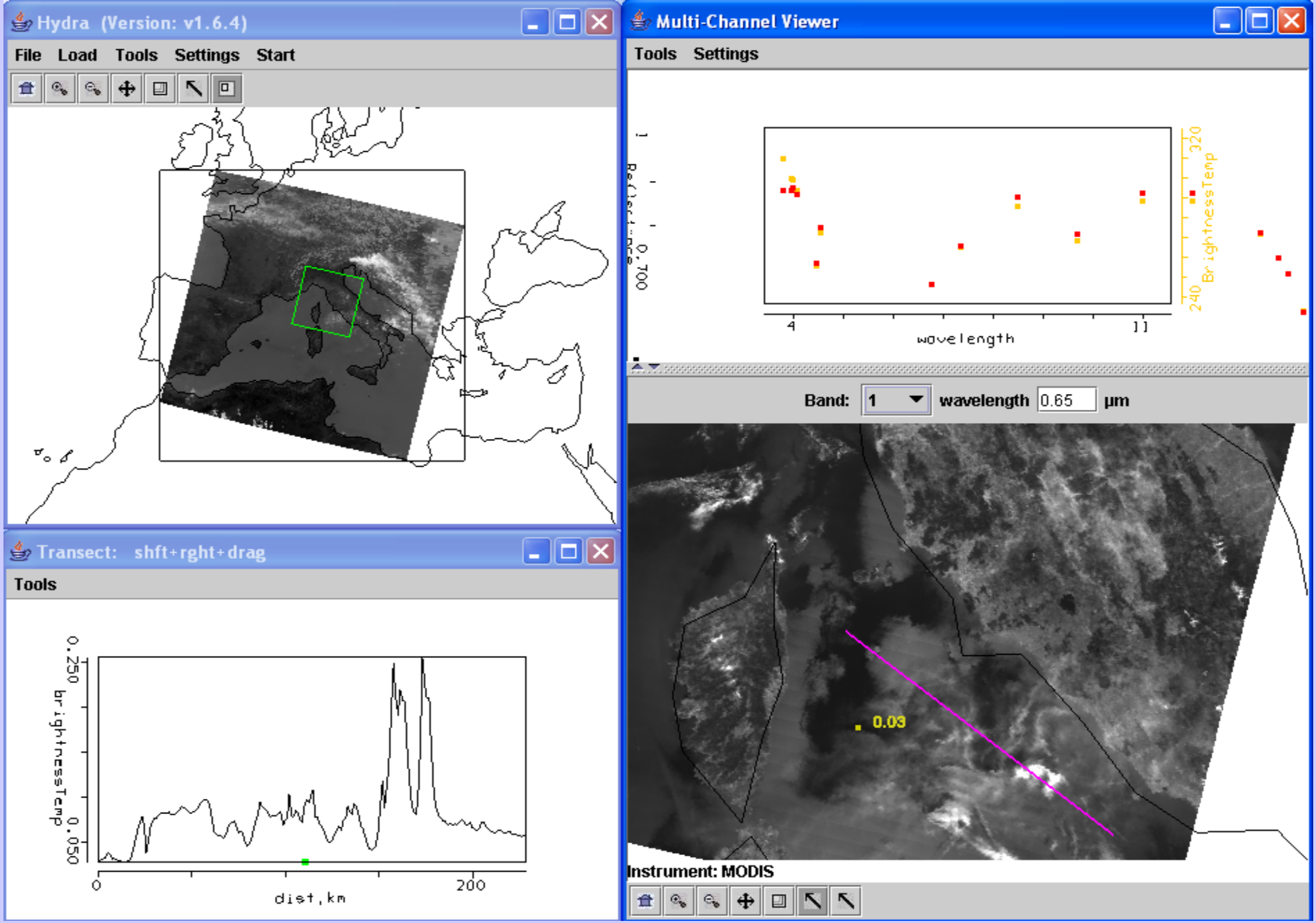

High clouds reflect more than surface at 0.65 µm

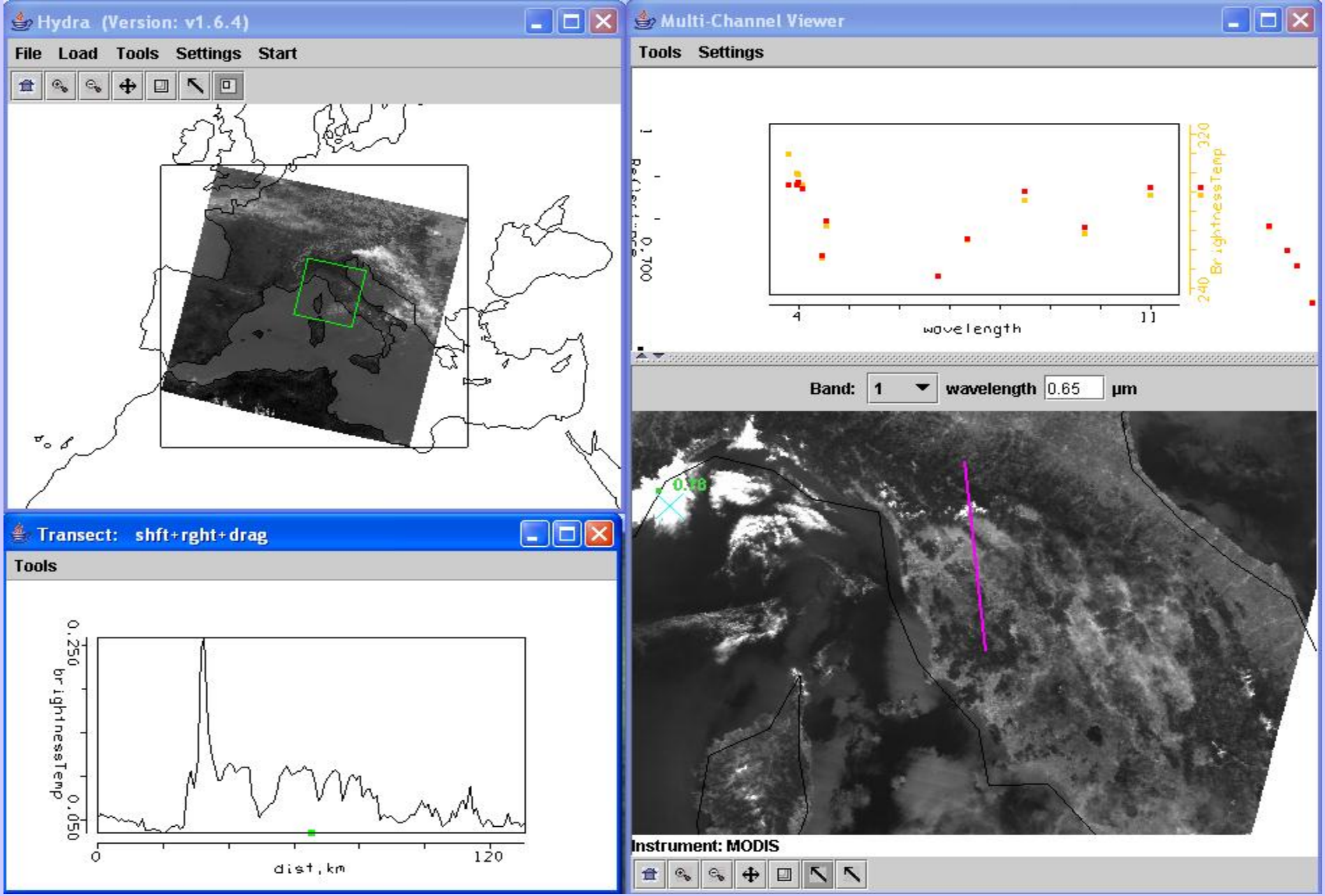

High clouds reflect more than surface at 0.65 µm, even over vegetation

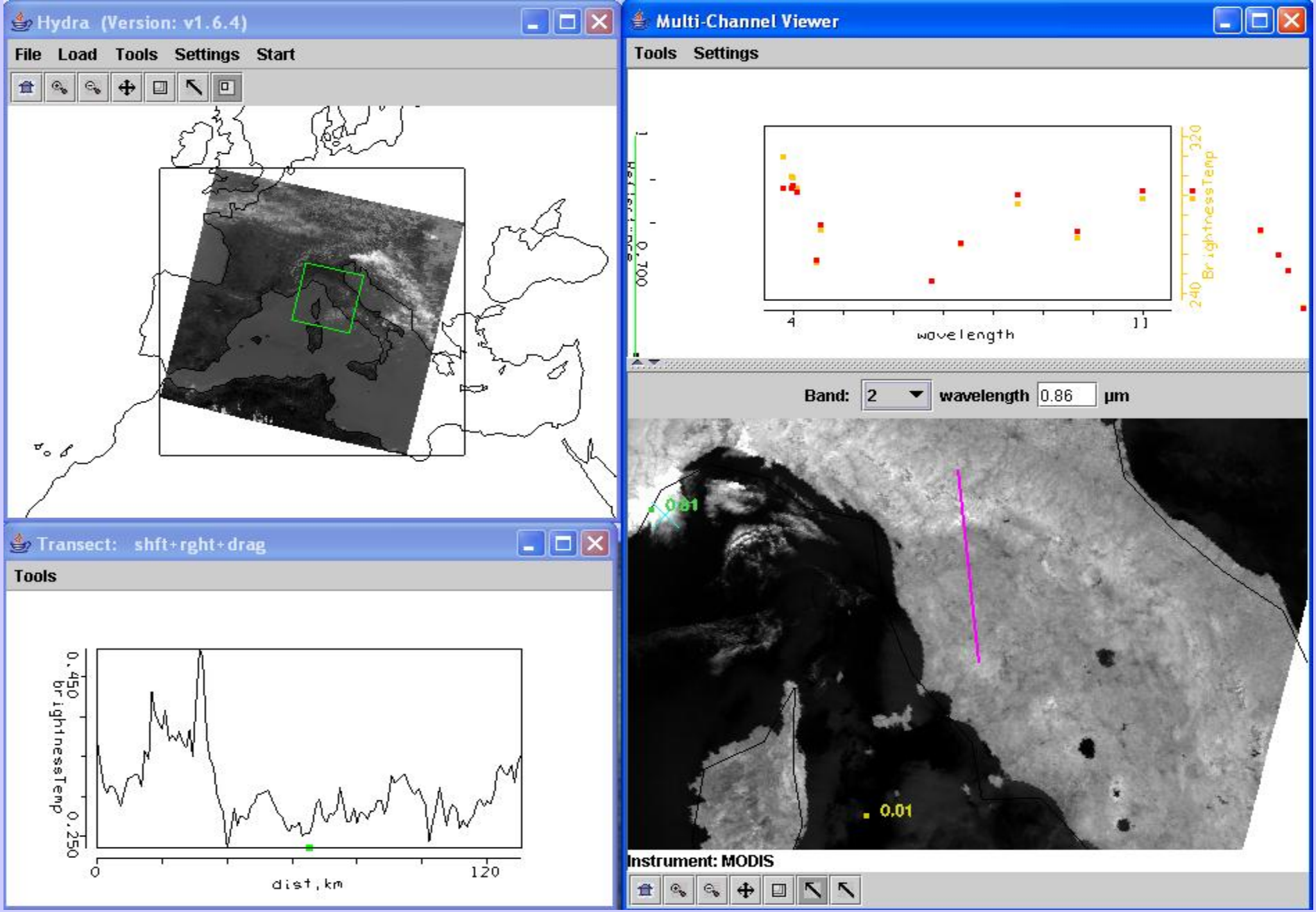

High clouds are more difficult to detect at 0.86 µm over vegetation

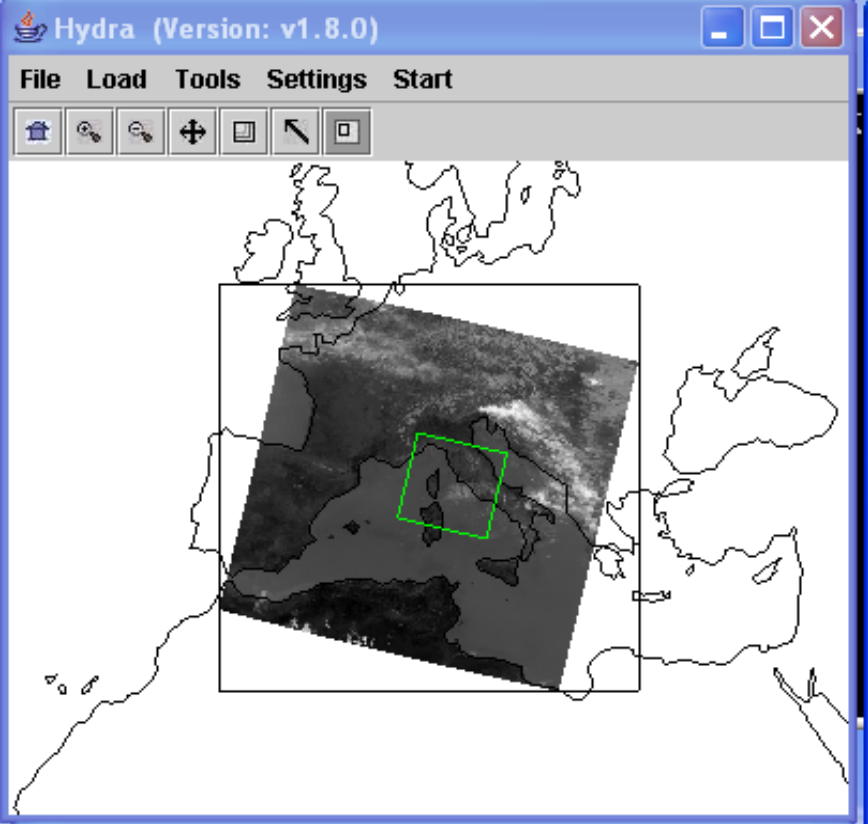
Hydra (Version: v1.8.0)
File Load Tools Settings Start

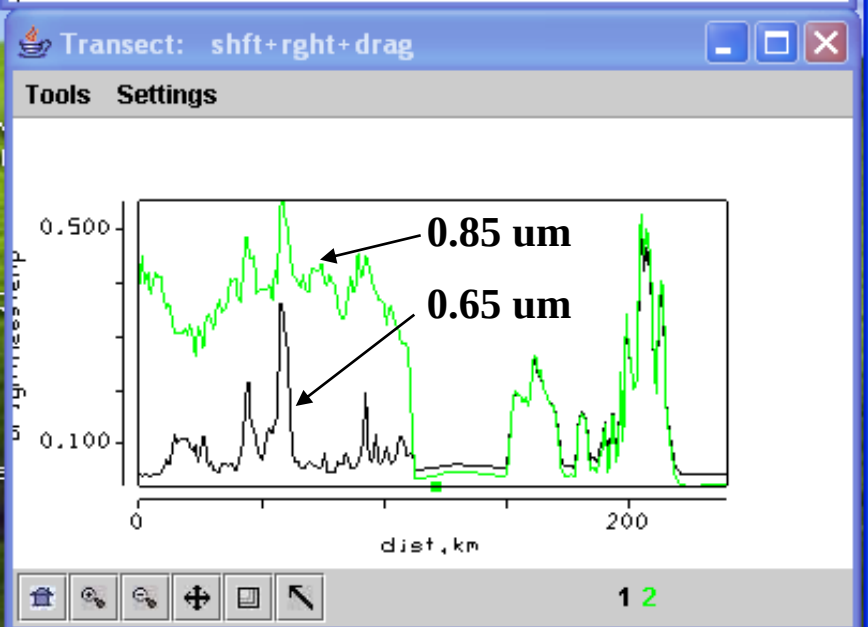
Transect: shft+rght+drag
Tools Settings
0.500
0.100
0.85 um
0.65 um
0
200
dist,km
1 2

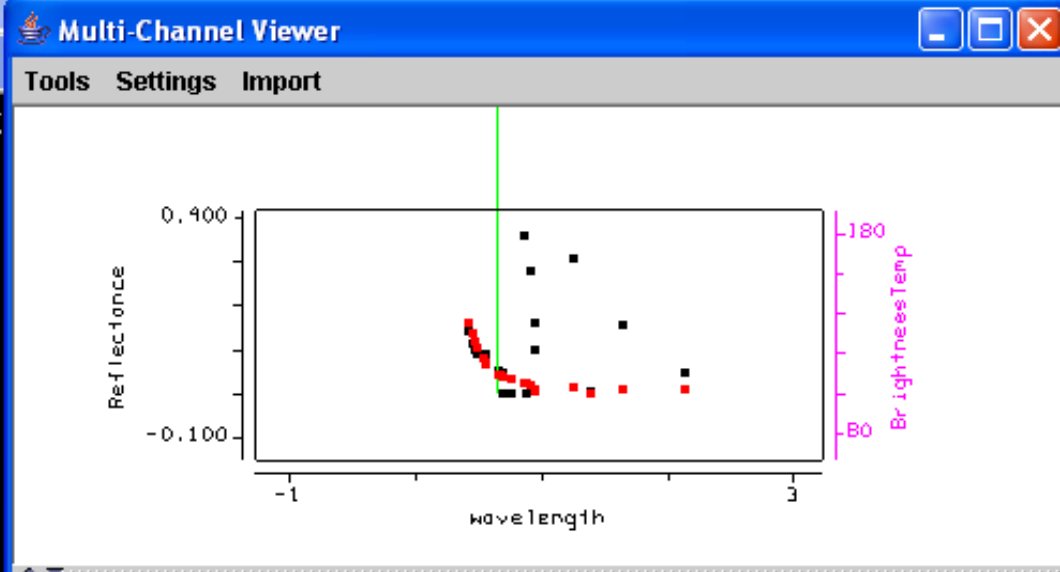
Multi-Channel Viewer
Tools Settings Import
0.400
-0.100
Reflectance
-1
3
wavelength
180
80
BrightneesTemp

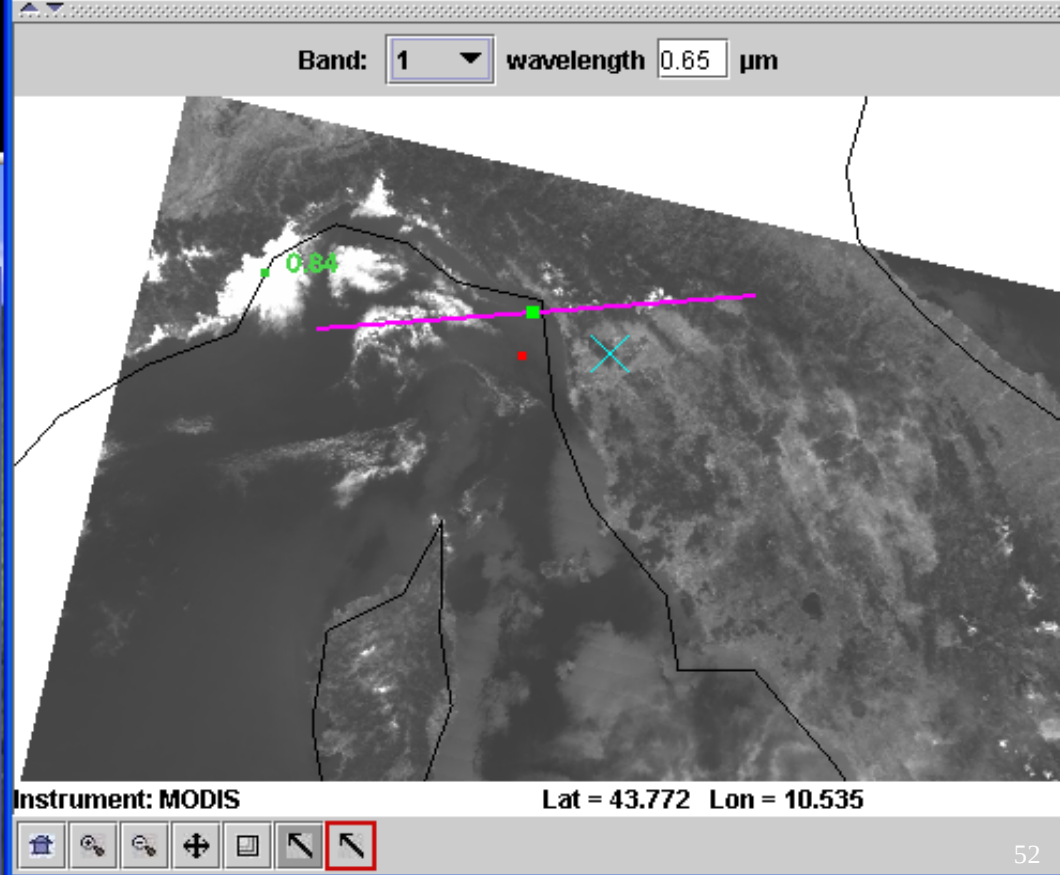
Band: 1 wavelength 0.65 µm
0.84
Instrument: MODIS
Lat = 43.772 Lon = 10.535

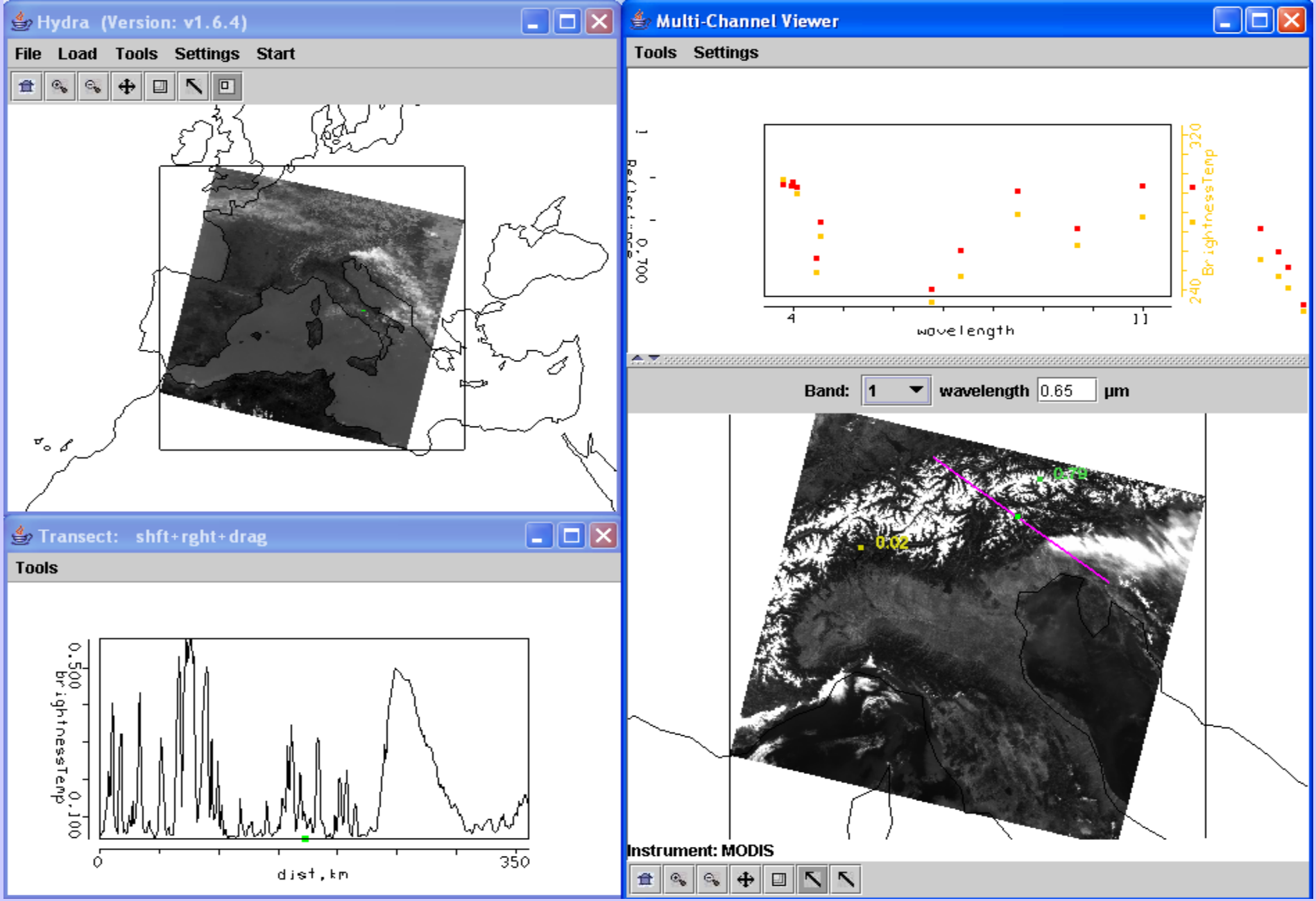

High clouds and snow both reflect a lot at 0.65 µm

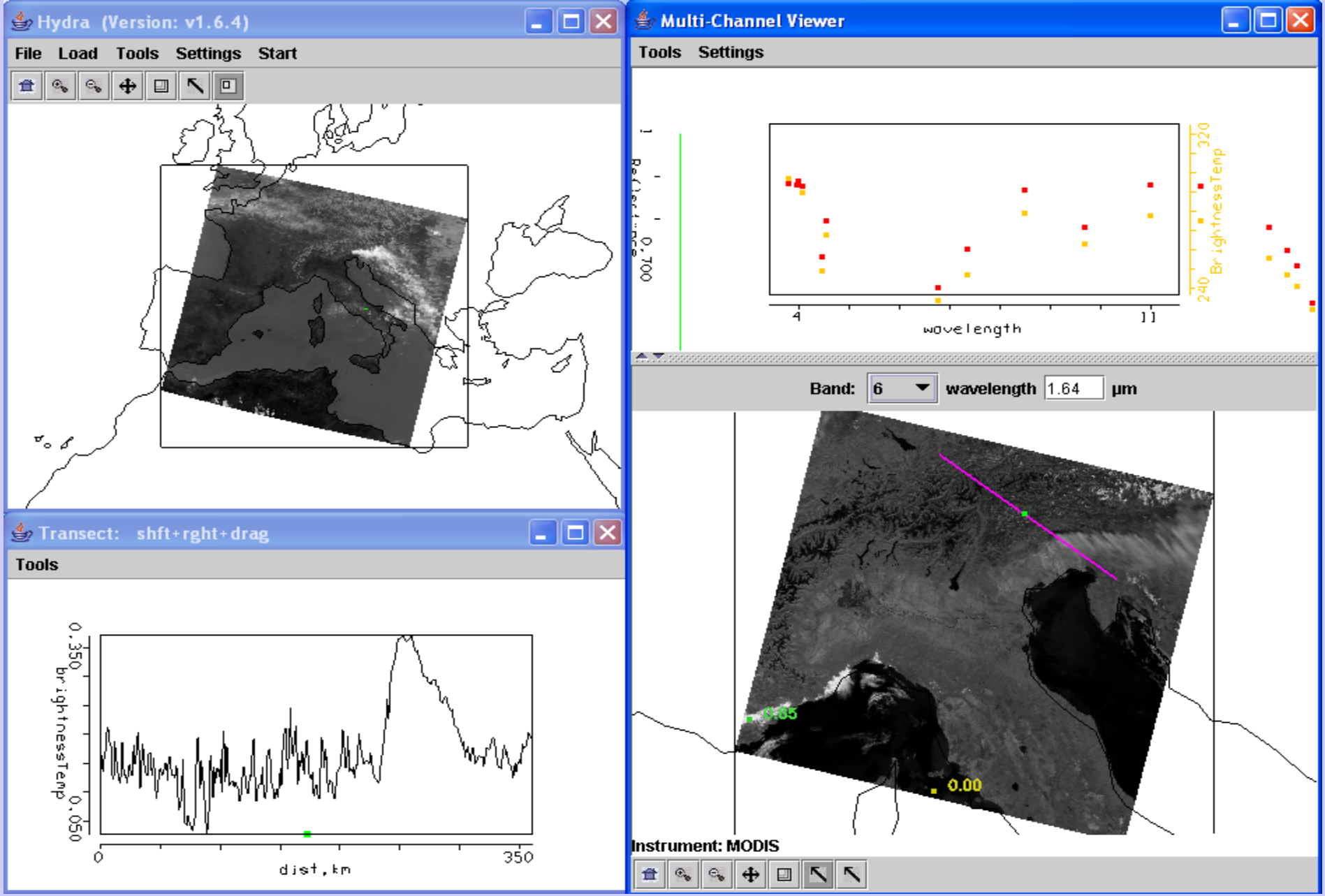

High clouds reflect but snow doesn't at 1.64 µm

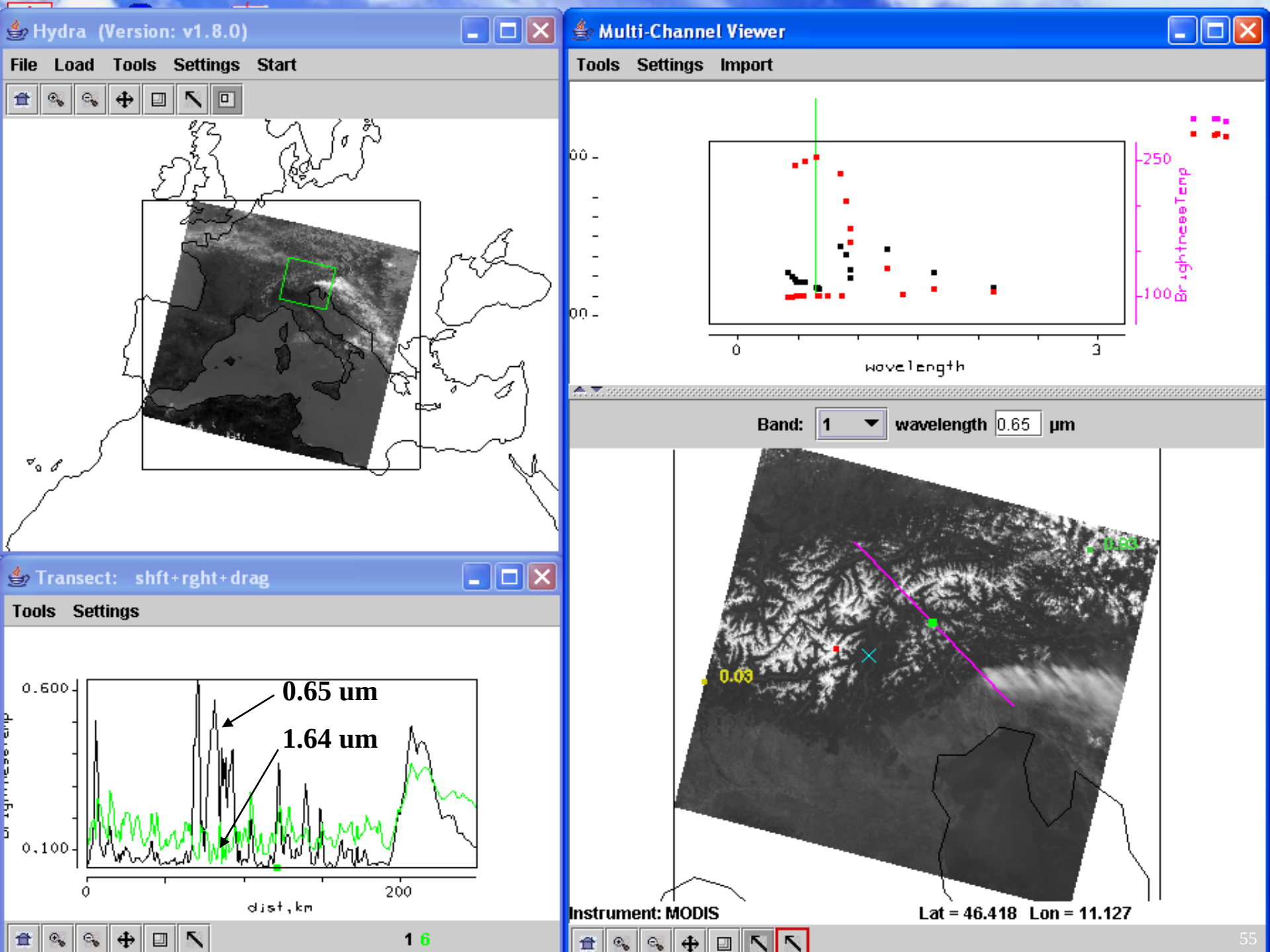
Hydra (Version: v1.8.0)
File Load Tools Settings Start
Multi-Channel Viewer
Tools Settings Import
250
100
BrightneseTemp
wavelength
Band: 1 wavelength 0.65 µm
Transect: shft+rght+drag
Tools Settings
0.600
0.100
0.65 um
1.64 um
0
200
dist,km
0.03
Instrument: MODIS
Lat = 46.418 Lon = 11.127
1 6

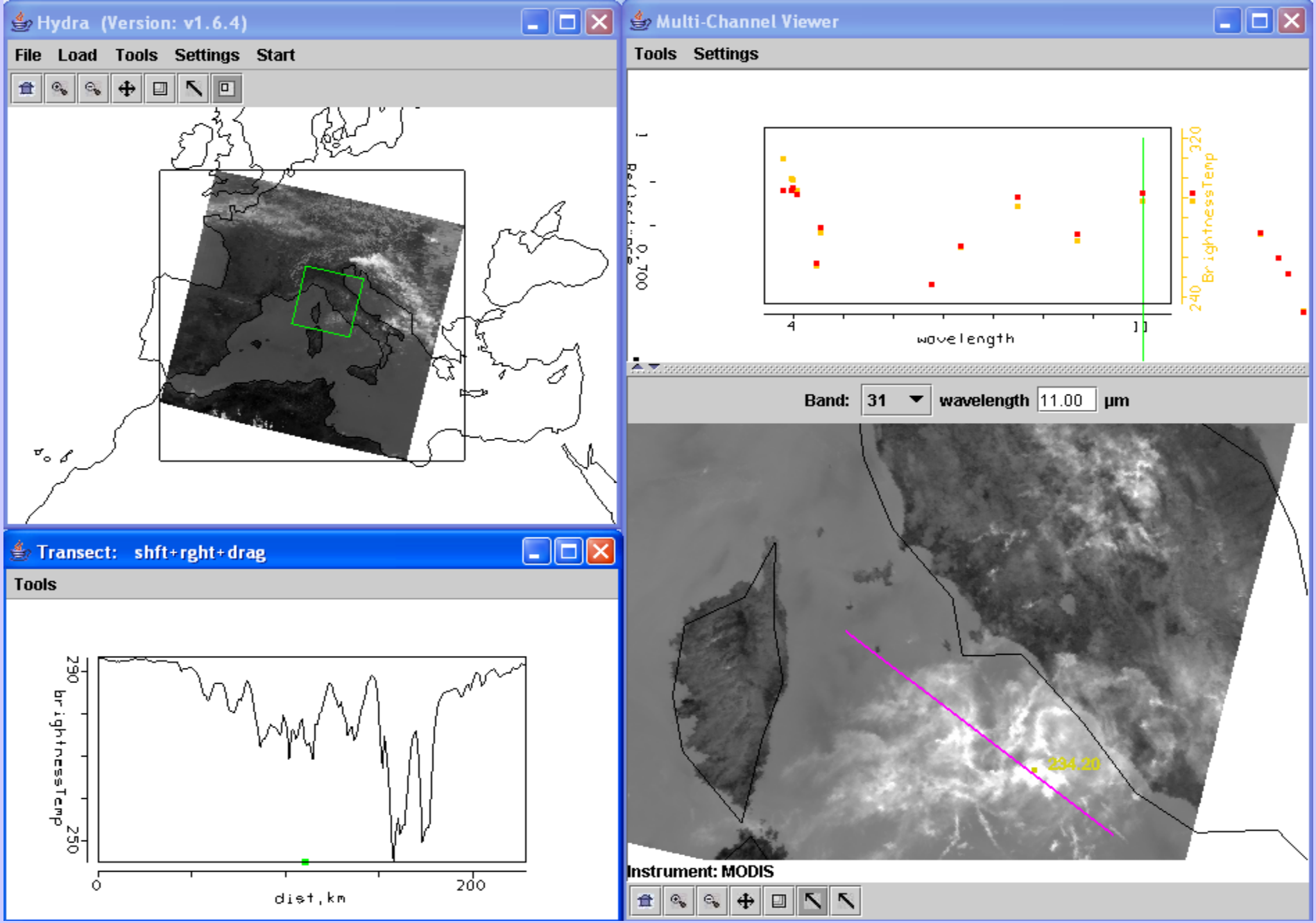

High clouds, cooler than surface, create lower 11 µm BTs

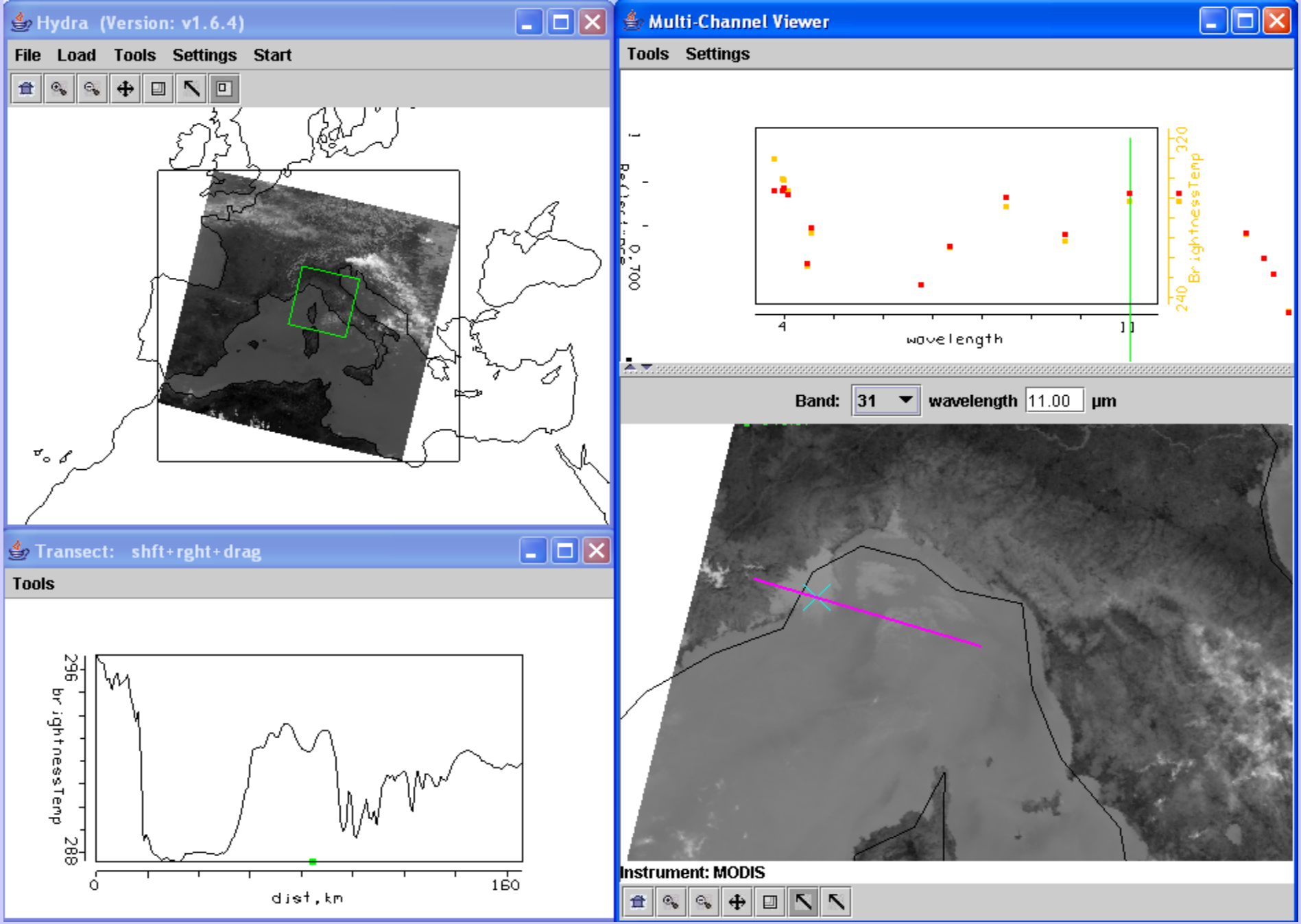

Low clouds, cooler than surface, create lower 11 µm BTs

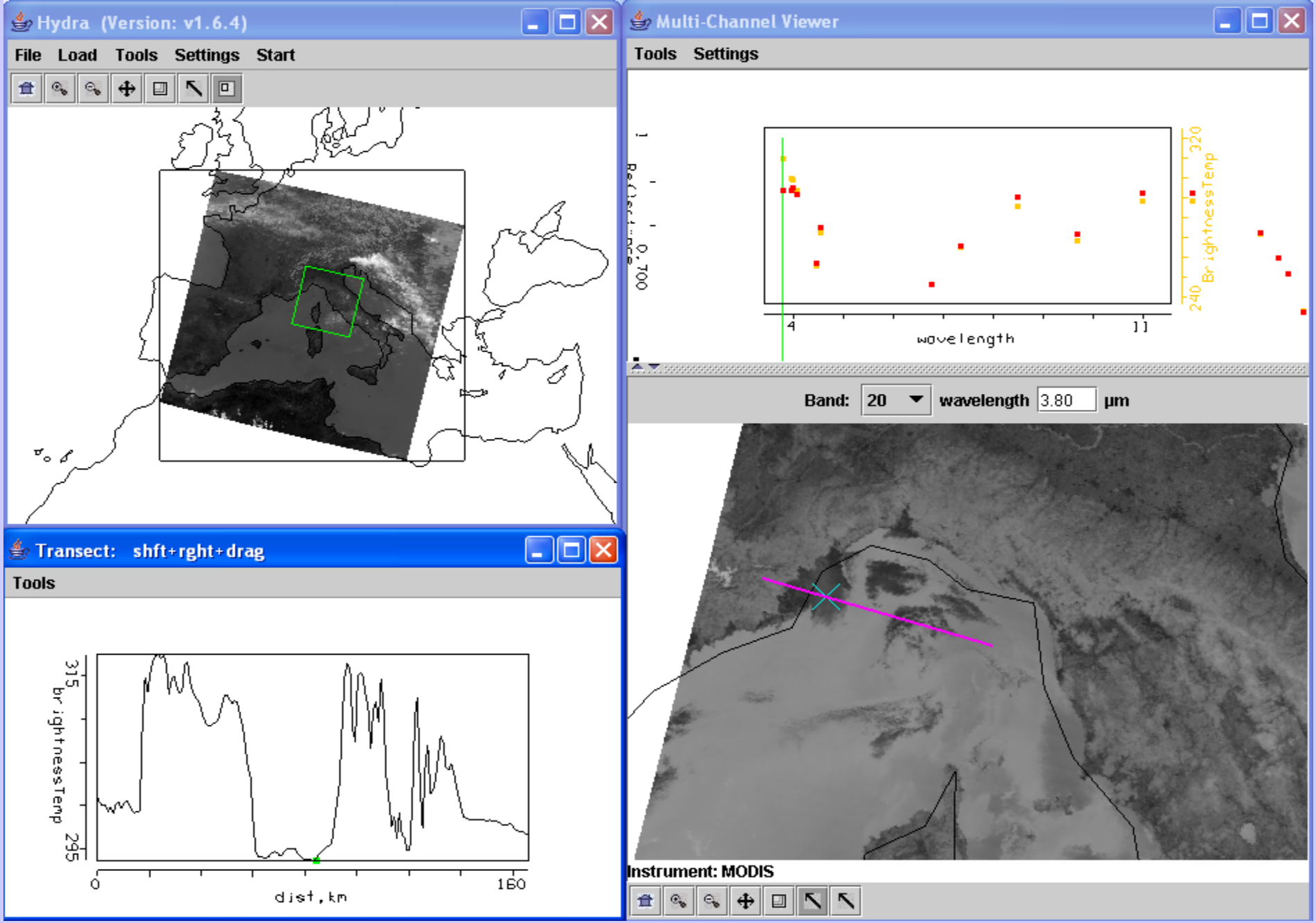

Low clouds reflecting create larger 4 µm brightness temperatures

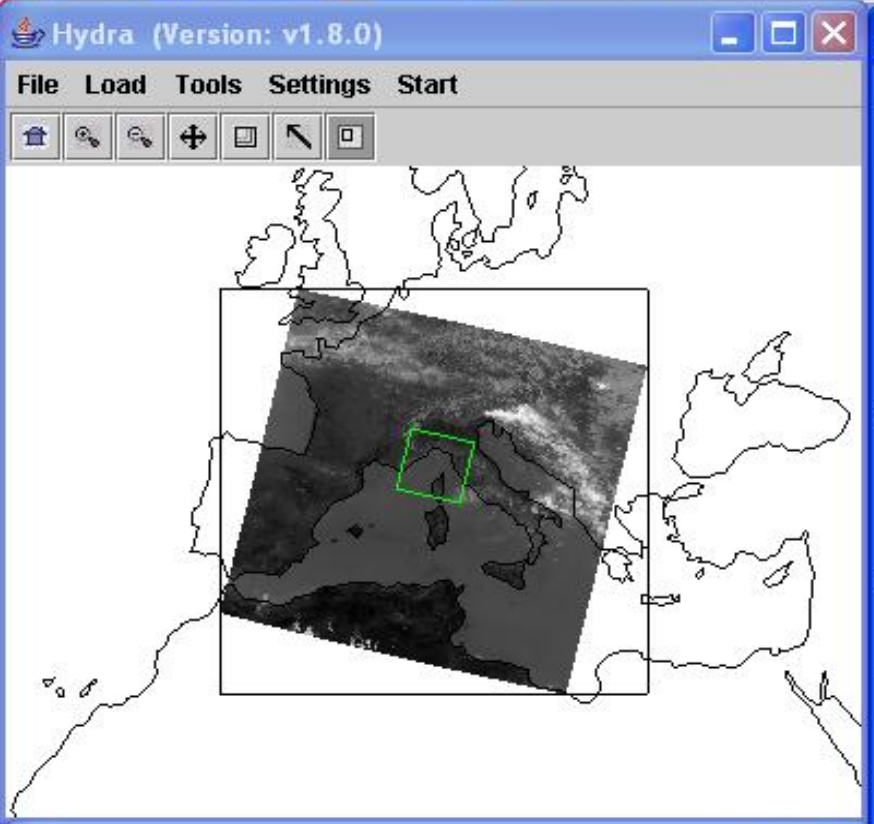
Hydra (Version: v1.8.0)
File Load Tools Settings Start

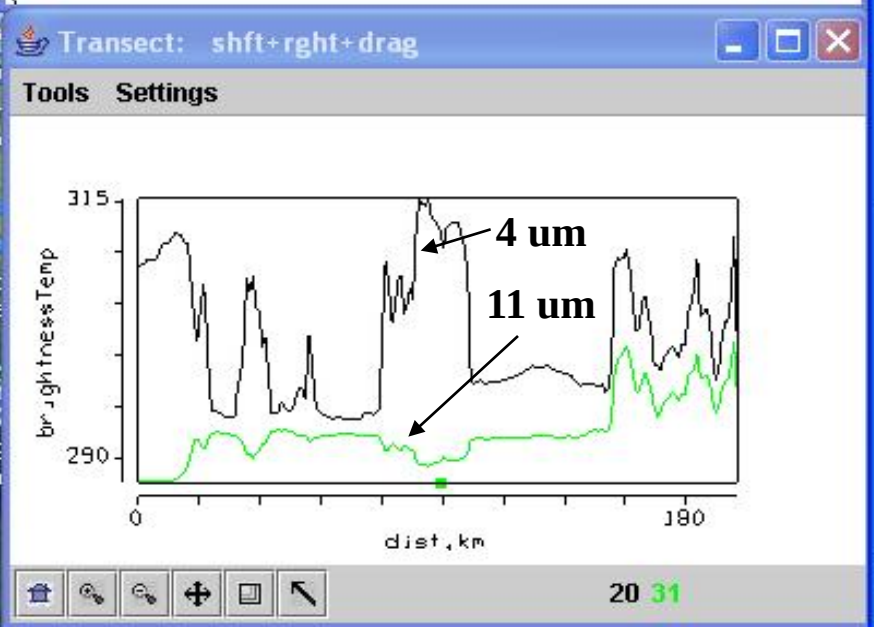
Transect: shft+rght+drag
Tools Settings
315
290
0
180
dist,km
4 um
11 um
20 31

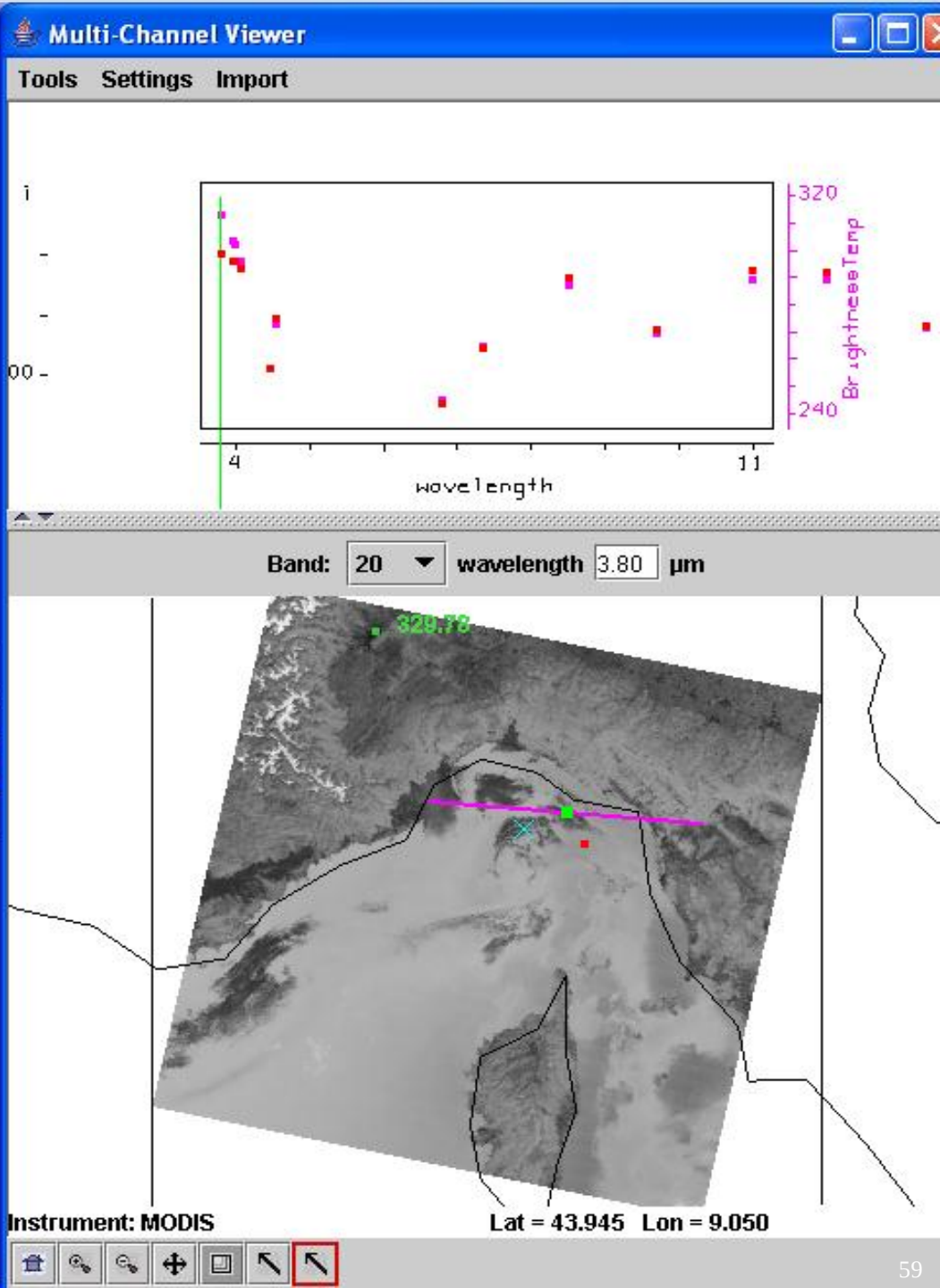
Multi-Channel Viewer
Tools Settings Import
320
240
4
11
wavelength
Band: 20 wavelength 3.80 µm
329.78
Instrument: MODIS
Lat = 43.945 Lon = 9.050

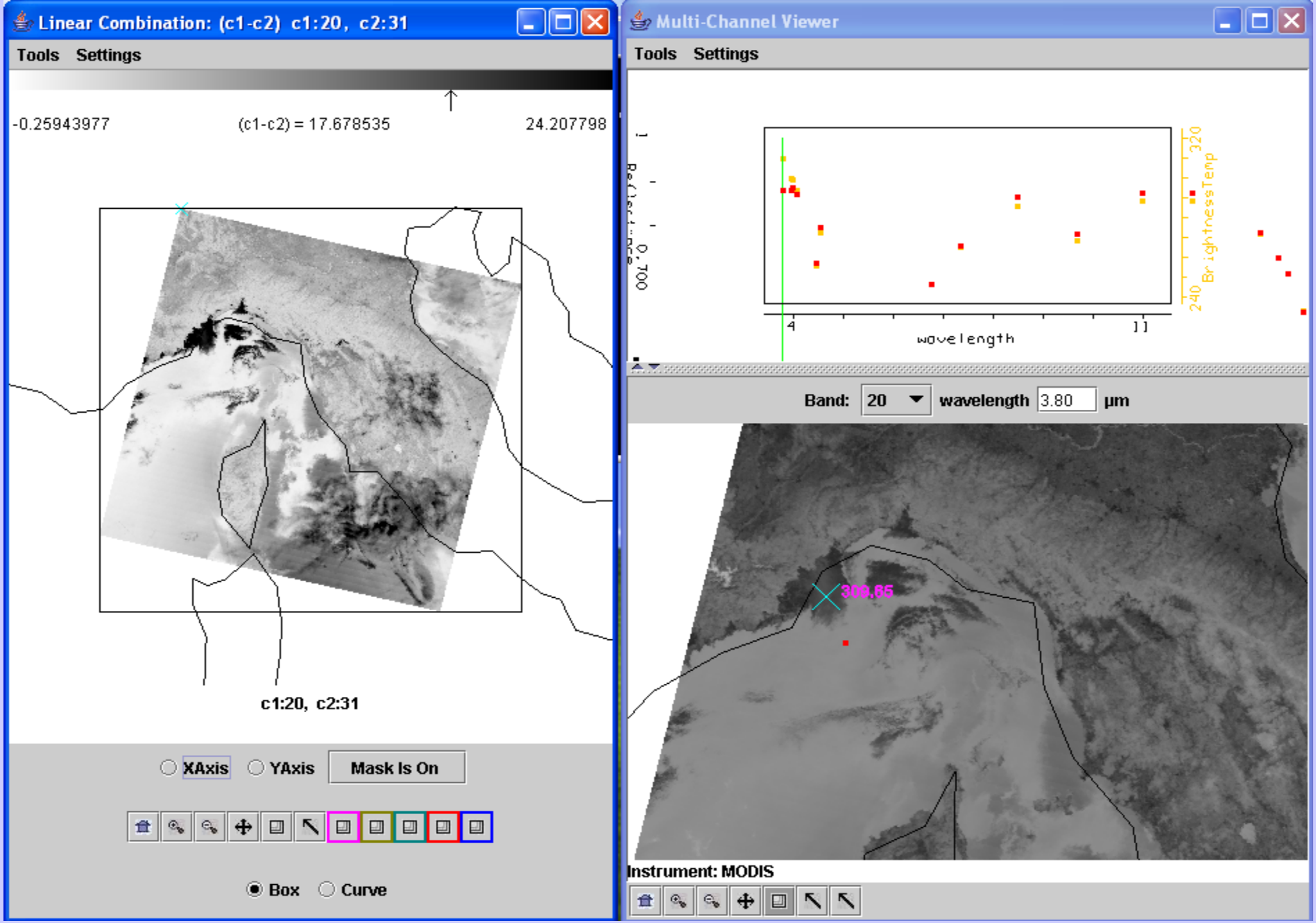

Detecting low clouds in 4-11 µm brightness temperature differences

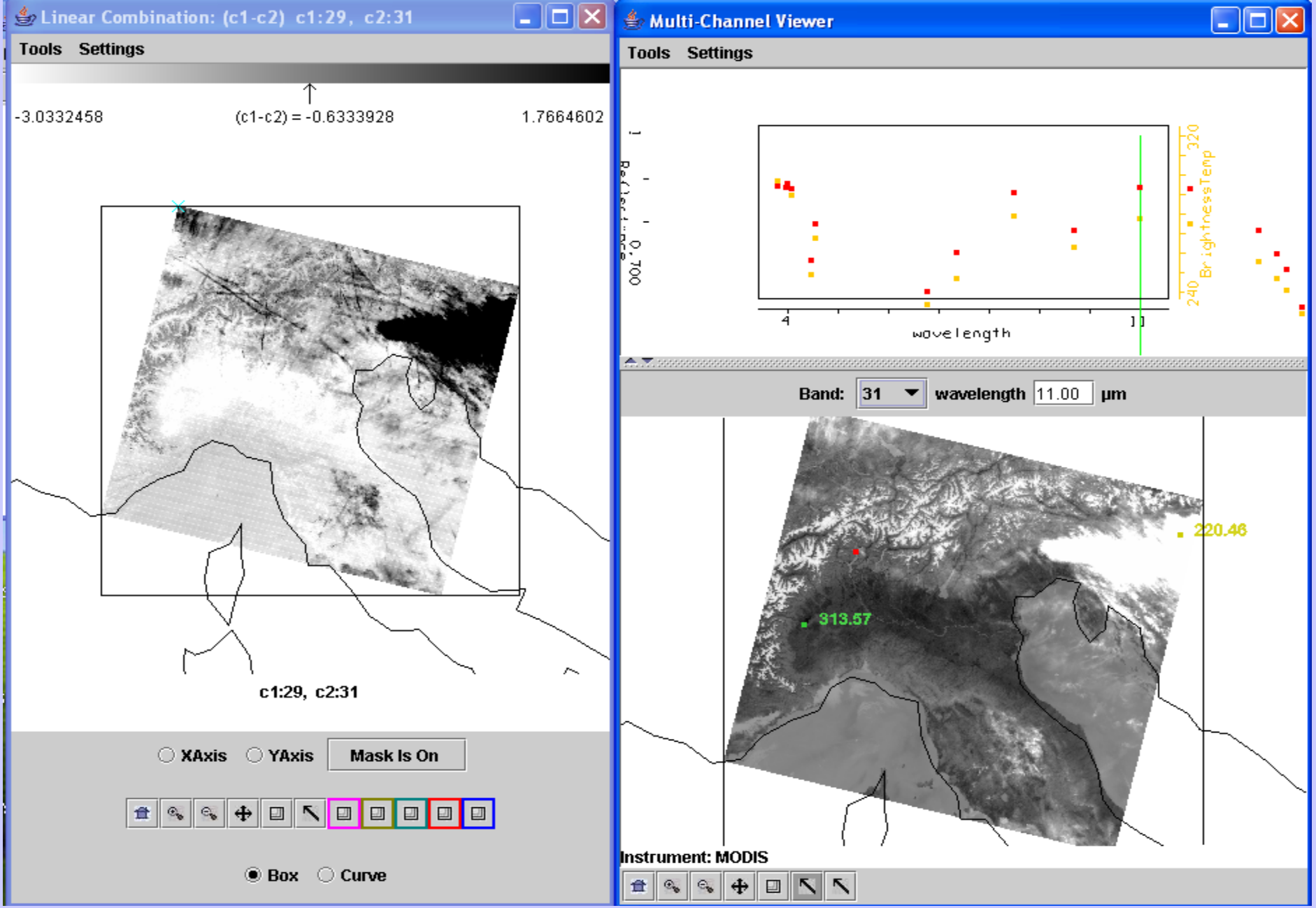

Detecting ice clouds in 8.6-11 µm brightness temperature differences

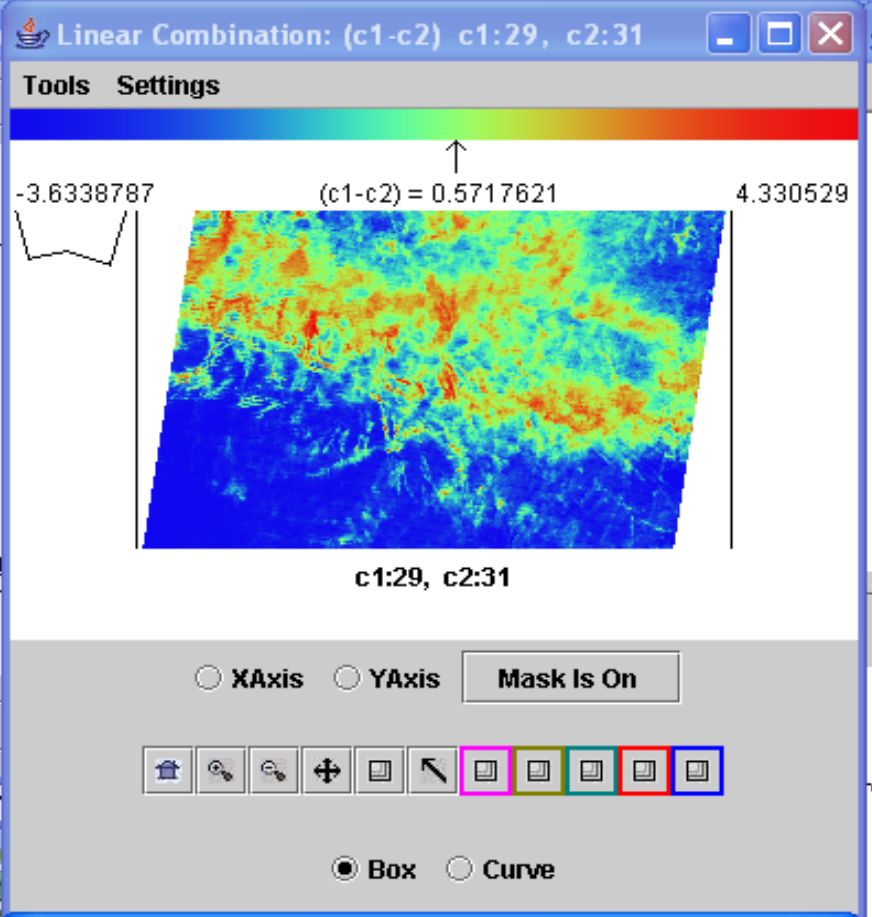
Linear Combination: (c1-c2) c1:29, c2:31
Tools Settings
-3.6338787
(c1-c2) = 0.5717621
4.330529
c1:29, c2:31
XAxis YAxis
Mask Is On
Box Curve

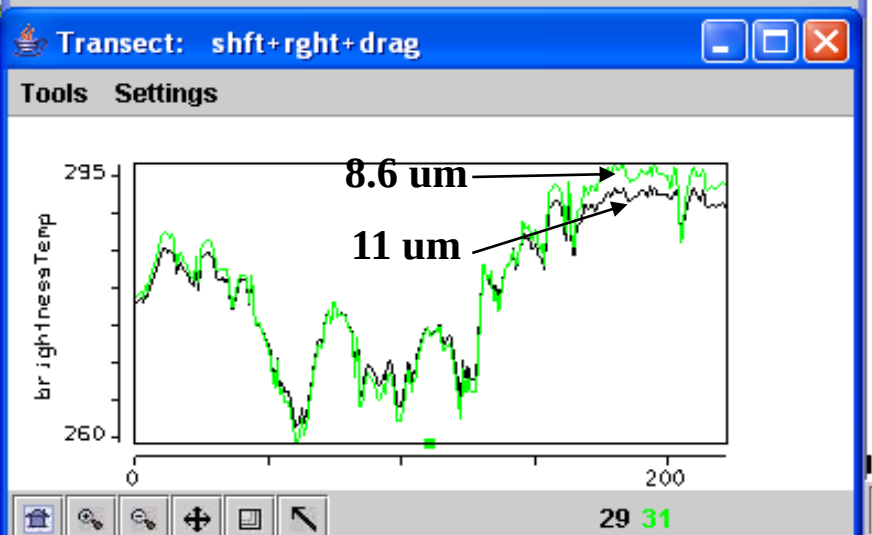
Transect: shft+rght+drag
Tools Settings
295
260
0
200
brightnessTemp
8.6 um
11 um
29 31

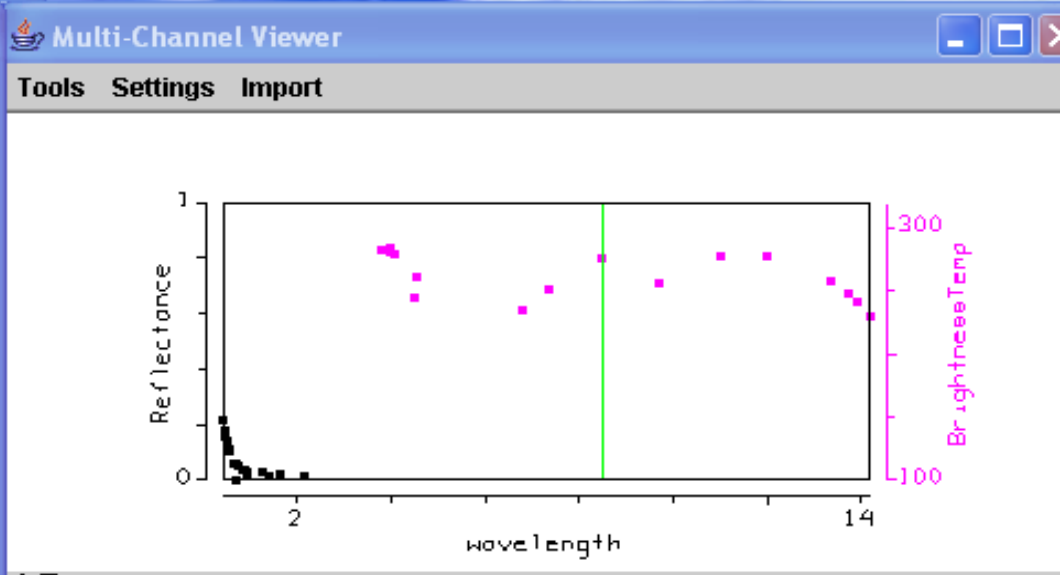
Multi-Channel Viewer
Tools Settings Import
Reflectance
1
0
2
14
wavelength
300
100
BrightnessTemp

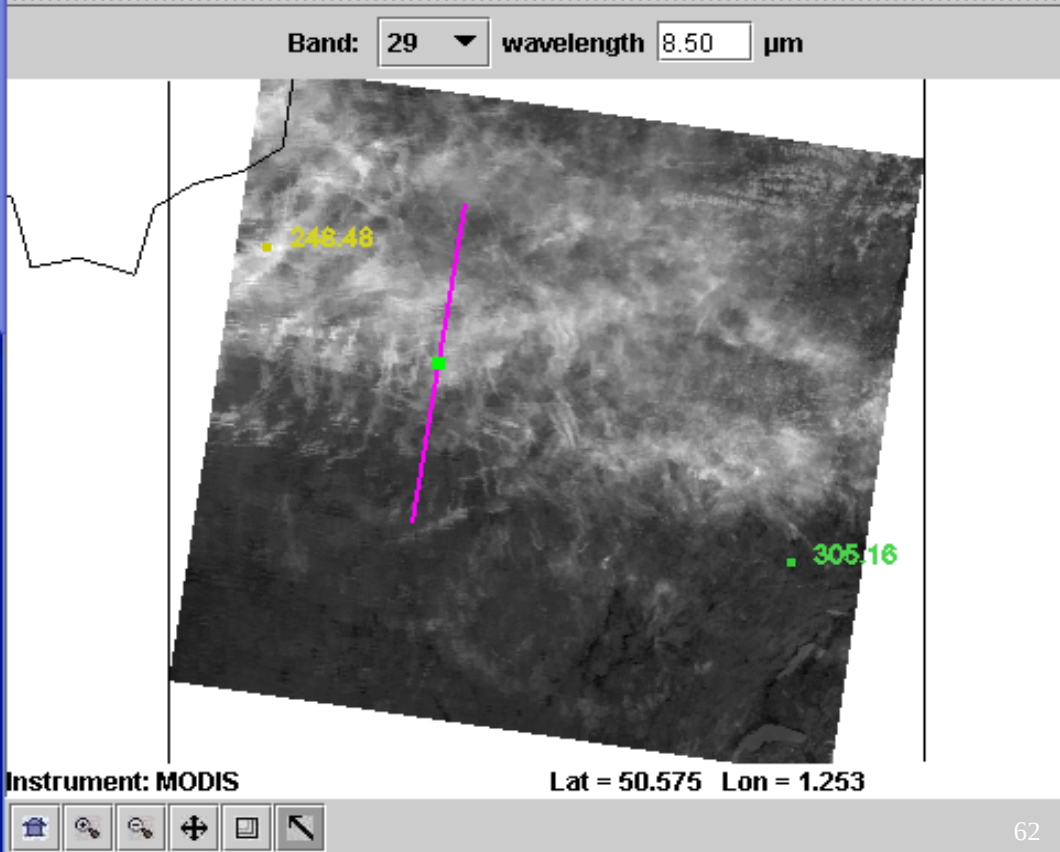
Band: 29 wavelength 8.50 µm
246.48
305.16
Instrument: MODIS
Lat = 50.575 Lon = 1.253

Optical properties of cloud particles: imaginary part of refraction index

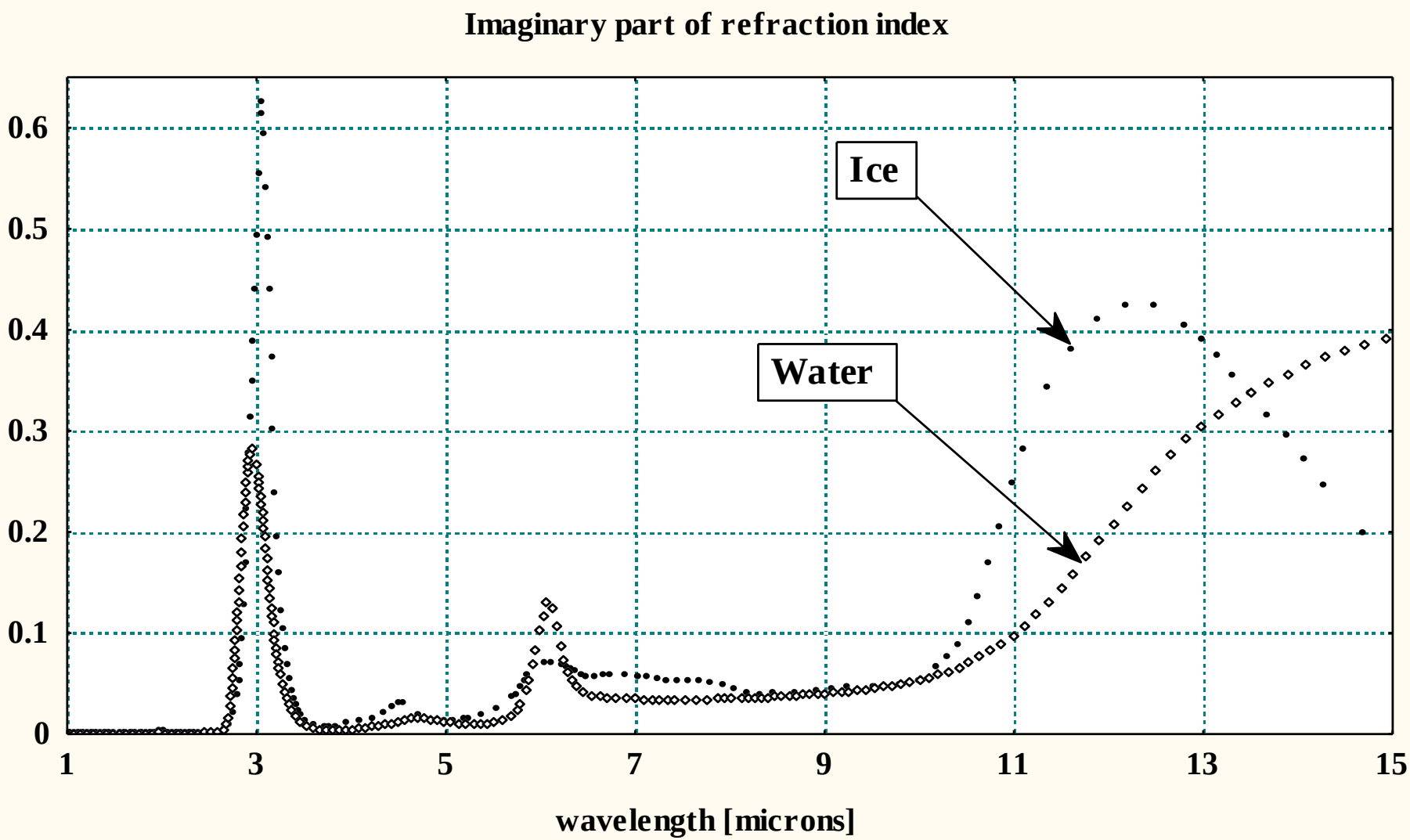

BT[8.6] – BT[11] will be positive for transmissive ice clouds

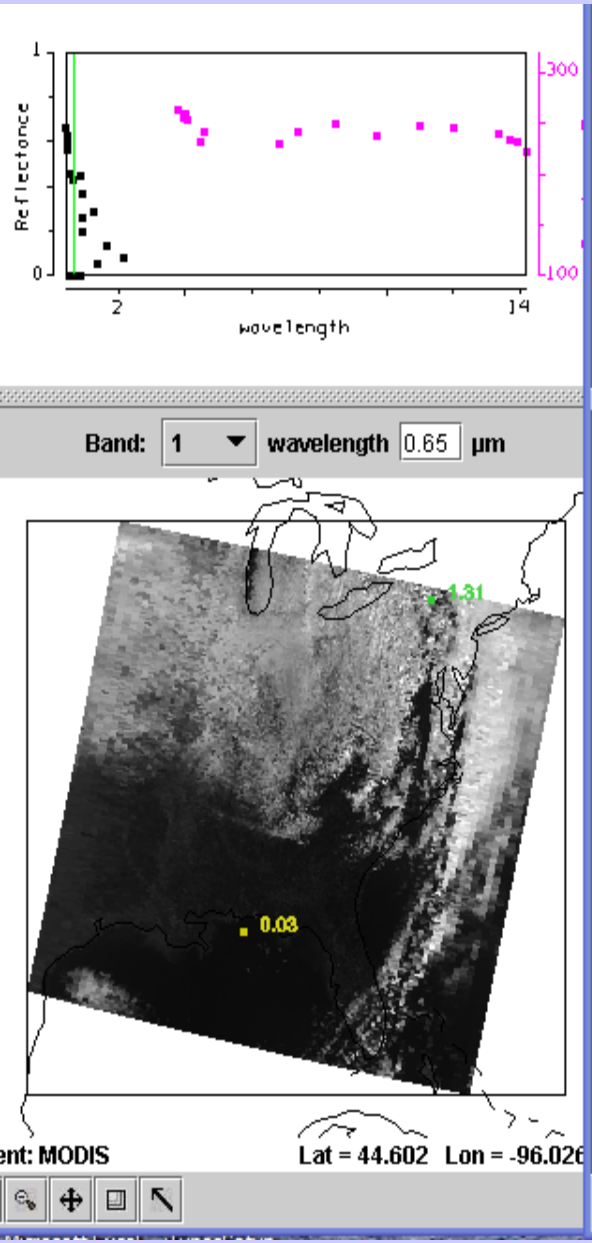
Reflectance
wavelength
Band: 1 wavelength 0.65 µm
1.31
0.03
Lat = 44.602 Lon = -96.026

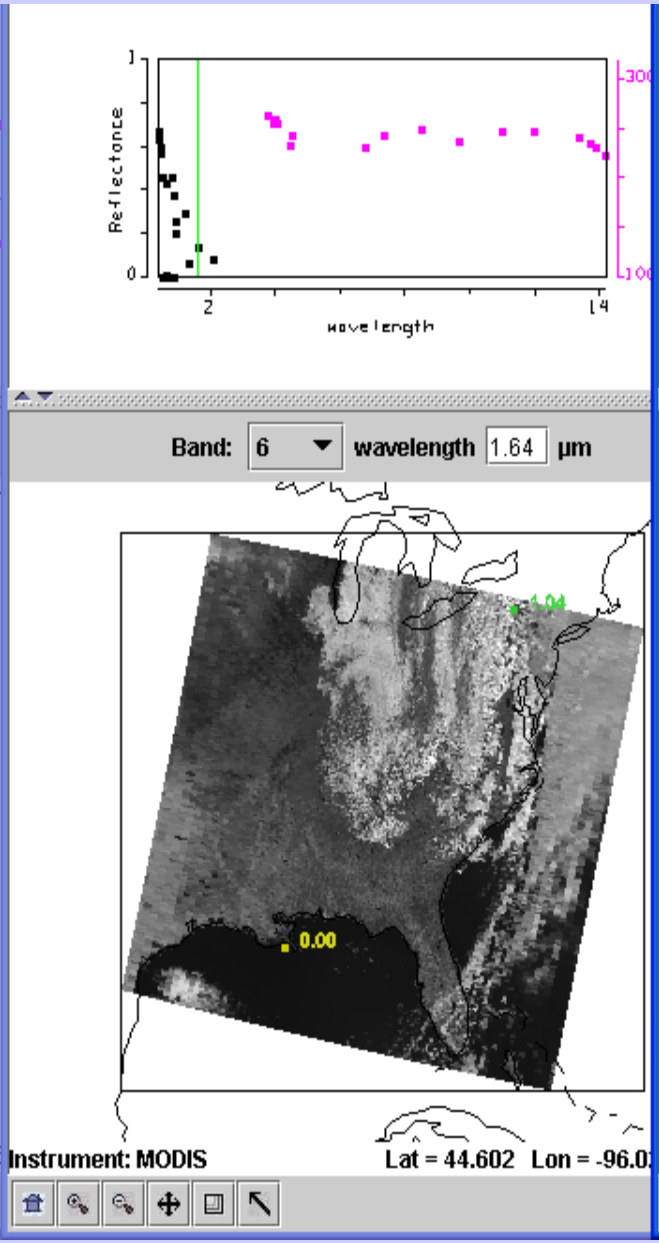
Reflectance
wavelength
Band: 6 wavelength 1.64 µm
1.04
0.00
Instrument: MODIS
Lat = 44.602 Lon = -96.0

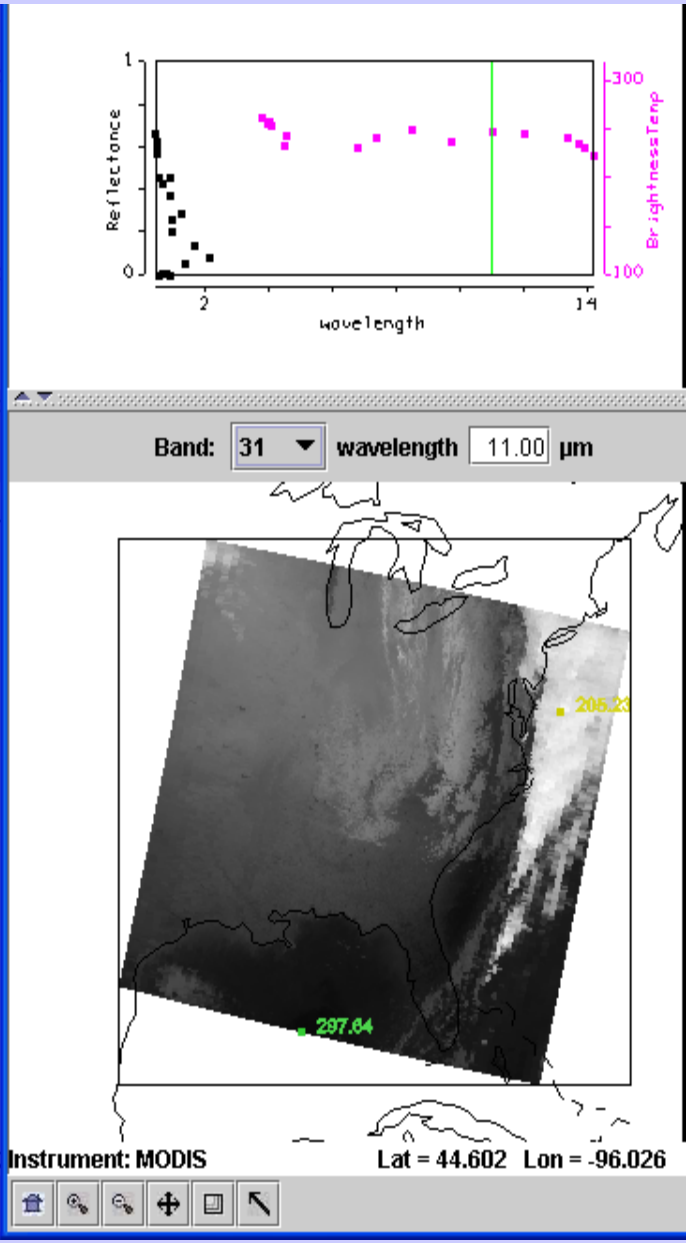
Reflectance
BrightnessTemp
wavelength
Band: 31 wavelength 11.00 µm
297.84
Instrument: MODIS
Lat = 44.602 Lon = -96.026

MODIS identifies cloud classes

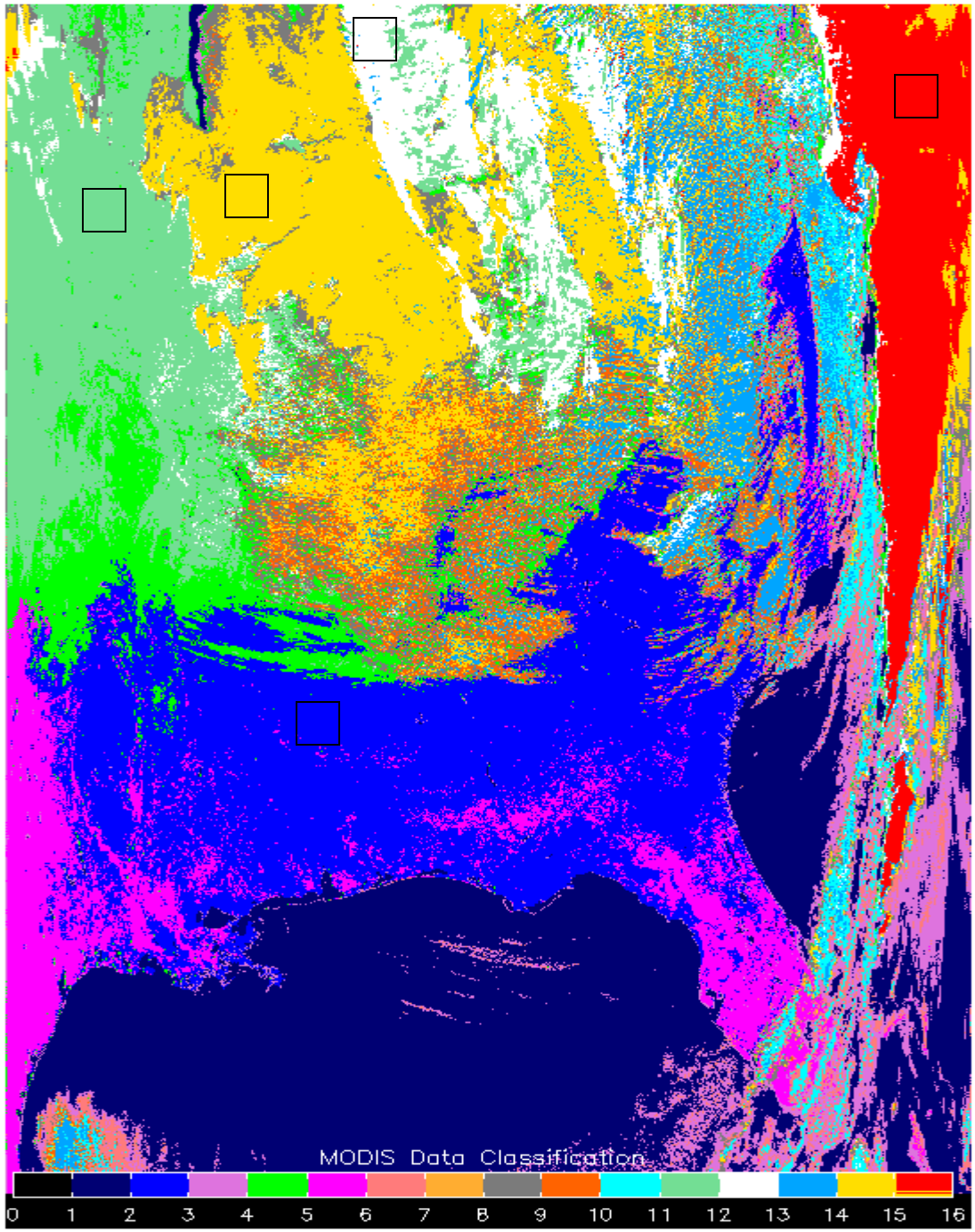

Hi cld

Mid cld

Lo cld

Snow

clr

Clouds separate into classes when multispectral radiance information is viewed

vis

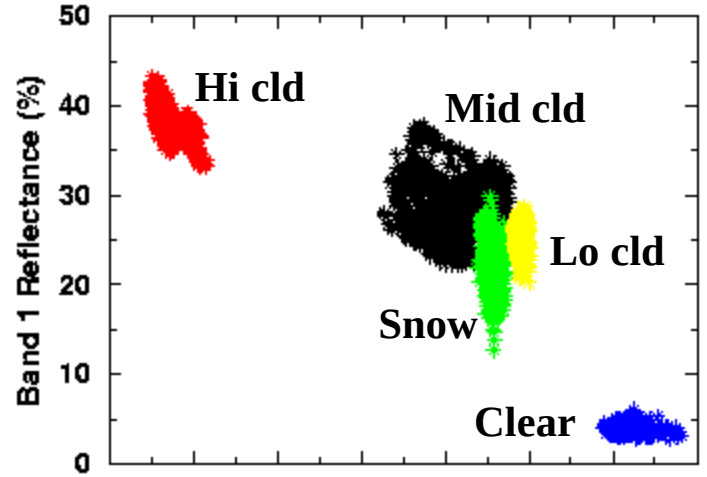

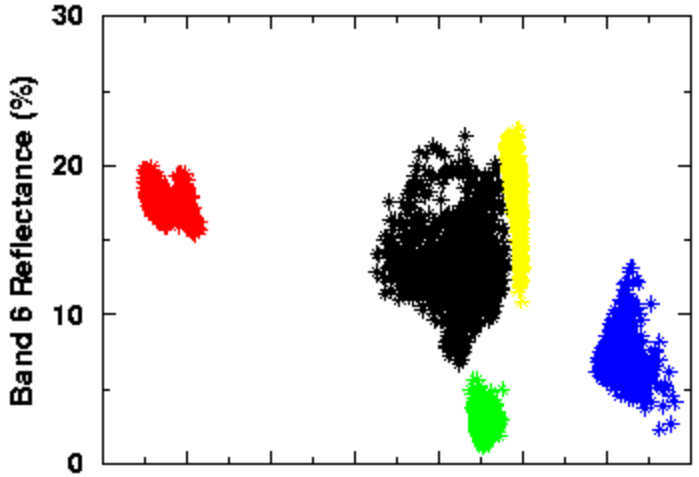

1.6 um

LSD 1.6 um

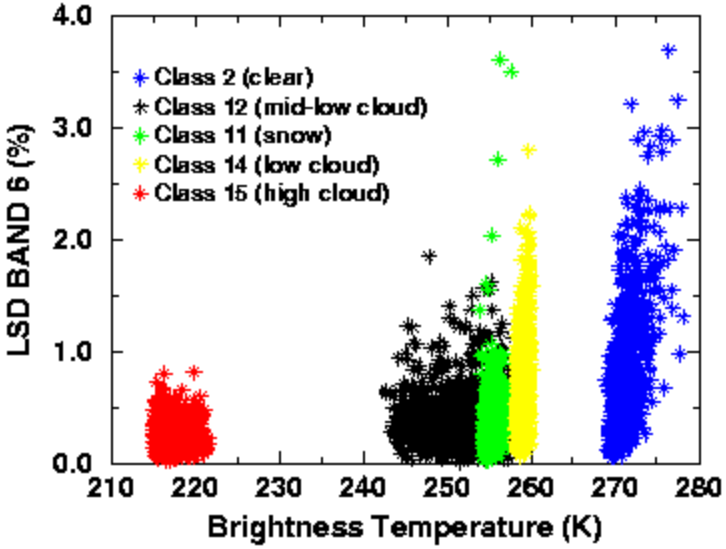

11 um

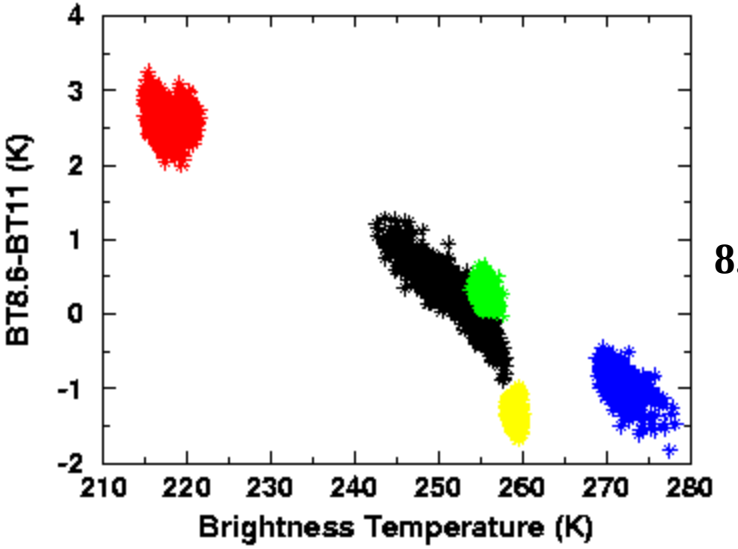

8.6-11 um

11 um

Cloud Mask Tests

• BT11	clouds over ocean
• BT13.9	high clouds
• BT6.7	high clouds
• BT3.9-BT11	broken or scattered clouds
• BT11-BT12	high clouds in tropics
• BT8.6-BT11	ice clouds
• BT6.7-BT11 or BT13.9-BT11	clouds in polar regions
• BT11+aPW(BT11-BT12)	clouds over ocean
• r0.65	clouds over land
• r0.85	clouds over ocean
• r1.38	thin cirrus
• r1.6	clouds over snow, ice cloud
• r0.85/r0.65 or NDVI	clouds over vegetation
• σ(BT11)	clouds over ocean

Cloud Properties

True Color Image
Cloud Mask
Land Classification
Cloud Opt Thickness
Cloud Eff Radius
Cloud Top Temp
Bispectral Phase

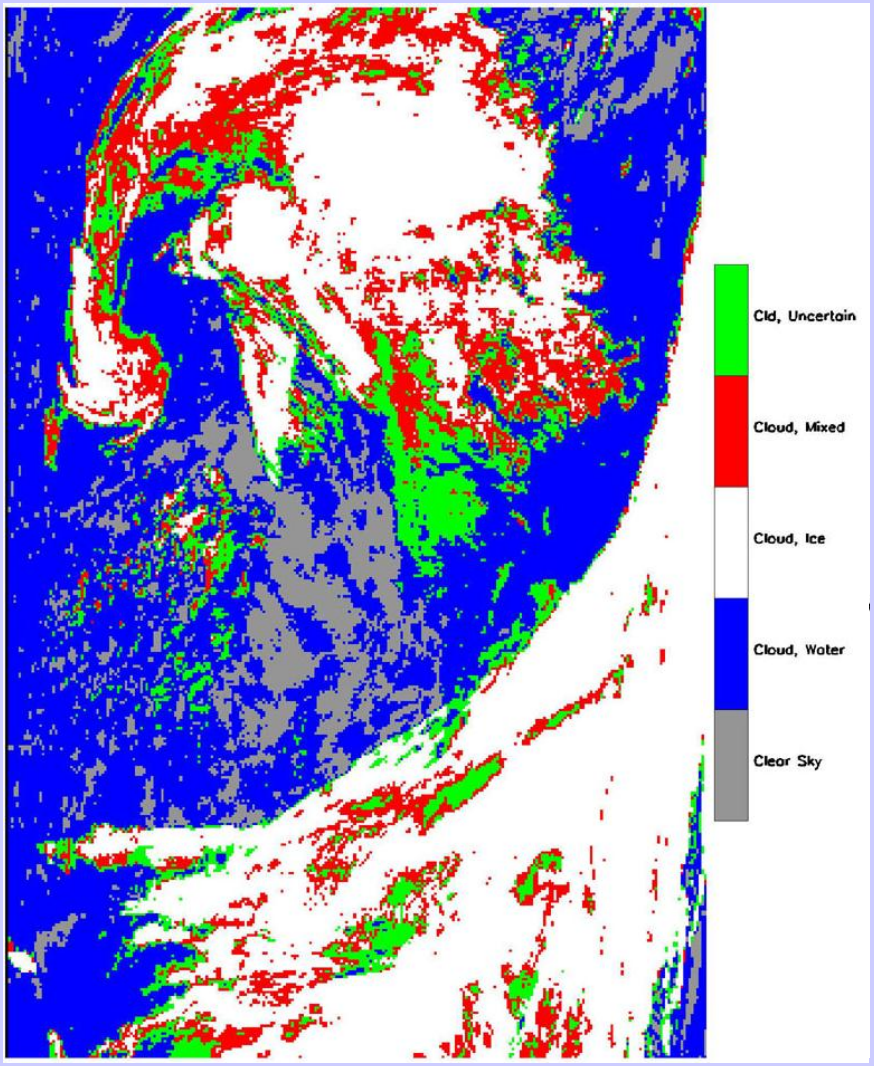

October 1, 2001

Monthly Mean Cloud Fraction (Cloud Mask)

(S. A. Ackerman, R. A. Frey et al. – Univ. Wisconsin)

April 2005
Aqua C5

Cloud_Fraction_Day_Mean_Mean

Cloud_Fraction_Night_Mean_Mean

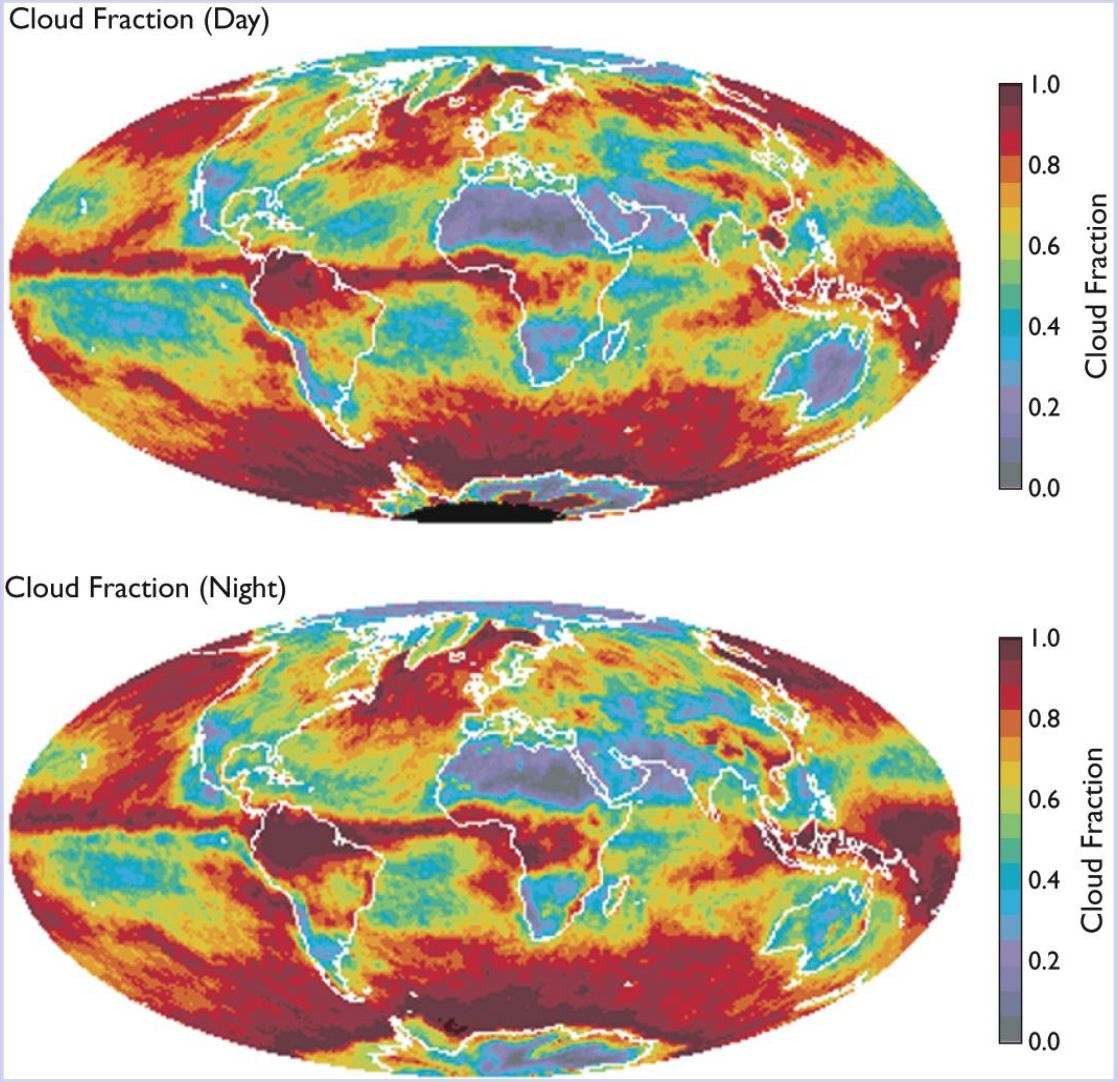

Monthly Mean Cloud-Top Properties

(W. P. Menzel, R. A. Frey et al. – Univ. Wisconsin)

April 2005
Aqua C5

Cloud_Top_Pressure_Mean_Mean

Cloud_Top_Temperature_Mean_Mean

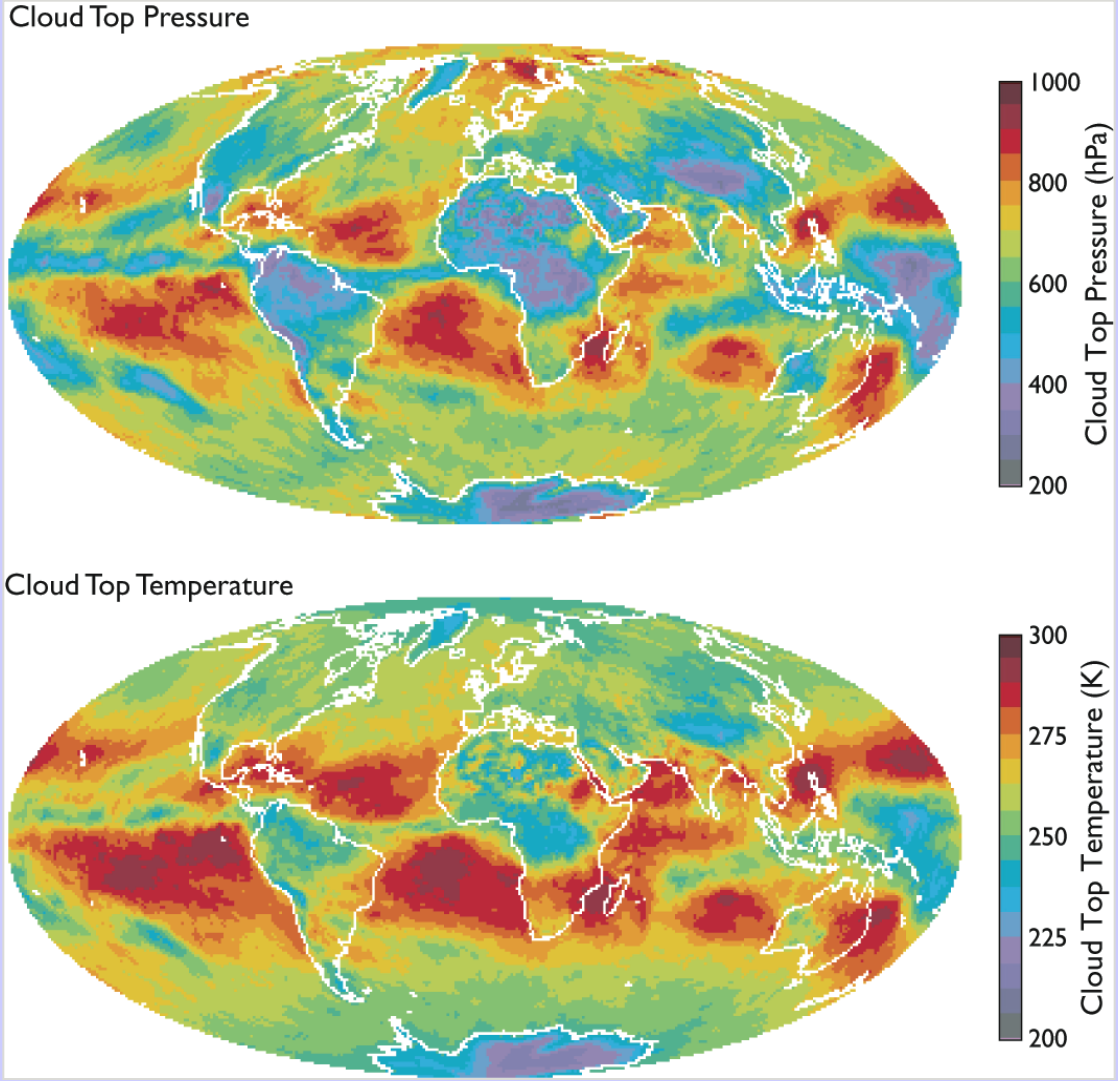

Monthly Mean Cloud Optical Thickness

(M. D. King, S. Platnick et al. – NASA GSFC)

April 2005
Aqua C5 (QA mean)

Cloud_Optical_Thickness
_Liquid_QA_Mean_Mean

Cloud_Optical_Thickness
_Ice_QA_Mean_Mean

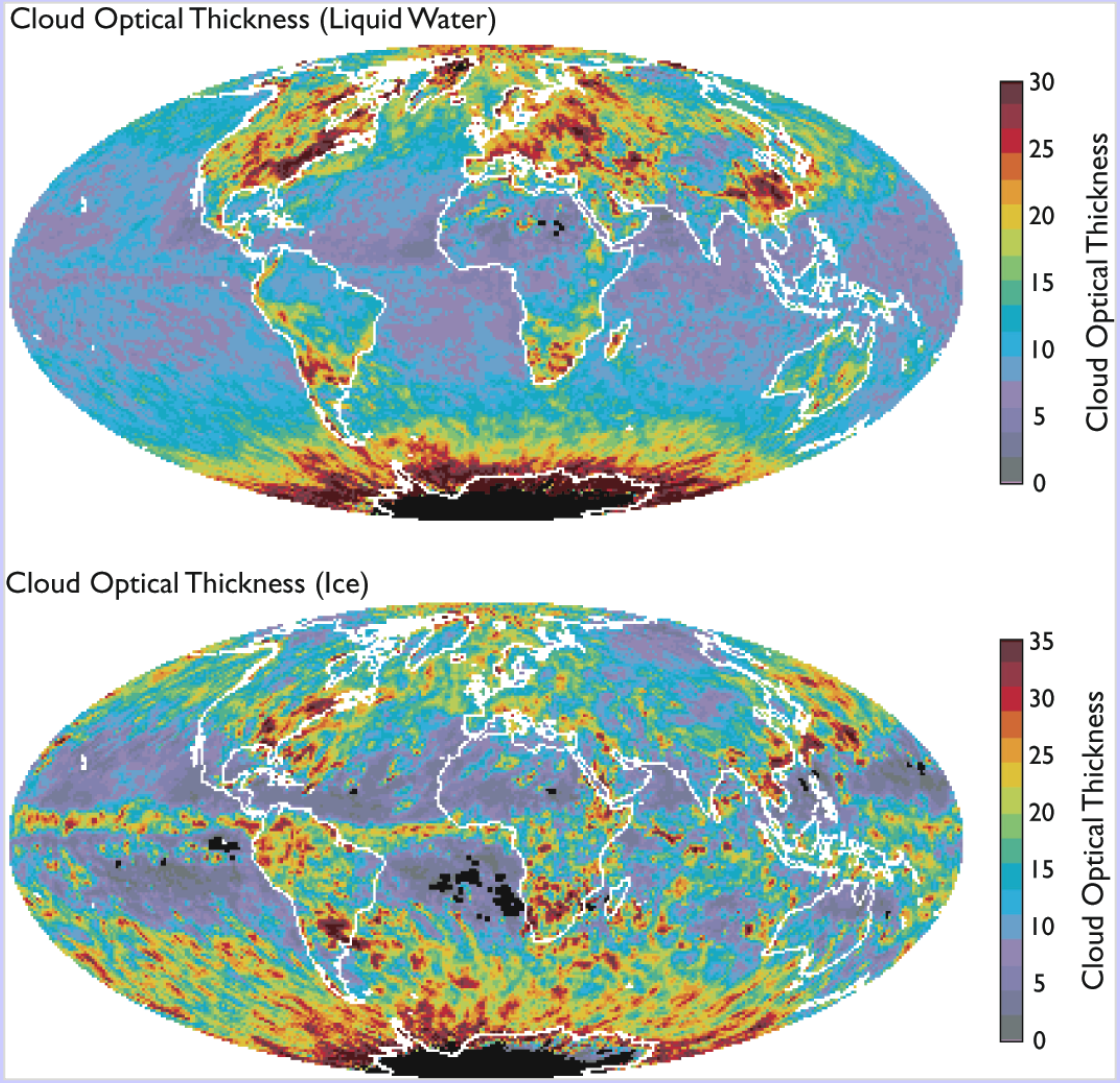

Monthly Mean Cloud Effective Radius

(M. D. King, S. Platnick et al. – NASA GSFC)

April 2005
Aqua C5 (QA mean)

Cloud_Effective_Radius _Liquid_QA_Mean_Mean

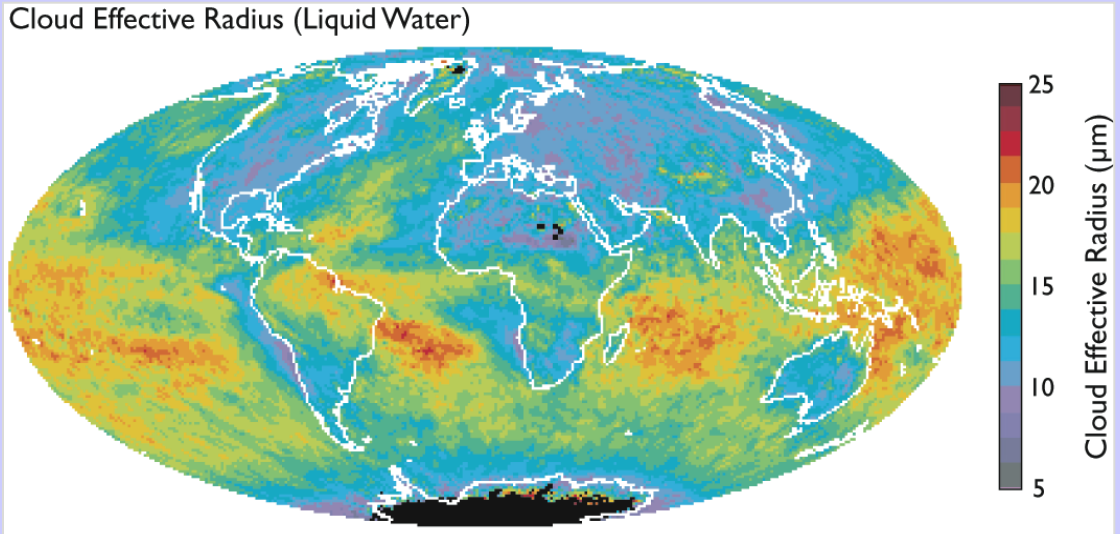

Cloud_Effective_Radius _Ice_QA_Mean_Mean

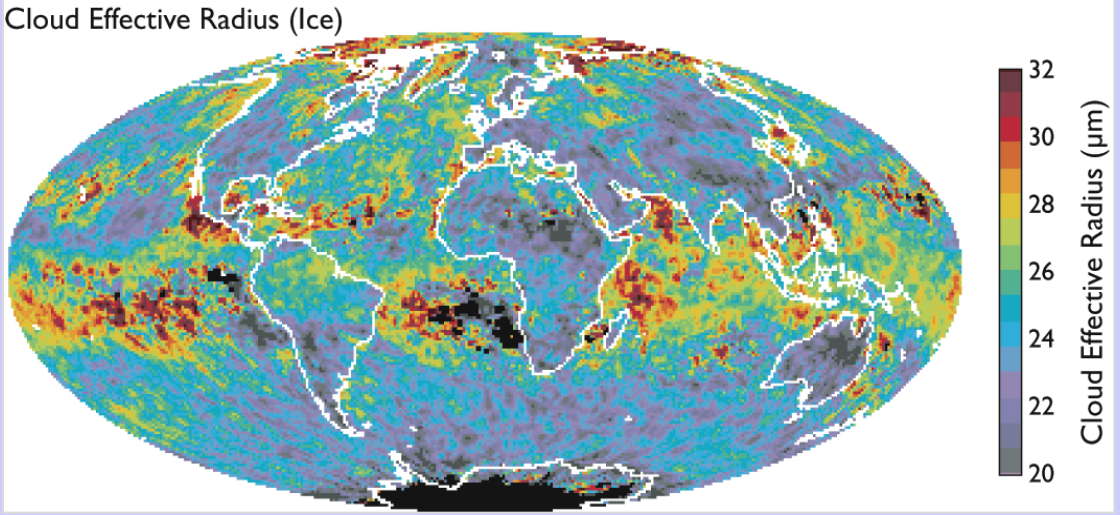

Cloud optical, microphysical properties retrieval space example

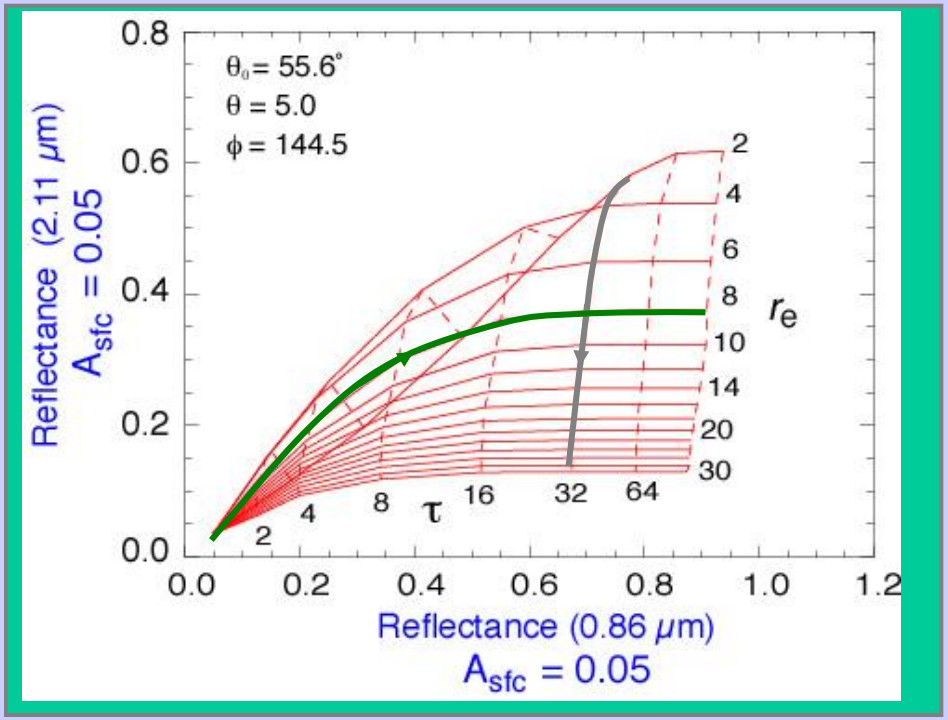

2.1 μm absorption increases with particle size, little effect at 0.86 μm

2.1 μm reflectance reaches limiting values with optical thickness

Liquid water cloud
ocean surface

S. Platnick, ISSAOS '02

Cloud parameter determinations from partly clear and partly cloudy FOVs

Radiance from a partly cloudy FOV

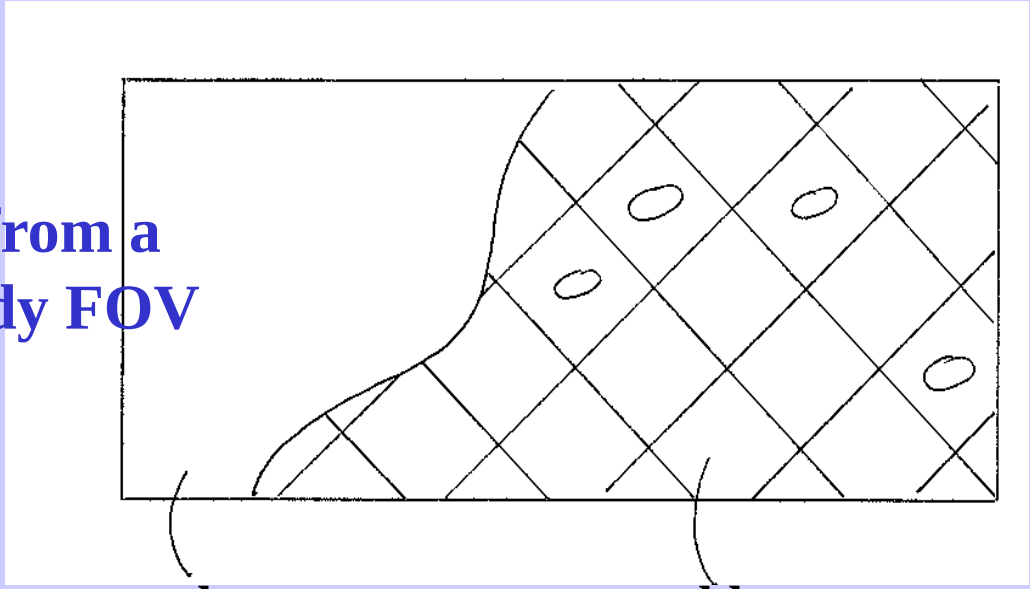

$R = [1-N]\, R_{clr} + N\, R_{cld}$

but $R_{cld} = [1-\varepsilon]\, R_{clr} + \varepsilon\, R_{bcd}$

where R_{bcd} represents opaque cloud radiance $B[T(P_c)]$

so together

$R = [1-N\varepsilon]\, R_{clr} + N\varepsilon\, R_{bcd}$

Two unknowns, ε and Pc, require two measurements

RTE in Cloudy Conditions

$$I_\lambda = \eta\, I^{cd}_\lambda + (1 - \eta)\, I^{clr}_\lambda \quad \text{where cd = cloud, clr = clear, } \eta \text{ = cloud fraction}$$

$$I^{clr}_\lambda = B_\lambda(T_s)\, \tau_\lambda(p_s) + \int_{p_s}^{o} B_\lambda(T(p))\, d\tau_\lambda \,.$$

$$I^{cd}_\lambda = (1-\varepsilon_\lambda)\, B_\lambda(T_s)\, \tau_\lambda(p_s) + (1-\varepsilon_\lambda) \int_{p_s}^{p_c} B_\lambda(T(p))\, d\tau_\lambda$$

$$+ \varepsilon_\lambda\, B_\lambda(T(p_c))\, \tau_\lambda(p_c) + \int_{p_c}^{o} B_\lambda(T(p))\, d\tau_\lambda$$

ε_λ is emittance of cloud. First two terms are from below cloud, third term is cloud contribution, and fourth term is from above cloud. After rearranging

$$I_\lambda - I_\lambda^{clr} = \eta\varepsilon_\lambda \int_{p_s}^{p_c} \tau_\lambda(p)\; dB_\lambda \,.$$

CO2 channels see to different levels in the atmosphere

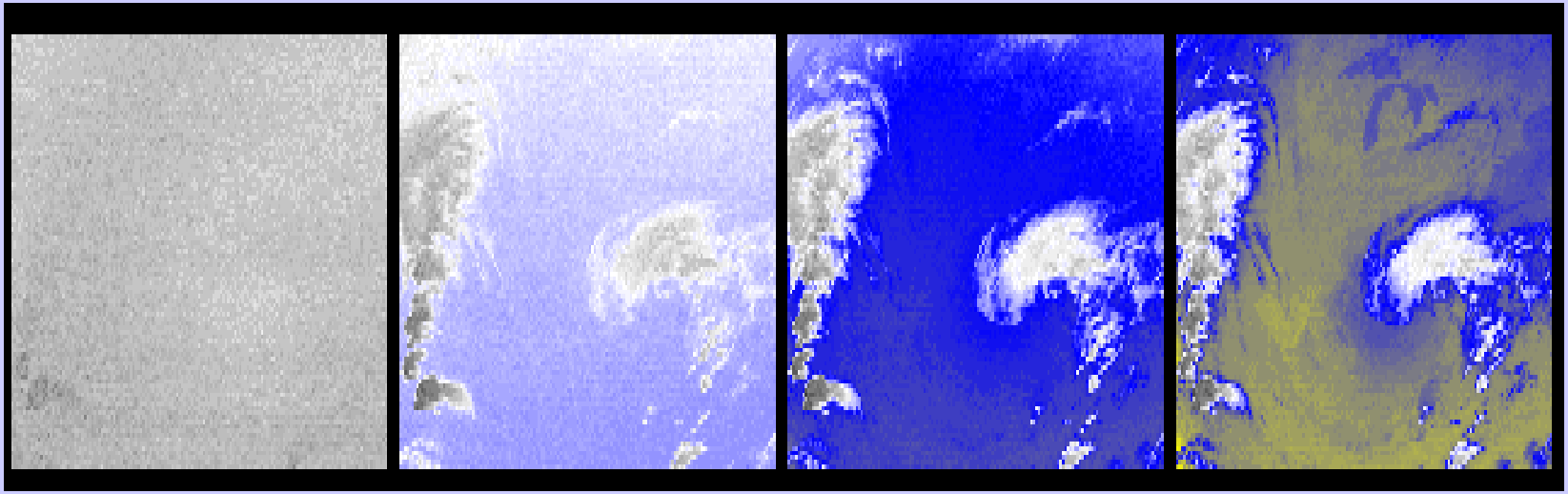

14.2 um 13.9 um 13.6 um 13.3 um

Different ratios reveal cloud properties at different levels

hi - 14.2/13.9
mid - 13.9/13.6
low - 13.6/13.3

Meas **Calc**

$$\frac{(I_{\lambda 1}-I_{\lambda 1}^{clr})}{(I_{\lambda 2}-I_{\lambda 2}^{clr})} = \frac{\eta\varepsilon_{\lambda 1}\int_{p_s}^{p_c}\tau_{\lambda 1}\,dB_{\lambda 1}}{\eta\varepsilon_{\lambda 2}\int_{p_s}^{p_c}\tau_{\lambda 2}\,dB_{\lambda 2}}$$

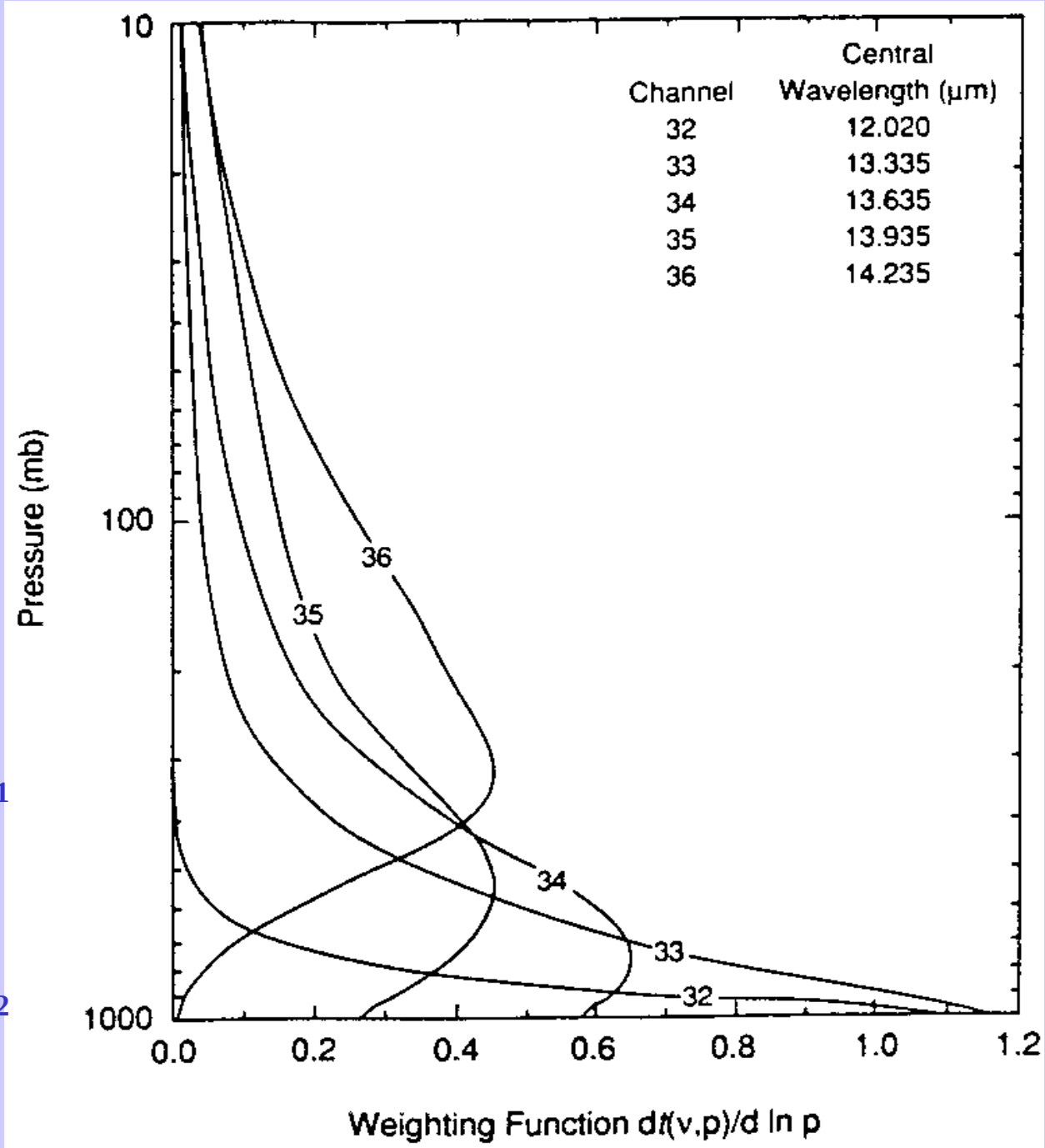

BTs in and out of clouds for MODIS CO_2 bands

demonstrate weighting functions and cloud top algorithm

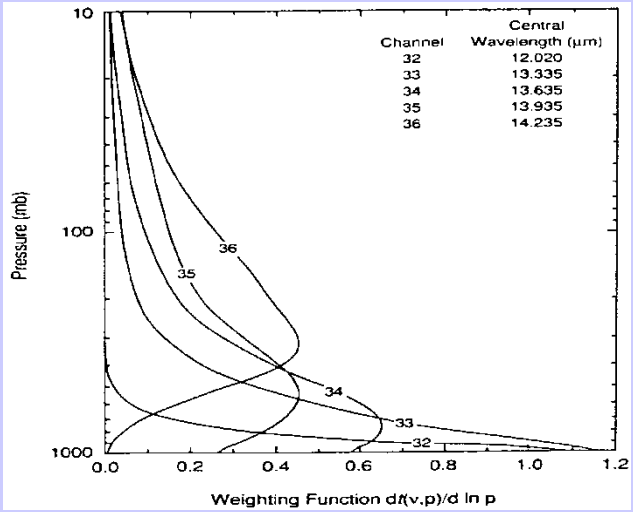

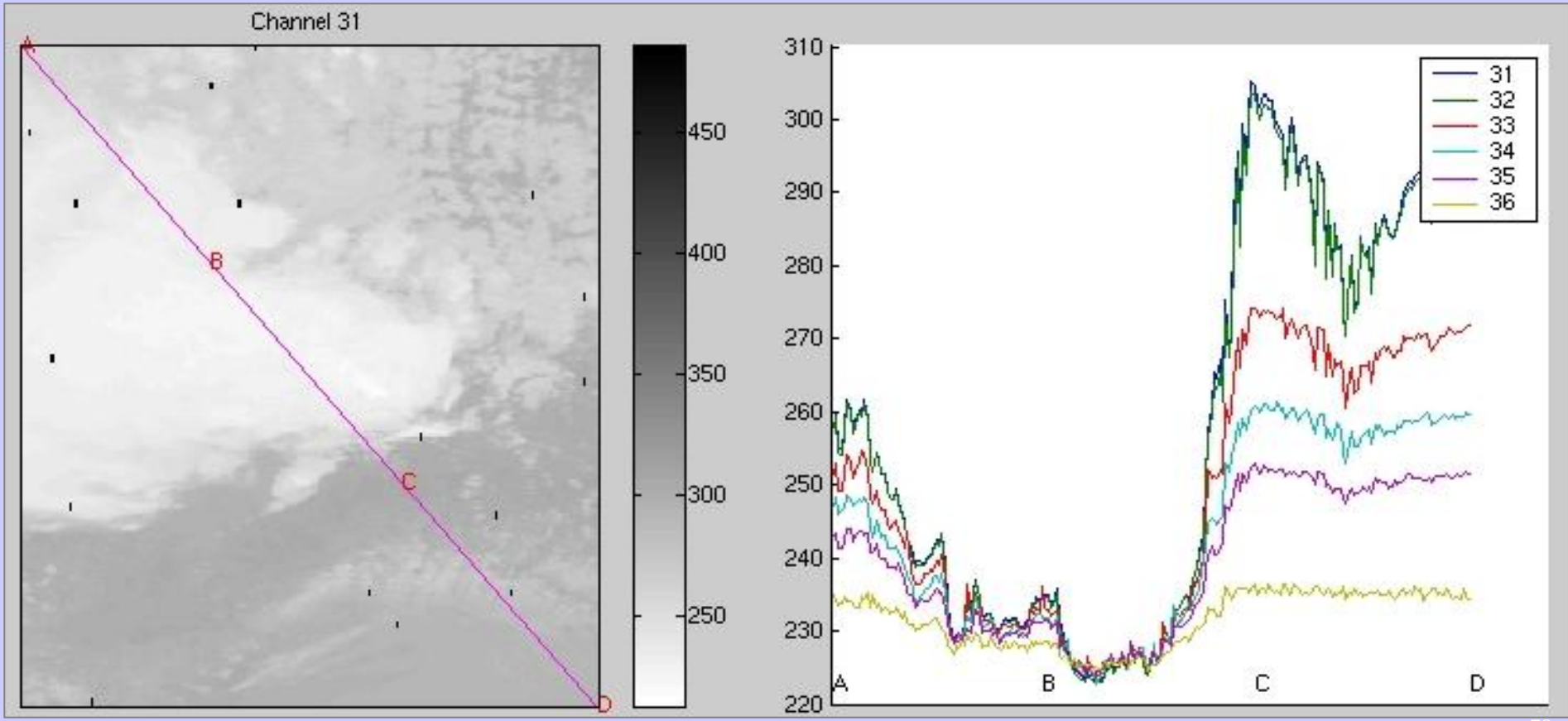

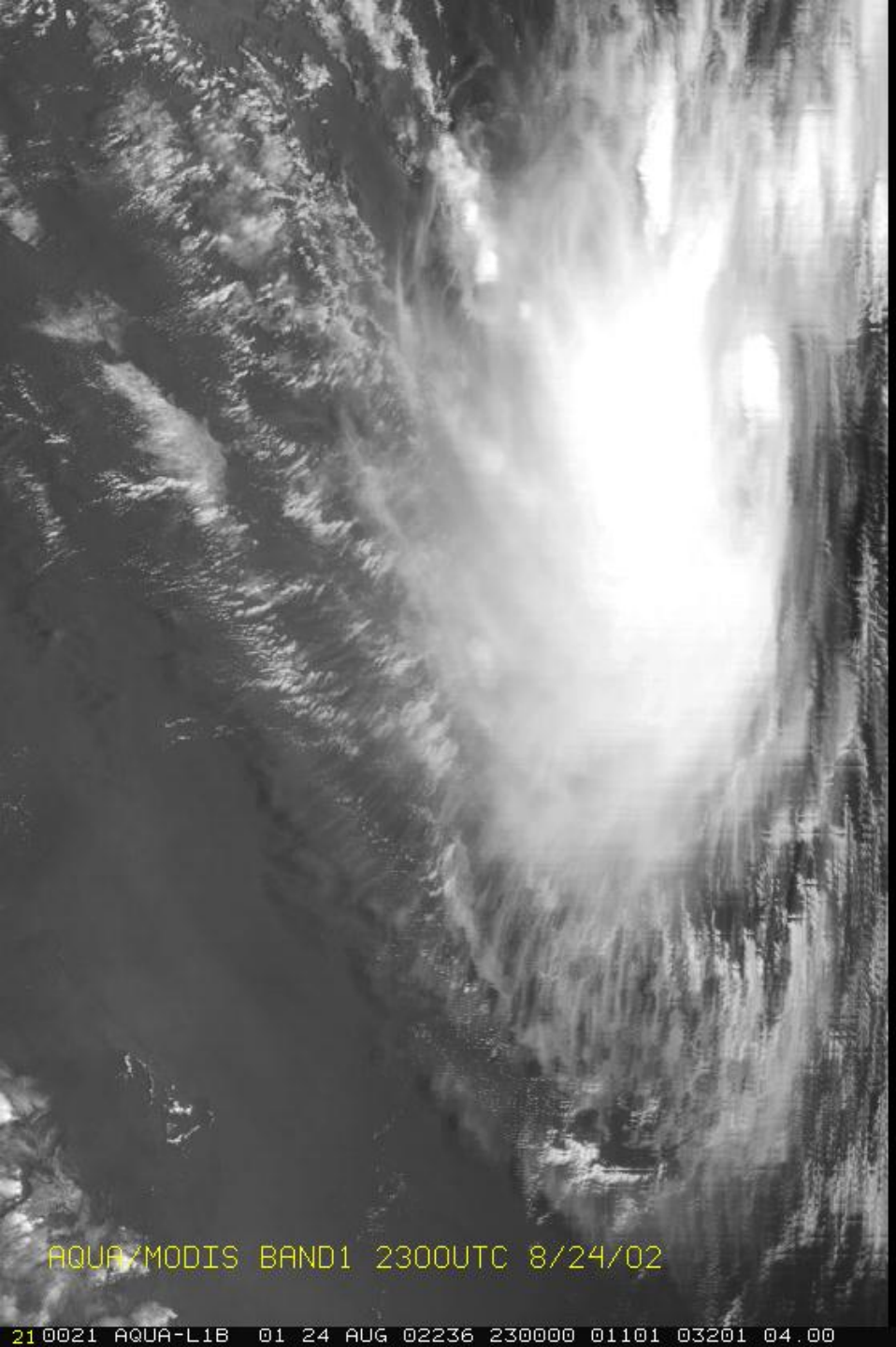
AQUA/MODIS BAND1 2300UTC 8/24/02
21 0021 AQUA-L1B 01 24 AUG 02236 230000 01101 03201 04.00

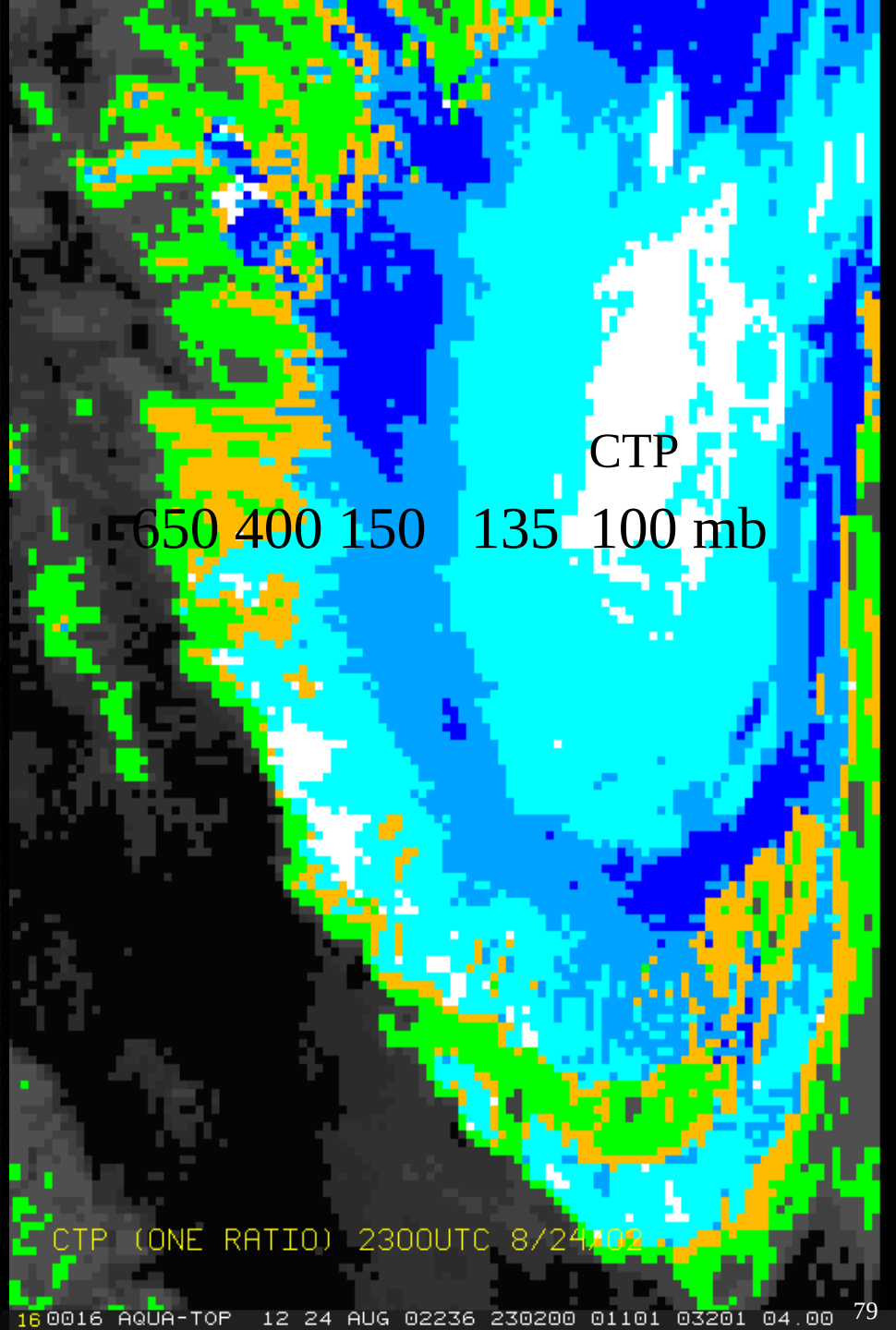
CTP
650 400 150 135 100 mb
CTP (ONE RATIO) 2300UTC 8/24/02
16 0016 AQUA-TOP 12 24 AUG 02236 230200 01101 03201 04.00

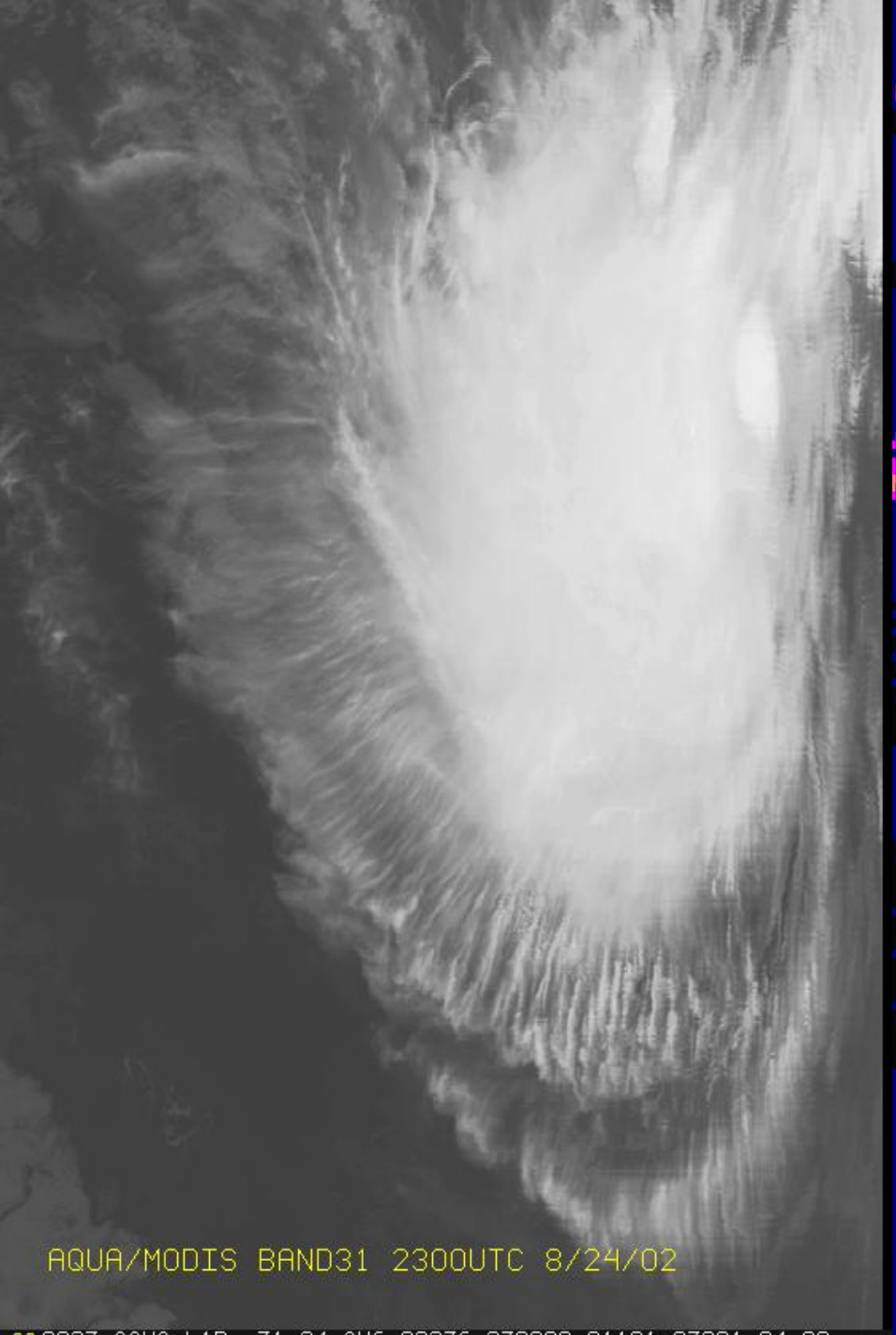
AQUA/MODIS BAND31 2300UTC 8/24/02
23 0023 AQUA-L1B 31 24 AUG 02236 230000 01101 03201 04.00

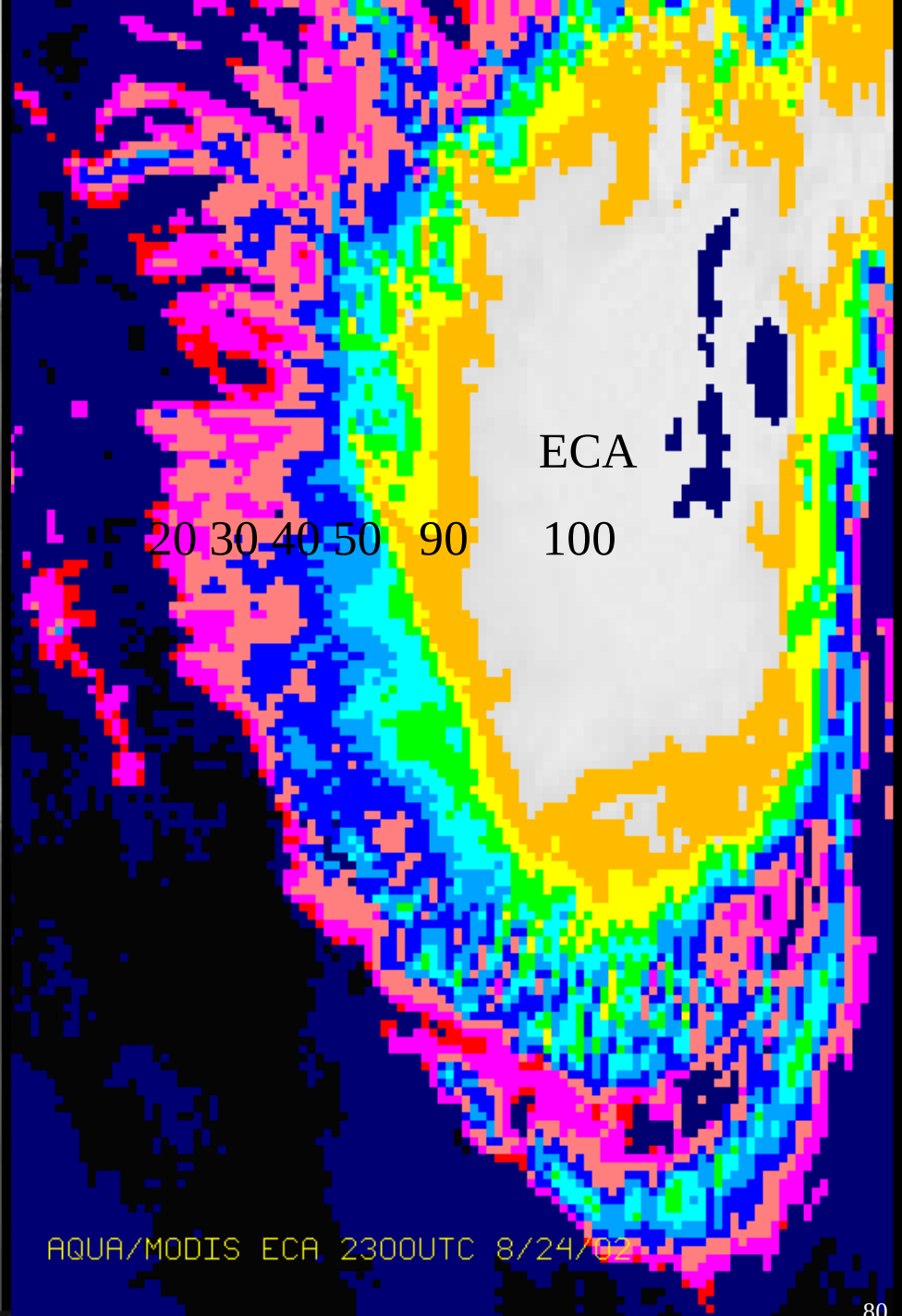
ECA
20 30 40 50 90 100
AQUA/MODIS ECA 2300UTC 8/24/02
25 0025 AQUA-TOP 22 24 AUG 02236 230000 01101 03201 04.00

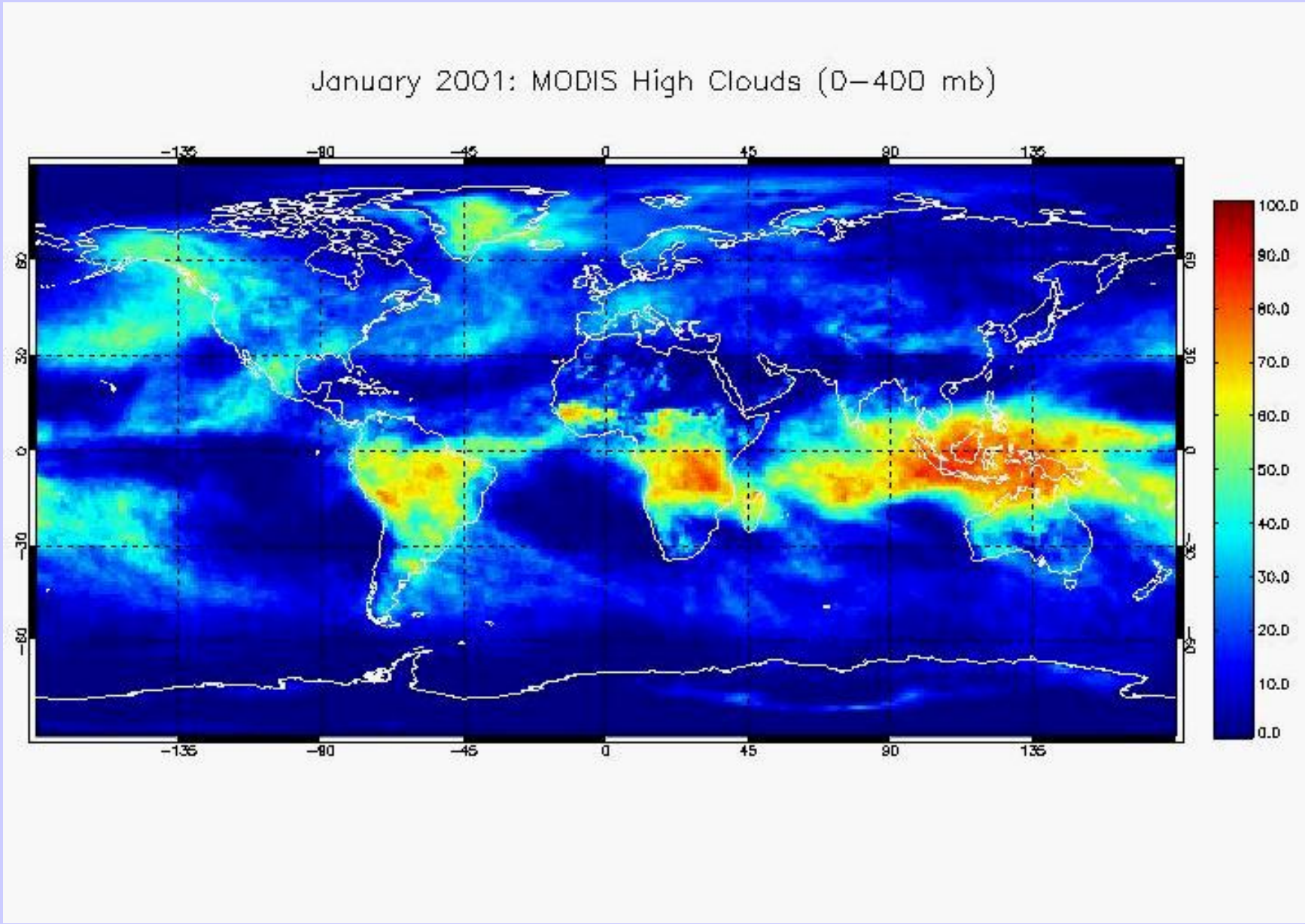
January 2001: MODIS High Clouds (0–400 mb)
-135
-90
-45
0
45
90
135
60
30
0
-30
-60
100.0
90.0
80.0
70.0
60.0
50.0
40.0
30.0
20.0
10.0
0.0

Strat Cloud identified when BTWV>BTIRW

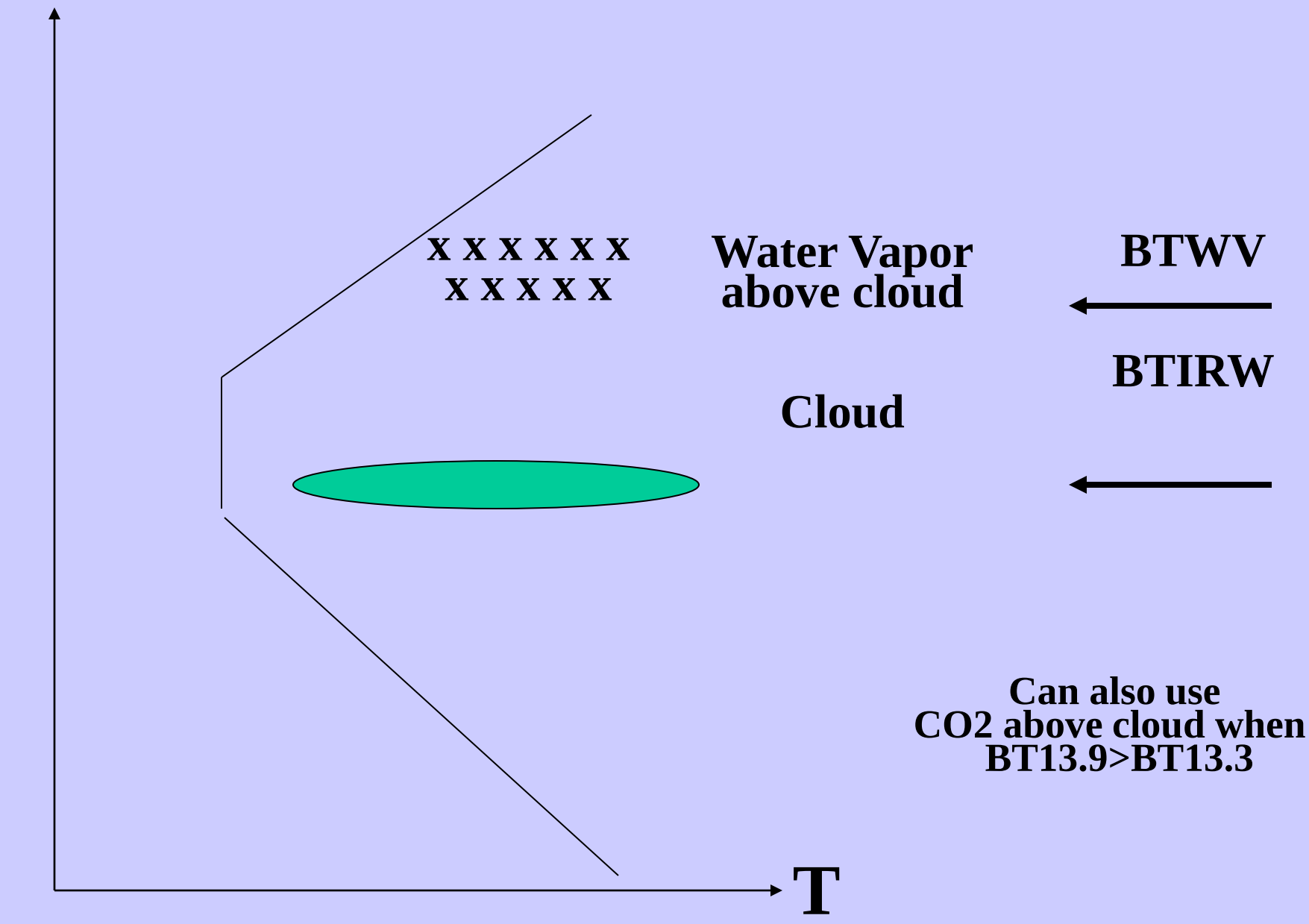

Can also use
CO2 above cloud when
BT13.9>BT13.3

Stratospheric Cloud Identification

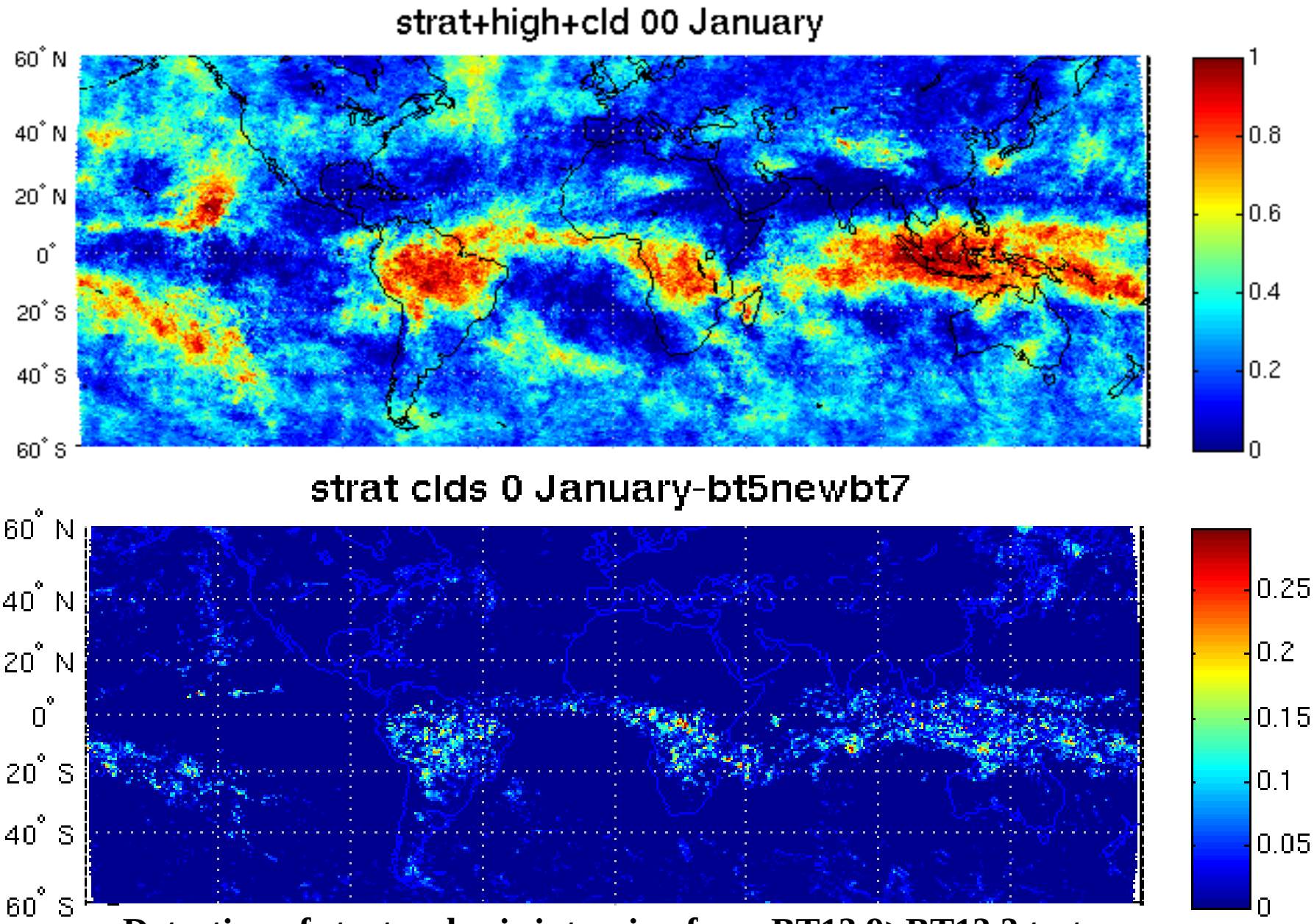

Detection of stratospheric intrusion from BT13.9>BT13.3 test

Transmission

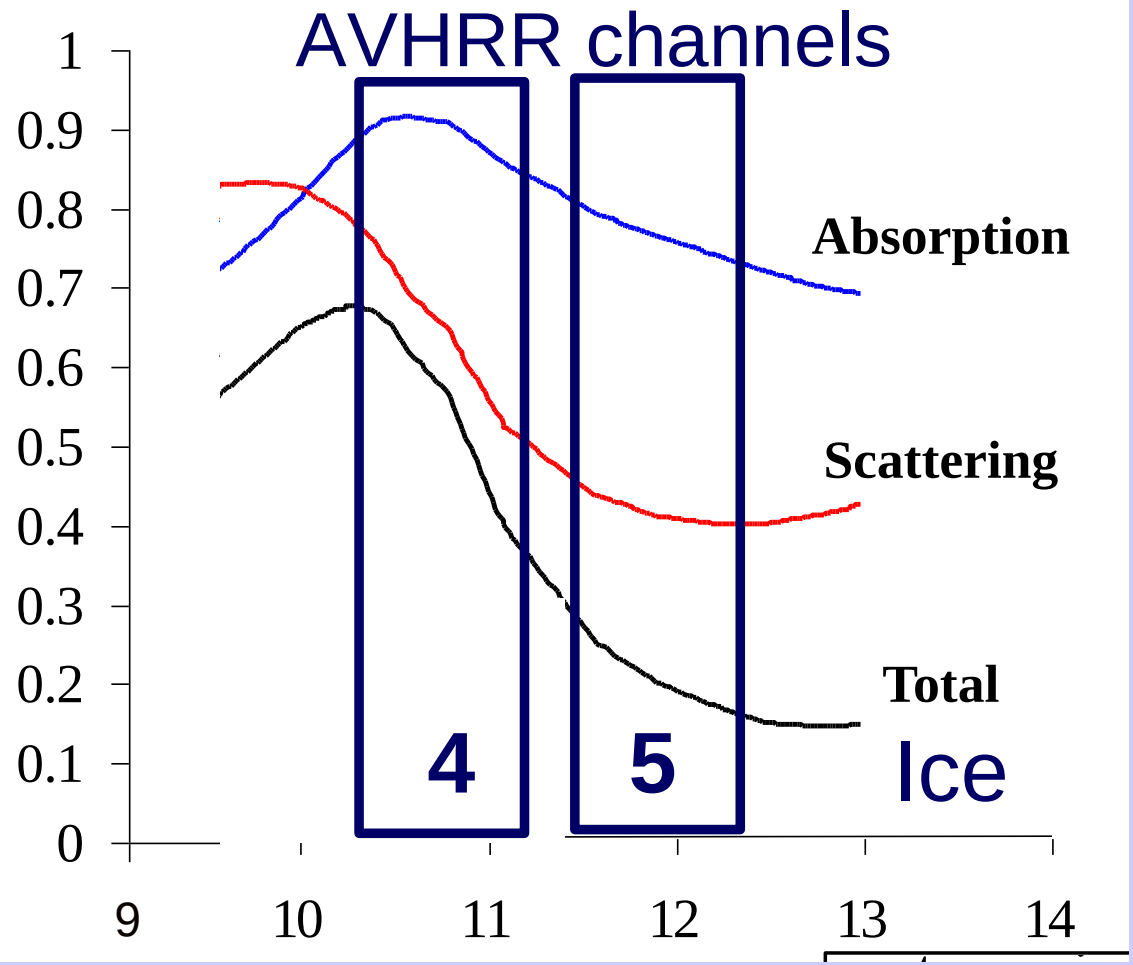

BT11-BT12 > 0 for ice

MODIS RGB Cloud Image

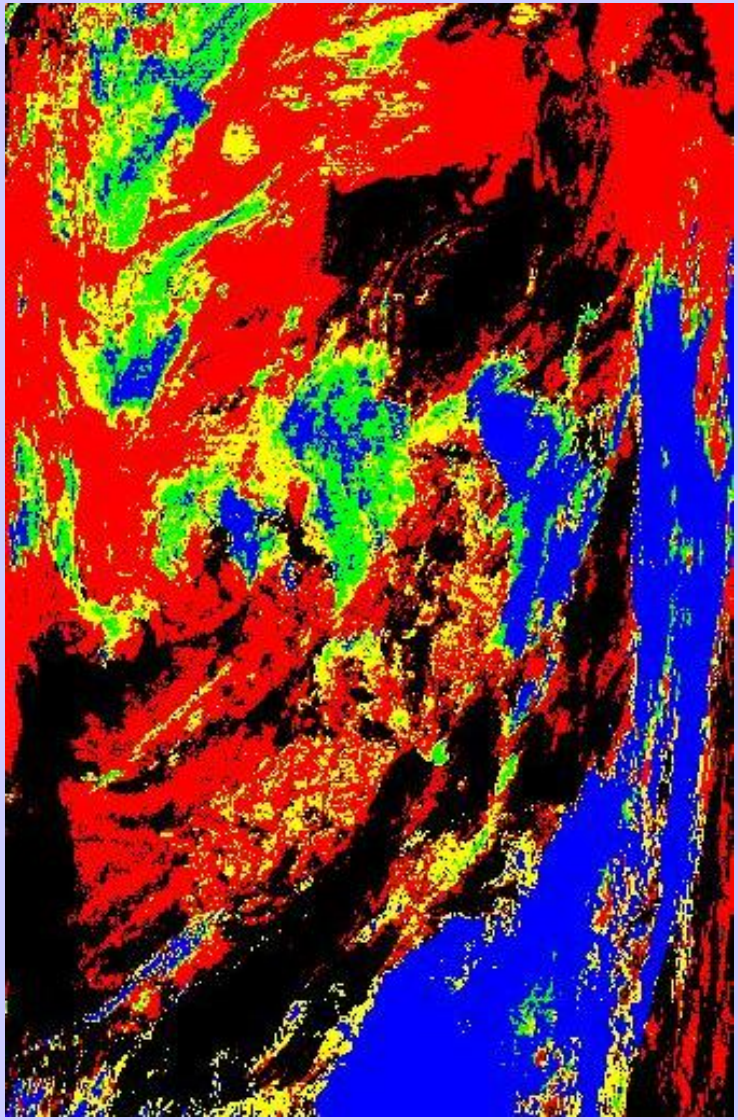

CIRRUS FORMATION BY CONTRAILS OVER CENTRAL U.S. IN GOES-8 IR IMAGERY October 26, 1996

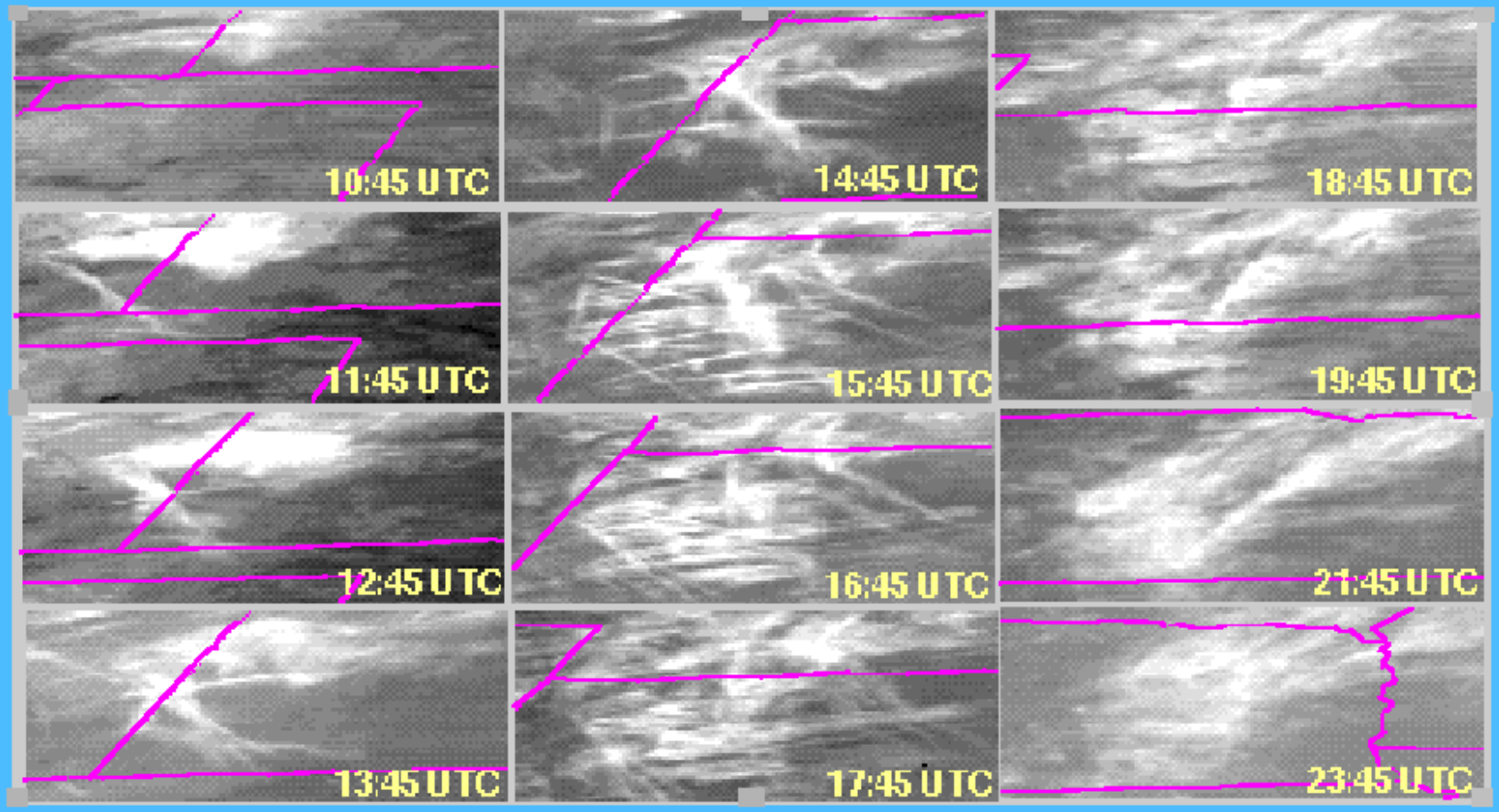

Minnis et al., *Science*, 1999

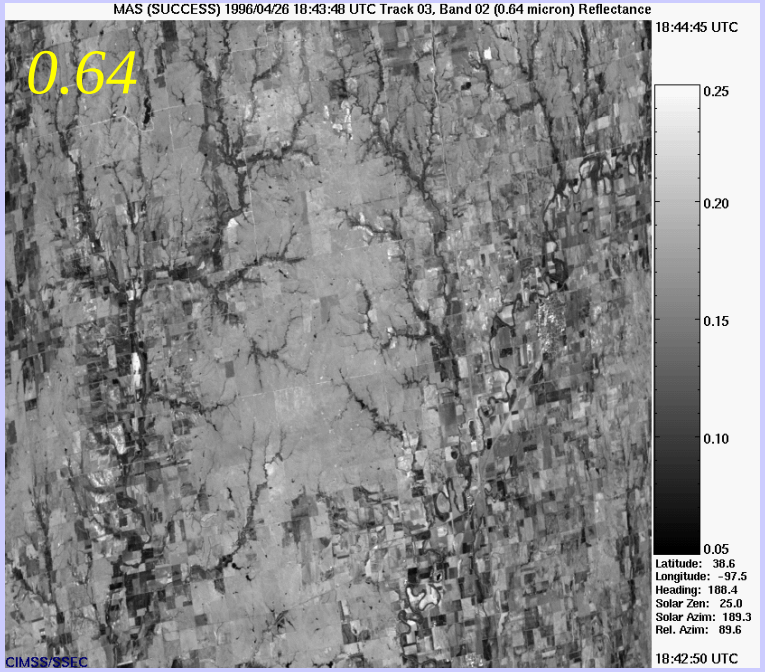
MAS (SUCCESS) 1996/04/26 18:43:48 UTC Track 03, Band 02 (0.64 micron) Reflectance
0.64
18:44:45 UTC
0.25
0.20
0.15
0.10
0.05
Latitude: 38.6
Longitude: -97.5
Heading: 188.4
Solar Zen: 25.0
Solar Azim: 189.3
Rel. Azim: 89.6
18:42:50 UTC
CIMSS/SSEC

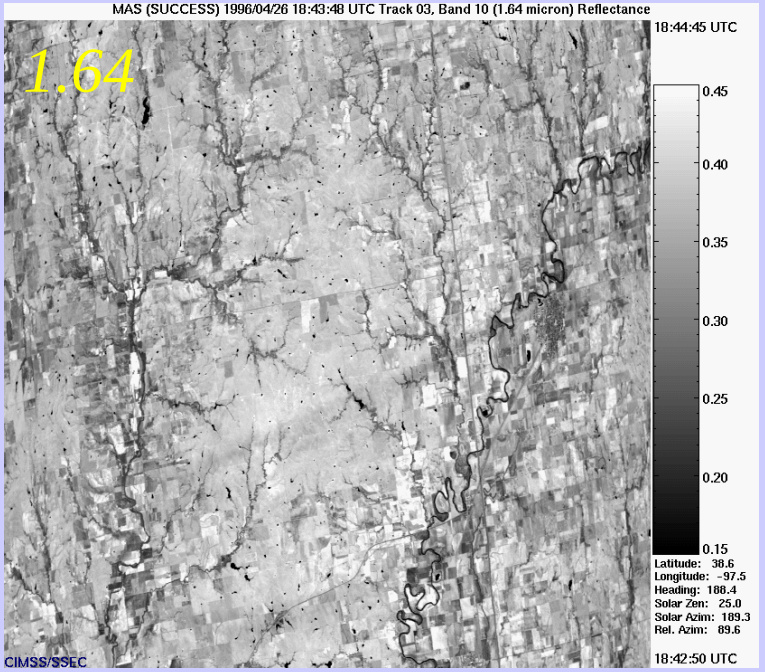
MAS (SUCCESS) 1996/04/26 18:43:48 UTC Track 03, Band 10 (1.64 micron) Reflectance
1.64
18:44:45 UTC
0.45
0.40
0.35
0.30
0.25
0.20
0.15
Latitude: 38.6
Longitude: -97.5
Heading: 188.4
Solar Zen: 25.0
Solar Azim: 189.3
Rel. Azim: 89.6
18:42:50 UTC
CIMSS/SSEC

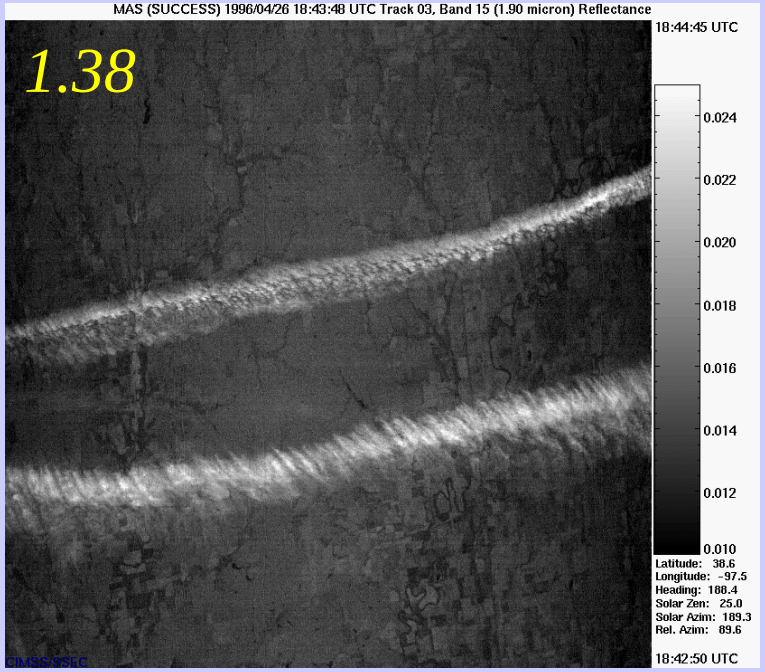
MAS (SUCCESS) 1996/04/26 18:43:48 UTC Track 03, Band 15 (1.90 micron) Reflectance
1.38
18:44:45 UTC
0.024
0.022
0.020
0.018
0.016
0.014
0.012
0.010
Latitude: 38.6
Longitude: -97.5
Heading: 188.4
Solar Zen: 25.0
Solar Azim: 189.3
Rel. Azim: 89.6
18:42:50 UTC
CIMSS/SSEC

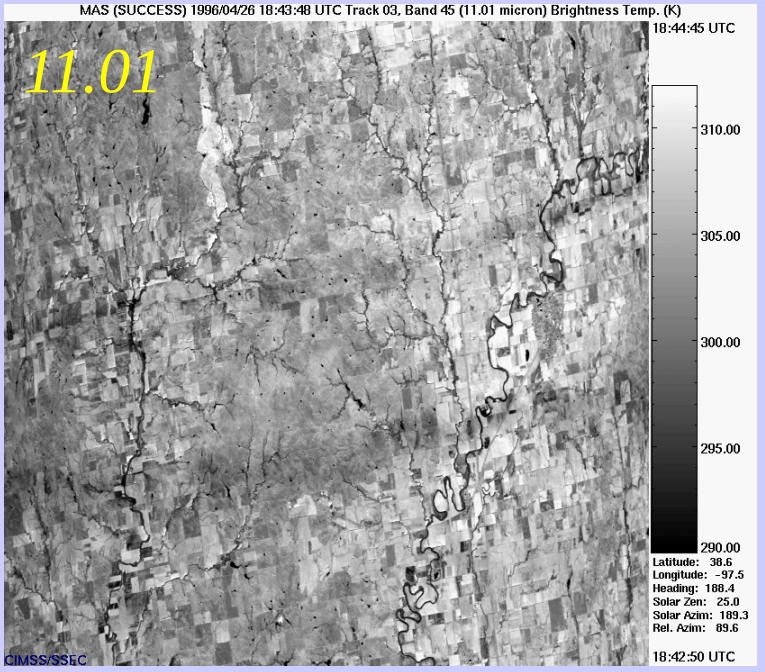
MAS (SUCCESS) 1996/04/26 18:43:48 UTC Track 03, Band 45 (11.01 micron) Brightness Temp. (K)
11.01
18:44:45 UTC
310.00
305.00
300.00
295.00
290.00
Latitude: 38.6
Longitude: -97.5
Heading: 188.4
Solar Zen: 25.0
Solar Azim: 189.3
Rel. Azim: 89.6
18:42:50 UTC
CIMSS/SSEC

Is cirrus related to air traffic?

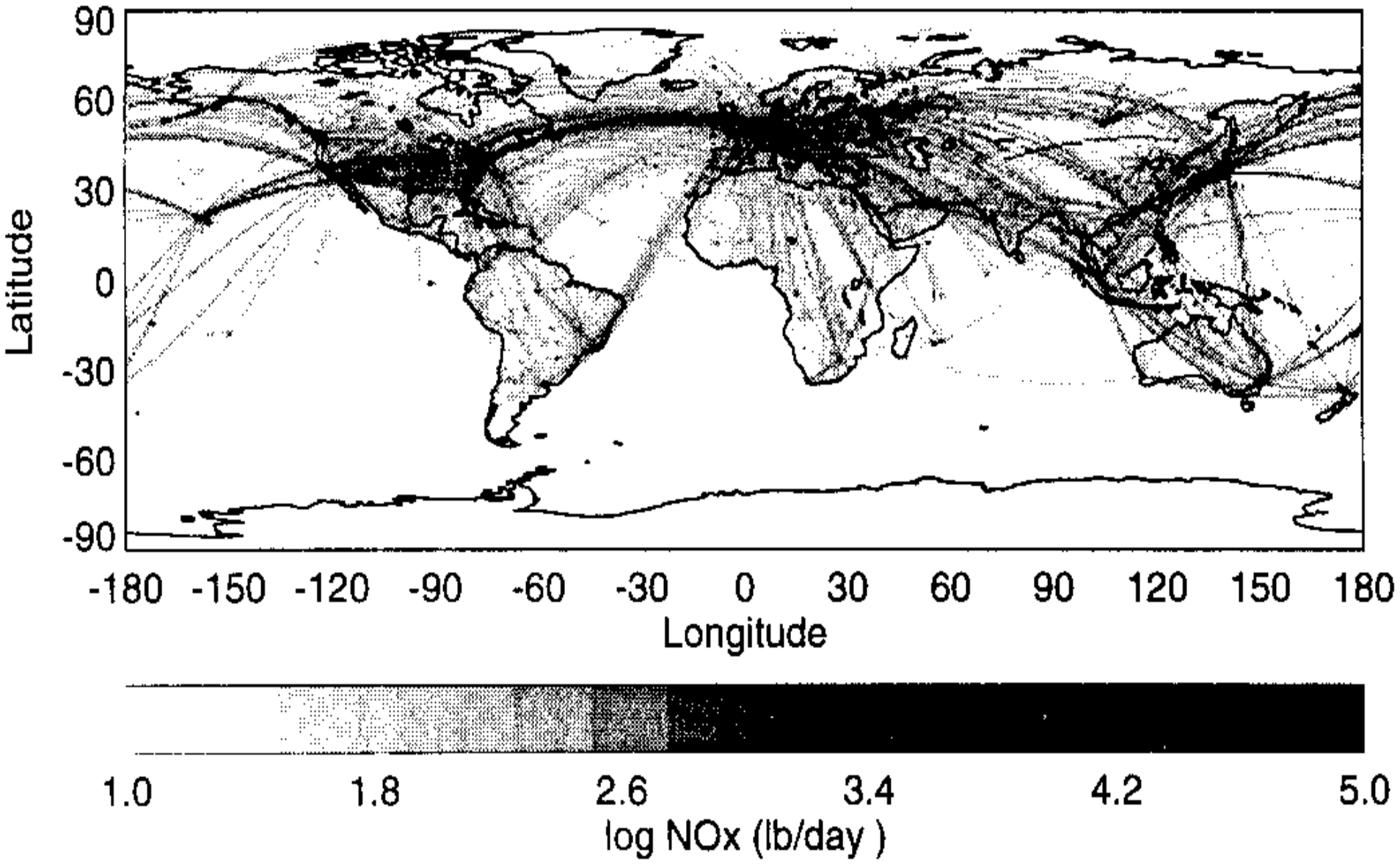

Ice Clouds have particles of many sizes and shapes

3 layer model

*1 km 10 to 50 um spheres

*1 km 300 um columns

*2 km 150 um aggregates and bullet rosettes.

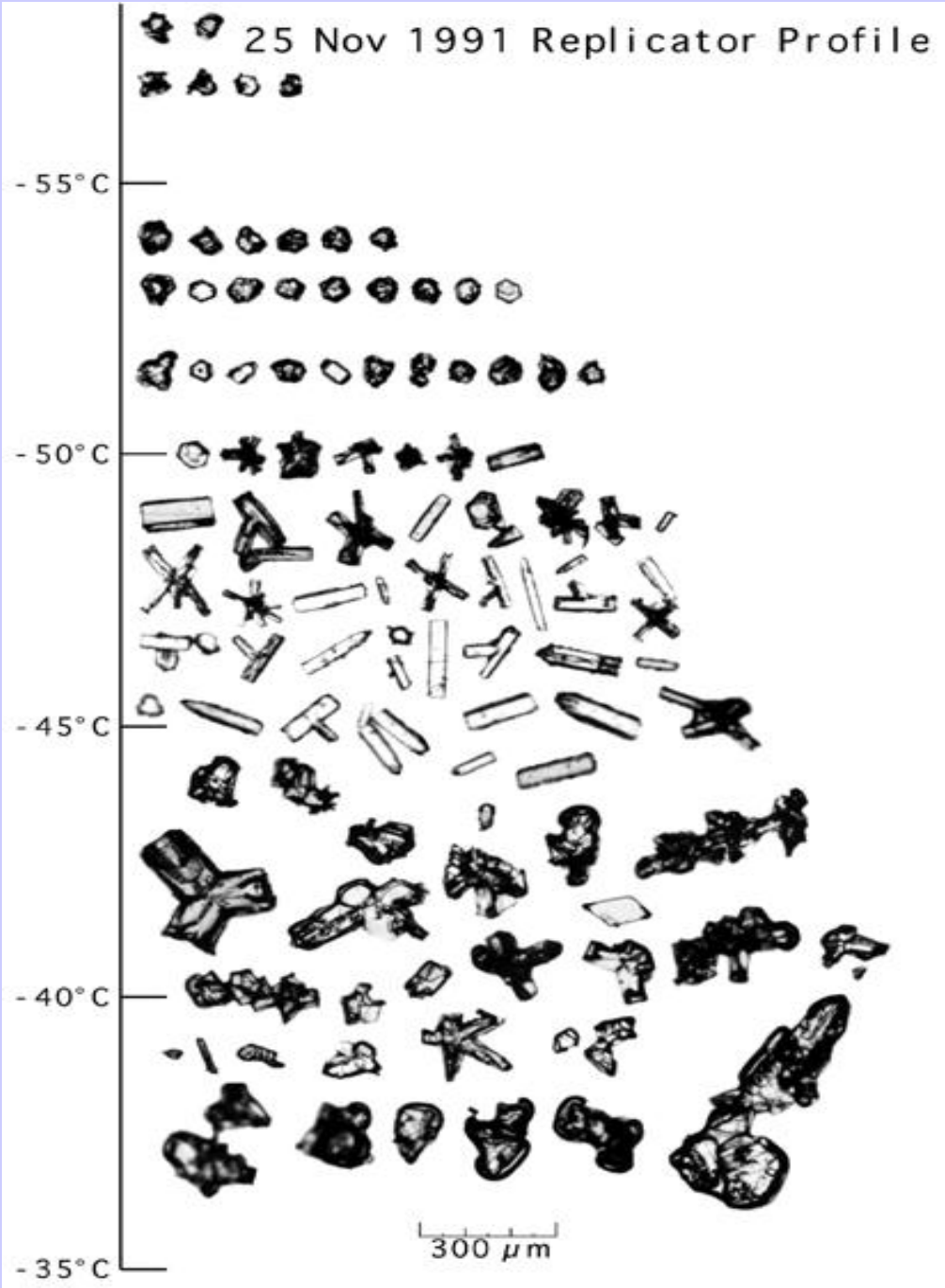

MODIS detects ship tracks

Ship Tracks occur in marine stratocumulus regions of the globe

- California, Azores, Namibia, and Peru

Conditions for formation

- High humidity
- Small air-sea temperature difference
- Low wind speed
- Boundary layer between 300 and 750 m deep

Enhanced reflectance of clouds at 3.7 µm

- Larger number of small droplets arising from particulate emission from ships

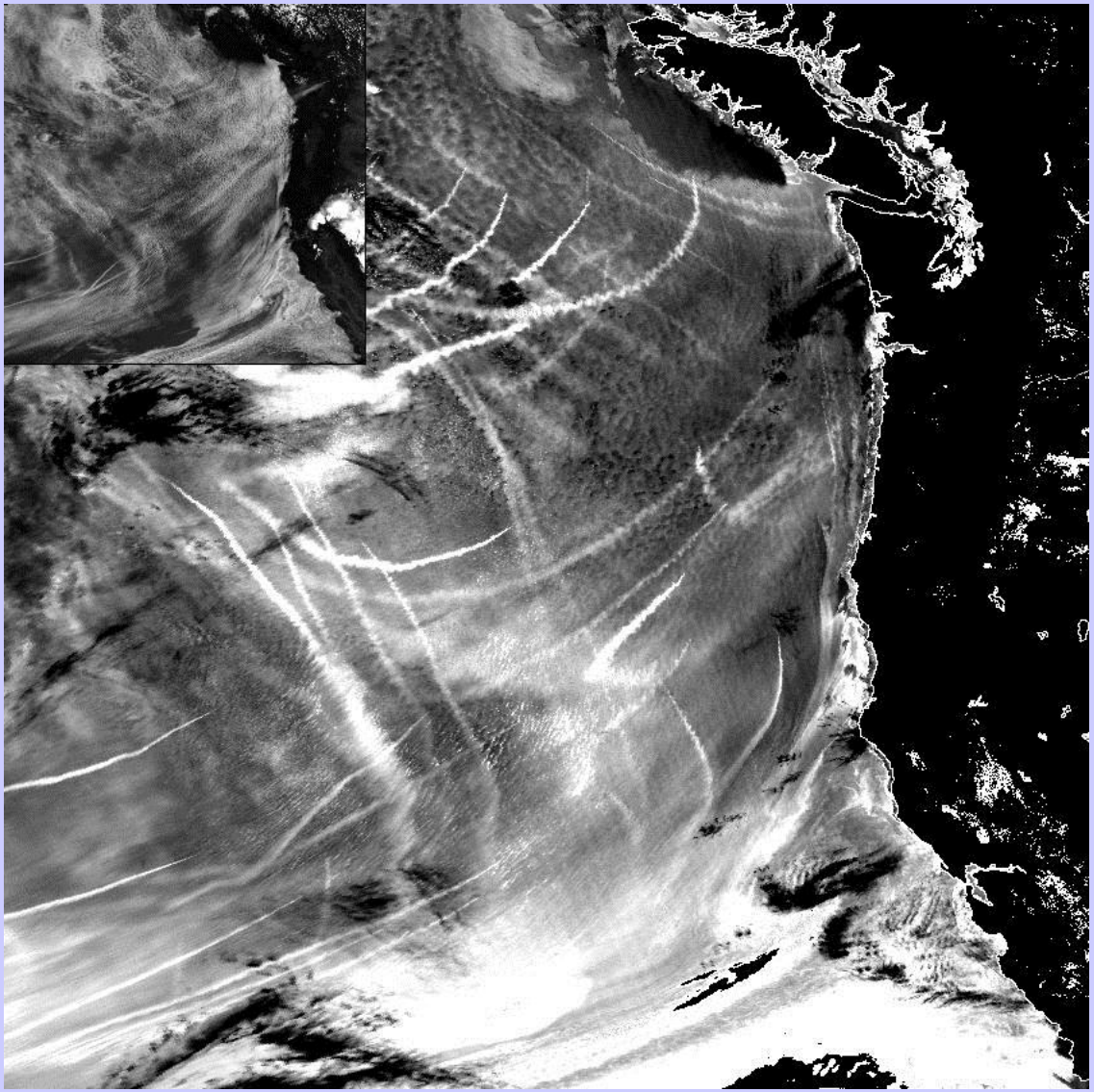

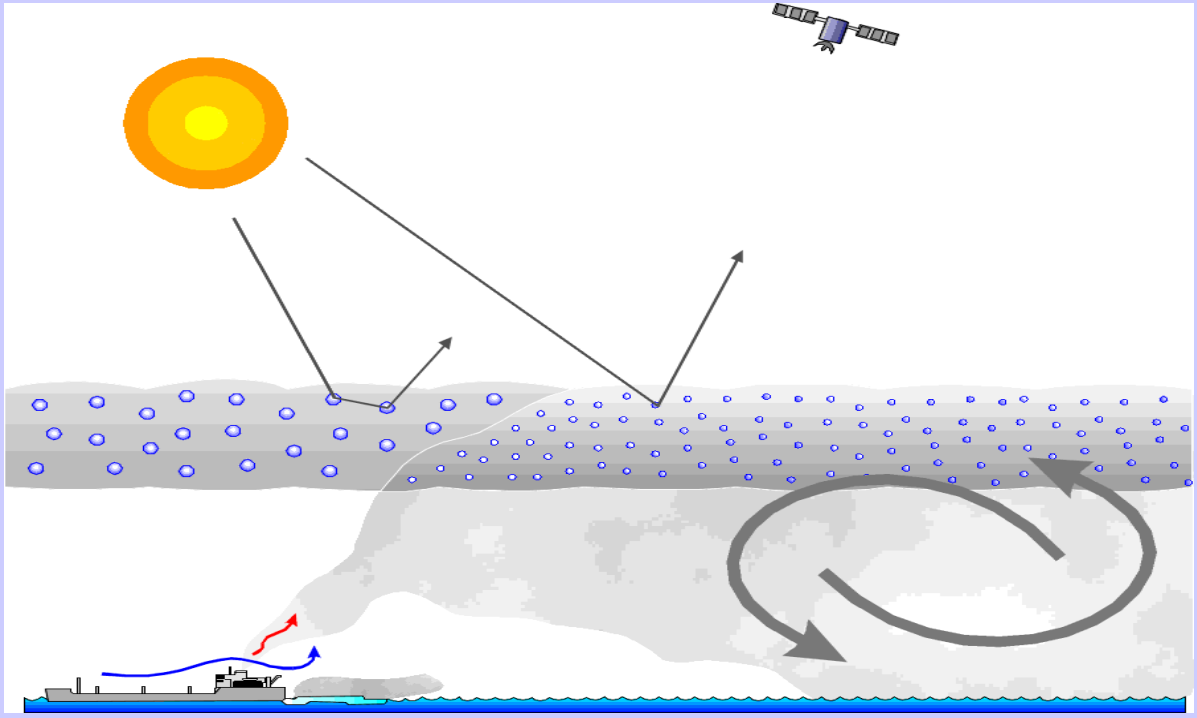

* Particles emitted by ships increase concentration of cloud condensation nuclei (CCN) in the air
* Increased CCN increase concentration of cloud droplets and reduce average size of the droplets
* Increased concentration and smaller particles reduce production of drizzle (100 μm radius) droplets in clouds
* Liquid water content increases because loss of drizzle particles is suppressed
* Clouds are *optically thicker* and brighter along ship track

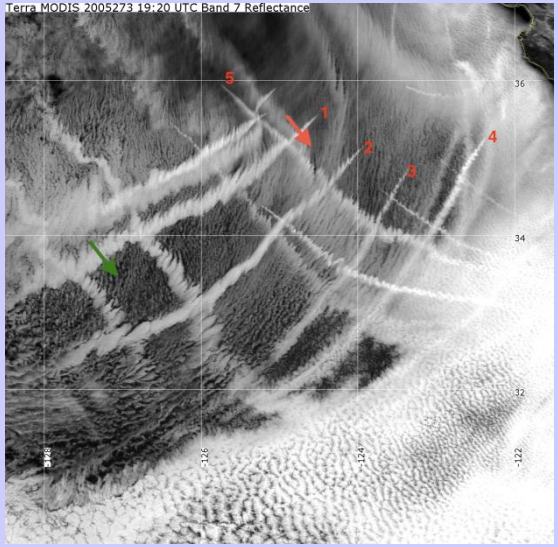
Terra MODIS 2005273 19:20 UTC Band 7 Reflectance
5
1
2
3
4
36
34
32
-126
-124
-122

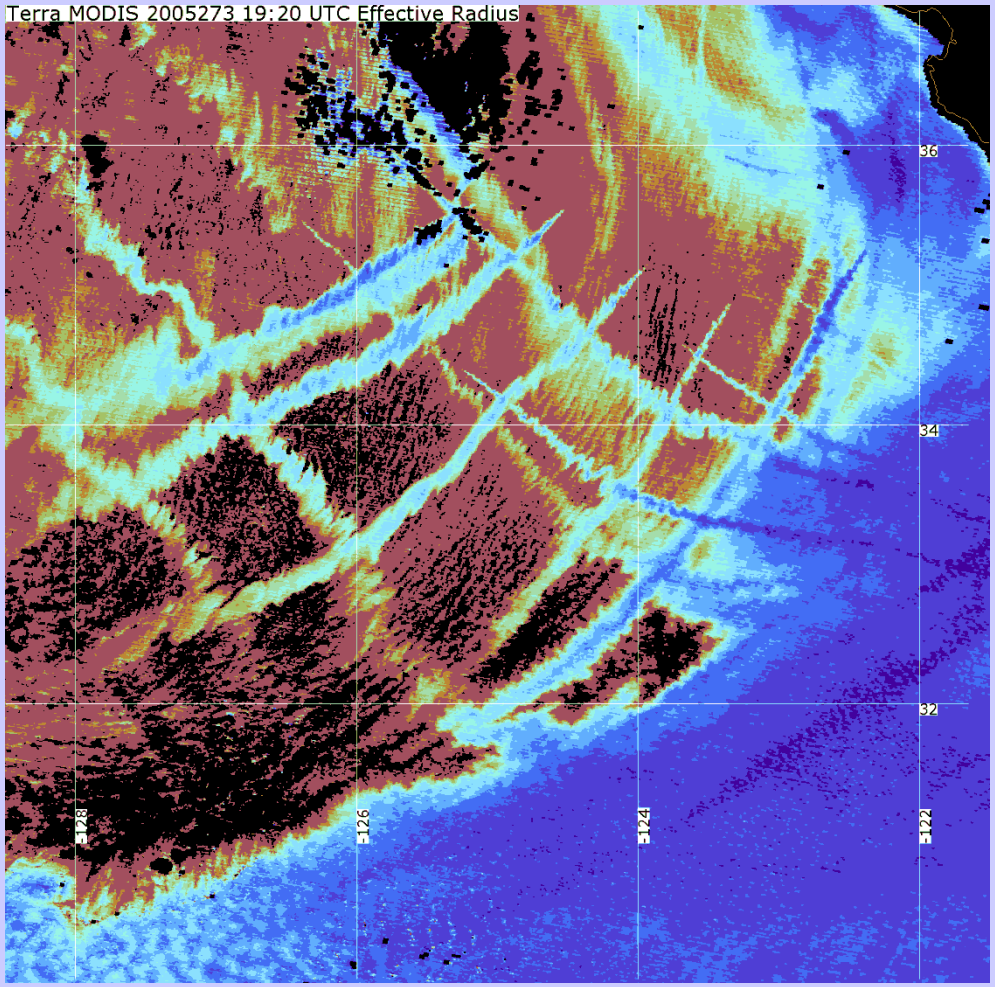
Terra MODIS 2005273 19:20 UTC Effective Radius
36
34
32
-128
-126
-124
-122

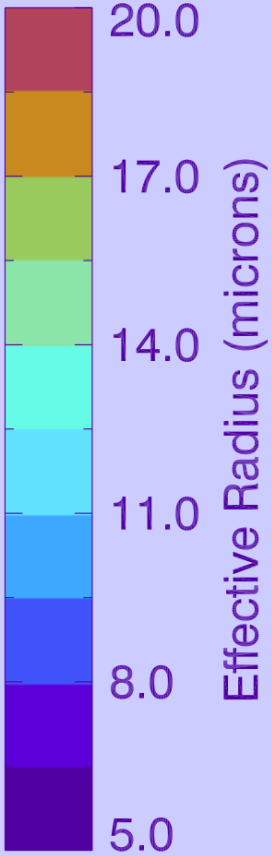
20.0
17.0
14.0
11.0
8.0
5.0
Effective Radius (microns)

Cloud Clearing

For a single layer of clouds, radiances in one spectral band vary linearly with those of another as cloud amount varies from one field of view (fov) to another

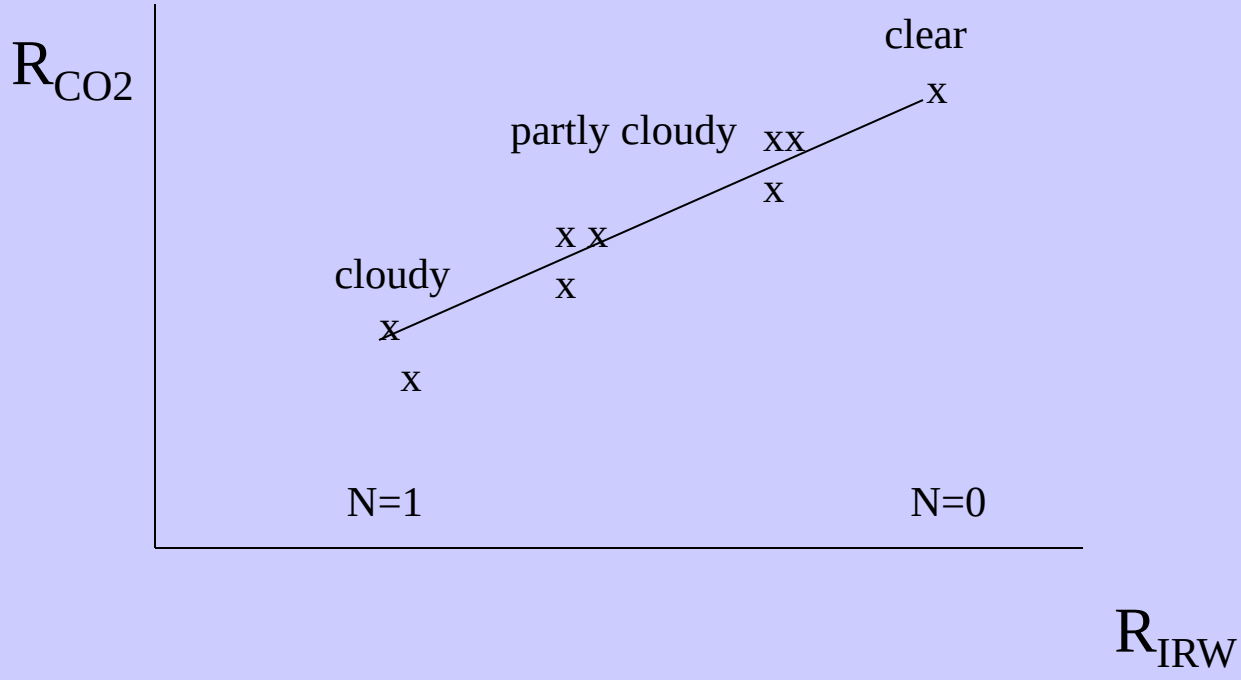

Clear radiances can be inferred by extrapolating to cloud free conditions.

Paired field of view proceeds as follows. For a given wavelength λ, radiances from two spatially independent, but geographically close, fields of view are written

$$I_{\lambda,1} = \eta_1 I_{\lambda,1}^{cd} + (1 - \eta_1) I_{\lambda,1}^{c} \quad ,$$

$$I_{\lambda,2} = \eta_2 I_{\lambda,2}^{cd} + (1 - \eta_2) I_{\lambda,2}^{c} \quad ,$$

If clouds are at uniform altitude, and clear air radiance is in each FOV

$$I_\lambda^{cd} = I_{\lambda,1}^{cd} = I_{\lambda,2}^{cd}$$

$$I_\lambda^{c} = I_{\lambda,1}^{c} = I_{\lambda,2}^{c}$$

$$\frac{\eta_1 \ (I_\lambda^{cd} - I_\lambda^{c})}{\eta_2 \ (I_\lambda^{cd} - I_\lambda^{c})} = \frac{\eta_1}{\eta_2} = \eta^* = \frac{I_{\lambda,1} - I_\lambda^{c}}{I_{\lambda,2} - I_\lambda^{c}} \ ,$$

where η^* is the ratio of the cloud amounts for the two geographically independent fields of view of the sounding radiometer. Therefore, the clear air radiance from an area possessing broken clouds at a uniform altitude is given by

$$I_\lambda^{c} = [\, I_{\lambda,1} - \eta^* I_{\lambda,2}] \,/[1 - \eta^*]$$

where η^* still needs to be determined. Given an independent measurement of surface temperature, T_s, and measurements $I_{w,1}$ and $I_{w,2}$ in a spectral window channel, then η^* can be determined by

$$\eta^* = [I_{w,1} - B_w(T_s)] \,/\, [I_{w,2} - B_w(T_s)]$$

and I_λ^c for different spectral channels can be solved.

Applications with Multispectral Remote Sensing Data

Satellite Remote Sensing

Energy Balance

VIS, IR, and MW Radiative Transfer

EOS Terra & Aqua MODIS

Multispectral Signatures

*(Ocean Color, SST, Snow/Ice, Vegetation, Aerosols, Clouds, **Moisture**, Fires, Volcanic Ash)*

Detecting Climate Trends

Water vapour evaluated in multiple infrared window channels where absorption is weak, so that

$$\tau_w = \exp[- k_w u] \sim 1 - k_w u \text{ where w denotes window channel}$$

and

$$d\tau_w = - k_w du$$

What little absorption exists is due to water vapour, therefore, u is a measure of precipitable water vapour. RTE in window region

$$I_w = B_{sw} (1-k_w u_s) + k_w \int_o^{u_s} B_w du$$

u_s represents total atmospheric column absorption path length due to water vapour, and s denotes surface. Defining an atmospheric mean Planck radiance, then

$$I_w = B_{sw} (1-k_w u_s) + k_w u_s \bar{B}_w \text{ with } \bar{B}_w = \int_o^{u_s} B_w du \Big/ \int_o^{u_s} du$$

Since B_{sw} is close to both I_w and B_w, first order Taylor expansion about the surface temperature T_s allows us to linearize the RTE with respect to temperature, so

$T_{bw} = T_s (1-k_w u_s) + k_w u_s \bar{T}_w$, where T_w is mean atmospheric temperature corresponding to B_w.

For two window channels (11 and 12um) the following ratio can be determined.

$$\frac{T_s - T_{bw1}}{T_s - T_{bw2}} = \frac{k_{w1} u_s (T_s - \bar{T}_{w1})}{k_{w1} u_s (T_s - \bar{T}_{w2})} = \frac{k_{w1}}{k_{w2}}$$

where the mean atmospheric temperature measured in the one window region is assumed to be comparable to that measured in the other, $T_{w1} \sim T_{w2}$,

Thus it follows that

$$T_s = T_{bw1} + \frac{k_{w1}}{k_{w2} - k_{w1}} [T_{bw1} - T_{bw2}]$$

and

$$u_s = \frac{T_{bw} - T_s}{k_w (\bar{T}_w - T_s)} .$$

Obviously, the accuracy of the determination of the total water vapour concentration depends upon the contrast between the surface temperature, T_s, and

the effective temperature of the atmosphere $\bar{T}_w$

Global TPW from Seemann

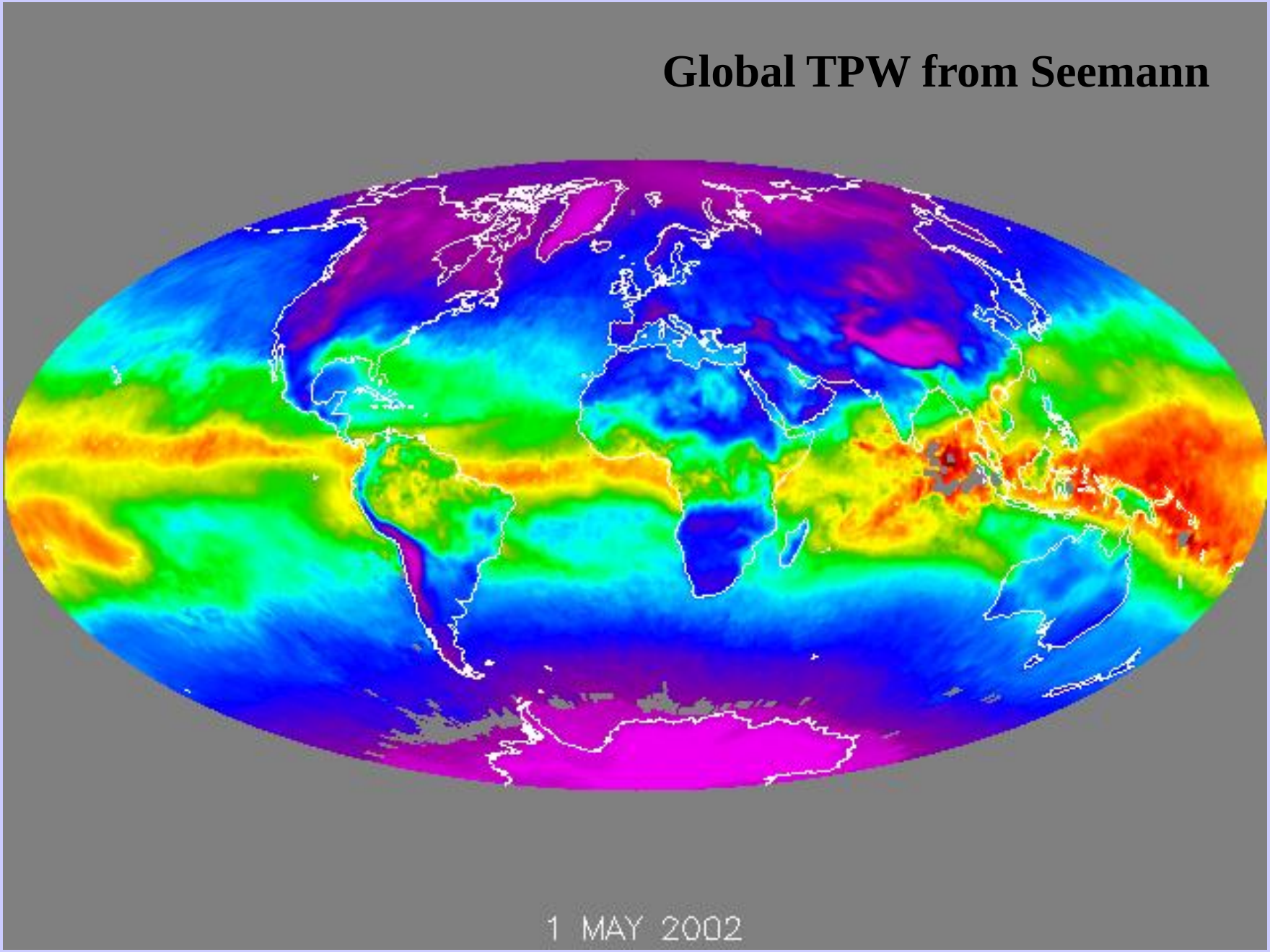

T(p)

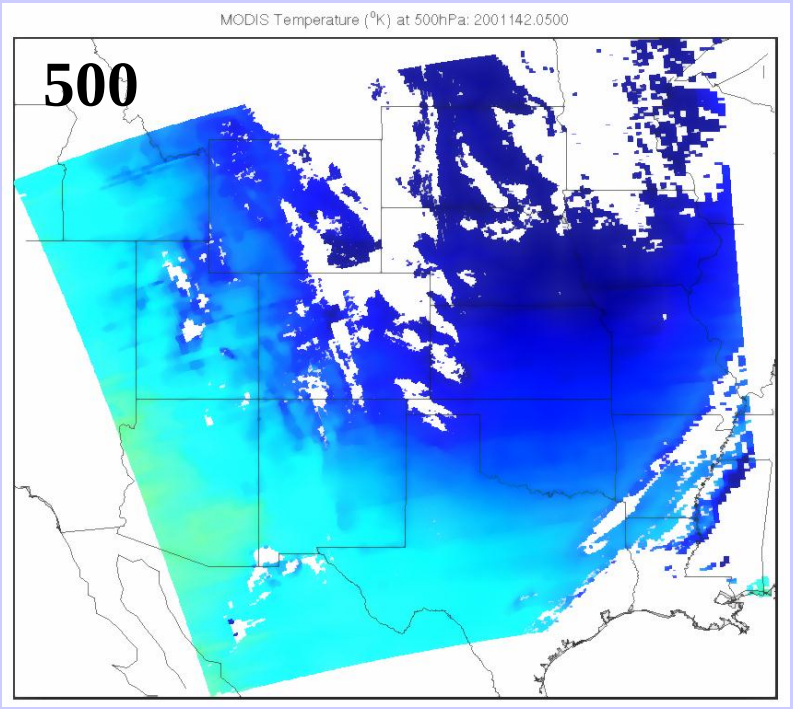
MODIS Temperature (°K) at 500hPa: 2001142.0500
500

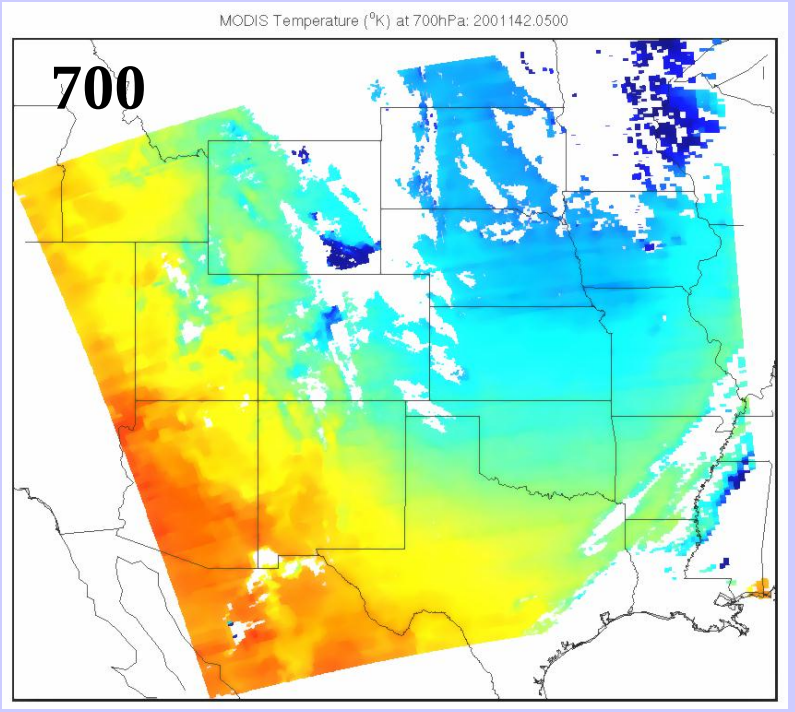
MODIS Temperature (°K) at 700hPa: 2001142.0500
700

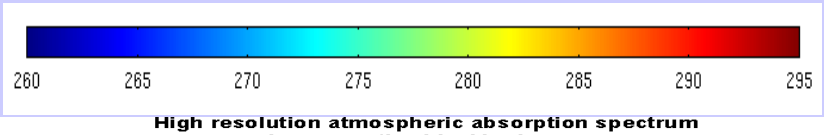
260
265
270
275
280
285
290
295

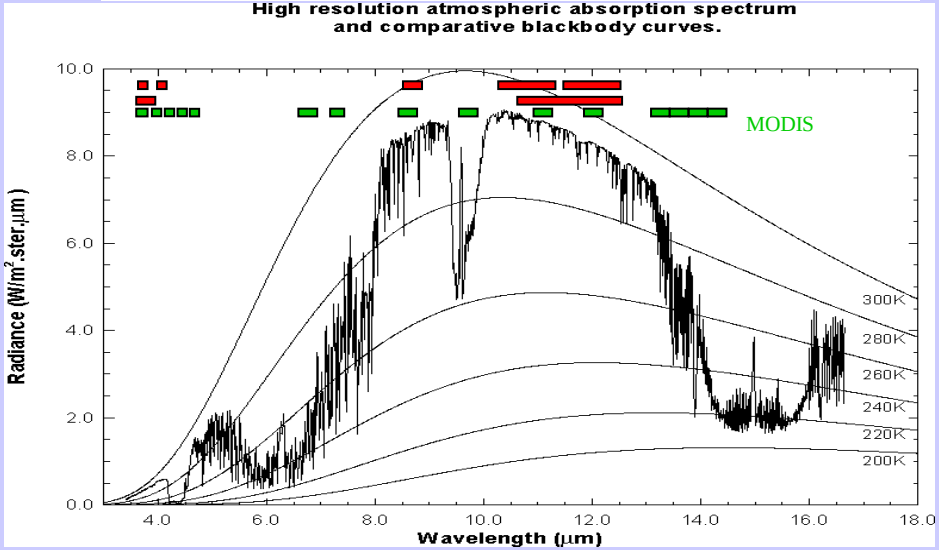
High resolution atmospheric absorption spectrum
and comparative blackbody curves.
MODIS
Radiance (W/m².ster.μm)
Wavelength (μm)
300K
280K
260K
240K
220K
200K

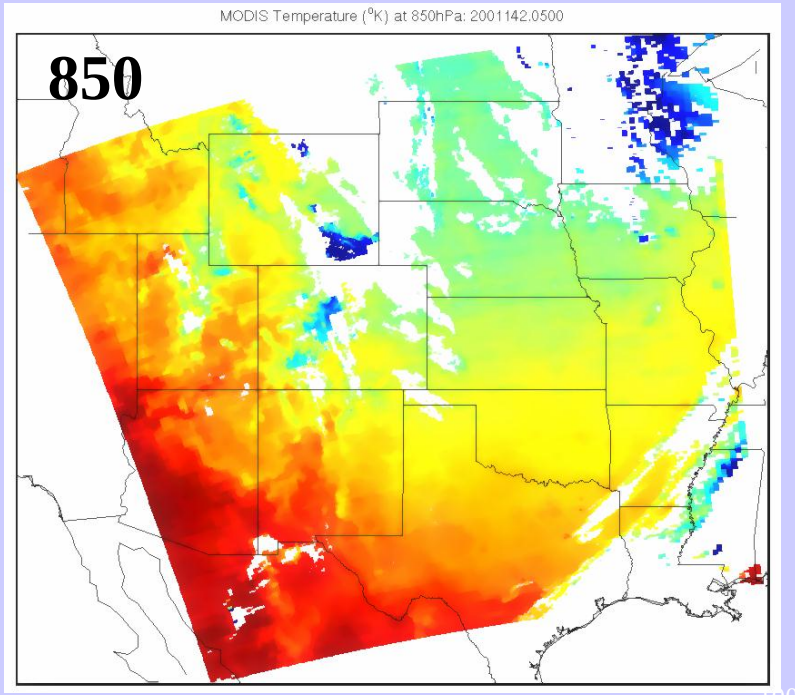
MODIS Temperature (°K) at 850hPa: 2001142.0500
850

MODIS TPW

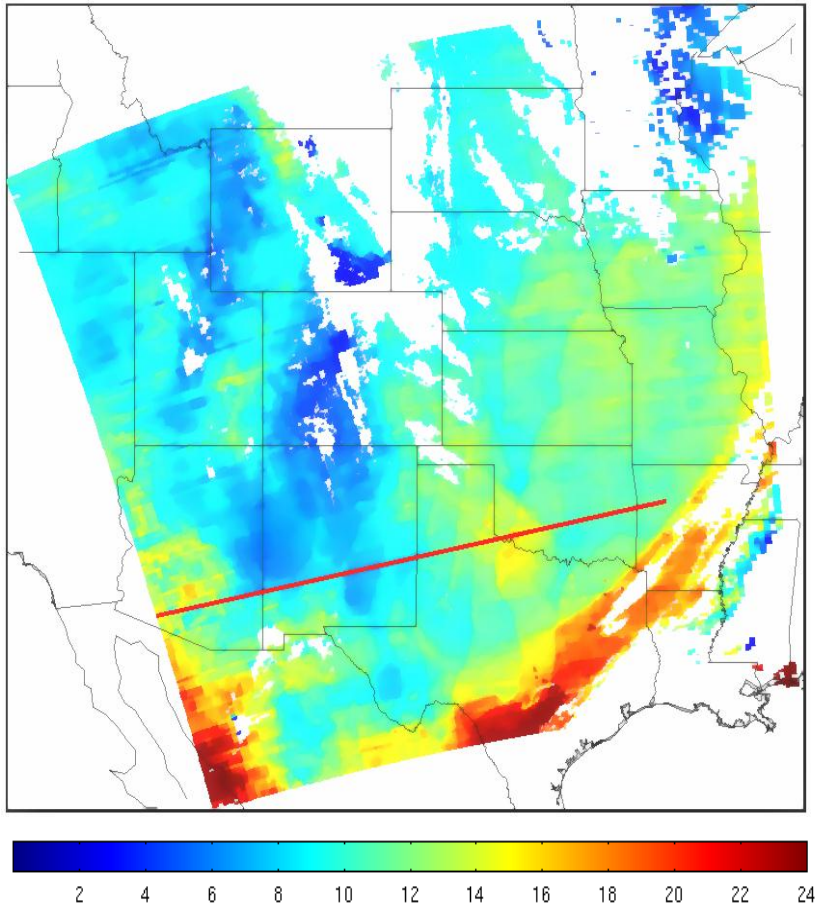

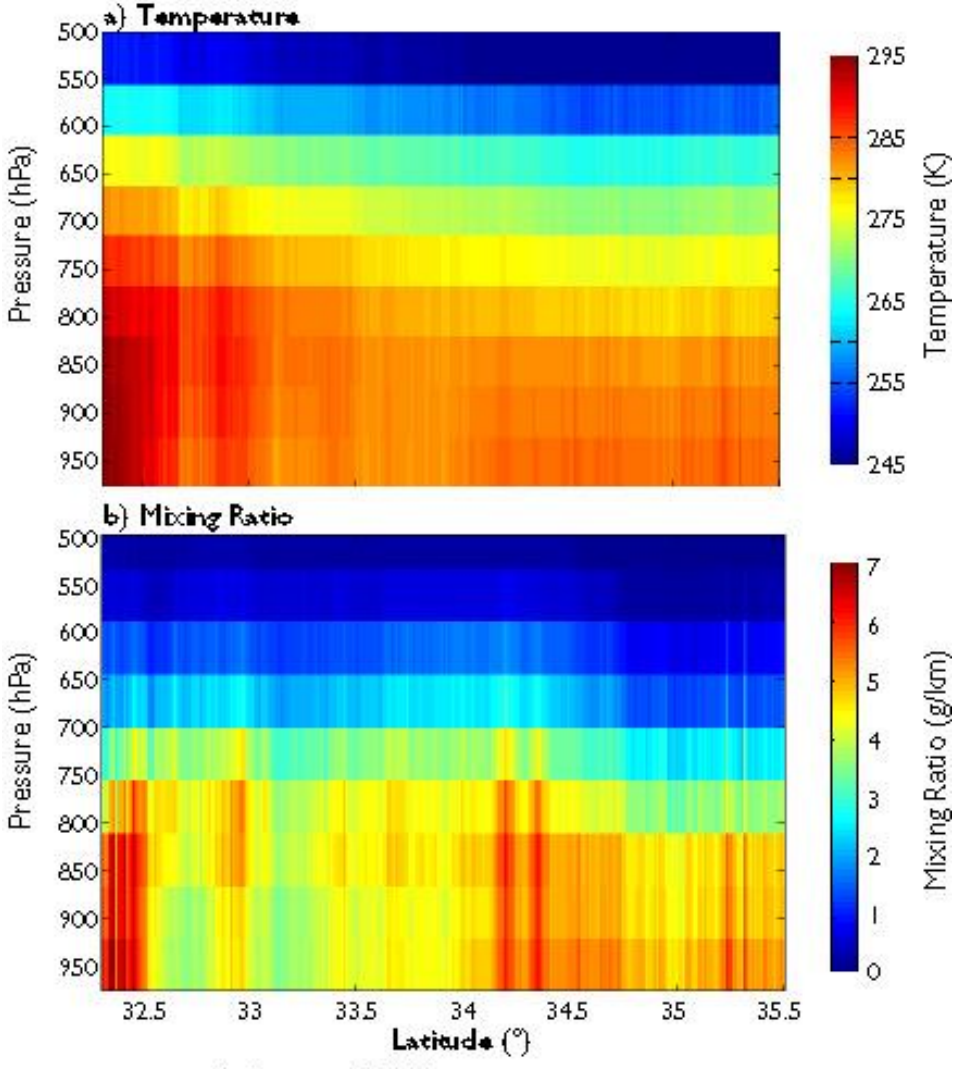

Clear sky layers of temperature and moisture on 2 June 2001

Applications with Multispectral Remote Sensing Data

Satellite Remote Sensing

Energy Balance

VIS, IR, and MW Radiative Transfer

EOS Terra & Aqua MODIS

Multispectral Signatures

(Ocean Color, SST, Snow/Ice, Vegetation, Aerosols, Clouds, Moisture, ***Fires, Volcanic Ash****)*

Detecting Climate Trends

Active Fire Detection

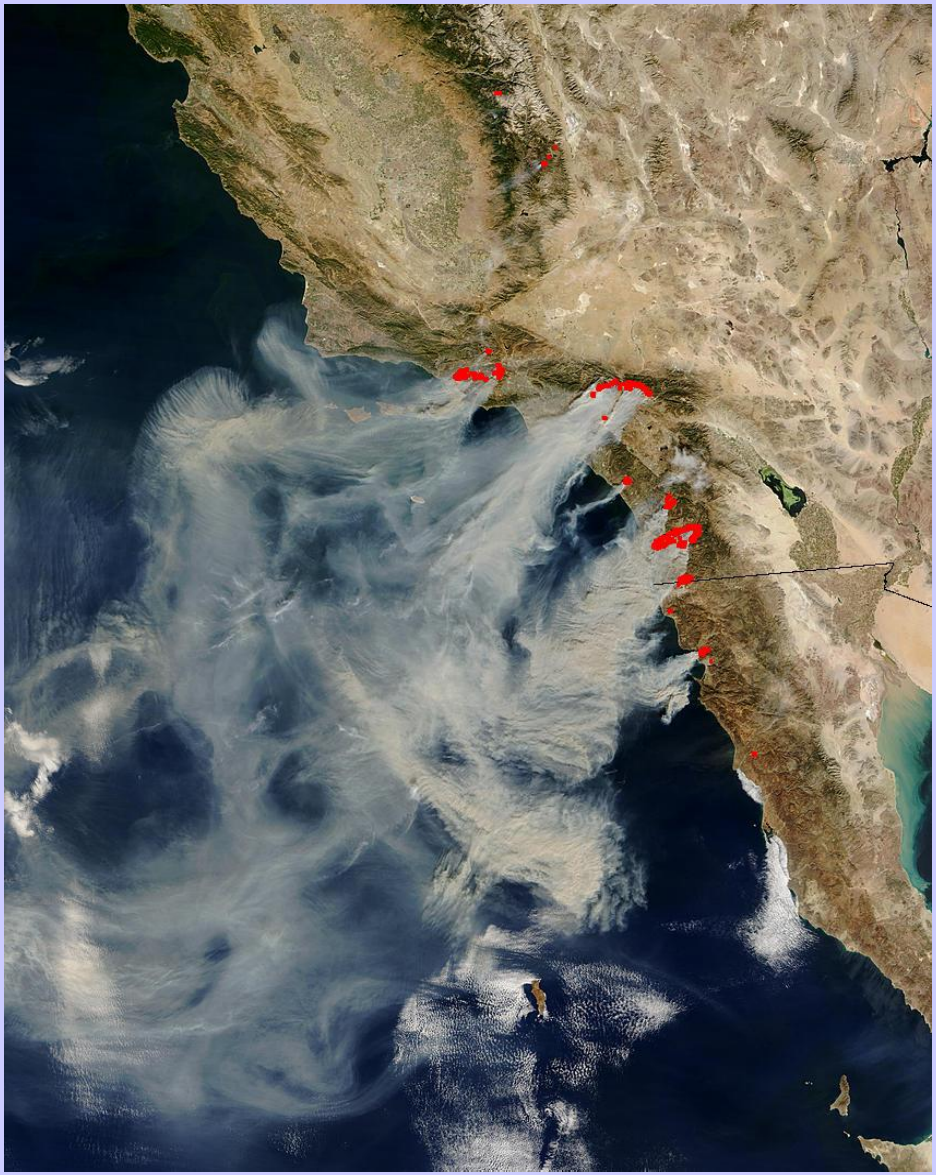

California – 10/26/03

- The algorithm considers the spectral signature (in middle and thermal infrared) of each pixel and compares it to the non-burning surrounding pixels
- The natural variability of the surrounding background is taken into account
- Fewer false detections than traditional threshold-based algorithms
- Sensitive enough to detect small fires

(Giglio et al., 2003)

The fire extent and temperature within a field of view can be determined by considering the upwelling thermal radiance values obtained by both channels (Matson and Dozier, 1981; Dozier, 1981). For a given channel, λ, the radiative transfer equation indicates

$$R_\lambda(T) = \varepsilon_\lambda B_\lambda(Ts)\,\tau_\lambda(s) + \int_0^1 B_\lambda(T)\,d\tau_\lambda$$

When the GOES radiometer senses radiance from a pixel containing a target of blackbody temperature T_t occupying a portion p (between zero and one) of the pixel and a background of blackbody temperature T_b occupying the remainder of the pixel (1-p), the following equations represent the radiance sensed by the instrument at 4 and 11 micron.

$$R_4(T_4) = p\,R_4(T_t) + \varepsilon_4\,(1-p)\,R_4\,(T_b) + (1-\varepsilon_4)\,\tau_4(s)\,R_4(solar)$$

$$R_{11}(T_{11}) = p\,R_{11}(T_t) + \varepsilon_{11}\,(1-p)\,R_{11}(T_b)$$

The observed short wave window radiance also contains contributions due to solar reflection that must be distinguished from the ground emitted radiances; solar reflection is estimated from differences in background temperatures in the 4 and 11 micron channels. Once T_b is estimated from nearby pixels, these two nonlinear equations can be solved for T_t and p. In this study, the solution to the set of equations is found by applying a globally convergent bisection technique followed by Newton's method.

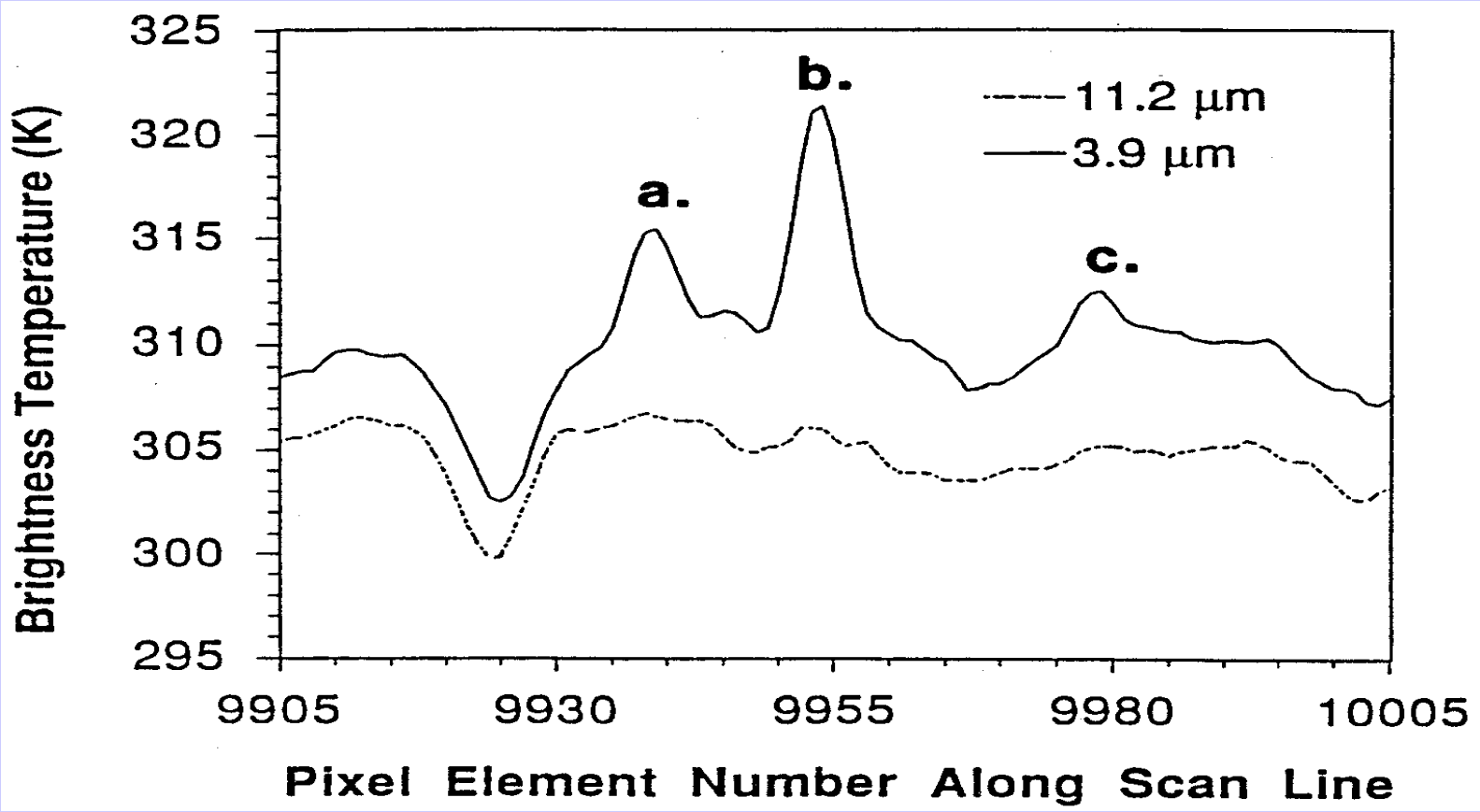

3.9 and 11.2 microns plotted for one scan line over grassland burning in South America; fires are likely at a, b, and c.

Portugal fires 3 Aug 2003

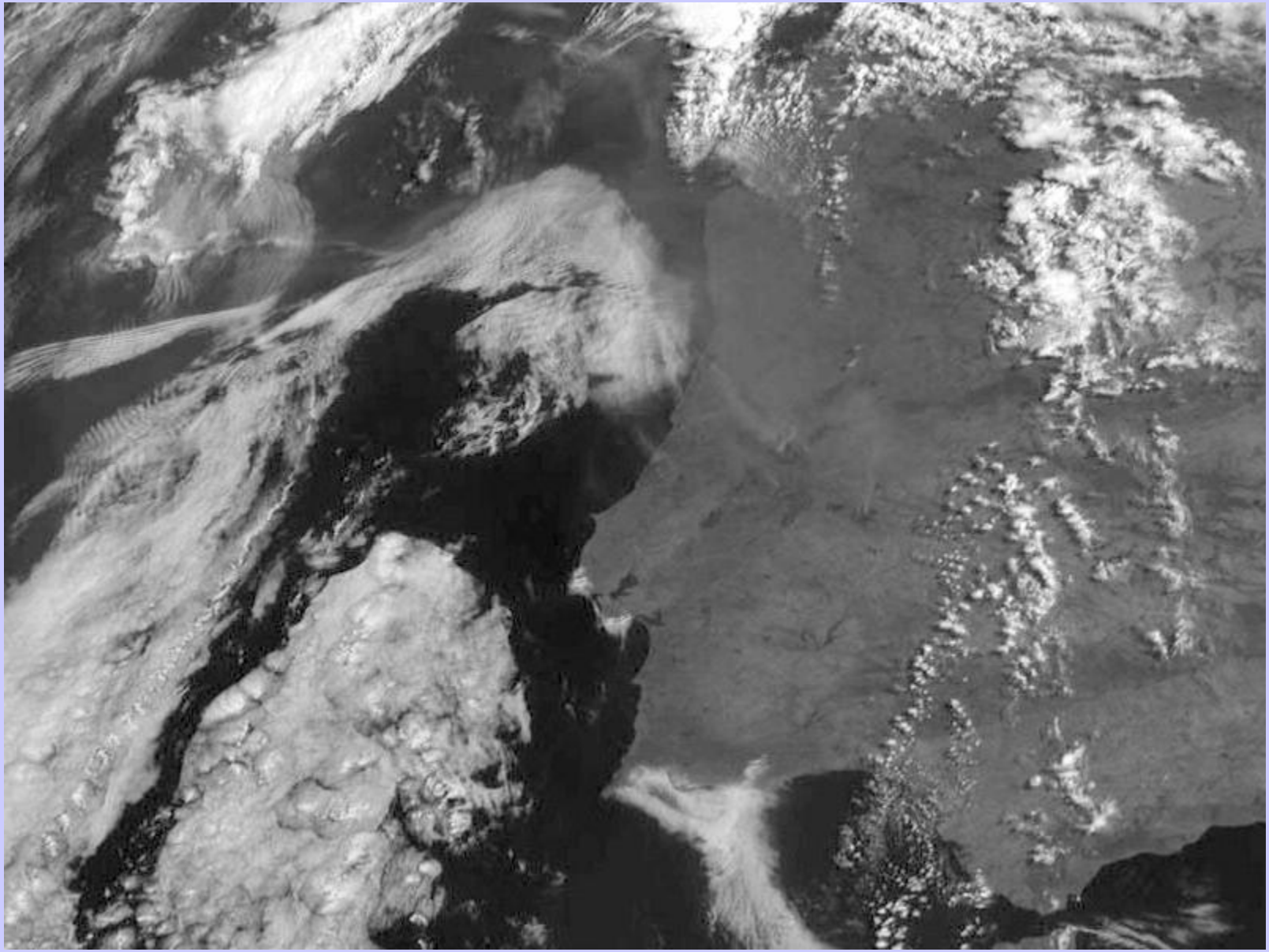

Ash Plume Detection

Mt. Cleveland Eruption 19 Feb 2001

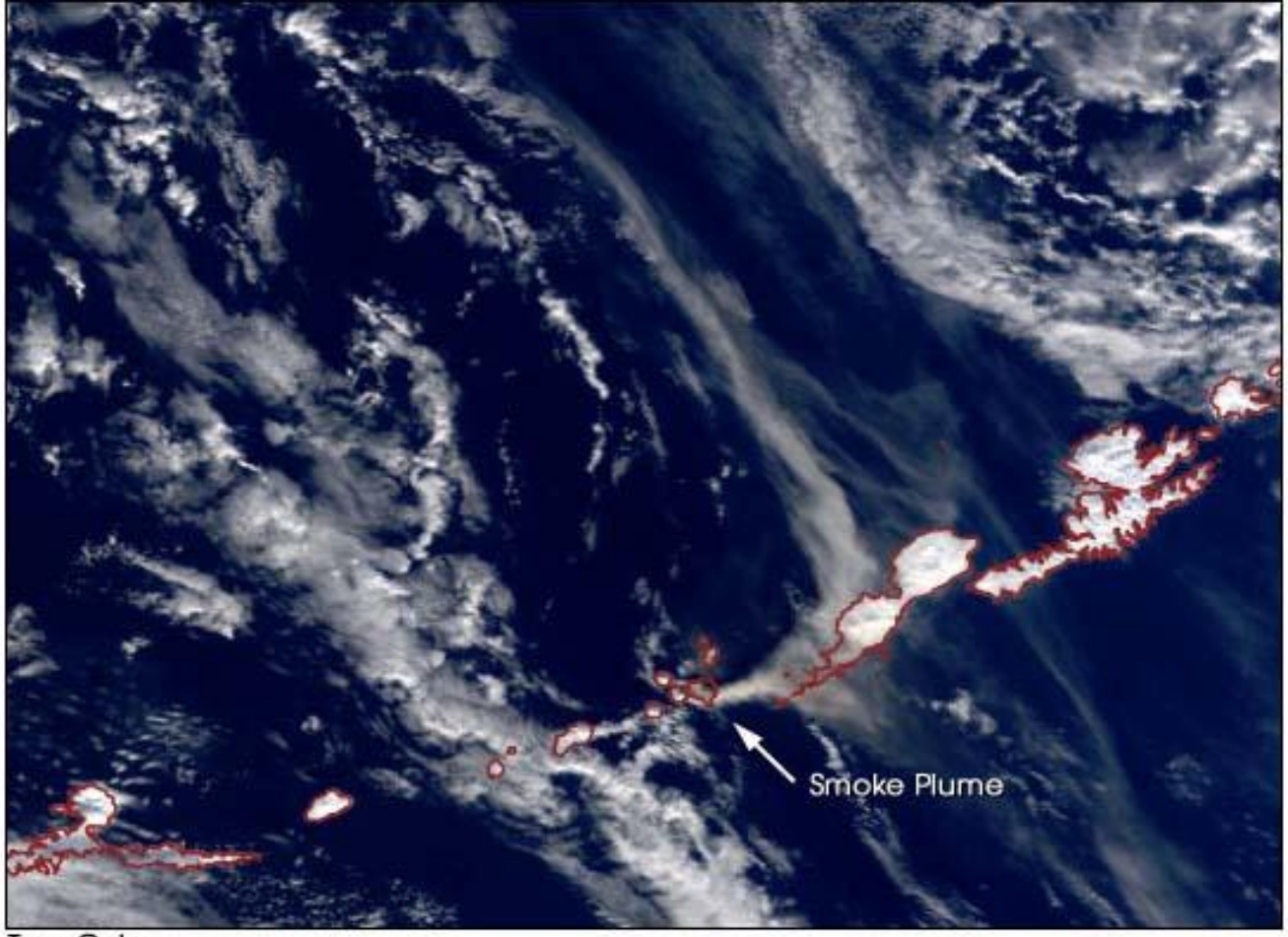

True Color

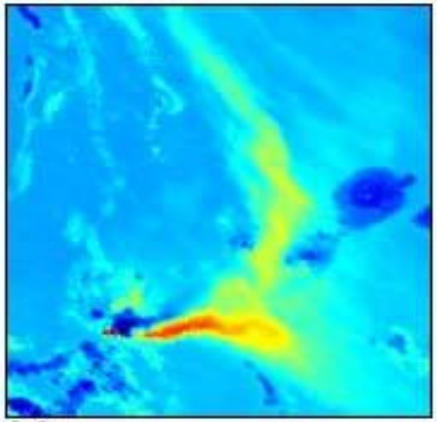

3.9μm

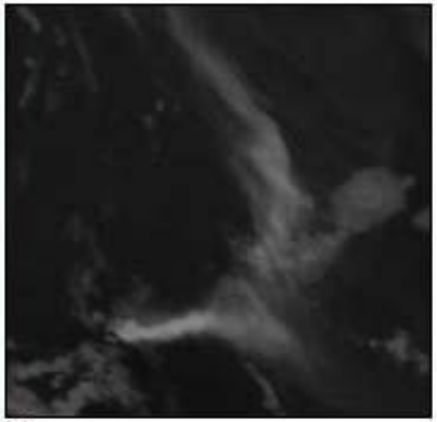

11μm

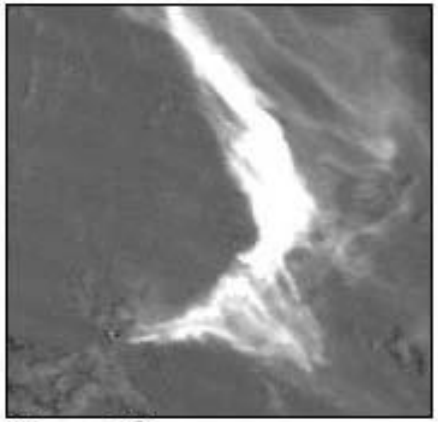

11μm - 12μm

Eyjafjallajökull Eruptions

March 20 to April 12, 2010 - non-ash eruptions, lava fountains

April 14 to May 23, 2010 - mostly explosive ash cloud producing *(ash was visible in satellite imagery 32 out of 41 days)*

Marco Fulle - www.stromboli.net


zh
aw
TECHNORAMA

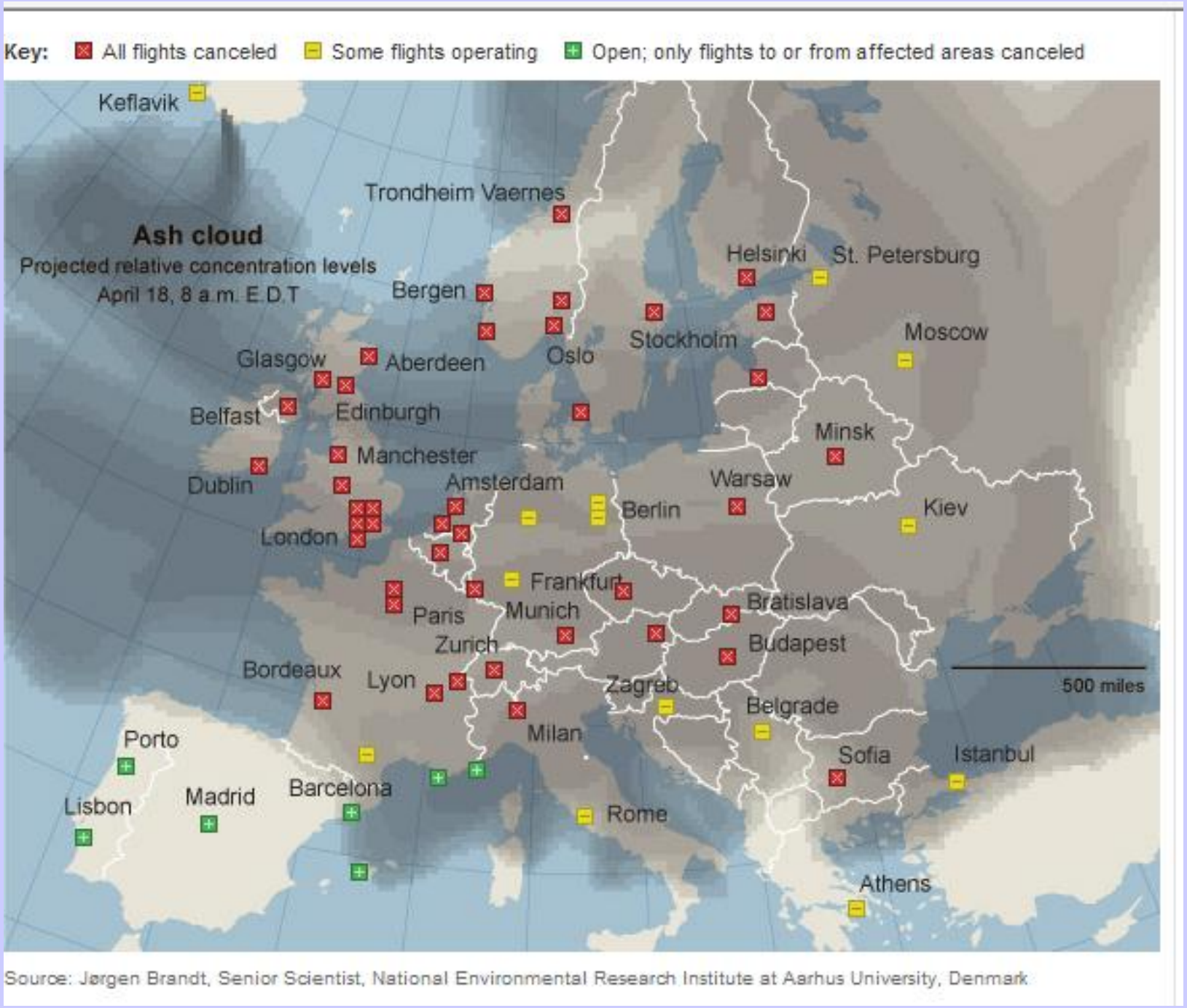

Source: Jørgen Brandt, Senior Scientist, National Environmental Research Institute at Aarhus University, Denmark

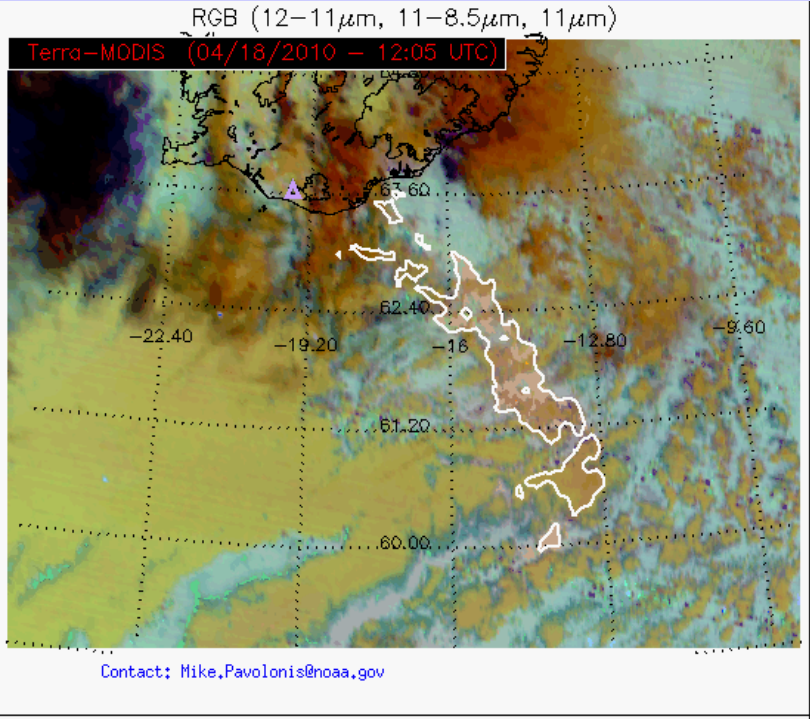

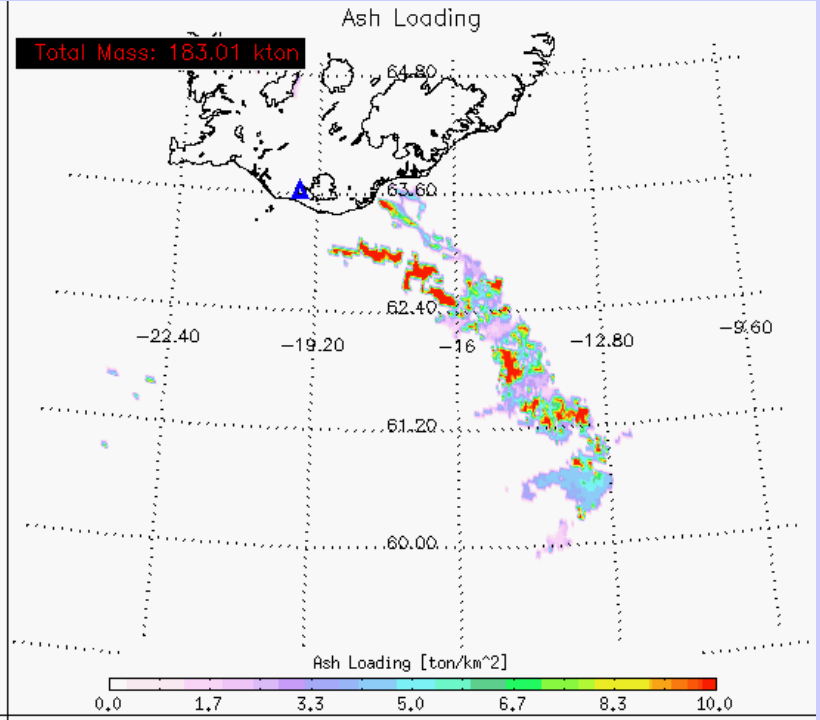

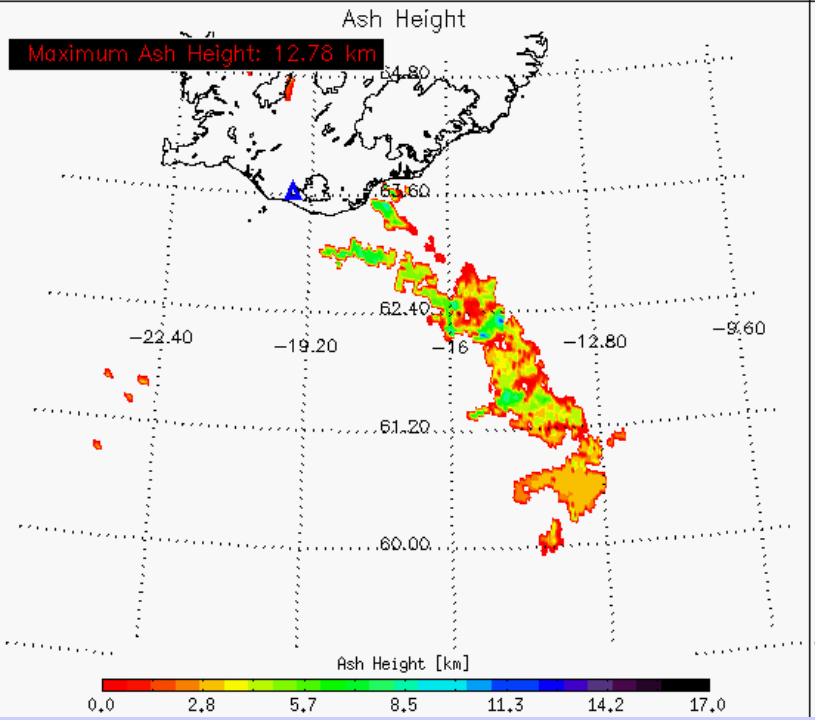

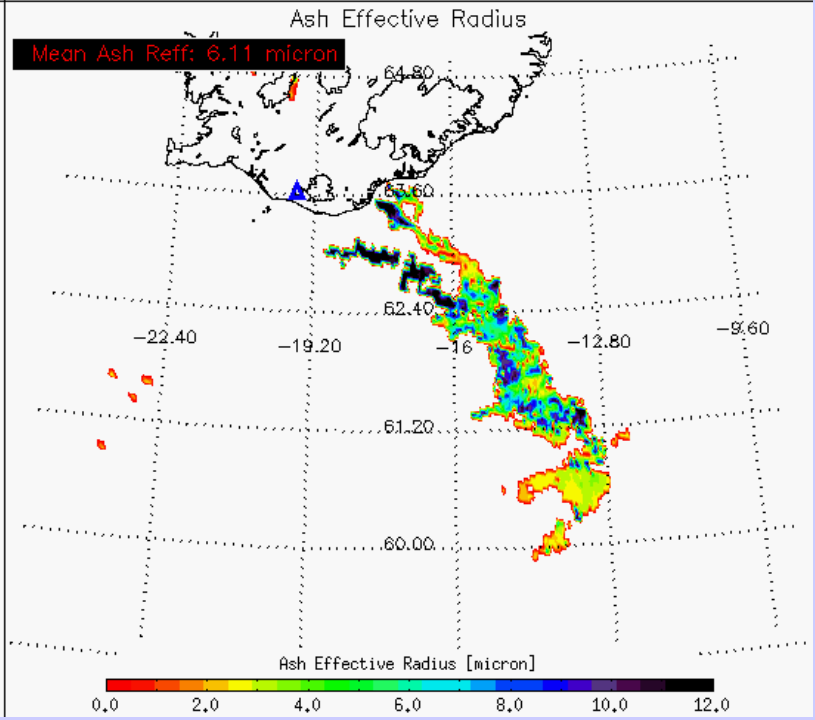

Terra-Aqua MODIS provide am & pm snapshots

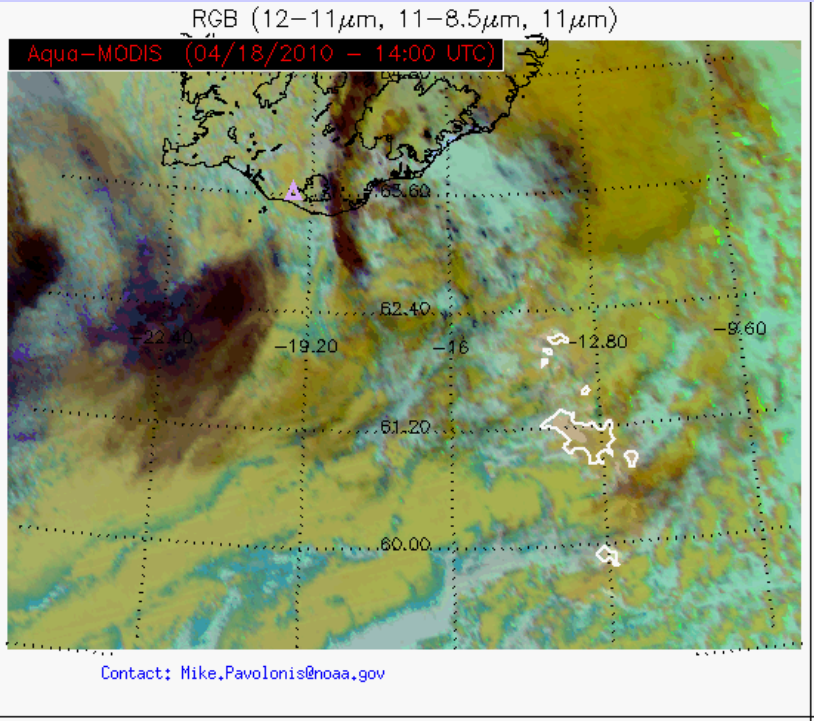

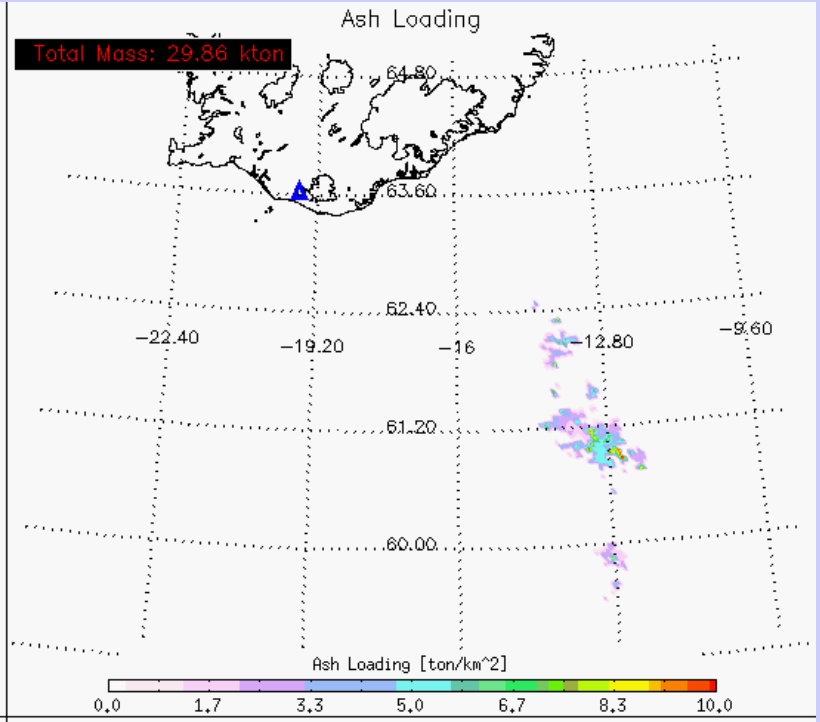

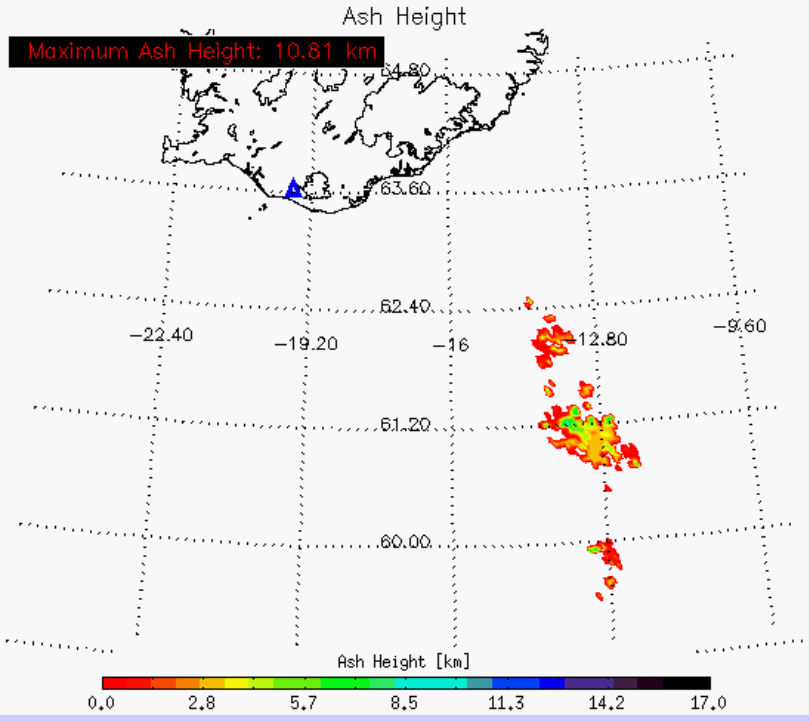

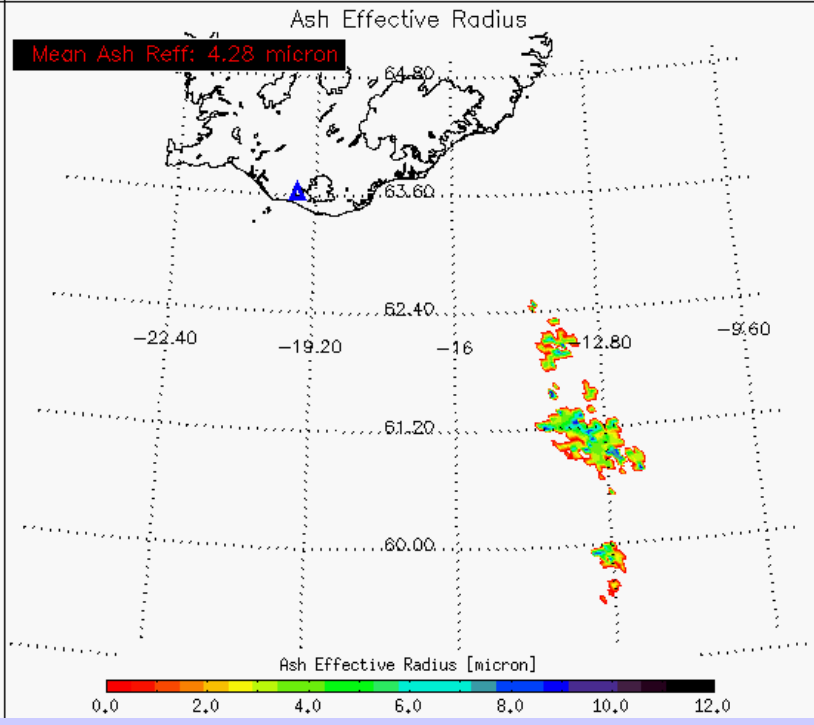

Terra-Aqua MODIS provide am & pm snapshots

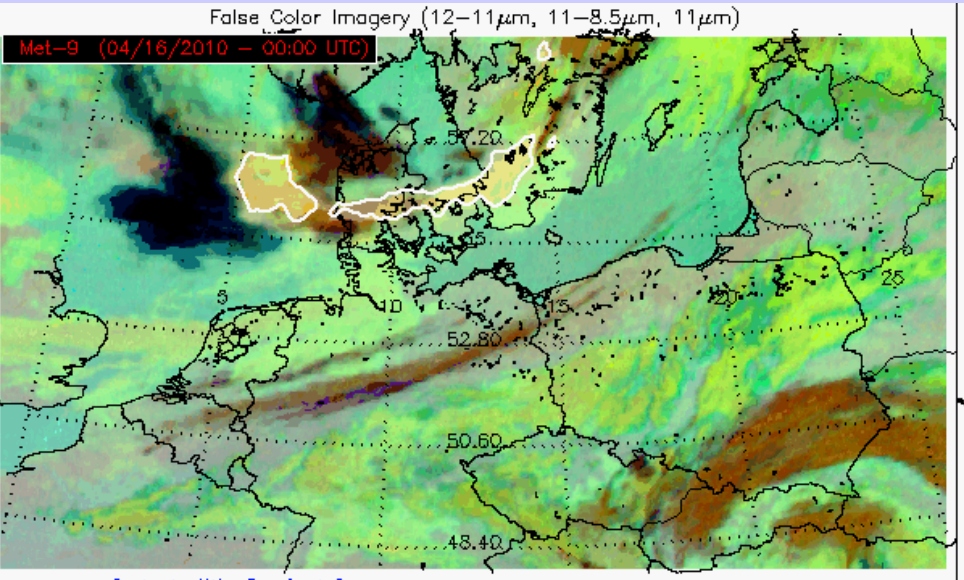

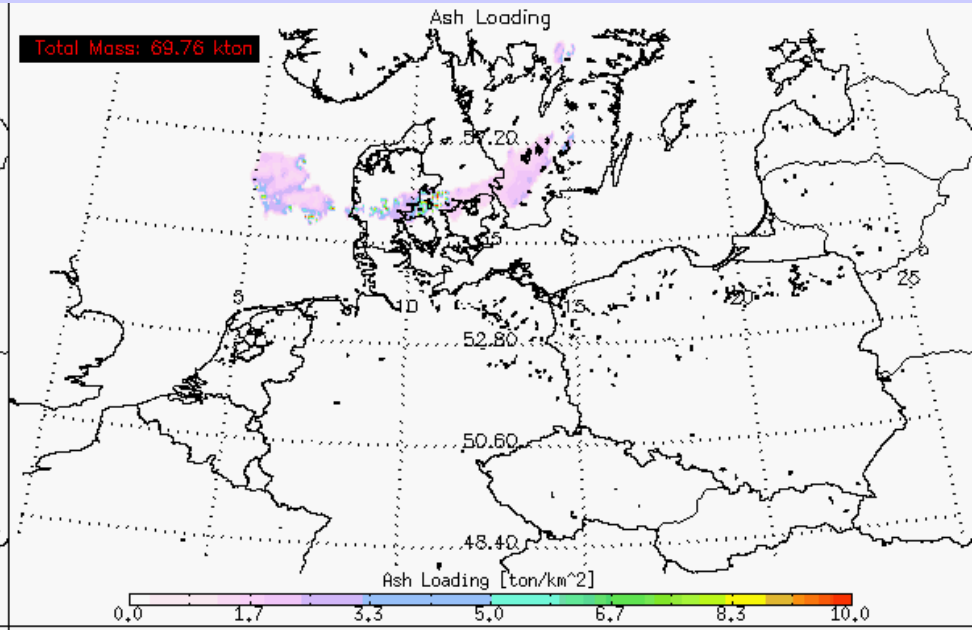

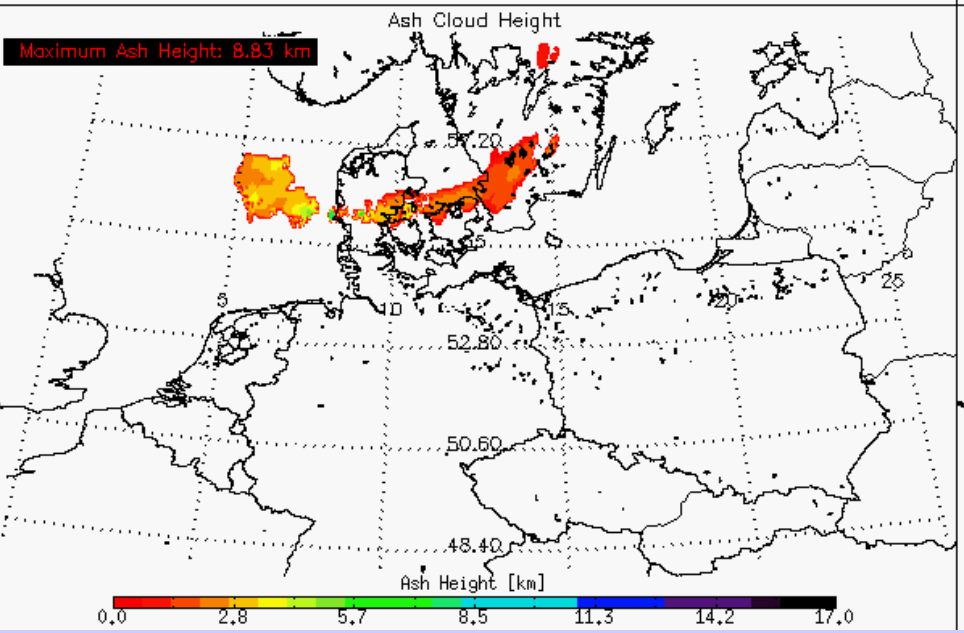

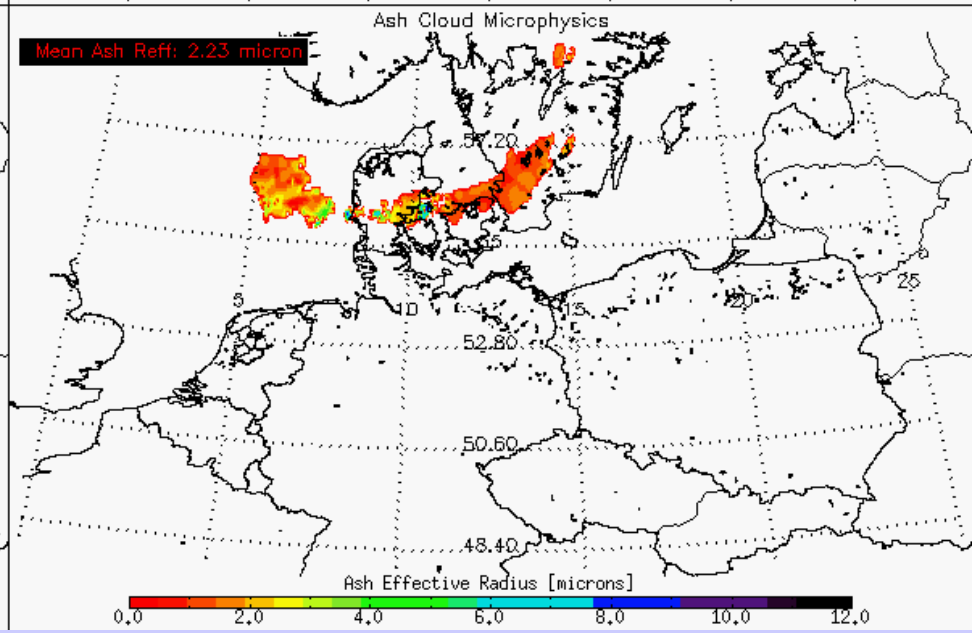

SEVIRI provides time continuous monitoring of ash location and amount

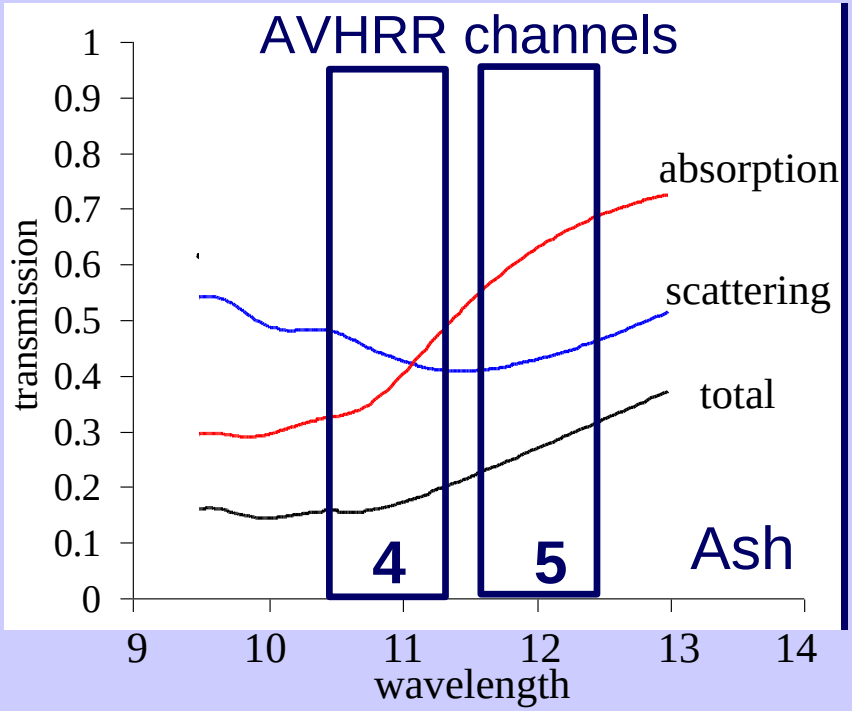

Investigating with Multi-spectral Combinations

Given the spectral response of a surface or atmospheric feature

Select a part of the spectrum where the reflectance or absorption changes with wavelength

e.g. transmission through ash

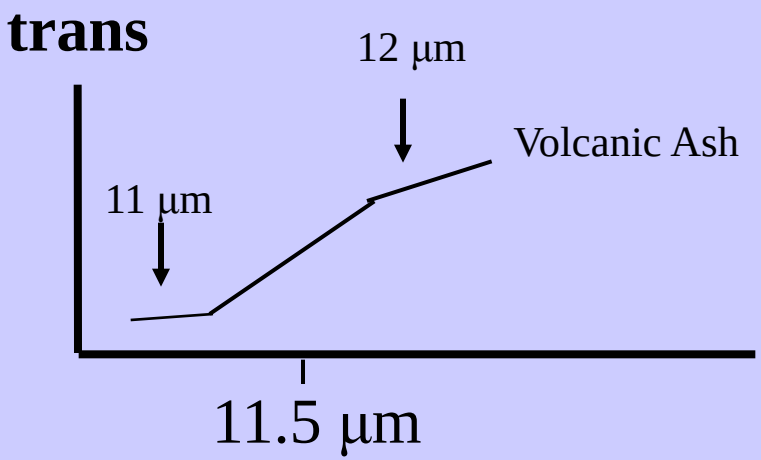

If 11 μm sees the same or higher BT than 12 μm the atmosphere viewed does not contain volcanic ash;
if 12 μm sees considerably higher BT than 11 μm then the atmosphere probably contains volcanic ash

Frank Honey, CSIRO 1980s

Applications with Multispectral Remote Sensing Data

Satellite Remote Sensing

Energy Balance

VIS, IR, and MW Radiative Transfer

EOS Terra & Aqua MODIS

Multispectral Signatures

(Ocean Color, Snow/Ice, Vegetation, Aerosols, Clouds, Moisture, Fires, Volcanic Ash)

Detecting Climate Trends

Key Areas of Uncertainty in Understanding Climate & Global Change

* Earth's radiation balance and the influence of clouds on radiation and the hydrologic cycle

* Oceanic productivity, circulation and air-sea exchange

* Transformation of greenhouse gases in the lower atmosphere, with emphasis on the carbon cycle

* Changes in land use, land cover and primary productivity, including deforestation

* Sea level variability and impacts of ice sheet volume

* Chemistry of the middle and upper stratosphere, including sources and sinks of stratospheric ozone

* Volcanic eruptions and their role in climate change

Climate System Energy Balance

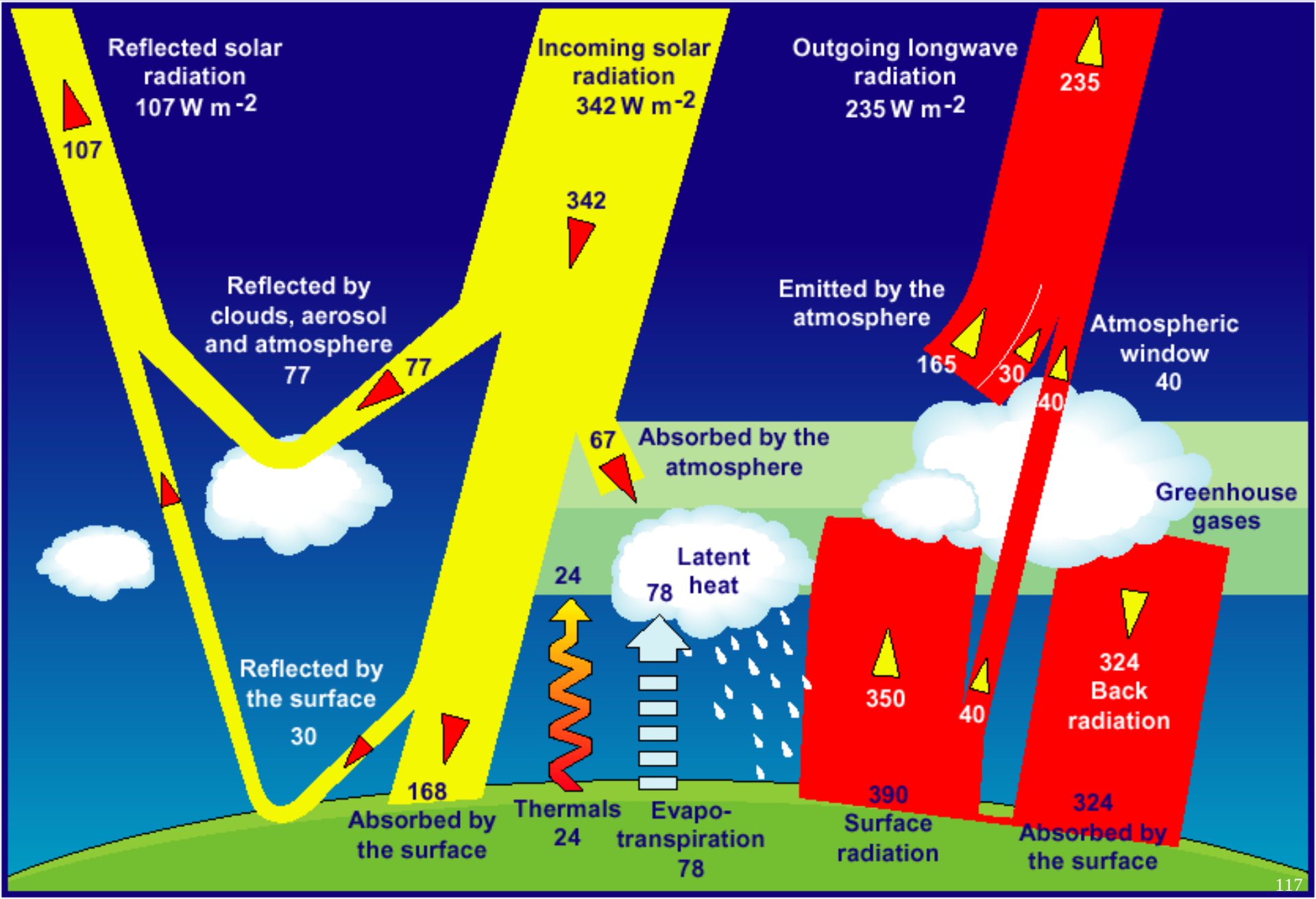

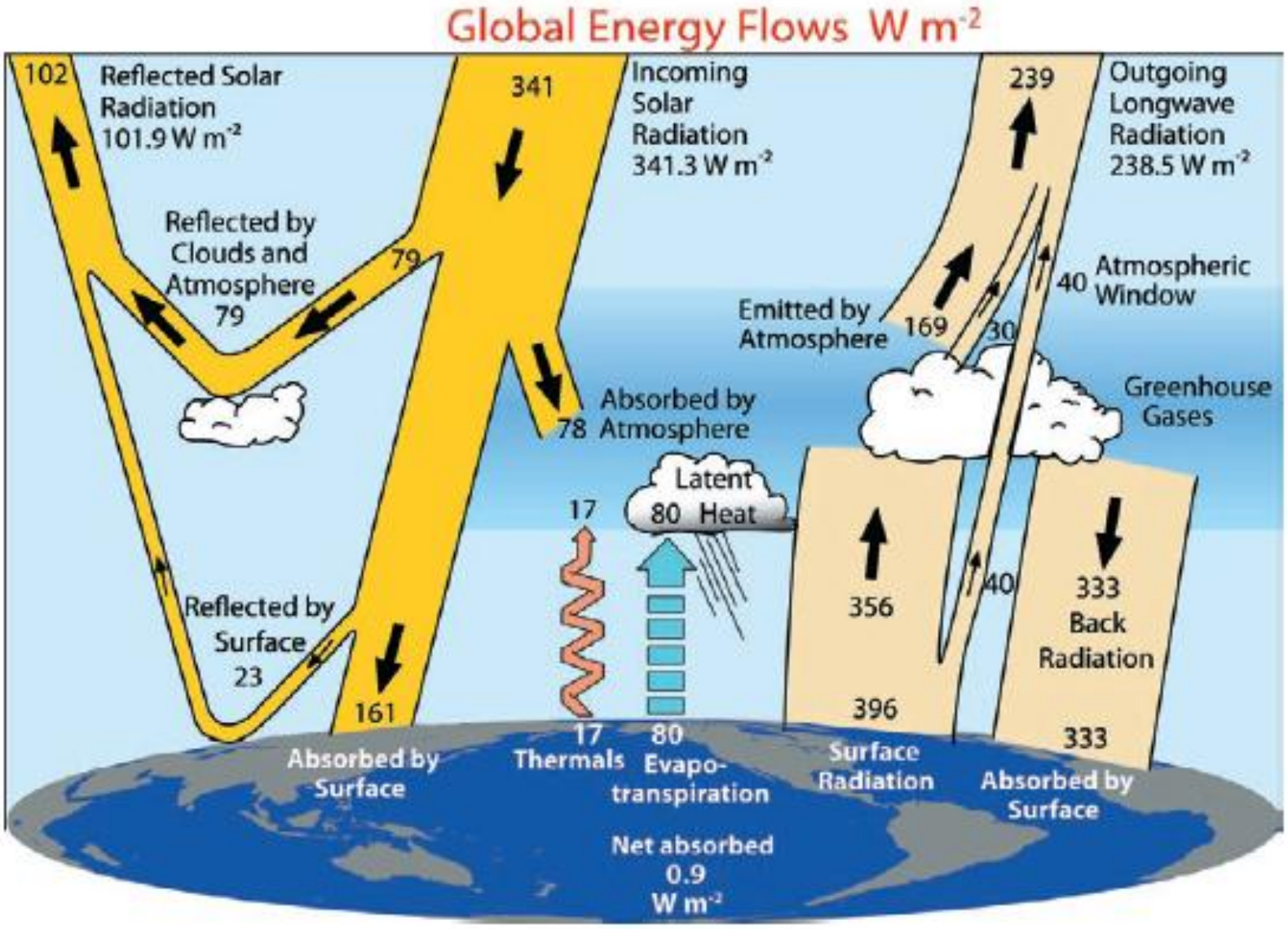

FIG. 1. The global annual mean Earth's energy budget for the Mar 2000 to May 2004 period (W m^{-2}). The broad arrows indicate the schematic flow of energy in proportion to their importance.

Trenberth et al, BAMS 2009

Major Climate System Elements

Carbon Cycle

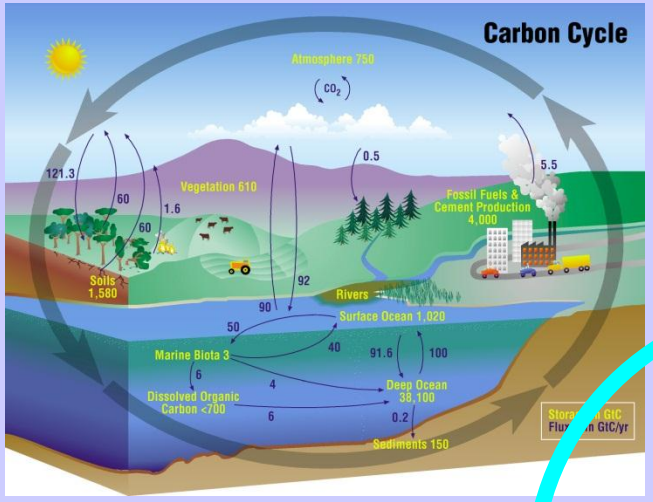

Water & Energy Cycle

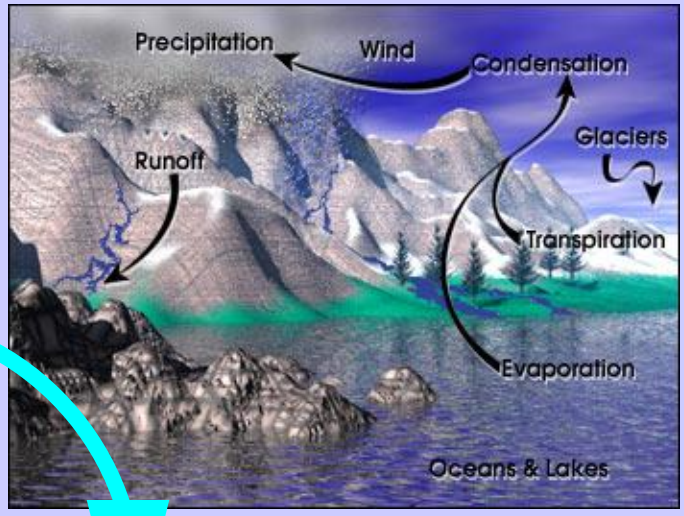

Coupled Chaotic Nonlinear

Atmospheric Chemistry

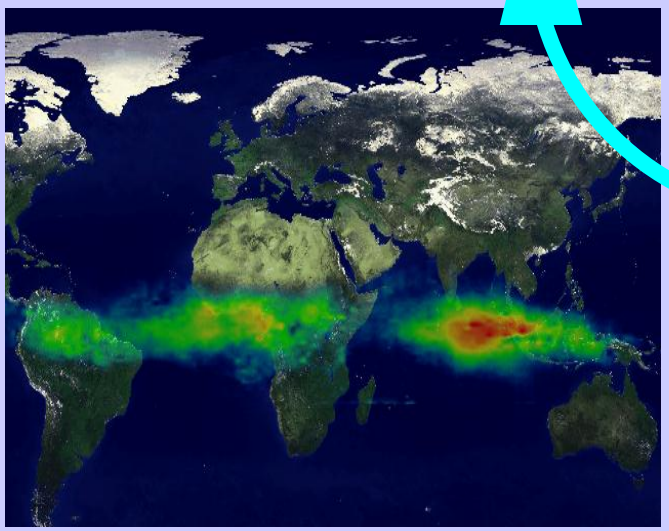

Atmosphere and Ocean Dynamics

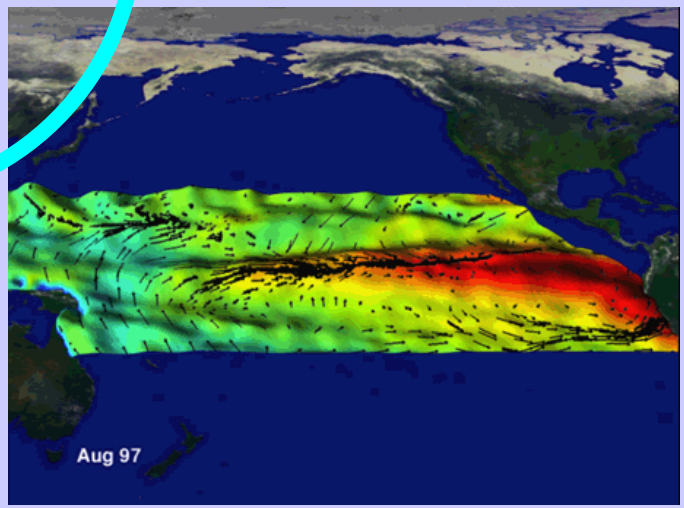

What global surface temperature change has occurred so far?

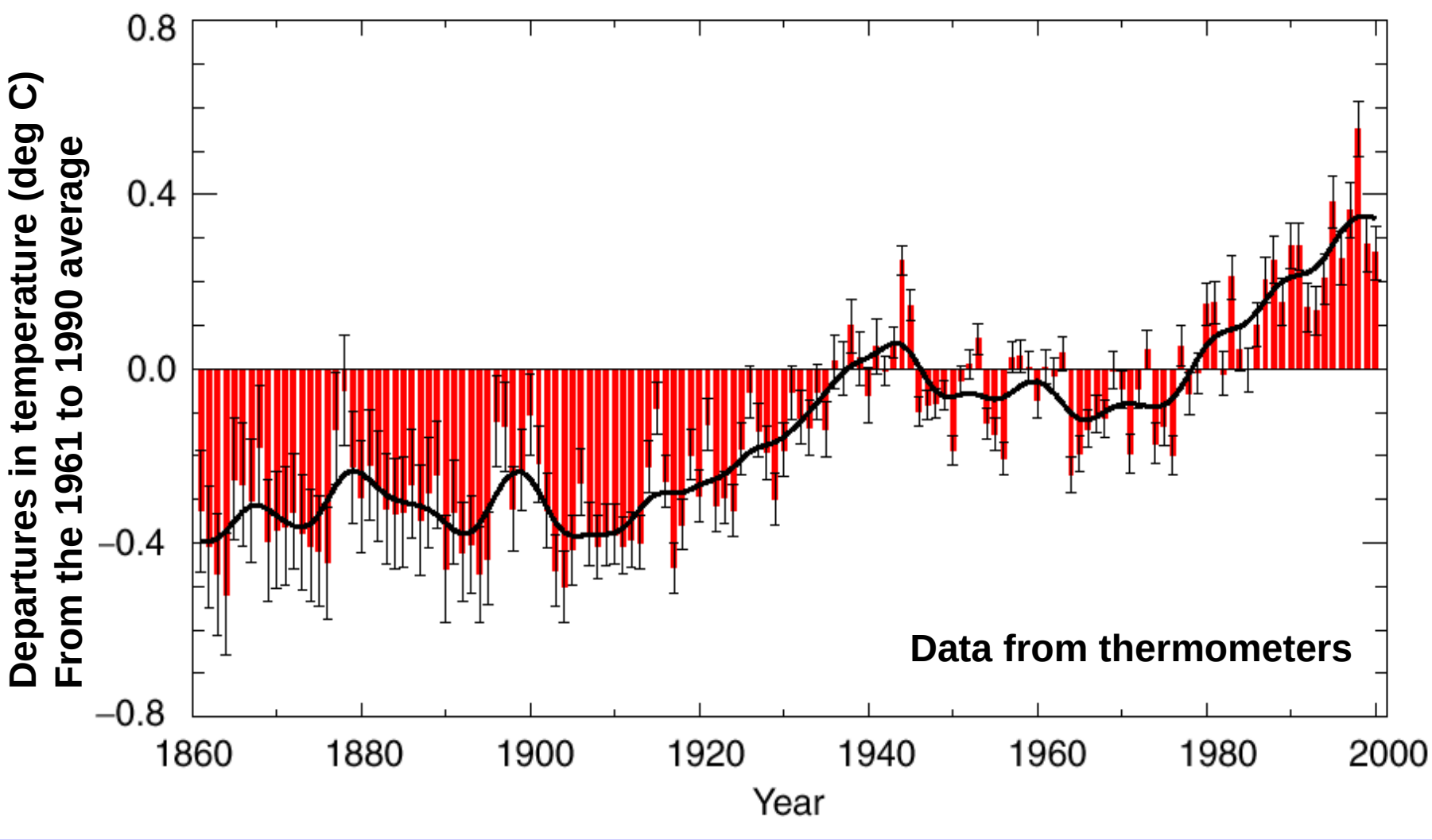

IPCC 2001

Human Influence on Climate

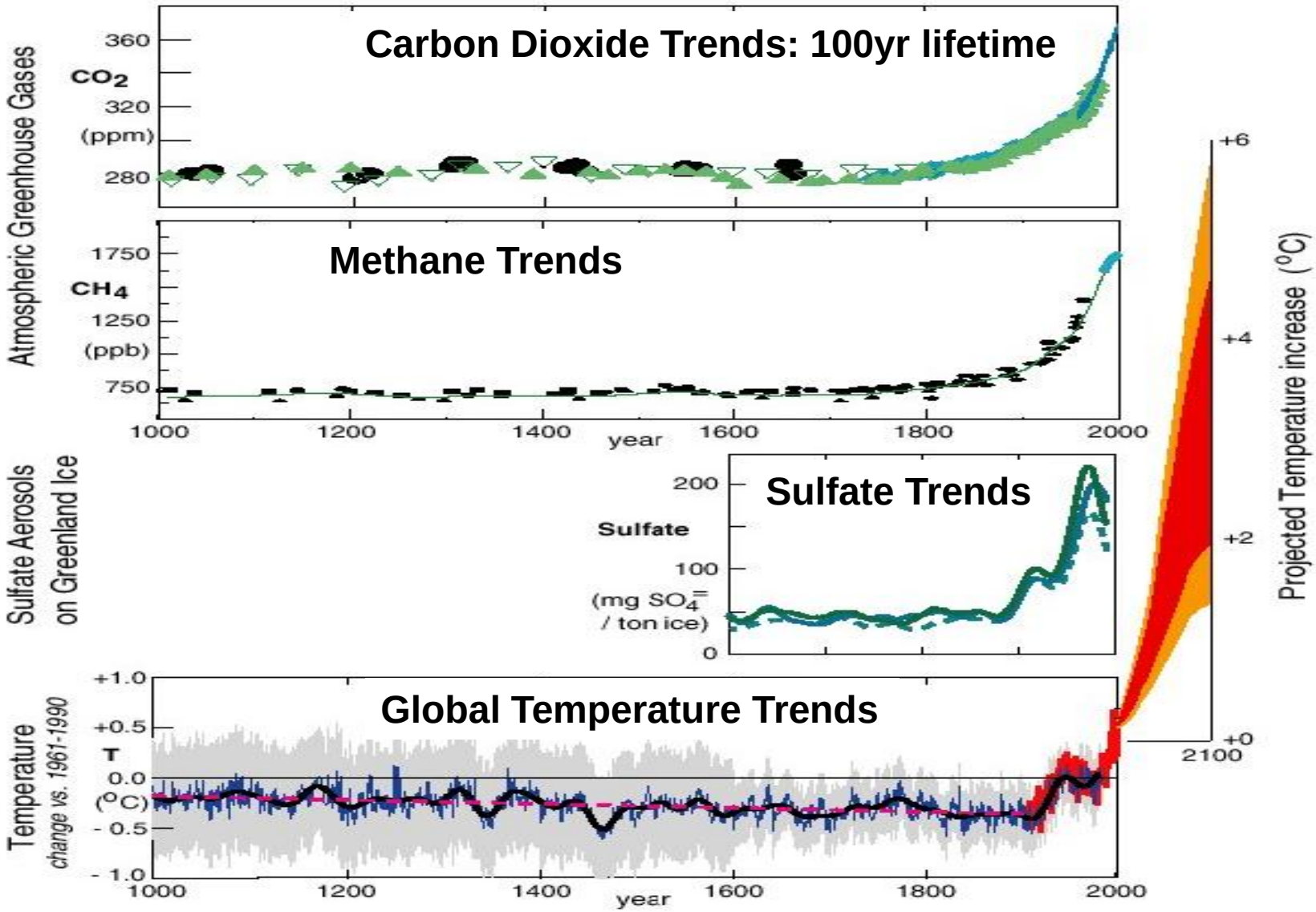

From M. Prather University of California at Irvine

Cloud Feedback is a key unknown

Stephens et al, 2005

- Climate Variability is key NOAA mission. It supports our mission for real-time cloud remote sensing.
- Clouds are major uncertainty in climate models. Satellite records are now long enough to begin to offer some relevant constraints if they are credible.
- The scientific relevance of the cloud climate records from EOS and NPOESS will be much larger if we can extend selected time series back in time using the AVHRR data.

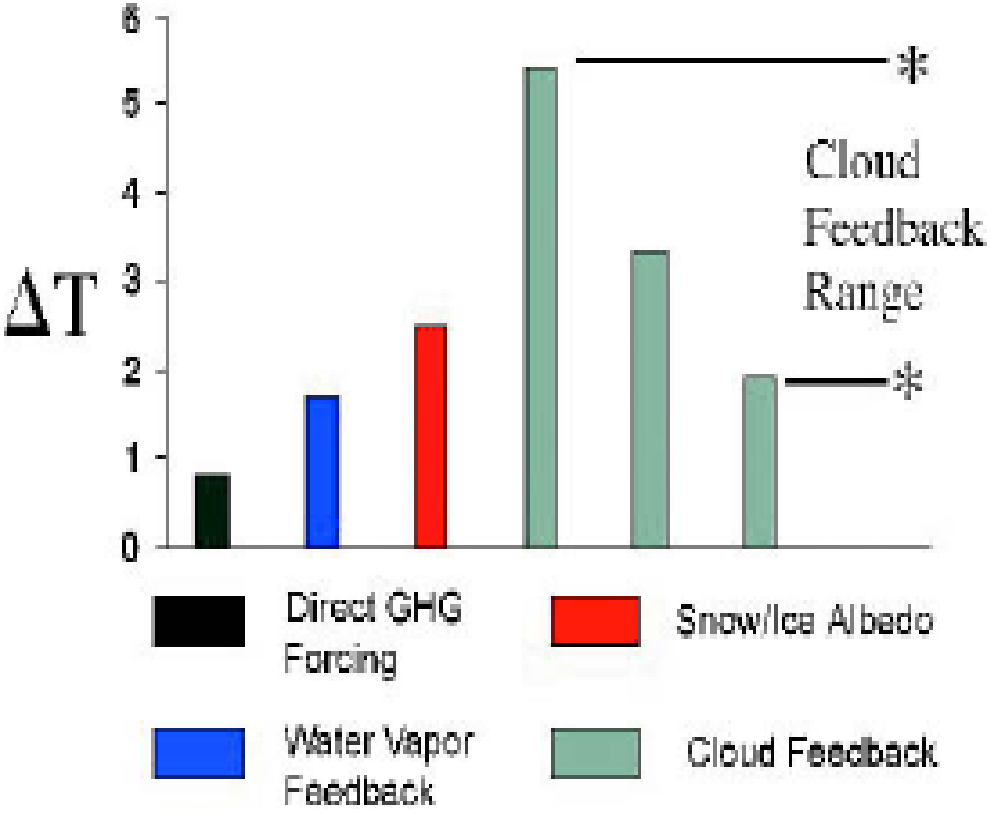

FIG. 13. The response of a single climate model to an imposed doubling of CO_2 as different feedbacks are systematically added in the model (adapted from Senior and Mitchell 1993). Different treatments of cloud processes in the model produce a large spread in predicted surface temperature due to CO_2 doubling.

Annual Cycle of Total Cloud Amount

0-30N Ocean

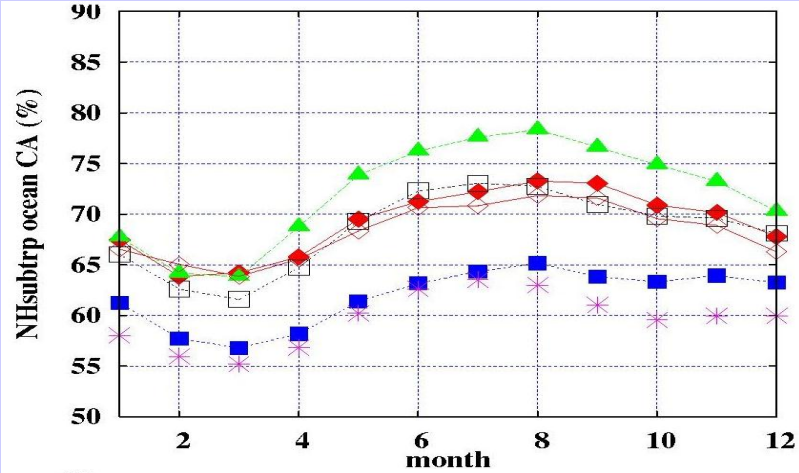

30S – 0N Ocean

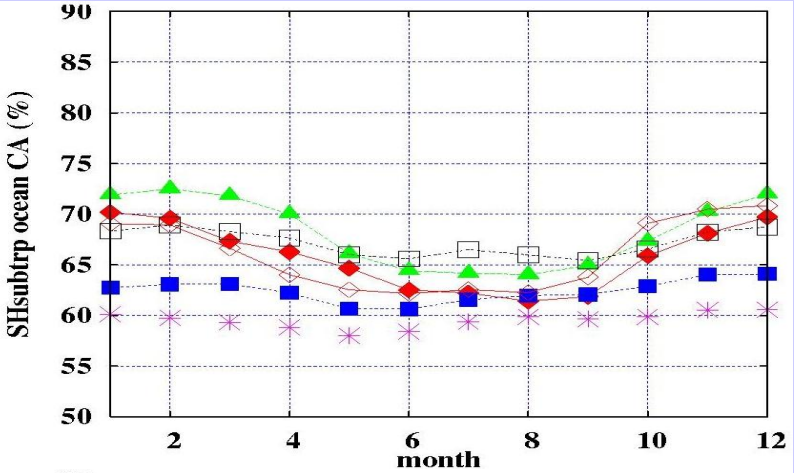

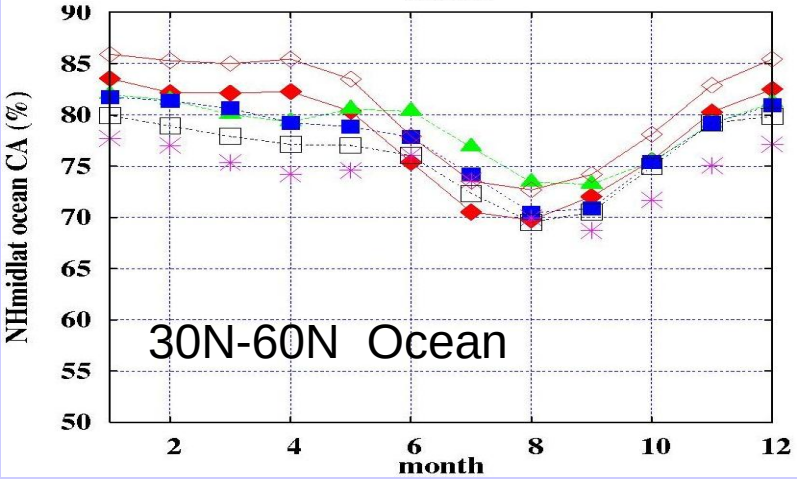

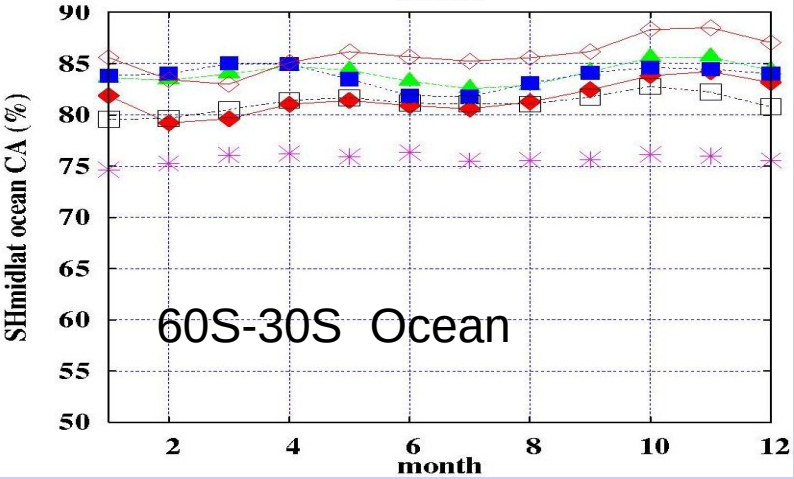

ISCCP, SOBS, UW/HIRS, TOVS/HIRS, PATMOS-x, MODIS

Seasonal cycles all agree through 10% spread on magnitudes.

Detection of High Cloud Differs Appreciably

A series of GEWEX workshops to assess the state of the various satellite cloud climatologies (ISCCP, HIRS, PATMOS-x, MODIS) found large disagreement in the high cloud long-term time-series. Work remains to be done.

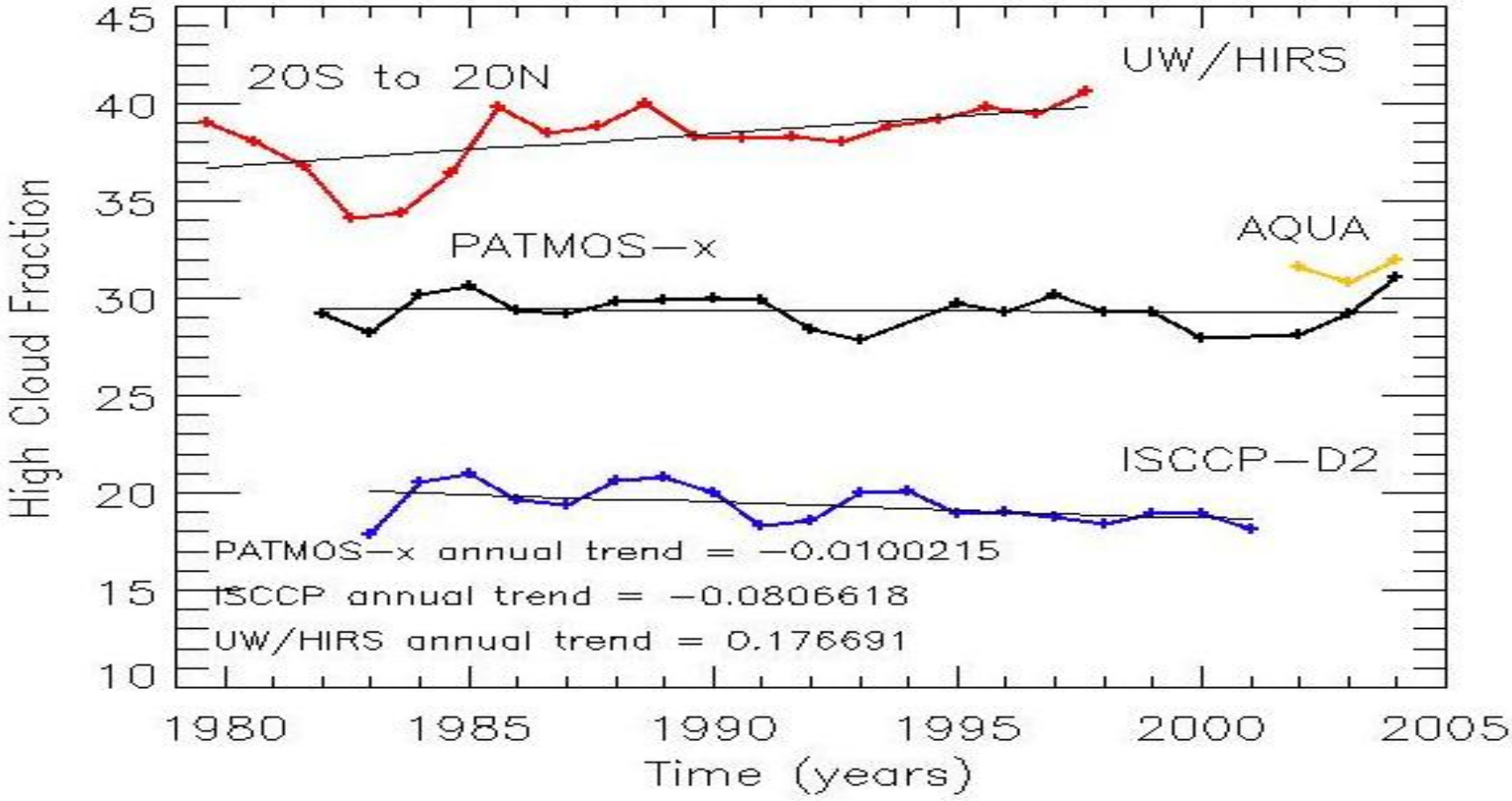

Striving for the Sustainable Society

"A place where humans and their use of the environment are in balance with nature"

"living in harmony with the environment and having resilience to natural hazards"